University of Fort Hare
Together in Excellence

LITHOSTRATIGRAPHIC CORRELATION, MINERALOGY AND GEOCHEMISTRY OF THE LOWER MANGANESE OREBODY AT THE KALAGADI MANGANESE MINE IN THE NORTHERN CAPE PROVINCE OF SOUTH AFRICA

By

Sonwabile Rasmeni

A dissertation submitted in fulfillment of the requirement for the degree of

MASTER OF SCIENCE IN GEOLOGY

In the

Department of Geology, Faculty of Science and Agriculture

University of Fort Hare, Alice 5700, Eastern Cape, South Africa

Supervisor : Professor Baojin Zhao

Co-supervisor : Professor Ken Liu

January 2012

DECLARATION

I declare that this dissertation is my own work except where proper referencing and acknowledgement are made. It has not previously been submitted for a degree requirement to any other University. I, therefore, submit it for the examination and award of the Degree of Master of Science (Geology) at the University of Fort Hare.

Signature

Sonwabile Kidwell Rasmeni **Date:** 30 January 2012

Department of Geology
Faculty of Science and Agriculture
University of Fort Hare, Alice
Eastern Cape, South Africa.

ACKNOWLEDGEMENT

I will forever be indebted to my supervisor Professor Baojin Zhao for his encouragement and valuable support through my series of life transitions especially in the last three years. He has managed to find time within his busy schedule and provided healthy discussions and guidance throughout the study. I also thank Professor Ken Liu for his co-supervision and positive input in the late stage of my study.

Grateful acknowledgment is also given to my family especially my parents, Mr and Mrs Rasmeni for their continuous support and prayers throughout my career. To the staff and students at Fort Hare Geology Department, I have benefited a lot. Special thanks to Dr Oswald Gwavava (H.O.D) for his support and Wendy Koll for proofreading and language correction. Professor Chris Harris of University of Cape Town is thanked for analyzing my samples for carbonate stable isotope.

I wish to express my special appreciation to Mining Qualification Authority (MQA) for the financial and spiritual support and developing me through their Capacity Development Program.

Mintek and their staff at mineralogy division are thanked not only for funding the project but also for their hospitality. They accommodated me in their residences for two months, produced polished sections, provided training and allowed me to use their sample preparatory lab and machines for my analyses.

I am grateful to Kalahari Resources Co. and their staff for logistical support and allowing me to participate into their project from the initial stages and providing me with their valuable data and unpublished mine information.

Lastly, friends are acknowledged for various roles they played.

LIST OF MAJOR MINERALS AND THEIR CHEMICAL FORMULA

Mineral	Chemical Formula
Barite	$BaSO_4$
Braunite	$Mn^{2+}Mn_6^{3+}SiO_{12}$
Calcite	$CaCO_3$
Garnet(Andradite)	$Ca_3F_2Si_3O_{12}$
Hausmannite	Mn_3O_4
Hematite	Fe_2O_3
Jacobsite	$Mn\ Fe_2O_4$
Kutnahorite	$Ca\ (Mn,Mg)(CO_3)_2$
Mg calcite	$(Ca, Mg)CO_3$
Mn calcite	$(Ca,Mn)CO_3$
Rhodochrosite	$MnCO_3$
Serpentine	$(Mg, Fe)_3Si_2O_5(OH)_4$

LIST OF ABBREVIATIONS

BIF → Banded Iron Formation

CGS→ Council for Geoscience

KMF → Kalahari Manganese Field

LMO → Lower Manganese Orebody

XRD → X-Ray Diffraction

XRF →X -Ray Fluorescence

ABSTRACT

The Kalagadi Manganese mine in the Kuruman area of the Northern Cape Province of South Africa contains reserves of Mn ore in excess of 100Mt. Mineralization in the mine lease area is restricted within the Hotazel Formation of the Voëlwater Subgroup, belonging to the Postmasburg Group, the upper subdivision of the Transvaal Supergroup. Surface topography is characterized by flat lying, undulation with minimal faulting and the ore are slightly metarmophosed. This study investigates the general geology of the mine, lithostratigraphic subdivision and correlation of the economic Lower Manganese Orebody (LMO) of the Kalagadi Manganese Mine in order to guide mining plan and operations once the mine is fully commissioned. At the commencement of this study, Kalagadi Manganese mine was a project under exploration with no specific geology of the mine lease area and no lithostratigraphic subdivision.

The study also aimed determining the extent of lithostratigraphic correlation between the LMO economic orebodies of the Kalagadi Manganese mine with that of underground Gloria and open-pit Mamatwan mines. Four methods including petrographic microscope, Scanning electron Microscope (SEM), X-ray diffraction (XRD) and X-ray fluorescence (XRF) analyses were applied mainly for the mineral identification, chemical composition and ore characterization of the Lower Manganese Orebody (LMO) at Kalagadi Manganese mine.

The results of this study indicates the following: **(1)** Eleven textural distinct zones with economic zones restricted to the middle while the lower grade zones are confined to the top and bottom of the LMO; **(2)** The economic zones, comprising of Y, M, C and N subzones attain an average thickness of 10 m and are graded at an average of 40% Mn while the Mn/Fe ratio varies from 6 to 9; **(3)** The most economic zones are M and N subzones which are mostly characterized by oxidized ovoids and laminae, a characteristic applicable even to other zones of economic interest; **(4)** Braunite is the main mineral of the manganese ore and is often integrown with kutnahorite and other minerals (hematite, hausmannite, Mg-calcite, calcite, jacobsite, serpentine and garnet) which are present in variable amounts; **(5)** The Mg-rich calcite $(Ca, Mg)CO_3$ is the second dominant manganese carbonate

mineral and it corresponds to elevated MgO concentration and is often associated with marine environment. The occurrence of the Mg−calcite is not common in the manganese ore of this area except for the Mn-calcite, which was not determined by XRD analyses in this study; **(6)** MnO is the most abundant major oxide in the manganese ore while other major oxides present in decreasing order of abundance are CaO, SiO_2, Fe_2O_3, and MgO. The oxides TiO_2, Na_2O, K_2O, Al_2O_3, and Cr_2O_3 are depleted and are mostly < 0.01wt% and < 0.001wt% respectively while P_2O_5 concentrations are low ranging from 0.02wt% to 0.3wt%. The trace element concentrations of Ba, Zn and Sr in most borehole samples are slightly elevated ranging from 100ppm to 3.9% (36000pm) while Co, Cu, Ni, Y, As, Zr, V and La rarely exceed 50ppm.

The enrichments of Cu, Zn, Ni, Co and V that are commonly associated with volcanogenic hydrothermal input in chemicals may reach up to 70ppm; **(7)** The mineralogical and geochemical characteristics of the manganese ore in the Kalagadi Manganese mine lease area are similar to that of Low-Grade Mamatwan-Type ore. The cyclicity (Banded Iron Formation ↔ Hematite lutite ↔ braunite lutite) and alternation of manganese and iron formation have been confirmed; and **(8)** The oxygen $\delta^{18}O$ isotope values (18‰ to 22‰) indicate a slight influence of metamorphism of the manganese ore. No positive correlation exists between $\delta^{13}C$ vs $\delta^{18}O$ values and Mn vs $\delta^{13}C$ values. Such observations indicate minimal action of organic carbon during manganese precipitation where the organic matter was oxidized and manganese content reduced. On the other hand, the manganese carbonates (CaO) are positively correlated with carbon isotope, this indicates diagenetic alteration, and the involvement of biogenic carbonate during the formation of manganese carbonates.

It is concluded that the lithostratigraphic subdivision at Kalagadi Manganese mine is best correlated physically, mineralogically and geochemically with that of Gloria mine operating in the Low Grade Mamatwan - Type ore while correlation with an open-pit Mamatwan mine is also valid.

TABLE OF CONTENTS

LIST OF FIGURES

LIST OF TABLES

CHAPTER ONE

INTRODUCTION

1.1 Mineral economics

The Kalagadi Manganese project started in 2006 (in an area covering 8, 000 ha) with the aim of exploring the manganese ore covered by Cenozoic Kalahari sands and other lithologies in the Kuruman area, Northern Cape Province of South Africa. Pre-feasibility studies followed by first phase of drilling were conducted to evaluate the ore deposit and underground structural features that may affect future mining activities, such as ore grade and mine safety.

The permission to use the available borehole data and material from the mine lease area for study purposes was sought and obtained from Kalahari Resources, which is the second major shareholder of the Kalagadi Manganese Mine. This study is therefore, based mainly on the borehole information obtained from the first and second phases of their drilling program.

The drill core data in the mine area have uncovered three manganese orebodies alternating with Banded Iron Formation (BIF) and directly overlain by at least three different lithologies to the surface. The lowermost orebody is the oldest and the most economic component in the Kalagadi Manganese mine lease. The Early Proterozoic manganese deposits such as those in the Northern Cape of South Africa, Minas Gerais of Brazil and Orissa of India represent a very important source of the world's manganese. The Kalahari Manganese Field (KMF) in South Africa contains the largest manganese resource in the world accounting for about 80% of the world's identified resources. According to estimates by the International Manganese Institute (2008), China was the

largest producer of Mn ores, followed by South Africa, Australia, Gabon, Brazil, India, Ukraine and other countries.

The demand for manganese ore increases with demand in the steel industry, various grades of steel products require different amounts of manganese and industrialized countries have long been linked with the demand in manganese. Manganese has many important applications but is largely (about 95 %) used by iron and steel industry due to its sulfur fixing, deoxidizing and alloying properties. Manganese is used by the chemical industry especially in dry cell batteries and is alloyed with aluminium and copper. It is further used in trace amount as plant fertilizer and animal feed and as a coloring agent (International Manganese Institute, 2008).

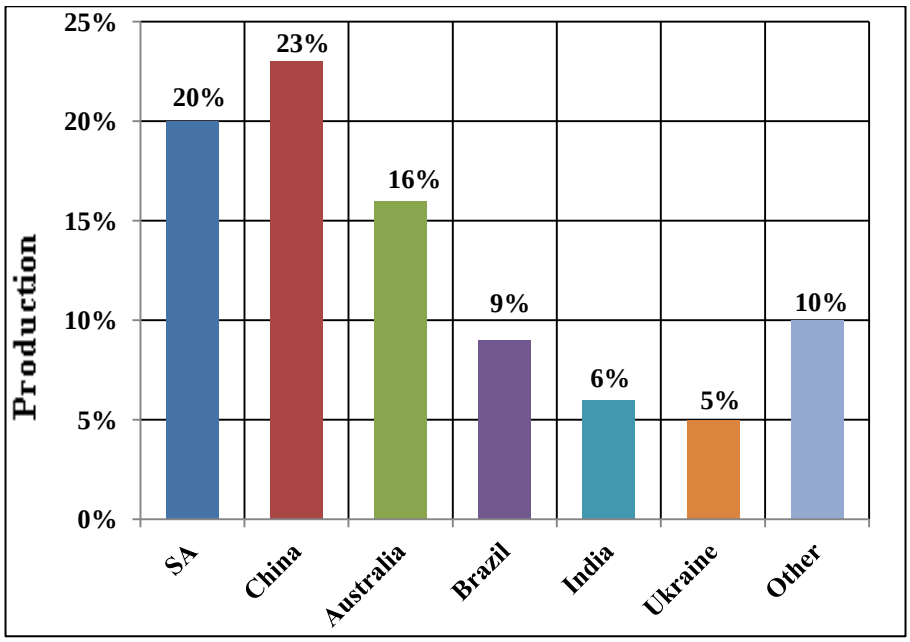

Figure 1.1. The world's manganese ore production per country in Million Metric Tons for the year 2008 (International Manganese Institute, 2008).

The first ever lithostratigraphic subdivision of the LMO in the entire Kalahari deposit was conducted at Mamatwan mine and the findings were later published by Nel et al. (1986). This study led to subdivision of the lowermost manganese orebody at Mamatwan mine into eleven distinct zones, based on physical characteristics of the ore such as colour, abundance of carbonate laminae, lenticles and ovoids orientation, banding and sizes. The mineralogy and geochemistry of the ores at Mamatwan mine were also studied to supplement the macroscopic observations.

These lithostratigraphic zones were further grouped into three categories: The Upper Low grade ore zone at the top; Central Economic grade ore zone in the middle; and the Basal Low grade ore zone towards the base of the orebody. Preston (2001) also conducted a similar study at Mamatwan mine and although the initial subdivision published by Nel et al. (1986) remained valid, some zones such as X, Y, M and C were further refined and subdivided into subzones that are macroscopically distinct and laterally consistent. Van Staden (2002) also conducted a similar study at Gloria mine, which is situated about 10 km from Kalagadi mine. At Gloria mine, about ten zones that are correlative on mineralogical and geochemical composition with those at Mamatwan mine but differ on the thickness were reported.

The methods applied in the study involve fieldwork and laboratory analyses. The aim was to identify and describe various zones of the LMO focusing on various parameters such as grain size, texture, composition, magnetic properties and colour. Graphic logs were created from drill core logs in order to give a visual impression of the entire section, correlate and compare equivalent sections in the entire mine lease area. Petrographic, mineralogical and geochemical studies of the manganese

ore were conducted in order to supplement macroscopic field observations. The information and data obtained from the field and petrographic analyses are presented in chapter 3, 4 and 5.

1.2 Background

The Kalagadi manganese mine is located in the north-central part of the extensively studied main Kalahari deposit of the KMF, about 65km NW of Kuruman in the Northern Cape Province of South Africa. The mine lease area is situated approximately 10km SW of Gloria mine and 15km NW of Mamatwan mine (Figure 1.2).

ArcelorMittal (50%), black women-owned Kalahari Resources (40%) and Industrial Development Corporation (10%) jointly own the Kalagadi Manganese mine. Geographically, the mine lease forms gently, wavy-sloping plains and basins with little or no visible outcrops except for the well-known Black Rock "Hill" (the only outcropping mound of manganese ore of the Hotazel Formation) located approximately 15km towards the north at an elevation of 1070m.

The mine lease is at a mean elevation of 1049m and windblown sand, thick calcretes and gravels of the Kalahari Formation cover its surface. Mining is to take place in an area of approximately 8,000ha incorporating three farms, Umtu Olivepan and Gama, stratigraphically located in the Hotazel Formation of the Postmasburg Group of the Transvaal Supergroup. The Hotazel Formation is the host to three manganese-rich orebodies intersected during drilling in the mine lease area. These manganese orebodies are termed the Upper, Middle and Lower manganese ore bodies and are found alternating with Banded Iron Formation (BIF). Exploitation in the entire Kalahari deposit has traditionally been focused on the lowermost orebody since it is regarded as the most economic and

well developed in the entire Kalahari deposit. The Mamatwan- Type ore is the most abundant in the Kalahari deposit accounting for nearly 97% of manganese ore with the remaining 3% being that of the thrusted and hydrothermally altered Wessel-Type ore.

The KMF, which is the focus area for this study encompasses all manganese mines in the Kuruman area and is further subdivided into five deposits that are structurally preserved as erosional relics of the Hotazel Formation, which comprises iron-formation with alternating units of manganese ore. Such erosional relics as depicted in Figure 1.2-B are mainly: The Kalahari deposit (sometimes referred to as Mamatwan-Wessel basin), the largest of the five deposits is known to contain an estimated resource of 13.6 billion metric tons of ore at 20 to 48 percent of manganese content (Miyano and Beukes, 1987) approximately 80% of the worlds known mineable manganese resource (Preston, 2001). The mine lease area is therefore restricted to the Low Grade Mamatwan-Type ore of the Kalahari deposit. Surface exposures in the mine lease area show flat-lying undulations and are covered by wind-blown sand, calcretes and gravels of the Kalahari Group. The LMO form the base Hotazel Fomation at a depth of the about 200 m.

The Kalahari deposit underlies a total area of about 525km^2 (Gutzmer and Beukes, 1995) stretching from Mamatwan mine in the south to the Wessels mine in the north. The Kalahari deposit is further divided into high-grade hydrothermally altered Wessel-Type in the north incorporating the Ncwaning, Wessels and the defunct Black Rock mine and the low-grade sedimentary Mamatwan-Type ore in the south, which incorporates the Mamatwan, Gloria and the Kalagadi mines.

The other two deposits are Hotazel and Langdon Annex lying east of the main deposit and are considered to be of higher grade but have been mined out. Kleyenstüber (1984) described the ore at Hotazel mine as massive black-brownish supergrade ore with manganese content reaching 60% with ovoids completely replaced by hausmannite. These deposits are known to represent portions of the Hotazel Formation that have been downfaulted into graben structures. The Avontuur and Leinster lying north of the main deposits are insignificant and contain a sub-economic low-grade jacobsitic type of ore.

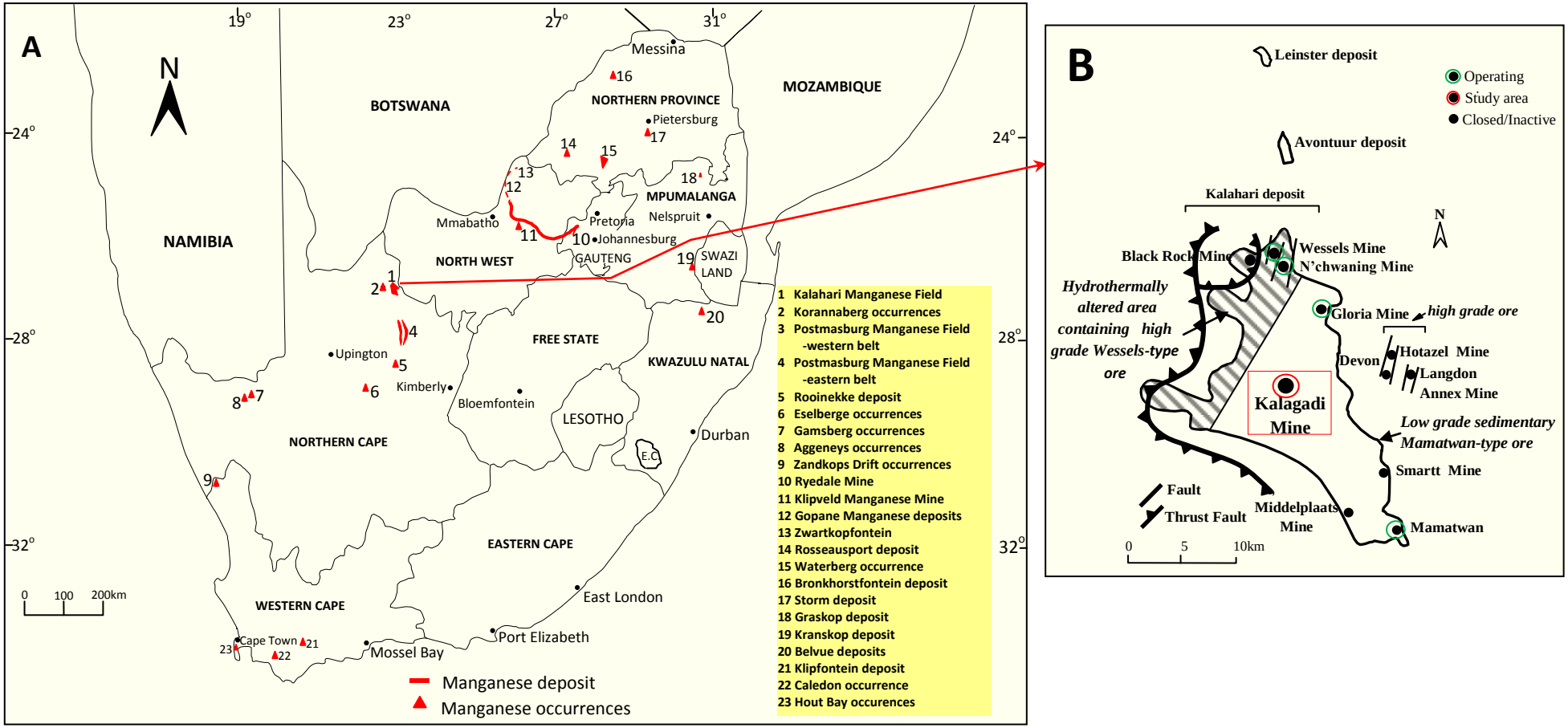

Figure 1.2 **A.** Map showing the location of the land-base manganese deposits in South Africa. Modified from Asrupt and Tsikos (2006). **B**. Enlaregd view of the Kalahari Manganese Field in the Northern Cape Province of South Africa showing the localition of a Kalahari deposit, the study area (red circles), active mines(green circles) and inactive mine.

1.3 Previous work

The KMF and the surrounding manganese mines have been extensively studied since the 1940s. The history of the KMF dates back to 1907 with the discovery of the Black Rock outcrop–bearing manganese ore. No further interest was shown to this "hill"up until 1941 when Boardman conducted the first detailed description of the manganese ore exposed at the Black Rock outcrop which was later acquired by Associated Manganese Mines of South Africa (ASSMANG) for mining purposes. Since then, more mines were opened and studies were conducted in the region. Aspects of previous work include general and detailed mineralogy and geochemistry; general geology of the specific mines and genesis of the manganese ore. Few studies focused on the BIF that are found alternating with manganese ores in the Hotazel Formation.

A lot of work had been done especially on the mineralogy and geochemistry of manganese ore but its genesis remained enigmatic for decades. The debate became more intense among the following authors: Beukes et al. (1982), Cornell and Schütte (1995), Beukes and Gutzmer (1996), De Villiers (1983) and Tsikos and Moore (1998). In an excellent review of an enigmatic association of iron and manganese in the KMF, Tsikos and Moore (1998) drew attention to the fact that the vast majority of commercial manganese deposits are of sedimentary character and proposed genetic models variously emphasize the importance of additional processes (e.g. sea-floor volcanic activity, sea level fluctuations, climate changes, biological productivity) as critical in the development of large accumulation of manganiferous sediment in depositional environments of various ages (Frakes & Bolton, 1992). The genetic models for Kalahari ores are grouped into three camps (Tsikos & Moore, 1998) and are:

(1) Large scale epigenetic replacement mechanism, whereby Kalahari manganese ores are thought to have formed as a result of younger hypogene replacement mechanisms at the expense of a suitable protolith, i.e. during a younger hypogene hydrothermal event (De Villiers, 1983).

(2) Submarine volcanogenic exhalative activity involving interaction between mid ocean ridge-type submarine volcanism and rapid precipitation of Mn and Fe-rich compounds (Cornel & Schütte, 1995).

(3) Pure chemical precipitation which places particular emphasis on various environmental parameters (sea-level fluctuations, climate change) involved in the deposition of iron and manganese minerals with volcanism acting either as a nearest (Beukes, 1983; Nel et al., 1986) or a remote (Tsikos and Moore, 1997) metalliferous source. The latter seems to have gained popularity amongst many authors.

More studies were conducted at KMF especially in the 1980s, focusing either on the manganese ores themselves or associated iron formation. Studies conducted by De Villiers (1983) suggested that Kalahari Manganese deposit is genetically related to the Postmasburg deposit and they were precipitated by hypogene solution thereby suggesting magmatic hydrothermal origin. A study by Beukes et al. (1982) recognized the presence of three chemo-sedimentary cycles of BIF and braunite lutite in the Hotazel Formation. Kleyenstüber (1984) made major contributions by identifying new minerals and subdividing the ores in the KMF into low-grade metamorphic Mamatwan-type ore, high-grade Wessels-type ore and uneconomic jacobsitic ore. Nel et al. (1986) published the first detailed mineralogical characterization of the lower manganese orebody at Mamatwan and subdivided the orebody into various zones, which were further grouped into Upper Low Grade zone,

Central Economic zone and Basal Low Grade zone at the bottom. Studies were also conducted on the geology and mining operations of specific mines of the KMF. Jennings (1986) conducted a study on the general geology and mining operations of the Middelplats mines. A study by Du Plooy (2002) focused mainly on the parameters that control the supergene alteration of the ferruginized zone at Mamatwan mine. The studies by Nel et al. (1986) and Preston (2001) were aimed at characterizing the LMO at Mamatwan mine while van Staden (2002) conducted similar studies at Gloria mine. Kleyenstüber (1993) gave an update on the important characteristics of the manganese ores and some minerals occurring in the KMF and hence tentatively suggested the volcanogenic sedimentary origin for the manganese ore.

The studies by Gutzmer (1996), Gutzmer and Beukes (1995 and 1997) and Burger (1994) were aimed mostly at mineralogical identification, mineral paragenesis and also delineated the role of structural features (faults and thrusts) during metasomatic alteration and upgrading of the ore in the northern parts of the Kalahari deposit. Studies by Tsikos and Moore (1997 and 1998); Abrupt and Tsikos (1998) and Tsikos et al. (2003) concentrated mainly on the association of BIF and manganese (Mn) ores.

These authors focused mainly on petrography, geochemistry, mineralogy and the review of the literature and proposed models for the deposition as well as isotopic compositions of the BIF and Mn ores. A study by Chetty (2008) was aimed at geometallurgical evaluation of the ores in the northern Kalahari deposit. The study focused on detailed mineralogical and geochemical characterization of the Mn ore genesis with the emphasis on alteration and has since broadly

classified the ores in the region into: least altered (LA), partially altered (PA) and advanced altered (AA) types.

1.4 Problem Statement

This study focuses on the characterization of the LMO in the Hotazel Formation at the Kalagadi Manganese mine in comparison with the correlative orebodies at underground Gloria and opencast Mamatwan mines operating in the low-grade Mamatwan-Type ore of the Kalahari deposit.

An economic geological prospect of the study is achieved by characterizing the manganese ores in the mine lease area and suggesting the zones of economic importance for future efficient mining. Interest in this study is enhanced by the fact that the Kalagadi Manganese project is considered as one of South Africa's first major greenfield manganese project in three decades especially in terms of expected production and involved investment.

The mine was expected to commence production at the end of 2011; critical mine planning and operating decisions require definitive and detailed information from physical, mineralogical and geochemical analysis of the ore composition to improve production and beneficiation. There is currently no published scientific information on the detailed geology of the mine lease area and no lithostratigraphic subdivision to aid in guiding mining operations once the mine is commissioned. It is known from an in-house company report that approximately 8m thick section of the economic loweremost orebody at the mine would be mined and processed. However, evidence on borehole material indicates that the LMO attains an average thickness of approximately 18m, so the remaining section will not be utilized. There is currently no lithostratigraphic subdivision in place to correlate

the mineralogy and chemistry of the LMO at Kalagadi mine with that of an underground Gloria mine and open-pit Mamatwan currently operating in the low grade sedimentary Mamatwan-Type ore of the Kalahari deposit.

Similar studies conducted at Mamatwan mine as published by Nel et al. (1986) and Preston (2001) and at Gloria mine by van Staden (2002) are hoped to have benefited the mines in terms of efficient mining. It is also essential and interesting to determine which subdivision among the three in those two mines is applicable and best correlated with that of Kalagadi Manganese mine.

Apart from the mineralogical characterization of the manganese ore, the paragenetic sequence of minerals determined in the study as well as genetic consideration for the manganese are ascertained. The expected output from the study would be useful in not only assisting and guiding the daily mining operations, but also in adding value to the existing knowledge as no similar study has been undertaken in the mine lease area.

1.5 Aims and Objectives

The purpose of the study is to gain a better understanding of physical, mineralogical and geochemical characteristics of the manganese ores and from the results, suggest the zones of high mineralization and possible ways of utilizing the larger thickness or more zones of the orebody than anticipated. The study also aims at investigating the controlling factors of mineralization and any influence of structural features on the quality of the ore across the mine lease area. The study seeks to compare and correlate the lithostratigraphic subdivision of the LMO at Kalagadi mine with the correlative orebody to the north at Gloria Mine and further to the south at Mamatwan Mine. Apart

from that, the paragenetic sequence, paleoclimate and paleogeographic conditions under which manganese was deposited are ascertained and described.

The work on the Kalahari manganese ores dates back to the 1940s and their characterization serves as a tool in guiding the mining operations even today (Nel et al., 1986). Mineralogy has been used occasionally as a tool in characterizing the genesis of manganese ores but often with difficulty due to mineralogical complexity such as fine-grained nature, opaqueness and similarity in hand specimens. Geochemical signatures can give useful and vital information on the environment of deposition and the path of mineral diagenesis. In the initial stages of the study, Kalagadi manganese project was on shaft sinking stages with further drillings in progress but access to borehole material was granted.

1.6 Outline of the dissertation

The study consists of following chapters:

Chapter 1: Introduction

This chapter includes a brief overview of mineral economics, background of the study, previous work on manganese ore of this region, problem statement and objectives of this study highlighting the rationale of the study and expected output. References used in the particular chapter are listed at the end.

Chapter 2: Lithostratigraphic correlation

This section aimed at introducing the regional and local geology and the stratigraphic location of the study. It also highlights the macroscopic field observations. Orebody and borehole correlation are conducted in order to obtain a complete view of the underground and surface geology, variation of the orebody with depth and any structural influence on the ore. Various zones are described macroscopically, the results and the new lithostratigraphic subdivision are presented. Lastly, the observations from the chapter are discussed and the conclusions are drawn. References are also listed at the end of the chapter

Chapter 3: Lithostratigraphic zone's mineralogy

Lithostratigraphic zones are described mineralogically and petrologically. This chapter includes: general introduction on the mineralogy of the manganese ore with reference to previous workers, sample preparation and methodologies applied in the laboratory as means of further characterizing various zones. The results on mineralogy and mineral genetic sequence are presented followed by discussion and conclusions. Refererences used in this chapter are listed at the end.

Chapter 4: Geochemistry

Introduction on mineral chemistry and laboratory methods and analyses are presesented. Results of major and trace element analyses are presented and discussed. The discussion includes the correlation between major and trace elements and the depositional environment of the manganese ore. Conclusions are made based on the results and discussion. References used in this chapter are also listed.

Chapter 5: Carbon and Oygen isotope

Introduction in this chapter includes the previous studies on the stable isotope of the carbonates of manganese ore of the entire KMF and other manganese deposits of various ages throughout the world. Methodologies applied on this chapter are described and and the results are presented. Discussion of the results in relation to other deposit and the conclusions are presented. References used are listed at the end.

Chapter 6: Summary and Conclusions

A very brief summary of the findings in this study is presented and the major conclusions are made where necessary.

Appendix

This section contains tables of XRD analyses for the two boreholes selected for detailed analyses

1.7 References

Astrup, J., and Tsikos, H. (1998). Manganese. *in* Wilson, M.J., and Anhaeusser, C.R. (eds), Mineral Resources of Southern Africa: Pretoria, South Africa, Council for Geosciences, Handbook 16, p. 450–460.

Beukes, N.J., and Gutzmer, J. (1996). A volcanic-exhalative origin for the world's largest Kalahari Manganese Field, A discussion of the paper by D. H. Cornell and S.S. Schütte, Mineral Deposita, Vol. 31, p. 242-245.

Beukes, N.J. (1983). Palaeoenvironmental setting of iron formations in the depositional basin of the Transvaal Super group, South Africa. In: Trendall, A.F., and Morris, R.C. (eds). Iron formations, facts and problems, Elsevier, Amsterdam, p. 131-209.

Beukes, N.J., Kleyestüber, A.S.E., and Nel, C.J. (1982). Volcanogenic-sedimentary cycles in the Kalahari Manganese Field. Sedimentology, Vol. 82, Geological Society of South Africa, Extended Abstracts, p. 93-97.

Boardman, L.G. (1941). The Black Rock manganese deposit in the south-eastern Kalahari: Geological Society of South Africa Transaction, Vol. 44, p. 51-60.

Burger, A.M. (1994). Fault controlled hydrothermal alteration of Palaeoproterozoic manganese ore in Wessels mine, Kalahari Manganese Field. Unpublished MSc. Dissertation, University of the Johannesburg, Johannesburg, South Africa).

Chetty, D. (2008). A geometallurgical evaluation of the ores of the northern Kalahari manganese deposit, South Africa, Unpublished PhD Thesis, University of the Johannesburg, South Africa).

Cornell, D.H., and Schütte, P. S.S. (1995). A volcanic-exhalative origin for the world's largest (Kalahari) Manganese field: Mineral Deposita, Vol. 30, p. 146-151.

De Villiers, J.E. (1983). The Manganese Deposits of Griqualand West, South Africa: Some Mineralogic Aspects: Economic Geology, Vol. 78, p. 1108-1118.

Du Plooy, A.P. (2002). Geochemistry and mineralogy of supergene altered manganese ore below the Kalahari unconformity in the Kalahari manganese field, Northern Cape Province, South Africa, Unpublished MSc. Dissertation, University of the Johannesburg, South Africa).

Frakes, L., and Bolton, B. (1992). Effects of ocean chemistry, sea level, and climate on the formation of primary sedimentary manganese ore deposits. Economic Geology, Vol. 87, p. 1207-1217.

Gutzmer, J., and Beukes, N.J. (1995). Fault controlled metasomatic alteration of Early Proterozoic sedimentary manganese ores in the Kalahari Manganese Field, South Africa. Economic Geology, Vol. 90, p. 823-844.

Beukes, N.J., and Gutzmer, J. (1996). A volcanic-exhalative origin for the world's largest Kalahari Manganese Field, A discussion of the paper by D.H. Cornell and S.S. Schütte, Mineral Deposita, Vol. 31, p. 242-245.

Gutzmer, J., and Beukes, N.J. (1997). Effects of mass transfer, compaction and secondary porosity on hydrothermal upgrading of Paleoproterozoic sedimentary manganese ore in the Kalahari Manganese Field, South Africa. Mineralium Deposita, Vol. 32, p. 250-256.

Gutzmer, J. (1996). Genesis and alteration of the Kalahari and Postmasburg manganese deposits, Griqualand west, South Africa. Unpublished PhD Thesis, University of the Johannesburg, South Africa).

Kleyenstüber, A.S.E. (1993). Significant characteristics of the manganese ores and some of the minerals occuring in the Proterozoic Kalahari Manganese Field, South Africa. Resource Geology Special Issue, No 17, p. 2-11.

Kleyenstüber, A.S.E. (1984). The mineralogy of the manganese bearing Hotazel Formation of the Proterozoic Transvaal Sequence in Griqualand West, South Africa. Transactions of the Geological Society of South Africa, Vol. 87, p. 257-272.

Miyano, T., and Beukes N .J. (1987). Physicochemical environments for the formation of quartz-free manganese oxide ores from the early Proterozoic Hotazel Formation, Kalahari Manganese Field, South Africa: Economic geology, Vol. 82, p. 706-718.

Nel, C.J. Beukes, N .J. and De Villiers, J.E. (1986). The Mamatwan manganese mine of the Kalahari manganese field, in Anhaeuser, C.R. and Maske, S., eds. Mineral deposits of Southern Africa: Johannesburg, Geological Society of South Africa, p. 963-978.

Preston, P.C.C. (2001). Physical and chemical characterization of the manganese ore bed at the Mamatwan mine, Kalahari Manganese Field, Unpublished MSc. Dissertation, University of the Johannesburg, South Africa.

Tsikos, H., and Moore, J.M. (1997). Petrography and geochemistry of the Palaeoproterozoic Hotazel iron-formation, Kalahari Manganese Field, South Africa: Implications for Precambrian manganese metallogenesis. Economic Geology, Vol. 92, p.87-97.

Tsikos, H., and Moore, J.M. (1998). The Kalahari manganese field: an enigmatic association of iron and manganese. South African Journal Geology Vol. 101 (4), p. 287-290.

van Staden, A. (2002). Characterization of the lowermost manganese ore bed of the Hotazel Formation, Gloria Mine, Northern Cape Province, Unpublished MSc. Dissertation, University of the Johannesburg, South Africa).

International Manganese Institute, (2008). Manganese Ore Production. Available online at http://www.manganese.org/about_mn/production.

CHAPTER TWO

LITHOSTRATIGRAPHIC CORRELATION

2.1 Introduction

During the last field visits to the Kalagadi Manganese mine, the manganese ores had been explored in at least 66 boreholes drilled across the mine lease area. The depth of each borehole ranges from 200m to 400m with spacing of 100m to 250m. The depth variation plots of the borehole material defines the basinal appearance with surface morphology displaying wavy undulating and flat lying plains at elevations between 1030m to 1049m due to slight folding and faulting that are often accompanied by erosion (Figure 2.3).

The lithologies above the Hotazel Formation decrease from the north of the mine lease area to the south, near the open-pit Mamatwan mine.The overlying lithologies then increase from the east to the west of the mine lease thereby displacing the orebody into deeper levels. The Kalagadi Manganese mine is designed as an underground mine operation where the orebody would be accessed using bord and pillar mining method.

The orebody is located at an average depth of 220m and two vertical shafts (the main and secondary shaft) that are designed to intersect the orebody at 250m service the mine. The main shaft will service personnel, machinery, inlet ventilation and the hoisting of ore while the secondary shaft will be used for returning ventilation and as an emergency outlet (Kalahari Resources, 2008). The drilled and blasted ore aggregates would be crushed and reduced in size into 150mm fines in the designated crushing stations before it is transported into a conveyor belt system to the shaft silos, from where it

will be lifted up to the surface (run of mine stockpile). The ore would be routed to the secondary and tertiary crushing and screening plant producing a lump washed ore reduced to < 6mm in size, which is the size required for the sinter process (Kalahari Resources, 2008).

The mine is designed for a production capacity of about 3Mt of run of mine ore per annum which will be reduced to 2.4Mt of manganese ore per annum when sintered to upgrade the manganese content by driving the carbonate content that impacts on the grade of the ore. Therefore monthly ore production would be between 250 000 tons to 200 000 tons, three times higher compared to other mines currently operating in the Kalahari Manganese Field.

2.2 Geological setting

2.2.1 Stratigraphy

The manganese ore of the Kalagadi mine is restricted to the Hotazel Formation of the Voëlwater Subgroup in the Postmasburg Group, the middle subdivision of the Transvaal Supergroup in the Kaapvaal craton. The Transvaal Supergroup had been traditionally divided into two groups, the upper Postmasburg group and the Ghaap Group below. However, recent study by Dorland (2004) proposed a new lithostratigraphic subdivision, the Elim Group as succeeding the Postmasburg Group within the Transvaal Supergroup. According to this new stratigraphic subdivision, the Lucknow and Mapedi/Gamagara Formations, which were previously grouped under Olifantshoek group, form the upper and lower parts of the Elim Group.

The manganese bearing Hotazel Formation of the Voëlwater Subgroup comprises three manganese rich ore layers, alternating with banded iron formation. These manganese ore layers are subdivided

into the Lower, Middle and Upper manganese ore bodies. Mining in the entire Kahahari deposit is focused to the LMO, which varies in grade from 30% to 40% Mn. The Middle orebody is of sub-economic value with varying thickness of between 1m and 5m. Very limited exploitation has taken place at the Upper orebody (Miyano and Beukes, 1987) which varies in thickness from 5m to 15m at Kalagadi mine.

The Hotazel Formation in the central and northern parts of the Kalahari deposit is reportedly overlain by dolomites and minor limestones of the Mooidraai Formation (Bau et al., 1999), shales and siltstones of the Mapedi/Gamagara Formation and quartzites of the Lucknow Formation in the Elim Group. Lithologies of the Olifantshoek Group in the Keis Supergroup (Van Niekerk, 2006) and/or the Dwyka diamictite of the Karoo Supergroup overlies the Elim group with the surface exposure covered by the younger Kalahari Formation containing sands, silt, clay, gravels and calcretes.

In the southeastern portion of the Kalahari deposit, the Hotazel Formation is near the surface and is directly overlain by sand, calcrete, gravel and clay of the Kalahari Formation. The Hotazel Formation in the mine lease area is rarely overlain by the Mooidraai Formation but by Dwyka Group and the Kalahari Formation (Figure 2.4 and 2.7). The majority of borehole intersections show succession of Dwyka and Kalahari Groups directly above the Hotazel Formation while the underlying Mooidraai Formation in many boreholes is not well preserved due to erosion by glacial movement during the deposition of Dwyka Formation (Figure 2.9 and 2.10). The Hotazel Formation rests directly on the basaltic andesites (massive lava flows, pillow lavas, and hyaloclastites) of the Ongeluk Formation (Schneiderhan et al., 2006) with variable thickness of 500m – 600m (Tsikos et

al., 2003) and the drilling end once this formation is intersected. A review of literature shows that Ongeluk Formation is then underlain by Makganyene diamictite forming the base of the Postmasburg Group.

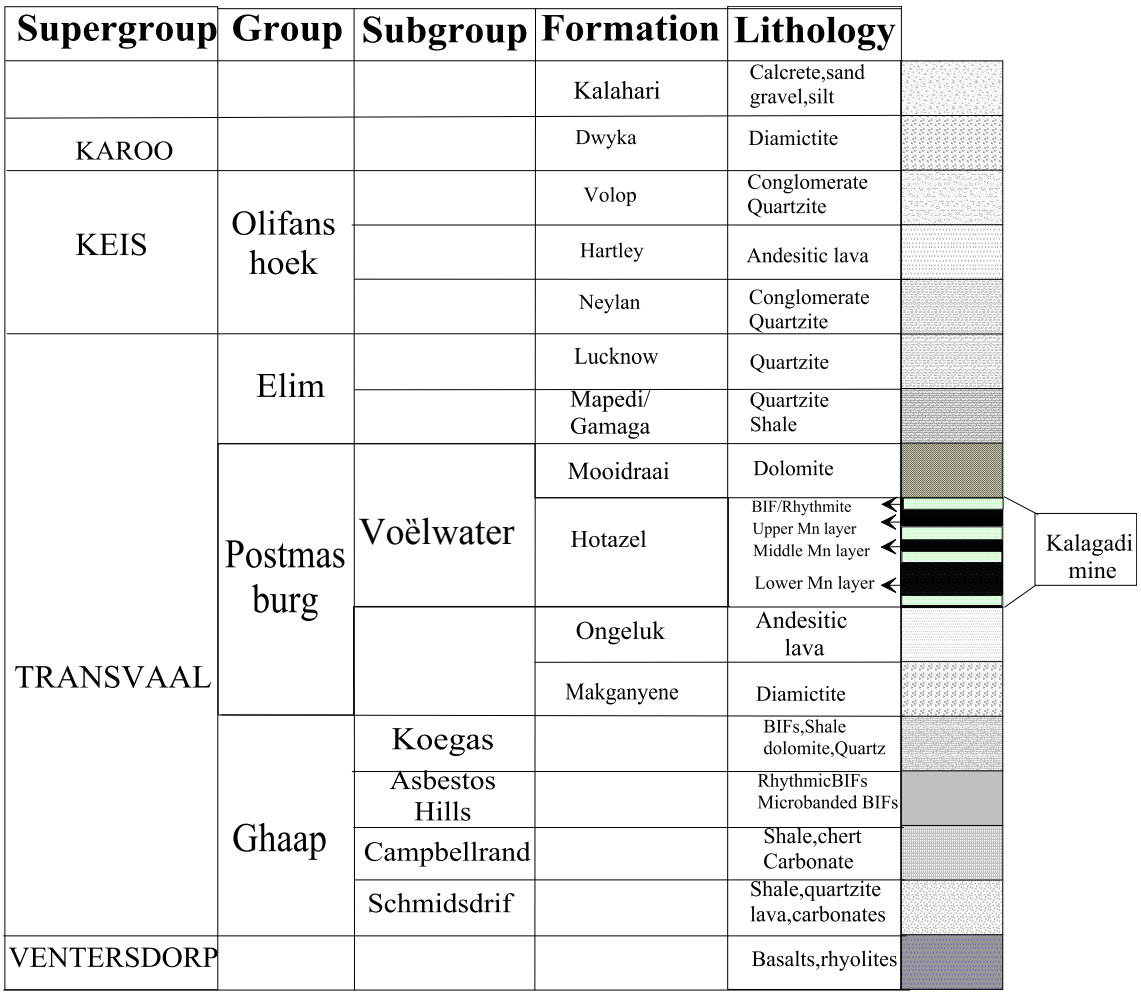

Figure 2.1. Simplified regional stratigraphic column of the Transvaal Supergroup in the Griqualand west sequence showing the location of the Hotazel Formation and Kalagadi mine. Brief description of certain lithological units is from literature sources: Dorland (2004); Van Niekerk (2006); and Polteau et al. (2006)

2.2.2 Metamorphic and Hydrothermal activity

The mine lease surface area shows no clearly visible structures to define the geology except for the flat lying, wavy features of the topography. The geological information therefore relied on material obtained from exploratory drilling.

The deposit is slightly faulted and the orebody is displaced to various levels. The hanging wall includes an alternation of BIFs with upper and middle manganese orebodies while the footwall comprises of a thin layer of iron formation and basaltic lava further below. The manganese ores at Kalagadi Manganese Mine are of diagenetic to early metarmophism with slight hydrothermally fluids mixed of meterioc water responsible during their formation.

There is generally no observable severe deformation and metamorphism defined in the entire Kalahari deposit except for the hydrothermal Wessel event recorded by Gutzmer and Beukes (1995) which is restricted to the faulted northern part, an area affected by east-verging thrust duplication and north-northeast-trending normal faulting (Tsikos et al., 2003).

The thrust fault (Figure 1.2-B) is thought to have acted as a channel-pathway for hydrothermal fluids, which precipitated manganese ores and altered the rocks, which they passed through (Gutzmer and Beukes, 1995). The economic manganese zones of the LMO at Kalagadi mine ranges in grade from 30% to 44% Mn and alternate with reddish to brownish-red hematite-lutite and reddish to greenish tinted BIF. The Hotazel Formation forms part of the Voëlwater Subgroup in the Postmasburg Group of the early Proterozic (2.7-2.2Ga) Transvaal Supergroup.

The Kalagadi mine is located in the southern central part of the Kalahari deposit and the manganese ore units are of low grade, carbonate-rich sedimentary Mamatwan-Type ore. Mineralization is restricted to the Hotazel Formation at an average depth of 250m above the Ongeluk Formation. The ore is black, shiny and metallic, with often white, brown to pinkish oxide or carbonate rich ovoids, lenticles and laminae. Apart from that, the ore displays various degrees of banding, laminations and subvertical natural fractures with carbonate infill contributing to some veining.

The top and bottom of the orebody is mostly capped by magnetic greenish or reddish tinted BIF and hematite-lutite. The dip of the orebody is towards the west at about 8^{o} to 10^{o} and the thickness of the Hotazel Formation (Mn ores and BIF) varies from 30m to 125m, preserving much of the normal stratigraphic sequence. This variation in thickness is attributed to the erosion below the Dwyka unconformity and rapid change of original thickness.

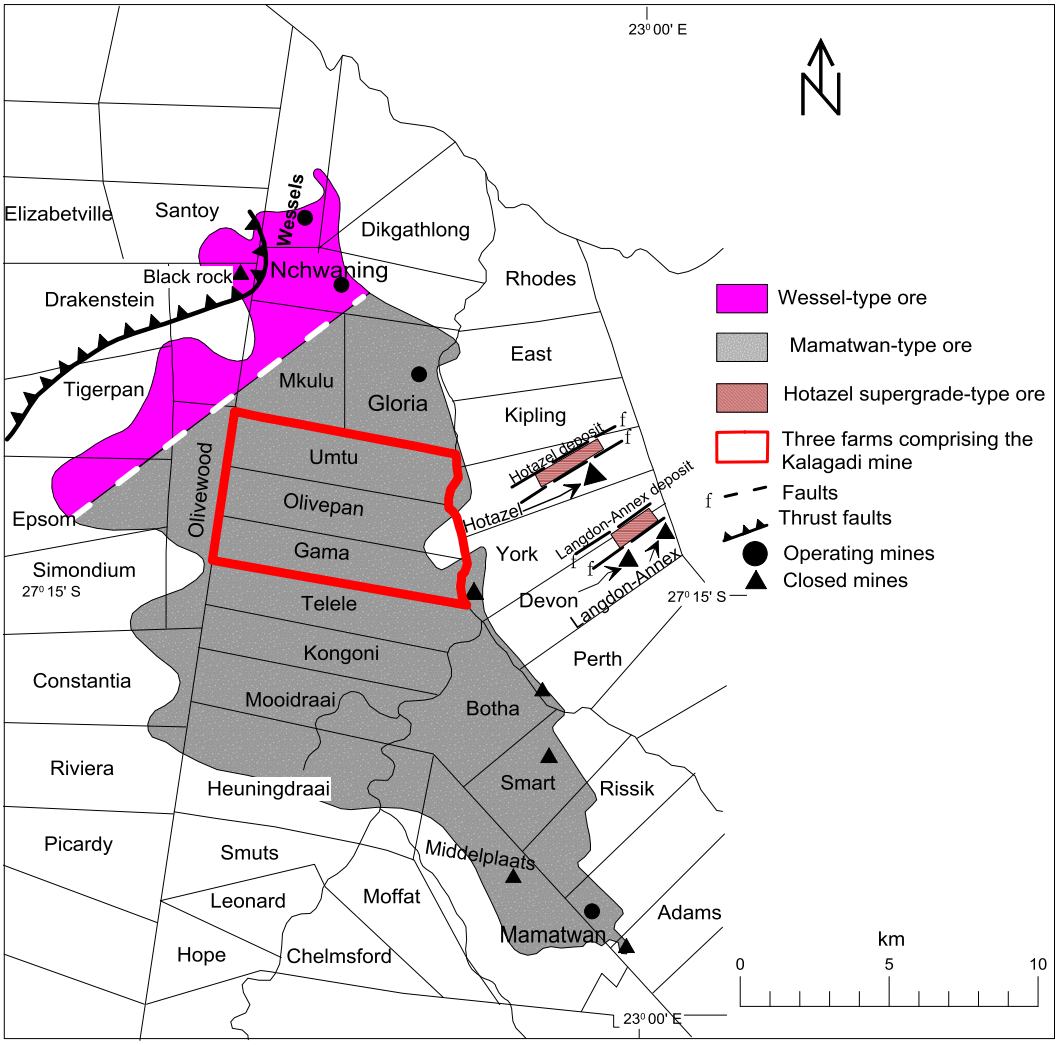

Figure 2.2 Map of the Kalahari Manganese Field showing the location of the Kalagadi Manganese mine lease area (incorporates Umtu, Olivepan and Gama farms), some of the closed mines and those that are currently operating in the Kalahari deposit (Wessels and Mamatwan-Type ore), Hotazel and Langdon-Annex deposit (modified after Asrupt and Tsikos, 1998).

2.3 Methodologies

Fieldwork was conducted on different occasions over a total period of four weeks and it included mostly logging of selected borehole material and observations during drilling programs. On the last field visit, about sixty boreholes had been drilled on the mine lease area with an additional six being drilled as the part of phase two drilling program. This provided an opportunity to observe during drilling, to work with unweathered material and also log the entire section of borehole material, from the softer Kalahari Formation to the top of the Ongeluk Formation.

The fieldwork including detailed borehole logging, cutting and identification of various zones of the LMO was conducted with the help of a geologist and technical assistants on site. The map with borehole localities was used in the selection of the boreholes of interest. Preliminary investigations and previously logged borehole information on the area was made available. The information obtained from borehole logging was then used to create graphic logs, subsurface and underground cross-sections in order to obtain two and three-dimensional perspectives of the mine lease and also to ascertain any presence of structural features that may create a problem during mining.

Nineteen orientated borehole drill cores were selected and logged in detail with the focus being on macroscopically recognizable features within the manganese ore body. The logged drill cores were chosen to represent those located near and those located away from faults. The aim of such selection was specifically to ascertain the influence of faulting on the quality and grade of the ore. The logged boreholes from east-west transverse are (19): SKR03, SKR04, SKR 31, SKR 05, SKR 40, SKR 17, SKR 08, SKR09, SKR 10, SKR 15, SKR 18, SKR 16, SKR 19, SKR 27, SKR 14, SKR 20, SKR 31, SKR 26 and SKR 65. The macroscopic field observations were tentatively used to subdivide the LMO into various zones guided by existing lithostratigraphic subdivisions analysed by Nel et al. (1986) and Preston (2001) at Mamatwan and van Staden (2002) at Gloria mine. Samples

representing specific zones in each drill core were carefully selected, marked, halved, washed and dried in direct sunlight in order to perform detailed laboratory analyses and further characterize the various zones, chemically and mineralogically.

The representative samples of both drill cores were left behind in the Kalagadi mine shed as required. Percussion equipment was used to drill through the softer Kalahari cover (0 to 130m) to the underlying Dwyka diamictite (130m to 220m). Diamond core drilling was then used to drill through dolomites of the Mooidraai Formation (220m to 230m), BIF and manganese-bearing lutites (about 230m to 250m) of the Hotazel Formation to the beginning of the Ongeluk lava (at depth of about 250m). Microsoft office package together with the following softwares were used to plot and create graphic logs: Surfer 10 and Grapher 8 were used to plot surface and underground 2D and 3 D graphical representation of the mine lease area based on borehole information. Graphic and borehole logs were created using Starter 2 plotting software package.

2.4 Results

2.4.1 Field work

The borehole material observations revealed differences in thickness of the three Manganese orebodies with the economic Lower orebody ranging from 15m to 25m. The uneconomic Middle and Upper orebodies attained a maximum of 4m and 14m respectively. The entire mine lease area is covered by 60m to 160m thick Tertiary Kalahari Group rocks comprising sand, clay, silt, shale, gravel and calcrete. The lithology encountered below is the 20m to 130m thick grey to dark gray poorly sorted diamictites of the clastic glacial Dwyka Group containing subangular to angular clasts of lava, rhyolites, hyloclastites and jaspilites as an indication of erosion of the underlying lithologies.

In certain areas the Dwyka Group is underlain by the greyish purple to pink banded, Fe-rich dolomites of the Mooidraai Formation belonging to the Voëlwater Subgroup in the Postmasburg group (SKR 40 in Figure 2.7). The Mooidraai Formation is characterized by white cherty and slightly reddish pure fragmented dolomites and it attains a maximum thickness of 100m (SKR 26 in Figure 2.7).

The Mooidraai Formation towards the base is magnetic with massive bands and this is attributed to grading of the sequence into a greenish to reddish BIF belonging to the Hotazel Formation. The BIF grades into manganese ores, which comprise red hematite-lutite, reddish-brown jacobsite-lutite and shiny black braunite-lutite. The alternating BIF and manganese (Mn) ores together constitute the Hotazel Formation and attain a maximum thickness of 125m. Apart from alternations of BIF and Mn ores, drill core material also revealed evidence of Hotazel Formation cyclic character (Banded Iron Formation ↔ Hematite lutite ↔ braunite lutite). In areas where the full Hotazel sequence is preserved, the low grade (18% to 25% Mn) Upper Mn orebody (Jennings, 1986)), poorly mineralized Middle Mn orebody and economic Lower Mn orebody were intersected.

The Upper Mn orebody at Kalagadi mine ranges in thickness from 5m to 20m, while the Middle layer ranges from 1m to 4m. Below the middle Mn layer is a thin layer comprising BIF and hematite lutite. The layer of BIF alternating with hematite-lutite and upper and middle Mn ore layers together comprise the base of the hanging wall. The Lower Mn layer ranges from 15m to 20m and represents the mineable and economic orebody. The orebody below is capped by hematite lutite, magnetic BIF and volcanic lava of the Ongeluk Formation and together they constitute the footwall. The Ongeluk lava below the Hotazel Formation is often intersected from 200m except on rare cases where it was intersected at 100m.

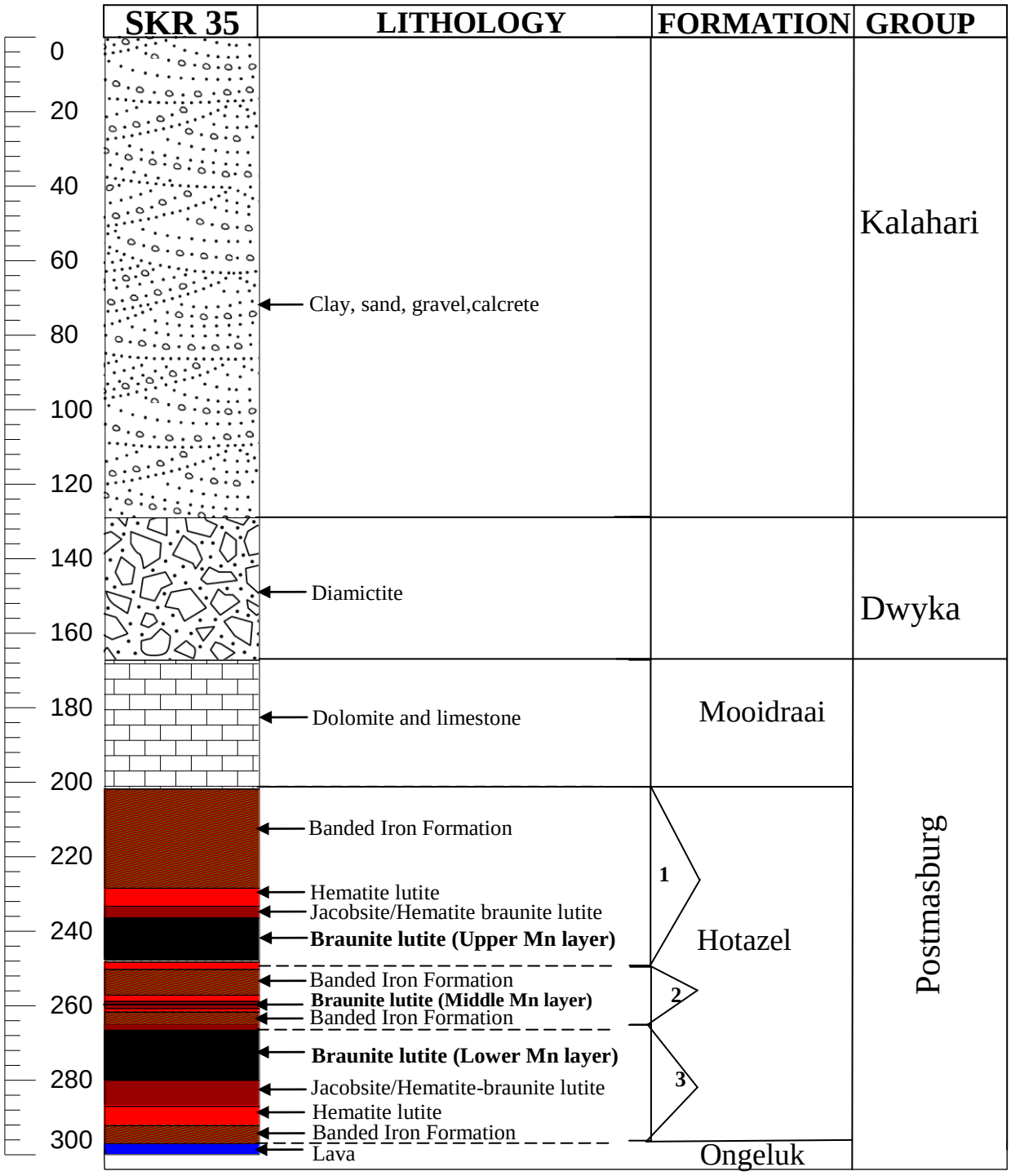

Figure 2.3 Borehole SKR35 at Kalagadi Manganese mine showing the stratigraphic location of the Hotazel Formation's cyclic character (1, 2 and 3) and the complete stratigraphy in the mine lease area. The middle Mn layer is less developed throughout the mine lease area while the upper Mn layer is poorly mineralized.

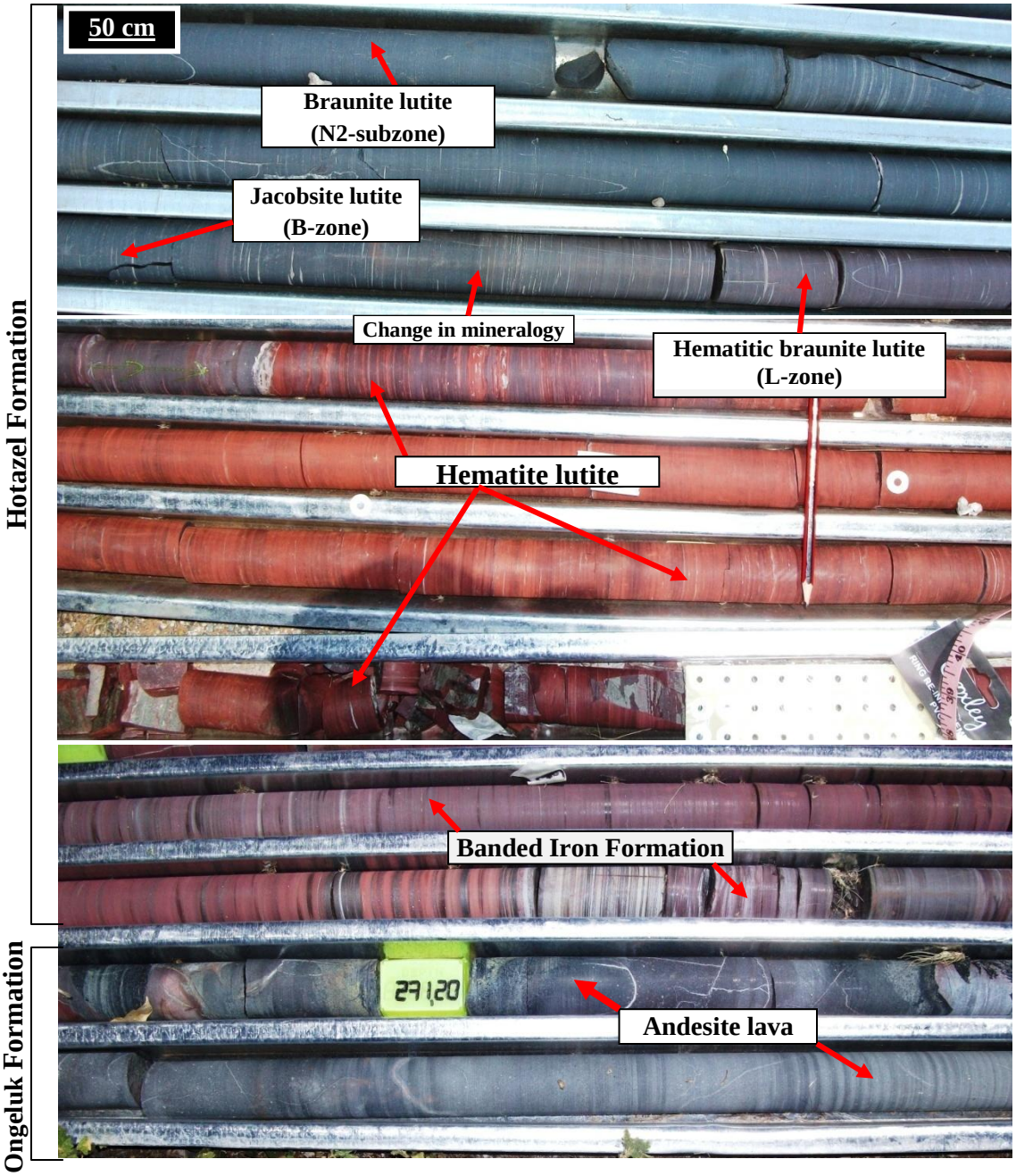

Figure 2.4 Drill cores showing the bottom section of the Lower manganese orebody. From the bottom is the grayish lava with white carbonate bands of the Ongeluk Formation grading upwards into a greenish to: brownish-red rhythmic Banded Iron Formation (BIF) – reddish pink hematite lutite (O-zone) – brown to black jacobsitic braunite lutite (B-zone) and black braunite lutite (N2-subzone).

2.4.2 Orebody and borehole correlation

Lithology and graphical logs were created to give a visual impression of the entire stratigraphic section across the mine lease area, depth localities and continuity of mineralization (orebody), and to delineate and confirm any evidence of structural features that may have been intersected during the drilling. Forty-four boreholes drilled across the mine lease area are plotted to create a graphical representation (Figure 2.6) of the mine lease area and the depth variation of borehole. The evidence from drilling material and geophysical analysis have delineated the presence of at least six normal faults, three striking in the SW-NW and other three in the SE – NE direction with a suspected dyke running across the SW – NW direction of the main shaft (Kalahari Resources, 2008).

The manganese ores are characterized by lenticular zones of hydrothermal alteration, fractures filled with carbonates and displaying various degrees of banding and scattered ovoids throughout. The Lower Manganese Oreboby is well developed and is capped by ferruginized zones at the top and bottom. The orebody varies from 12m to 20m in thickness and widens laterally across the mine lease area unless it is displaced by faulting. Economic mineralization is represented by braunite-lutite (sometimes referred to as manganolutite) and the shiny metallic appearance of the ore is attributed to the presence of hausmannite. The high-grade ores are mostly concentrated in the center of the mine lease and decrease sideways towards the farm boundary.

The two boreholes SKR 40 and SKR 65 highlighted in Figure 2.5 were selected for detailed analytical and petrographic studies. The SKR 40 is located away from structural features and hence no evidence of either faulting or erosion was found below the Dwyka unconformity. The complete

sequence of the Hotazel Formation is well preserved at SKR40 and the economic lowermost manganese orebody attains a maximum thickness of 23m and is restricted to a depth between 292m and 315m. The Mooidraai Formation below the Dwyka unconformity forms a thin layer of about 3m. The SKR 65 differs from SKR 40 in that it is faulted and eroded. Glacial processes have eroded the middle and upper Mn layers forming part of the Hotazel sequence together with overlying lithologies of the Mooidraai formation during deposition of Dykwa Group (Figure 2.7).

The lowermost manganese orebody at SKR 65 is restricted to 246m and 266m and attains a maximum thickness of 20m. The mineralogical and chemical comparison between the two boreholes is discussed in chapter three and four separately. The stratigraphic variation across the mine lease area is consistent except for the displacement of the orebody by a series of normal faults that cut across the mine lease in the SW-NE direction to the SE-NW direction. The EW profiles show gentle dipping of the orebody to the west in both the northern and southern portion of the main shaft.

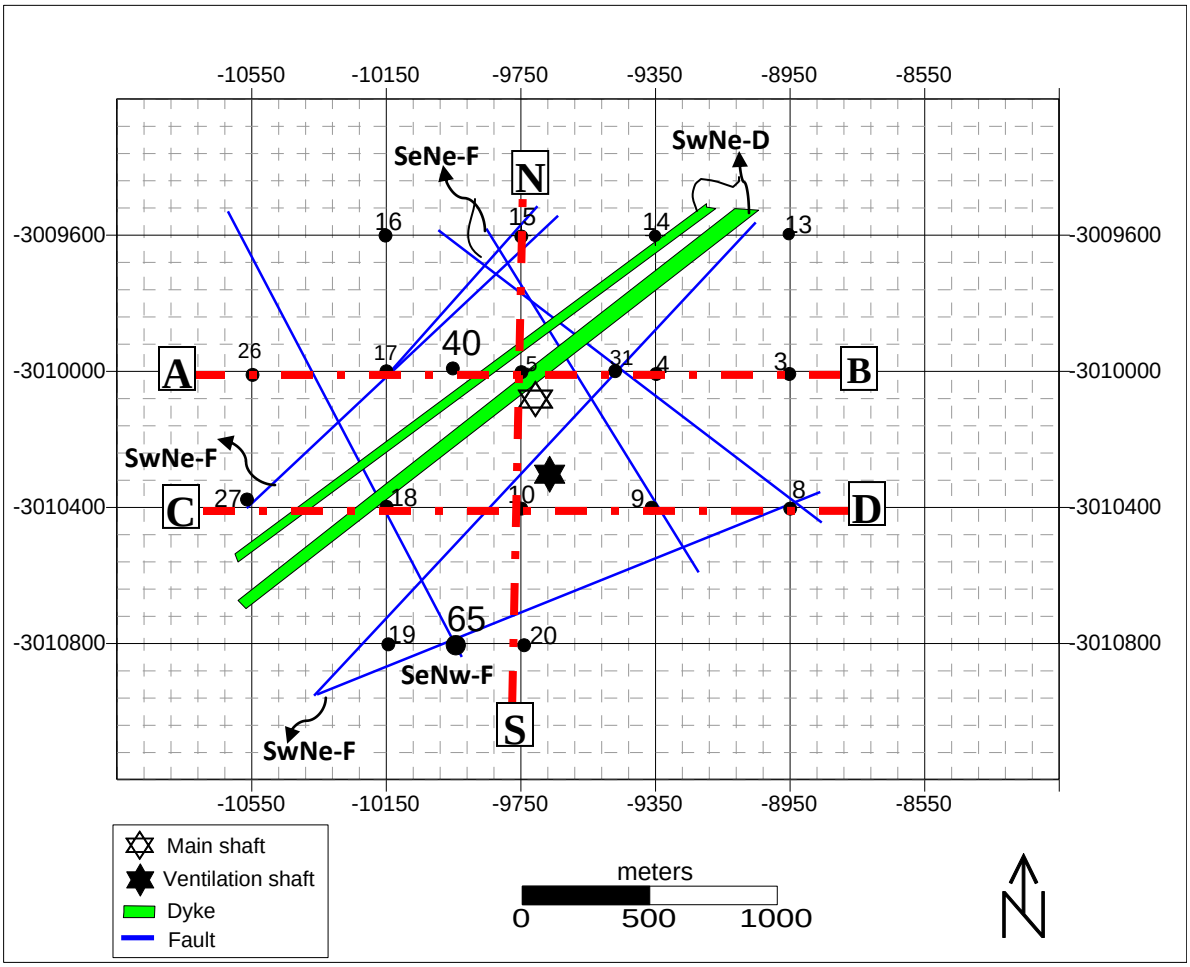

Figure 2.5. Map showing the localities of logged boreholes represented by their numbers. The borehole SKR 65 and SKR 40 highlighted in bold were selected for detailed laboratory analyses. Also shown are series of normal faults (F) striking in the South West – North East (SwNe-F) and South East – North West (SeNw-F) direction as well as suspected dykes (D) running across the SW-NE direction as evident on earlier geophysical investigations at the Umtu farm lease area (modified from Kalahari Resources, 2008). Dotted line **A-B** represents cross section shown in for Figure 2.9 and 2.10, **C–D** represented in Figure 2.11 and 2.12 and **S – N** for Figure 2.13

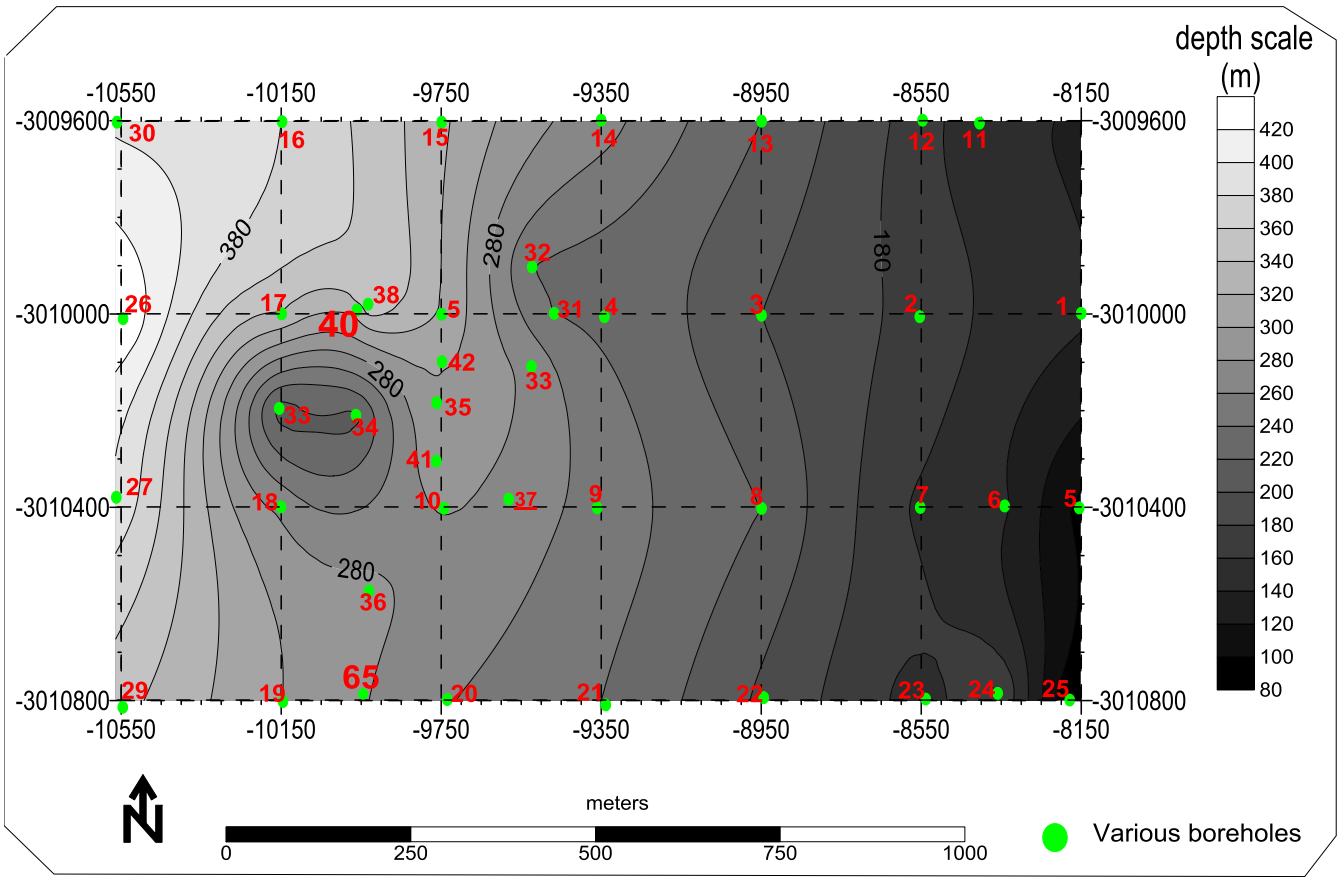

Figure 2.6. Contour map showing depth variation of boreholes drilled on the study area (Umtu farm). Note the low lying areas (depression/basin) displayed by various boreholes and the general increase in thickness from east to west causing the orebody to be displaced to deeper levels. Borehole coordinates data supplied by Kalahari Resources (2008).

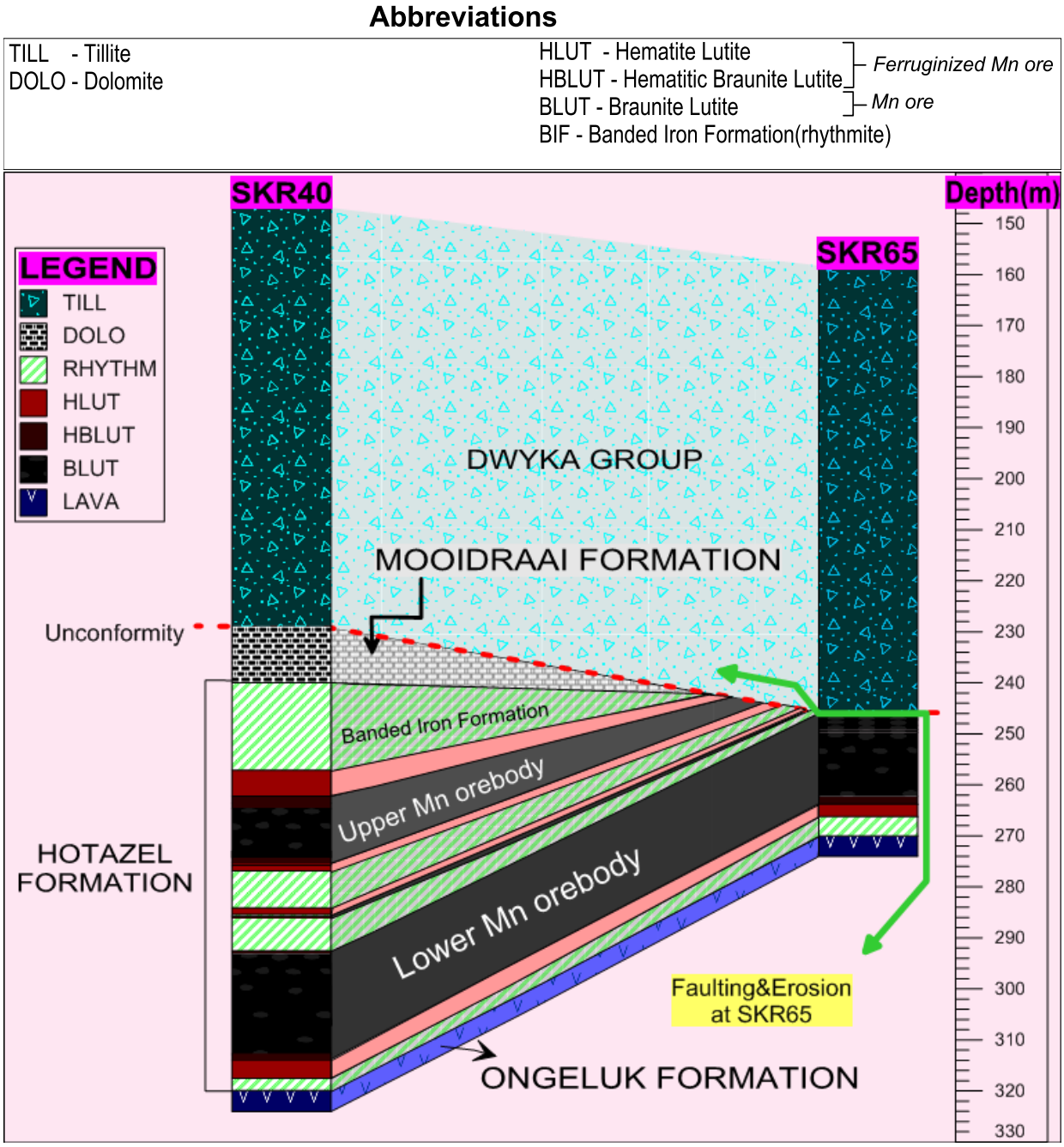

Figure 2.7 Stratigraphic comparison between borehole SKR 40 and SKR 65 selected for detailed study. The general stratigraphic sequence in the mine lease area is shown by SKR 40 while in SKR 65 the Mooidraai Formation together with BIF, Upper, Middle and uppermost zone of the Lower Manganese Orebody has been eroded prior deposition of Dwyka Group.

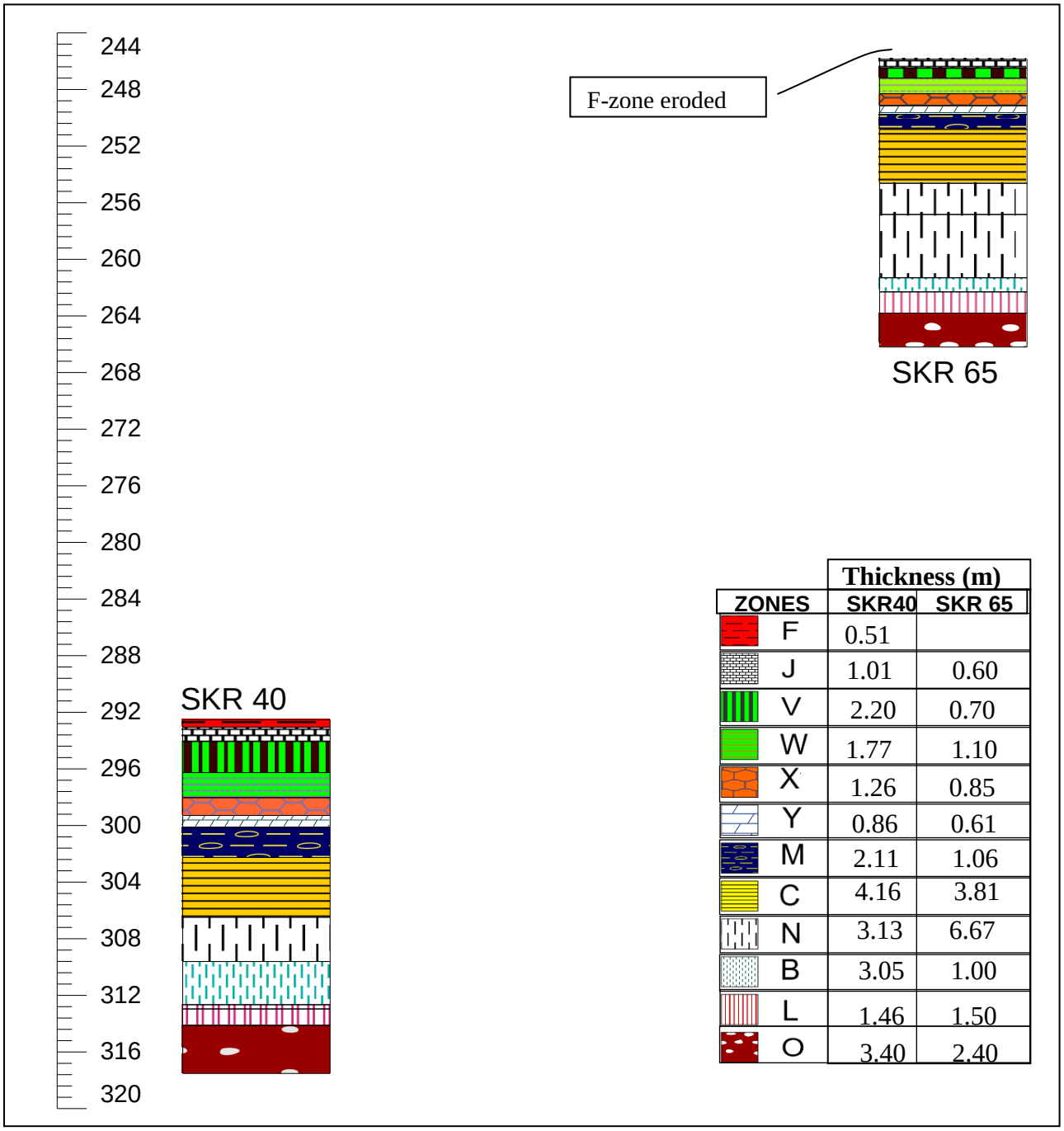

ZONES	Thickness (m) SKR40	SKR 65
F	0.51	
J	1.01	0.60
V	2.20	0.70
W	1.77	1.10
X	1.26	0.85
Y	0.86	0.61
M	2.11	1.06
C	4.16	3.81
N	3.13	6.67
B	3.05	1.00
L	1.46	1.50
O	3.40	2.40

Figure 2.8. Comparisons of various zones at borehole SKR 40 and SKR 65.

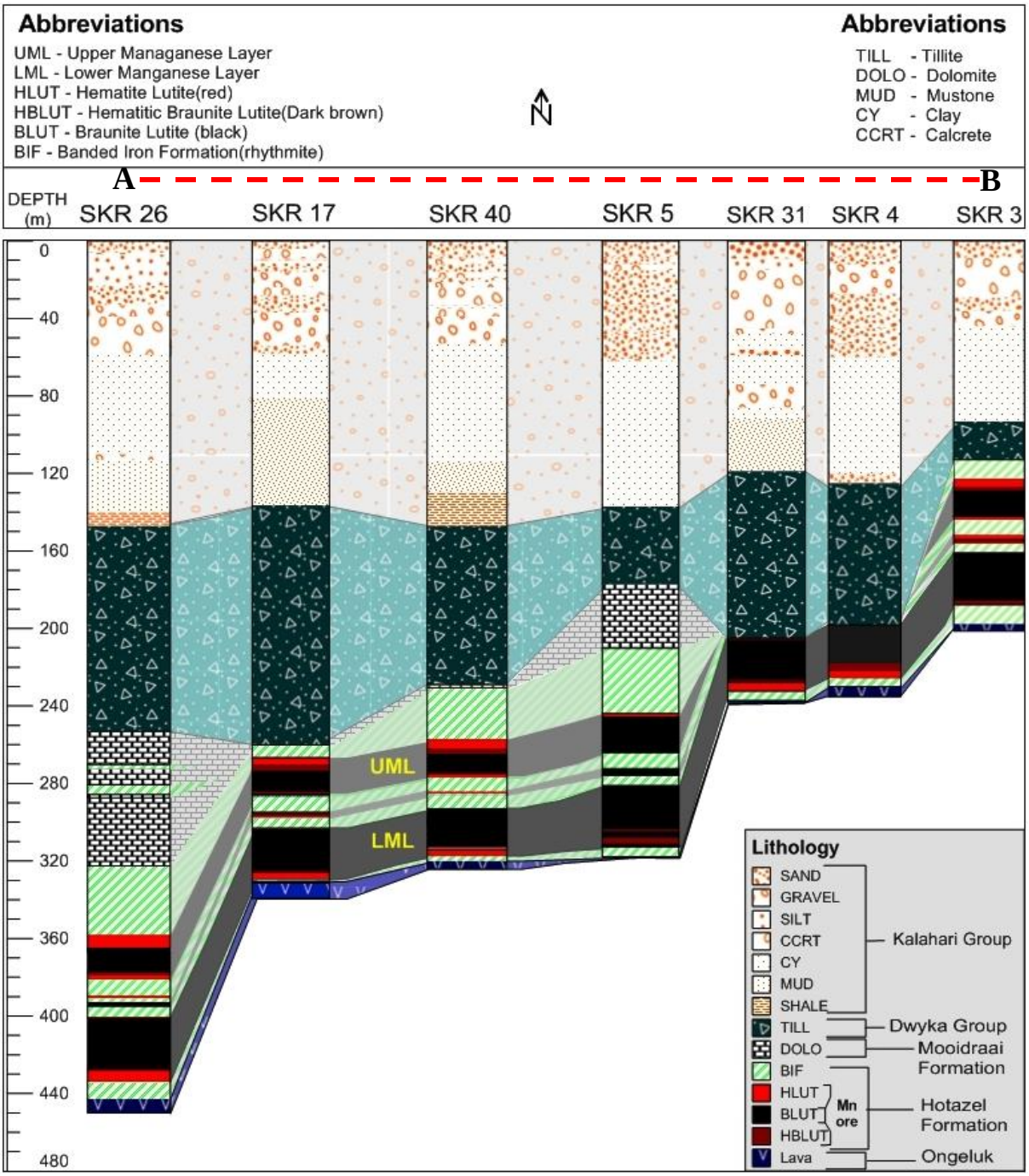

Figure 2.9 East- west (A-B) profile showing depth correlation of various drill core logs selected from the northern section of the main shaft. Faulting and erosion if observable on certain boreholes and that has resulted to the orebody displaced even on deeper levels.

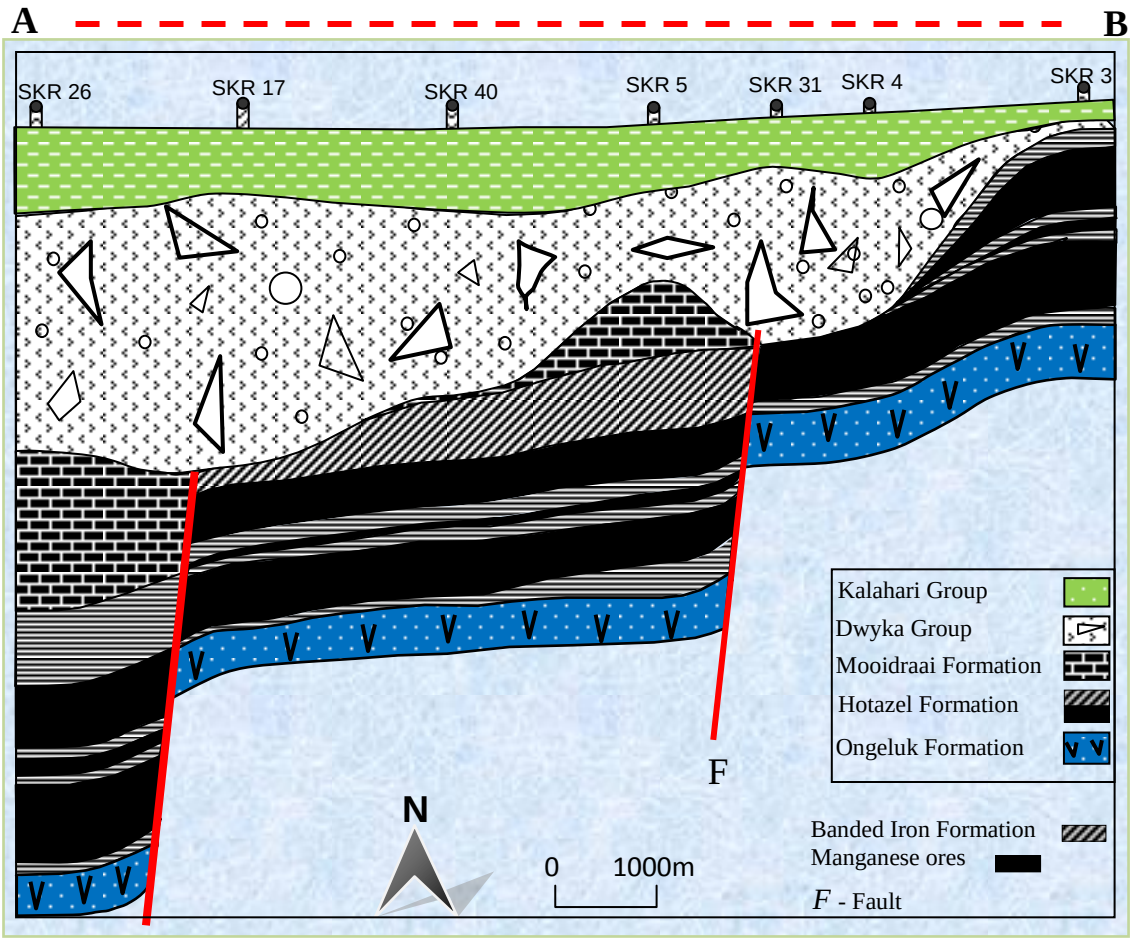

Figure 2.10. East- west (A-B) cross-section showing depth correlation of drill core logs, north of the main shaft. Note the evidence of erosion at borehole SKR 31 and SKR 4 below the Dwyka unconformity where the underlying lithologies has been eroded except the only lowermost orebody. Also, note the displacement of section due to the two normal faults striking in the SW-NW direction and dipping of the orebody at about 10° to the west. The displacement of the orebody ranges from 90m in the eastern portion of the mine lease to 100m in the eastern portion.

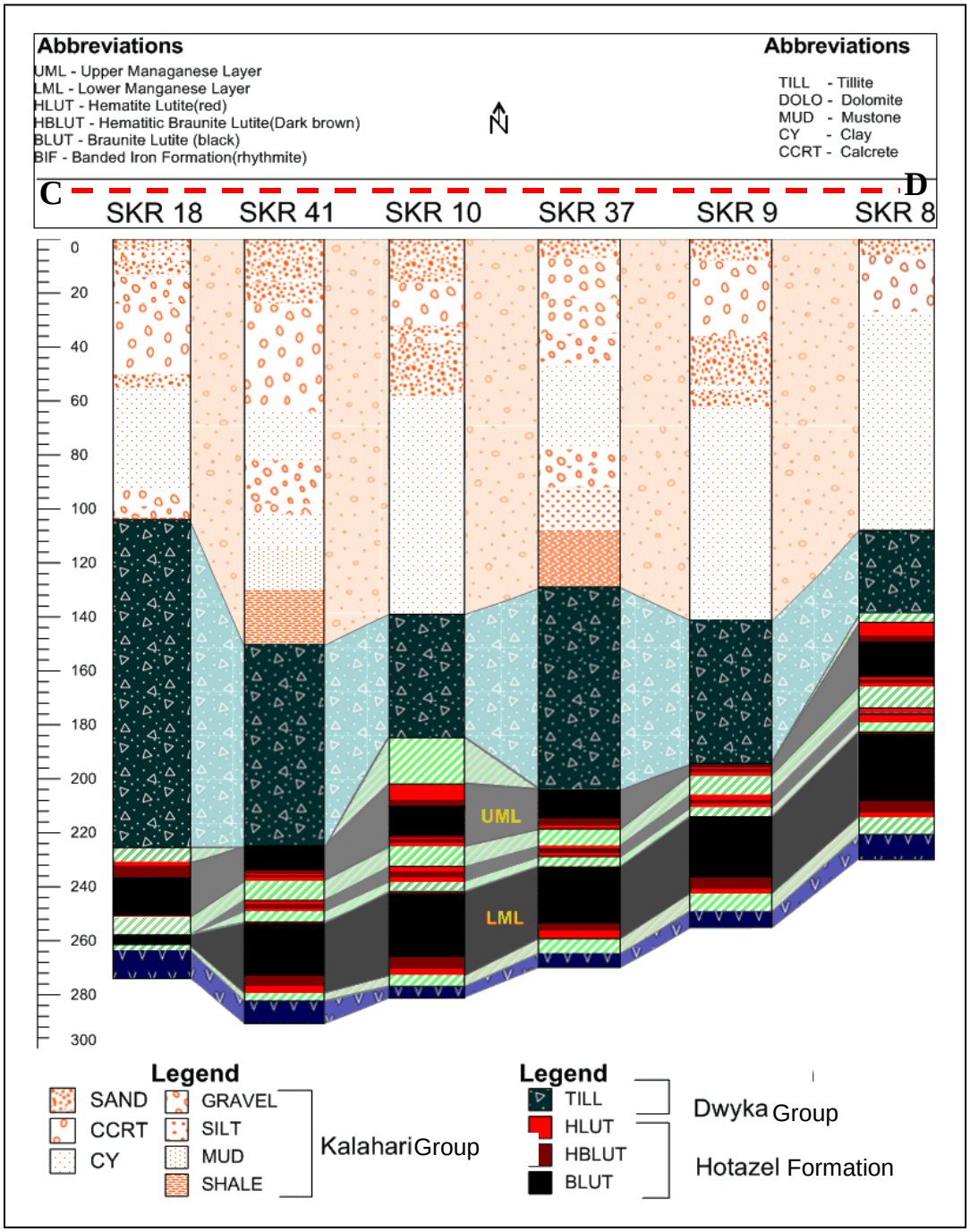

Figure 2.11. East- west profile showing depth correlation of various drill core logs from the southern parts of the main shaft. The orebody is gentle dipping to the west and the Mooidraai Formation has been eroded.

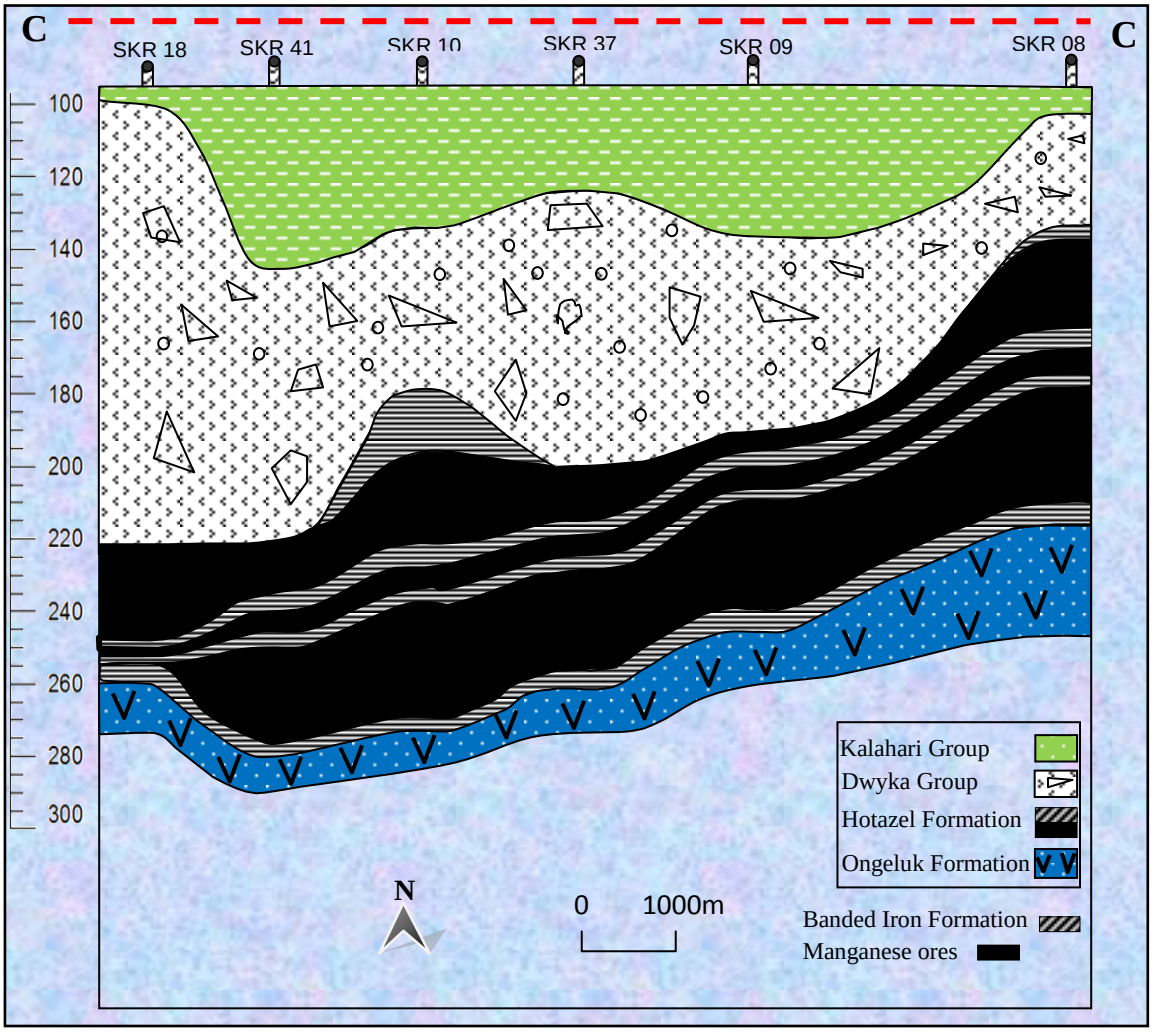

Figure 2.12. East- west cross-section showing depth correlation of drill core logs from the southern part of the main shaft. The orebody dip gentle to the west with no evidence of faulting except erosion below the Dwyka Group.

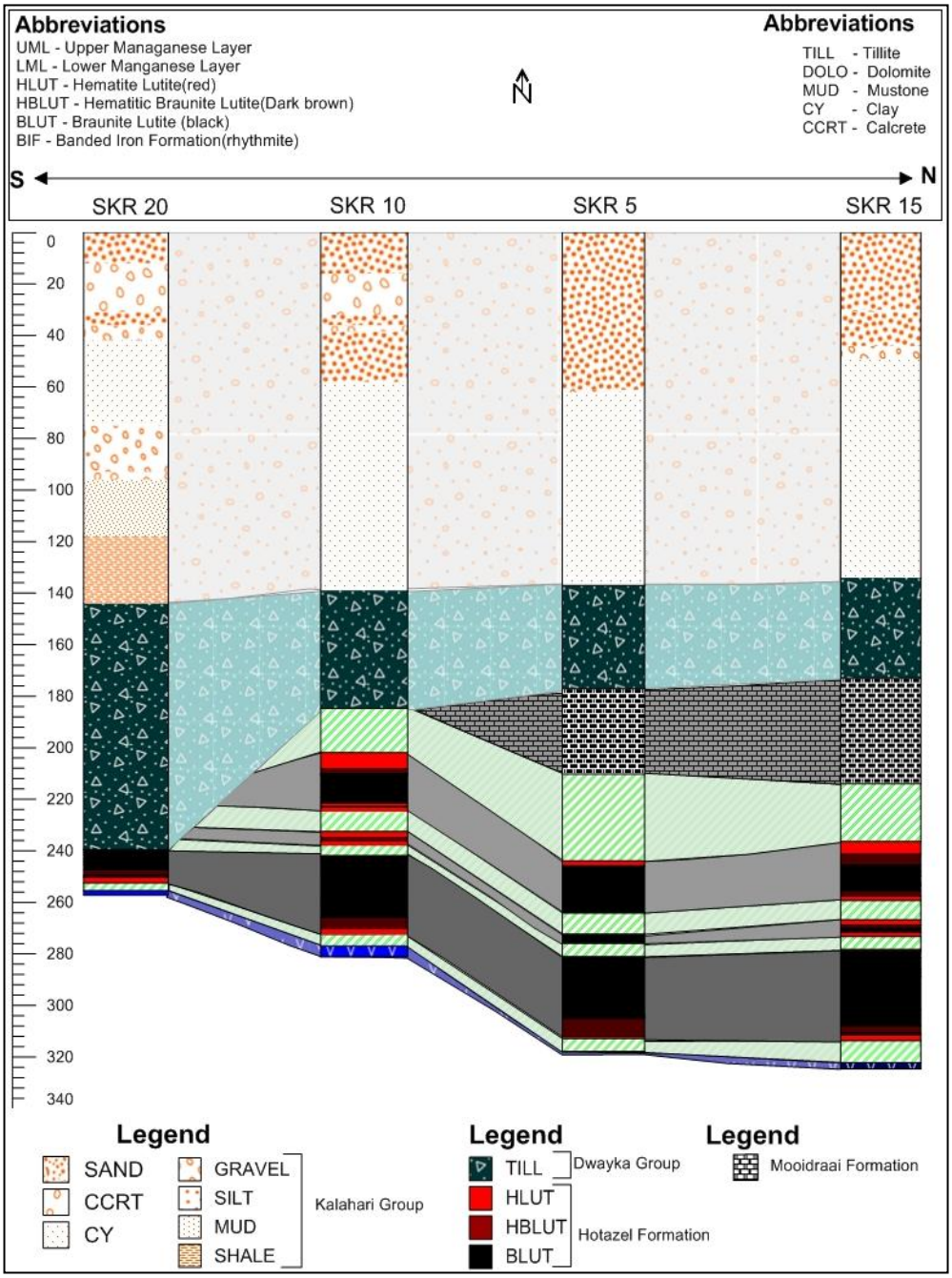

Figure 2.13. North- south profile showing depth correlation of various borehole logs in the mine lease area. The general stratigraphic thickness decreases towards the south and the Mooidraai Formation and upper portions of the Hotazel Formation below Dwyka unconformity are eroded.

2.4.3 Lithostratigraphic zones

The lithostratigraphic zonation is a method of subdividing the orebody into various zones focusing on various parameters such as grade, observable physical, mineralogical and chemical characteristics of the ore in order to determine the mineable zones.

The Lower Manganese Orebody at Kalagadi mine attains a maximum thickness of 20m, almost half that of Mamatwan mine which is 45m and 5m thicker than that of Gloria (15m). The macroscopic field description of lithostratigraphic zones at Kalagadi mine is based mainly on the observable minerals, physical properties of the ore such as colour, lustre, occurrence and abundance of ovoids, lenticles (stretched ovoids) and laminations.

Macroscopic description of various zones based on texture is difficult due to similarity of manganese ore in hand specimen and is described microscopically. The ovoids, lenticles and laminations observed either are filled by oxides (white) or carbonate (brown, light grey) minerals.

The LMO is subdivided and described according to the previous lithostratigraphic studies conducted and published in Nel et al. (1986) and Preston (2001) at Mamatwan mine located to the south, approximately 20km and by van Staden (2002) at Gloria Mine located north-east, approximately 10km from the Kalagadi mine lease area. A total of 20 sample aliquots representing various zones in both drill core SKR 40 and SKR 65 were analyzed petrographically, mineralogically and chemically to further characterize and compare between different zones.

The orebody at Kalagadi mine is subdivided into eleven distinct zones excluding the transition zone and such zones are summarized in Figure 2.14.

Av.Thicknes (m)	Zone		Av. MnO (wt%)	Description	
				Banded Iron Formation	
0.6		F	0.16*	Red to brownish red hematite - lutite with small white carbonate ovoids and fine laminae.	UPPER LOW GRADE ZONES
1.1		J	10.63*	Brownish grey jacobsitic braunite- lutite with abundant small and few medium-sized brownish-white carbonate ovoids and laminations.	
1.6		V	40.03	Banded braunite-lutite with small and large brown-rimmed white ovoids forming a "bird-eye" appearance.	
1.2		W	36.60*	Laminated braunite - lutite containing dominant irregularly and spherical shaped brown carbonate ovoids and lenticles widely scattered throughout.	
2.1		X	40.12	Banded braunite-lutite with carbonate ovoids of various sizes. The ovoids are small, widely scattered at the top and closely spaced towards the base.	
2.4		Y	42.00	Braunite-lutite containing white and abundant brown laminae, thick lenticles and small, amalgamated oxide rich ovoids.	ECONOMIC HIGHER GRADE ZONES
4.3		M	59.04	Massively textured braunite-lutite displaying a black metallic appearance, ellipsoidal and irregularly shaped brownish-white oxide dominated and irregulary shaped ovoids of various sizes (0.25 - 1 mm). The ovoids are partially altered.	
3.3		C	44.15	Dark-grey, dusty, massively banded braunite-lutite containing white and brownish white oxidized ovoids and thin laminae. The ovoids are dense and small at the top and are massively banded with white carbonate bands and medium sized ovoids towards the base.	
3.4		N1	49.92	Massively banded braunite-lutite with abundant small to medium size oxidized ovoids, and laminae and thick white lenticles. Ovoids and laminae are partially filled by hausmannite and braunite.	
3.2		N2	47.80	Braunite-lutite containing slightly scattered small to medium-sized (0.1 to 1.8mm) white oxide-rich ovoids and laminae. The ovoids display various degree of alteration and oxidation, either partially or completely.	
2.0		B	31.20	Laminated brownish-black jacobsitic braunite-lutite containing white and brown carbonate ovoids, laminae and well developed brownish-white lenticles.	BASAL LOW GRADE ZONES
2.8		L	13.96*	Brownish- red hematite-lutite with small widely scattered pink and white carbonate ovoids, thick pinkish white lenticles and thin white carbonate laminae. This zone shows a rhythmic appearance and is magnetic towards the base.	
	H H	O	–	Reddish pink hematite lutite with white and purple carbonate laminae	

Figure 2.14 Lithostratigraphic subdivision of the Lower Manganese Orebody at Kalagadi Manganese mine from the bottom to the top with average grade of MnO (wt%) and brief description of each zone. The * indicates samples that are not averaged due to insufficient sample material. – means not submitted.

The following is the macroscopic lithostratigraphic description of the Lower manganese orebody, from bottom to the top.

The LMO at Kalagadi Manganese mine is underlain by a thin layer of dark-red to greenish tinted magnetic and rhythmic BIF and together constitute the base of the Hotazel Formation. The base of the LMO is characterized by pinkish red hematite-lutite with massive white to grey carbonate laminae and ovoids of various sizes (Figure 2.15-A). Such description are comparable with O-zone (transition bed between LMO and iron formations and Ongeluk lavas), first described at Mamatwan mine.

The transition bed attains a maximum thickness of ±4m at Kalagadi Manganese mine and grades upwards into a brownish red hematite-lutite with pink-rimmed white lenticles, laminae and oblate ovoids of various sizes. Small white ovoids (0.68mm) contribute to the banded appearance of the ore and may attain a maximum thickness of 1.3mm while lenticles may be up to 3cm in size. The above characteristics correspond to **L-zone** also described at Mamatwan mine and Gloria mine.

The L-zone grades upwards into **B-zone** characterized by laminated magnetic brownish-black jacobsite-lutite containing white and brown carbonate ovoids and laminae of various sizes and well developed brownish-white lenticles. The magnetic character of this zone is attributed to the presence of jacobsite mineral in the ore.

The jacobsitic B-zone grades into a massively banded and laminated black metallic braunite-lutite of **N-zone** with small white ovoids and thin laminae. The N-zone at Kalagadi Manganese mine represents the base of the central economic zone and is well developed reaching a maximum

thickness of 6m. The N-zone is further subdivided into **N1** and **N2** subzones based on observed consistency in abundance of ovoids at the top and laminae at the base in almost all the logged boreholes (Figure 2.16-C-E). The **N2**-subzone is a greyish black braunite lutite with predominantly small white ovoids and laminae while the **N1-** subzone is a massively banded, black braunite-lutite with abundant thick white ovoids, laminae and lenticles.

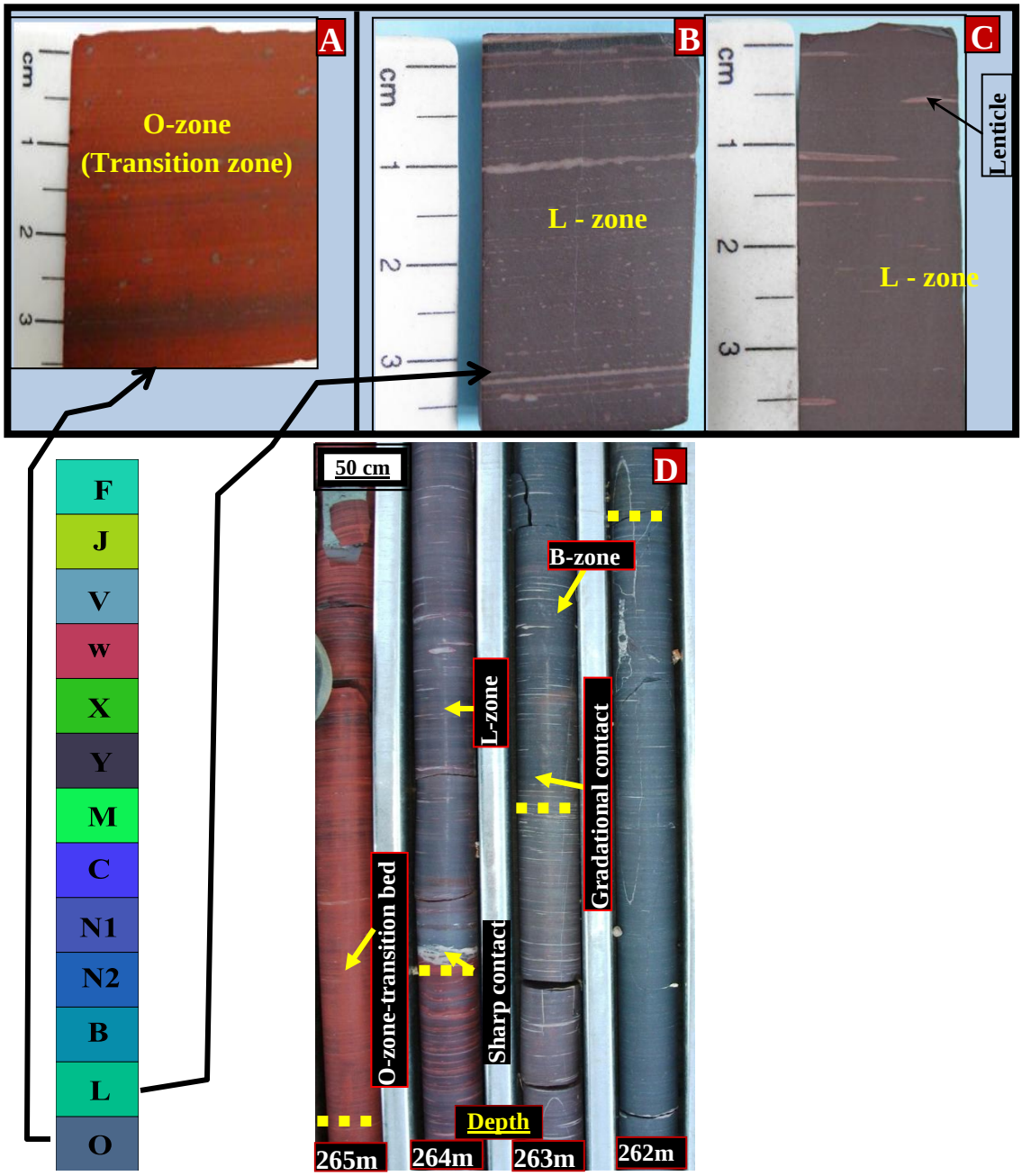

Figure 2.15. **(A)** Reddish-pink O-zone with white and gray laminae and up to 1.3mm size ovoid. **(B and C)** shows purplish red hematitic braunite lutite of L-zone with white to pinkish-white 0.6mm to 1.3mm size ovoids, 4mm to 30mm lenticles and fine laminations**. (D).** Shows borehole specimen in a core tray. Below is a reddish pink hematite lutite (O-zone) grading upwards into brownish red hematitic L-zone. Note the sharp contact from the transitional zone to the L-zone and a gradational contact to B-zone.

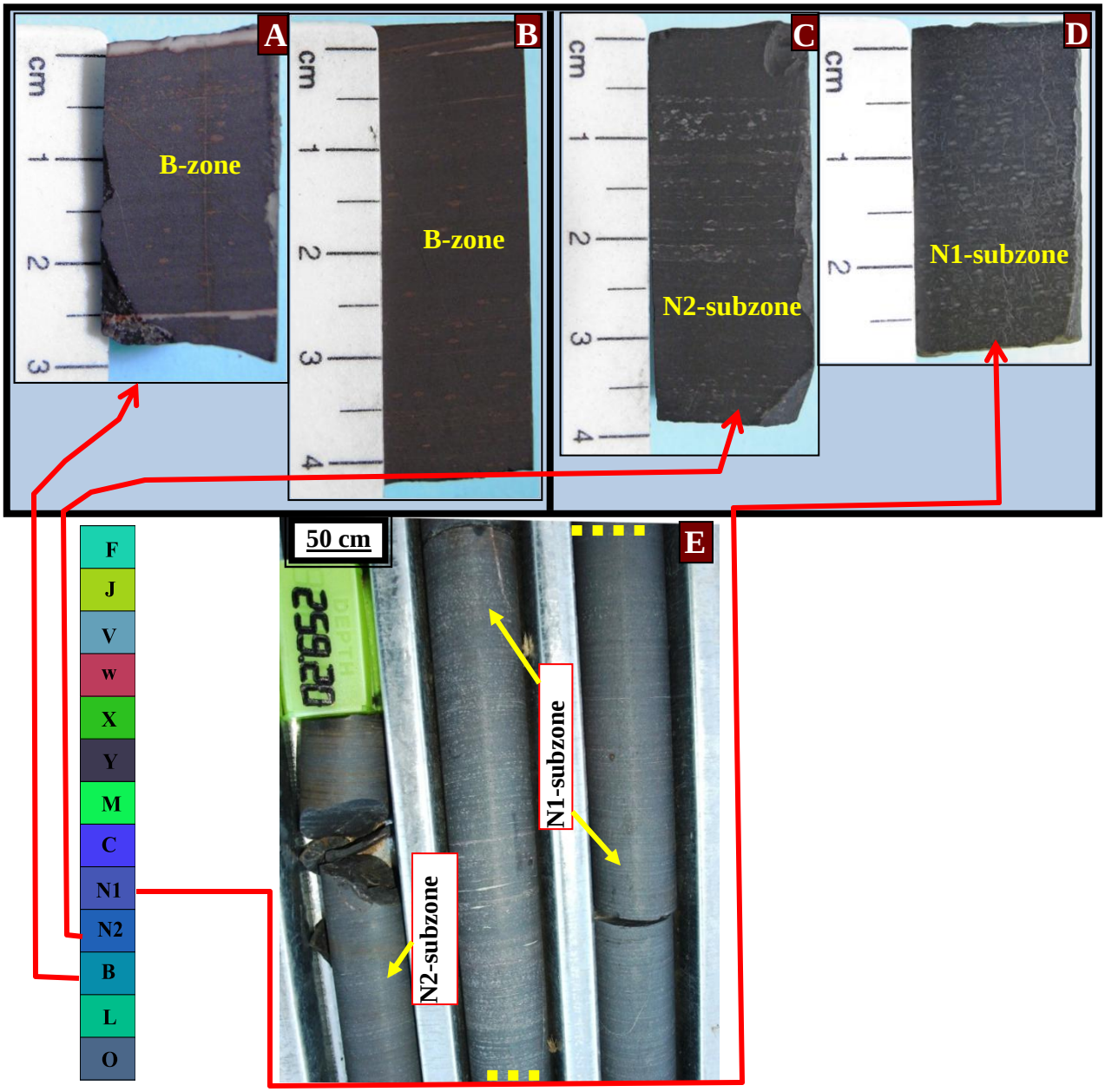

Figure 2.16 (A) - (B). The **B-zone** as observed from the two boreholes characterized by thick pinkish white laminae, brown lenticles and ovoids of various sizes from 0.1-1.800mm)**. (C).** Shows the **N2-subzone** characterized by banded braunite lutite with white laminae and irregularly shaped ovoids ranging in sizes from about 0.07 – 0.75mm). **(D).** Shows a massively banded braunite lutite with thick white carbonate laminae and lenticles of up to 0.9mm (**N1- subzone**). **(E).** Shows typical of N1 and N2 subzones as observed on borehole specimen in a core tray.

The **N1-subzone** grades into **C-zone** a dusty fine laminated braunite-lutite that is characterized by abundant minute white to brown ovoids, lenses and laminae (Figure 2.17). This zone massively banded with brownish black and white thin laminae and white ovoids at the top. The C-zone grades into a metallic and massively textured braunite-lutite with ellipsoidal brownish-white ovoids of various sizes.

The metallic appearance of the ore in most boreholes is attributed to the abundance of hausmannite compared. Such characteristics correspond to **M-zone** as described at Gloria mine. The massively textured braunite-lutite of M-zone at Kalagadi mine gradationally becomes finely laminated at the top with dominant white and brown carbonate laminae and ovoids. The small to medium-sized amalgamated ovoids contribute to some brown laminations.

The merged brown laminae and ovoids provide an ore with a brownish black appearance. This corresponds to **Y-zone** and this zone is not well developed in all the logged boreholes. The zone encountered above Y-zone is characterized by brown abundant, small and closely spaced ovoids at the base contributing to some brown laminations. The small ovoids often alternate with medium-sized ovoids that become widely scattered upwards (Figure 2.18-A and B). Similar descriptions correspond with X-zone.

The **W-zone** is encountered above the X-zone and is characterized by abundant brown and few white closely spaced carbonate ovoids of various sizes contributing to the observed prominent banding and lamination in the ore. The ellipsoidal and irregularly shaped ovoid alternate and they often lend a brownish dark appearance to the ore. The W-zone grades into **V-zone**, a thinly

laminated braunite-lutite with small to medium size and ellipsoidal brownish-white ovoids. The ovoids are white in the core and become brown on the rims lending a “bird-eye” appearance. The V-zone grades into a brownish red jacobsitic hematite - lutite with abundant small and few medium-sized brownish-white carbonate ovoids. Such descriptions correspond with the **J-zone** also described at Gloria mine.

The jacobsitic J-zone grades into F-zone, a dark red hematite - lutite with occasionally concentric medium sized white and widely scattered small carbonate ovoids, fine laminae and bands. The F-zone is the youngest and is either overlain by a layer of BIF, middle Mn layer, and upper Mn layer of the Hotazel Formation, Mooidraai Formation and/or Dwyka Group.

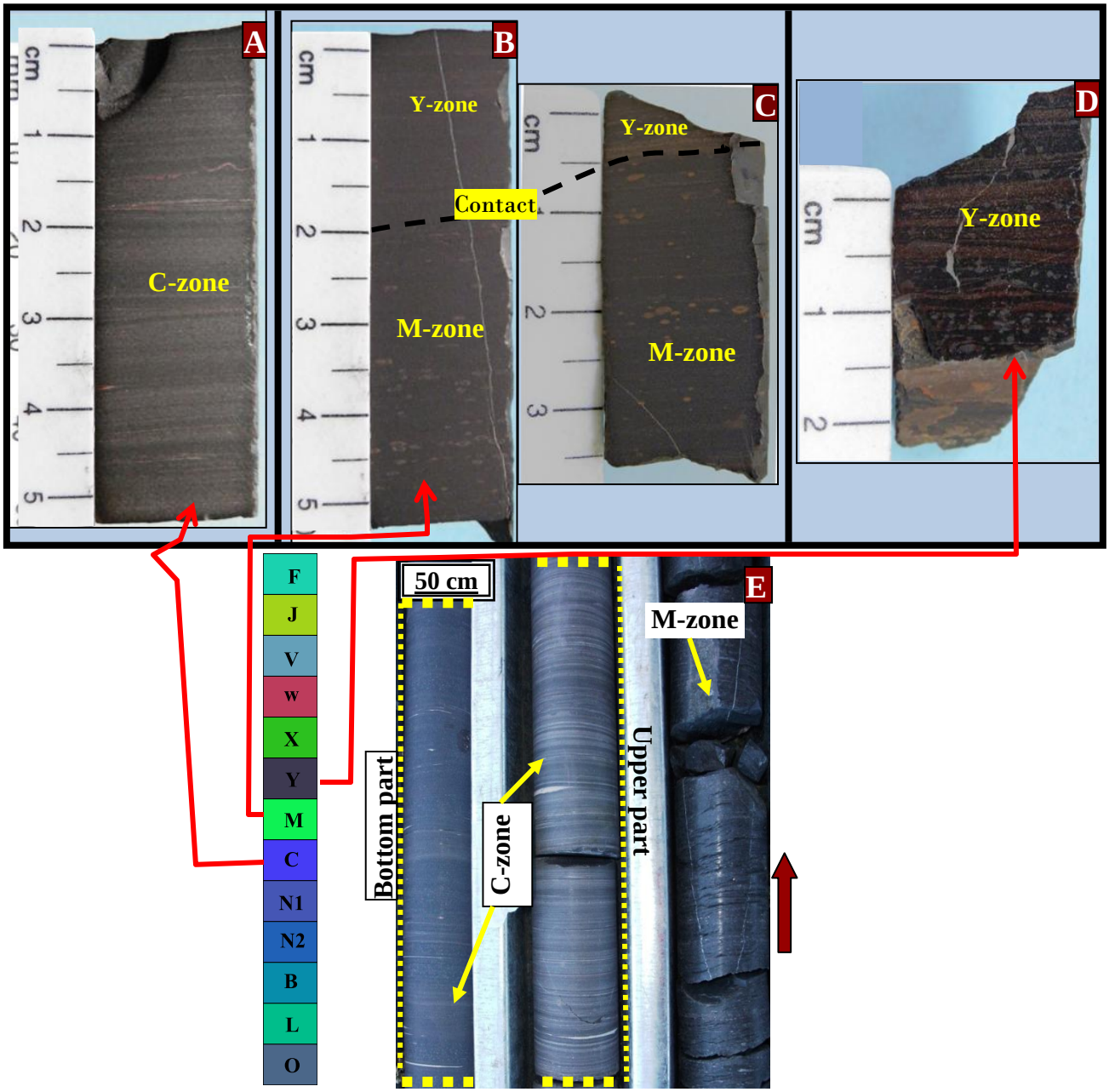

Figure 2.17 (A). C-zone characterized by white and brown massive bands, small ovoids and fine laminae. **(B)** - **(C)**. M-zone (bottom) contains thick brown and grayish-white laminae, lenticles and spheroidal ovoids ranging in size from 0.25mm – 1.6mm and grades into Y-zone (top). **(D)** Polished **Y-zone** characterized by white and abundant brown laminae, thick white lenticles and small abundant amalgamated brown ovoids (0.05 – 0.1mm). **(E).** Borehole specimen of C and M-zones in a core tray.

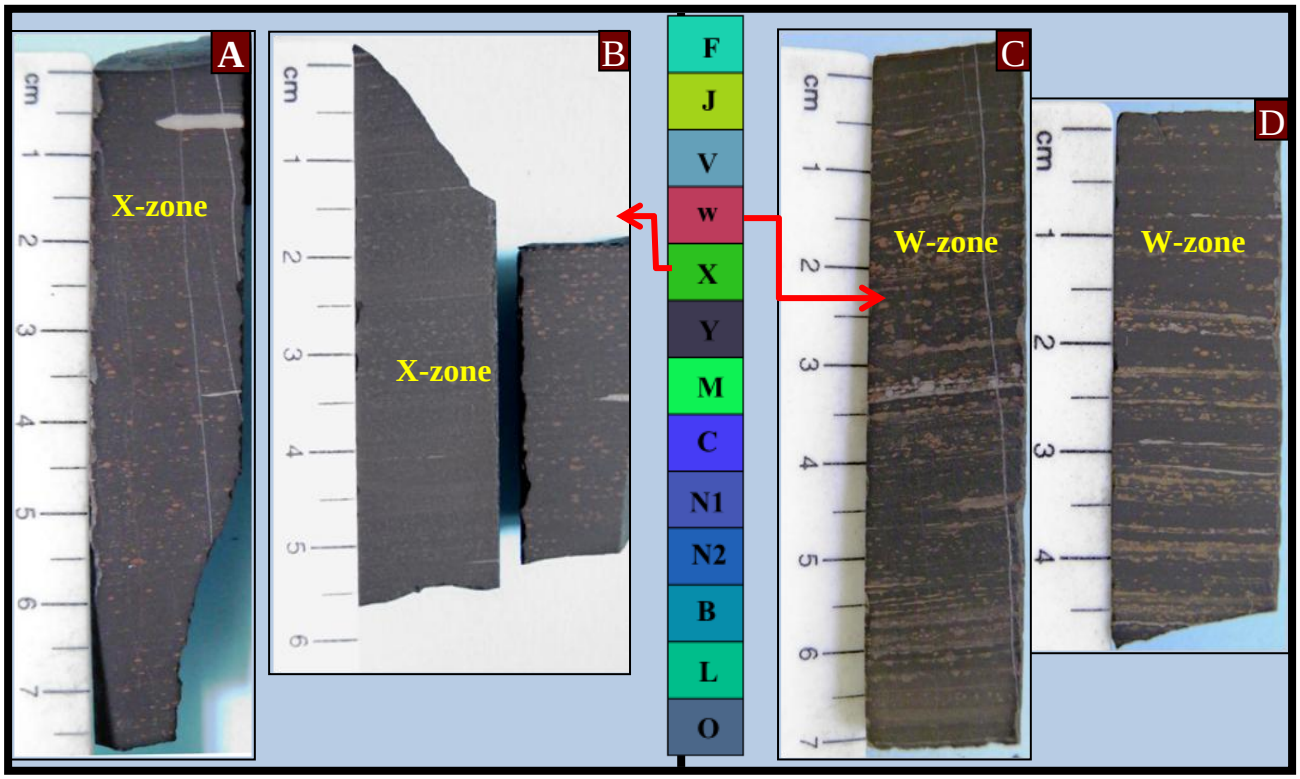

Figure 2.18 (A) - (B). Typical of X-zone with 0.8mm sized and closely spaced abundant brown ovoids at the bottom and widely scattered medium sized (1.7mm) ovoids at the top. **(C) - (D).** W-zone as observed on borehole SKR 40 and SKR 65 displaying white and brown carbonate laminae with 0.125mm to 1.4mm sized and irregularly shaped ovoid.

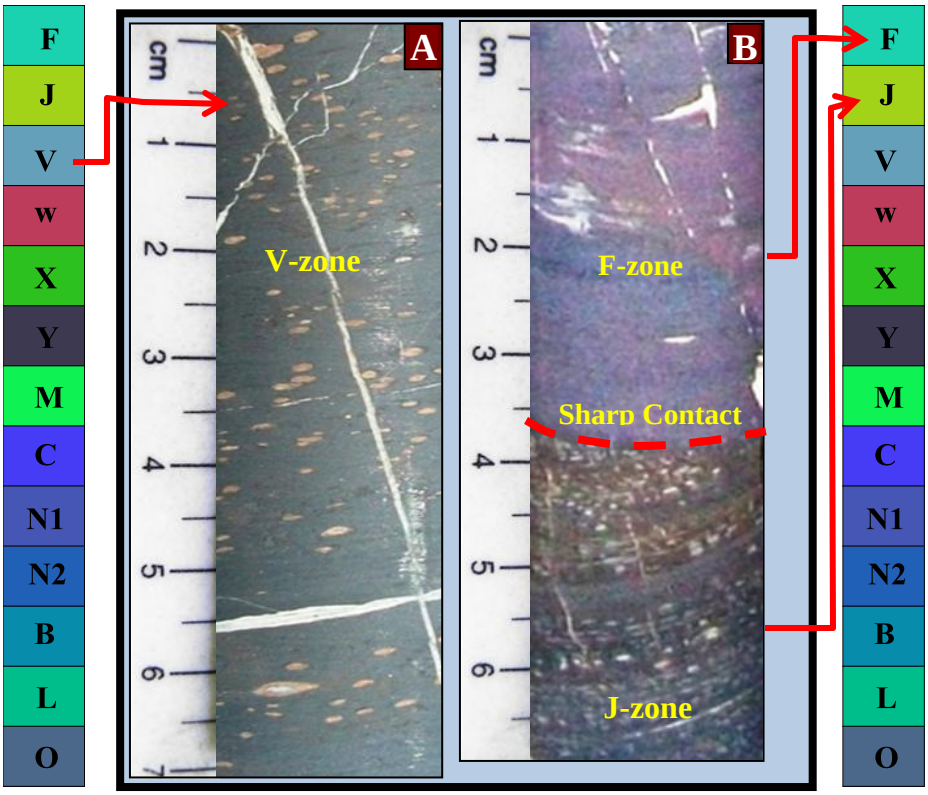

Figure 2.19 (A). Typical of V-zone showing thick carbonate veins and ovoids ranging in size from about 0.08 - 10mm. The ovoids are white in the core and brown on the rims giving an ovoid a "bird eye" appearance. **(B).** Shows a massively banded J-zone (bottom) containing white carbonate ovoids and laminae of various sizes from about 0.06 -1.2mm) and F-zone (top) is characterized by brownish red hematite-lutite with fine white laminae and small to medium sized ovoids (0.8 - 0.15mm).

2.5 Discussion

The LMO at Kalagadi mine as observed from the study is comparable with earlier studies conducted by Preston, (2001) at Mamatwan mine and van Staden (2002). The pioneering work on the lithostratigraphic subdivision published by Nel et al. (1986) at Mamatwan is also worth mentioning. Detailed mineralogy and chemistry of the manganese ore at Kalagadi Mnganese mine are discussed in Chapter 3 and 4.

A table summarizing all the observations in each zone from above-mentioned authors is presented at the end of this chapter. The following is a brief summary of the correlative zones of the LMO as compared with the results from the study are also made.

A transition zone also referred to as O-zone (Figure 2.15-A) was only described by Nel et al. (1986) at Mamatwan mine as "purplish red hematite-lutite with prominent pink carbonate laminae". The zone encountered above is the L-zone as observed in Figure 2.15-B. Characteristics for this zone are comparable with those of Gloria mine by van Staden (2002) which are described as reddish-black to purplish-red hematite-lutite with white carbonate bands and ovoids and lenticles with manganese content ranging mostly from about 21% to 22%.

Preston (2001) at Mamatwan mine described the same zone as, "laminated hematite lutite with thick pink carbonate laminae" and such description seem to be comparable with that of the transition zone as suggested in this study and by Nel at al. (1986). The L-zone grade grades into jacobsitic B-zone (Figure 2.16 - A and B) described at Gloria mine by van Staden (2002) and at Mamatwan mine by Preston (2001) as brownish red to purplish-black, magnetic jacobsite-lutite containing ovoids and laminae of various sizes with manganese (Mn) content varying at (24%–32%) and (29%–32%) respectively.

However, at Kalagadi mine, the manganese content in this zone may reach 29% and whole rock analyses are comparable with those of the other two mines. Braunite, kutnahorite, hematite, jacobsite and hausmannite are present in variable amounts from all the three mines. It should however be noted that earlier studies published by Nel et al. (1986) cannot be positively correlated as B-zone precedes L-zone in a lithostratigraphic sequence.

The jacobsitic B-zone grades into N-zone, which is further, subdivided into N2 and N1 subzones at Kalagadi mine (Fig. 16–C to E) whereas on the other two mines, this zone is described as a unity. This zone is described by van Staden (2002) at Gloria mine and by Preston (2001) at Mamatwan mine as laminated braunite/mangano-lutite with abundant, irregularly shaped white ovoids and laminae with manganese (Mn) content ranging from 29% to 32% and 28% to 36% respectively.

It is, however, important to note that at Kalagadi Manganese mine, the white ovoids and laminae in N-subzones are mostly rich in oxides (braunite and hausmannite) and the Mn content varies from 36% to 40% at N1-subzones and 36% to 39% at N2-subzone. The chemical and mineralogical analyses in these three mines show major similarities. Nel et al. (1986) recorded few braunite rich ovoids in N-zone of Mamatwan mine together with white and brown carbonate ovoids, bands and laminae. C-zone (Figure 2.17-A) above the N1-subzone is macroscopically described by van Staden (2001) as braunite-lutite containing light brown carbonate and dark braunite rich laminae with abundant white carbonate lenses and widely scattered ovoids. Nel et al. (1986) at Mamatwan had given mine similar descriptions. Later studies by Preston (2001) at Mamatwan mine led to further subdivision of C-zone into C1 and C2 – subzones, whereby the former is characterized by fine laminations, small brown carbonate ovoids and thin white

laminae while the later shows “alternating brown, white, red and dark brown laminae, with brown laminae being the most abundant”. It is interesting to note that C-zone at Kalagadi mine could have been further subdivided (Figure 2.17-E) but that was hindered by inconsistence on the observed individual characteristics on other boreholes. However, the combined descriptions for these zones are slightly compatible with those of Kalagadi mine.

The manganese (Mn) content for C-zone at Kalagadi mine may reach up to 35% (chapter 3) whereas at Gloria mine it attains a maximum of 40%. Observations on whole rock analyses are uniform in all the three mines with braunite, kutnahorite, hematite, hausmannite, and serpentine as common minerals. The shiny, dark braunite-lutites of M-zone (Figure 2.17 – B and C) are massively textured with greyish-white ellipsoidal to irregularly shaped carbonate ovoids (van Staden, 2002) and inclusions of hausmannite (Nel et al. 1986). However, the M-zone at Mamatwan mine was further subdivided by Preston (2001) into M1, M2, M3 and M4 based on certain observable textural differences.

The M-zone at Kalagadi Manganese mine is not well developed and hence cannot be further subdivided. It is interesting to note that M-zone is considered the most economic zone in all the mines currently operating in the Mamatwan-Type ore with manganese content at Kalagadi mine reaching an average of 45% while Gloria and Mamatwan mines attains a maximum of 43% and 40% respectively.

The M-zone grades upwards into Y-zone (Figure 2.17 – B, C and D) best described by Nel et al. (1986) as massively textured dark grey to brownish grey stained braunite lutite with prominent white and brown carbonate laminae. At Kalagadi Manganese mine however, close observations shows that most ovoids are rich in braunite. The characteristics of Y-zone at Gloria mine could

not be distinguished from those of X and Y-zone defined by Nel et al. (1986) at Mamatwan mine and hence were rather grouped as XY zone (van Staden, 2002). However, it was noted that such characteristics are more inclined to those of Y-zone rather than X-zone at Mamatwan mine.

Later studies by Preston (2001) at Mamatwan mine led to further subdivision of Y-zone into Y1, Y2, Y3 and Y4 – subzones (from top to bottom). The Y-zone at Kalagadi Manganese mine is best correlated with Y3-subzone, which is characterized by grey, red and dark brown matrix containing fine red and white laminae of various sizes. The manganese (Mn) content of Y-zone Kalagadi Manganese mine attains an average of 33% while at Mamatwan mines it is approximately 29% (Nel et al. (1986).

The X-zone (Figure 2.18 - A and B) was described at Mamatwan mine by Nel et al. (1986) as, "dark grey ore with large concentrically banded white carbonate ovoids and brown to white carbonate nodules." On the other hand, the X-zone at Mamatwan mine was further subdivided by Preston (2001) into three subzones, X1, X2 and X3 and their combined characteristics are slightly compatible with the X-zone at Kalagadi mine.

These three X-subzones as observed in the work of Preston (2001) can be summarily described, as dark grey braunite-lutite containing large abundant, spherical, and flattened elliptically small carbonate ovoids that are parallel to bedding thereby lending a laminated appearance to the ore. The above-mentioned macroscopic features as noted by these two authors are acceptable; the contrasting feature of X-zone at Kalagadi mine is that the ore is rather characterized by abundant brown carbonate ovoids with few white nodes and few thick white carbonate laminae (Figure 2.18-A). The average manganese (Mn) content of X-zone at Kalagadi mine is 31% and at

Mamatwan mine, Nel et al. (1986) reported an average of 38% while an average from Preston (2001) shows an approximate 29%.

The zone encountered above the X-zone is the W-zone (Figure 2.18 – C and D) described by Preston (2001) and Nel et al. (1986) as banded braunite - lutite containing alternating bands of white and brown carbonate ovoids and laminae of various sizes. Van Staden (2002) at Gloria had given mine almost similar descriptions for the same zone. However, at Kalagadi mine, W-zone is characterized by abundant brown ovoids contributing to massive banding, laminations and brownish dark appearance of the ore.

The manganese (Mn) is gradually declining compared to X-zone below reaching an average of 30% at Kalagadi mine, 31% at Gloria mine (van Staden, 2002) and 29% at Mamatwan mine (Nel et al. (1986). The V-zone (Figure 2.19-A) is the dark grey braunite with widely scattered, brown large oblate carbonate ovoids which often bear a white core. Van Staden (2002) gave similar descriptions for the V-zone at Mamatwan mine by Preston (2001) and at Gloria mine.

The chemical and mineralogical characteristics are similar in all three mines. The brownish red jacobsitic hematite lutite above V-zone at Gloria mine is termed J-zone by van Staden (2002) and its descriptions are comparable with those of Kalagadi Manganese mine for the same zone (Figure2.18–B). The top of the orebody is capped by F-zone (Figure 2.18-B), a purplish red hematite-lutite (Nel et al. 1986) with few white carbonate ovoid and laminae. The same zone was described at Mamatwan mine by Nel et al. (1986) and at Gloria mine by van Staden (2002). A diagram showing the degree of correlation between the LMO of Mamatwan mine and Gloria mine with reference to Kalagadi mine is presented below.

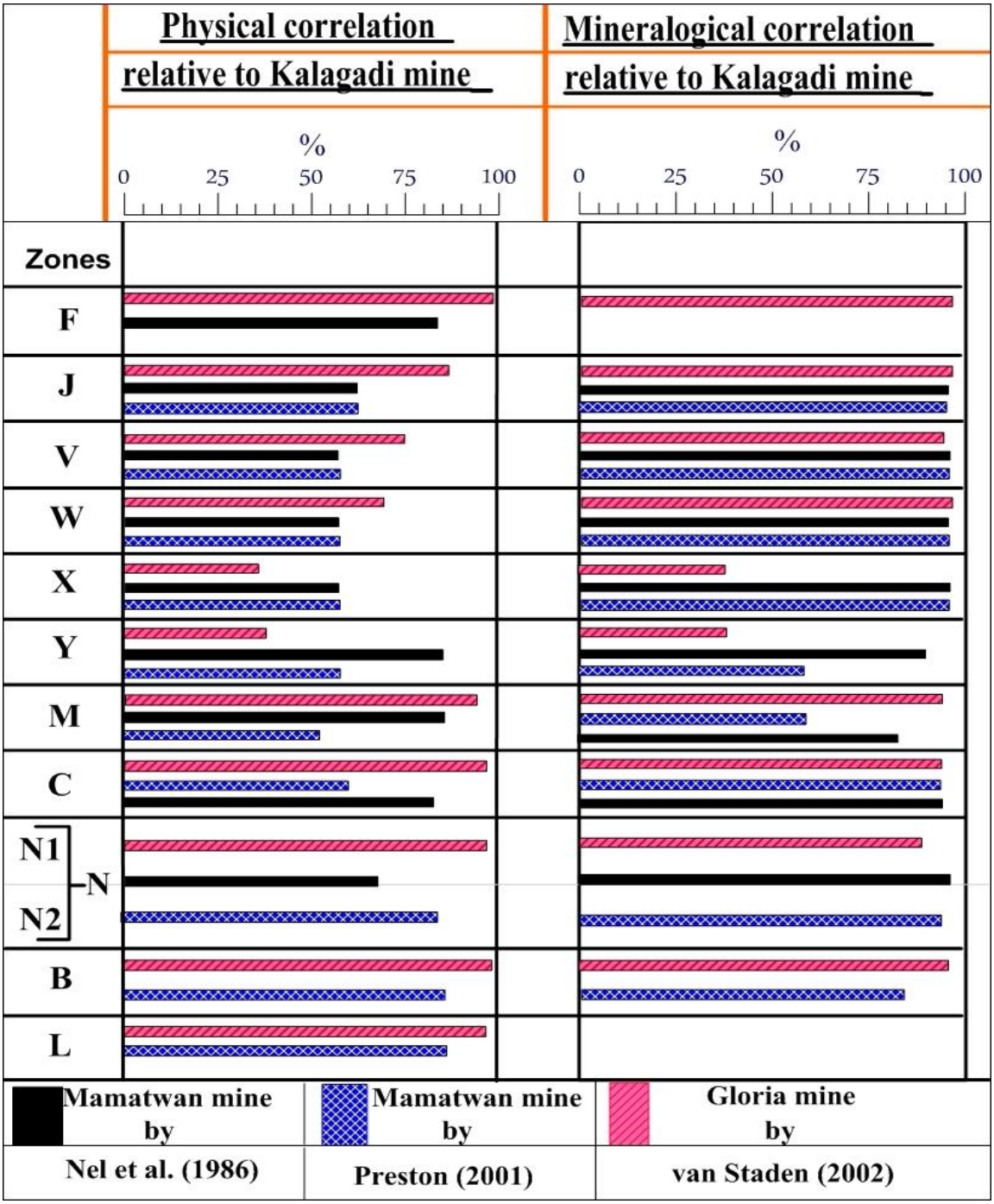

Figure 2.20 Comparisons of the Lower Manganese Orebodies at Mamatwan mine and Gloria mine relative to Kalagadi Manganese mine. Based on physical characteristics, C-zone at Gloria mine by van Staden (2002) is 92% correlated with Kalagadi mine while Mamatwan mine by Nel et al. (1986) and Preston (2001) shows a correlation of 85% and 60% respectively. The correlation is based on colour, grain size and the presence of the Mn-bearing minerals and gangue minerals.

2.6 Conclusions

Fieldwork analyses and the data interpretion show that:

1) The orebody occurs at an average depth of 220m, which is suitable for underground mining methods.
2) Apart from faults and suspected dykes, detailed fieldwork analyses and core logging suggest that the northern part of the mine lease area is faulted and the orebody has been displaced to deeper levels while in the southern portion the sequence is uniform throughout.
3) Various zones of the LMO at Kalagadi Manganese mine are physically, chemically and mineralogically correlated with a similar orebody mined at the Mamatwan open-pit mine situated in the south and Gloria underground mine situated in the northeast.
4) It is evident that the LMO at Kalagadi Manganese mine is best correlated with that of Gloria mine in all aspect while correlations with Mamatwan are also valid.
5) Various zones, which are considered the economic (chapter 3 and 4), are macroscopically distinct especially when the borehole material is unweathered.

2.7 References

Bau, M., Romer, R.L., Lüders, V., and Beukes, N.J. (1999). Pb, O, and C isotopes in silicified Mooidraai dolomite (Transvaal Supergroup, South Africa). Implications for the composition of Paleoproterozoic seawater and 'dating' the increase of oxygen in the Precambrian atmosphere: Earth and Planetary Science Letters, Vol. 174, p. 43–57.

Dorland, H. (2004). Provenance ages and timing of sedimentation of selected Neoarchean and Paleoproterozoic successions on the Kaapvaal Craton. Unpublished PhD thesis, University of Johannesburg, South Africa.

Gutzmer, J., and Beukes, N.J. (1995). Fault controlled metasomatic alteration of Early Proterozoic sedimentary manganese ores in the Kalahari Manganese Field, South Africa. Economic Geology, Vol. 90, p. 823-844.

Internet, 2009. *Tittle of web page.* www.kalahariresources.co.za, visited in 2009 and 2011.

Jennings, M. (1986). The Middleplaats manganese ore deposit, Griqualand West. In: Annhaeusser, C.R., and Maske, S., (eds.), Mineral deposits of Southern Africa. Geological Society of South Africa., Johannesburg, Vol. 1, p. 979-983.

Miyano, T., and Beukes N .J. (1987). Physicochemical environments for the formation of quartz-free manganese oxide ores from the early Proterozoic Hotazel Formation, Kalahari Manganese Field, South Africa.Economic geology, Vol. 82, p. 706-718.

Nel, C.J., Beukes, N .J., and De Villiers., J.E. (1986). The Mamatwan manganese mine of the Kalahari manganese field, in Anhaeuser, C.R. and Maske, S., eds., Mineral deposits of Southern Africa. Johannesburg, Geological Society of South Africa, p.963-978.

Schneiderhan, E. A., Gutzmer, J., Strauss, H., Mezger, K., and Beukes, N.J. (2006). The chemostratigraphy of a Paleoproterozoic MnF- BIF succession – the Voëlwater Subgroup of the Transvaal Supergroup in Griqualand West, South Africa. South African Journal of Geology. Vol. 109, p. 63-80.

Polteau, S., and Moore, J.M., and Tsikos, H. (2006). The geology and geochemistry of the Palaeoproterozoic Makganyene diamictite. Precambrian Research, Vol. 148 (3&4). p. 257-274.

Preston, P.C.C. (2001). Physical and chemical characterization of the manganese ore bed at the Mamatwan mine, Kalahari Manganese Field, Unpublished MSc. Dissertation, University of the Johannesburg, Johannesburg, South Africa.

van Staden, A. (2002). Characterization of the lowermost manganese ore bed of the Hotazel Formation, Gloria Mine, Northern Cape Province, Unpublished MSc. Dissertation, University of the Johannesburg, South Africa).

Van Niekerk, H.S. (2006). The origin of the Kheis Terrane and its relationship with the Archean Kaapvaal Craton and the Grenvillian Namaqua Province in Southern Africa, unpublished MSc. Dissertation, University of Johannesburg, South Africa.

Tsikos, H., Beukes, N.J., Moore, J.M,. and Harris, C. (2003). Deposition, Diagenesis, and Secondary Enrichment of Metals in the Paleoproterozoic Hotazel Iron Formation, Kalahari Manganese Field, South Africa. Economic Geology, Vol. 98, p. 1449–1462.

CHAPTER 3

LITHOSTRATIGRAPHIC ZONE'S MINERALOGY

3.1 Introduction

Many authors including Nel et al. (1986) and Kleyenstùber (1984) have described the detailed mineralogy of the manganese ores in the entire Kalahari Manganese Field. The general mineralogical studies were conducted at the Kalahari deposit and some mines with the focus on either the manganese ore or the associated Iron Formations. Studies from other authors such as Beukes (1983), de Villiers (1983), Nel et al. (1986), Jennings (1986), Gutzmer (1996), Gutzmer et al. (1997), Tsikos & Moore (1998), Tsikos et al. (2003), Preston (2001), van Staden (2002) and Chetty (2008) shed some light on the mineralogy of the Kalahari deposit. The identifications of various minerals in various zones were accomplished using XRD, reflected light microscopy and Scanning Electron Microscopy.

3.2 Methodologies

3.2.1 Sample preparation

Apart from hand specimen identification of the manganese ore, analytical studies were applied in order to determine the geochemistry, mineralogy and mineral geochemistry of manganese ore. The two drill cores, SKR 40 and SKR 65, were selected for detailed petrographic, mineralogical and geochemical analyses. A representative sample of about 8cm by 4cm in length and width of each zone of the LMO at both boreholes was selected based on macroscopically recognizable characteristics.

These representative samples halved in the laboratory using a diamond saw and were dried in an oven. One quarter was used to prepare polished thin and polished sections and the remaining quarter was crushed into small chips and ground into fine powder using a jaw crusher and a tungsten carbide mill. Any remaining or unused sample material was properly recorded and kept for future reference.

Great care was taken to prevent any form of contamination in order to produce accurate results. This was achieved by thoroughly cleaning the instrument after each sample crushed or ground in order to prevent contamination from the previous material. The mill was cleaned several times by grinding quartz sand into fine powder and was finally rinsed with ethanol to remove traces of quartz. Great care was taken not to over pulverize the sample as this would destroy the crystal structure and hence produce abnormal peaks during XRD analyses. The overall time each sample took to be ground into fine powder was recorded as certain minerals in the manganese ores display different levels of hardness.

3.2.2 Mineralogical and Petrological analyses

A total of twenty-two polished sections representative of each zone from both drill cores SKR 40 and SKR 65 were quartered and prepared for different analytical purposes. One quarter was used to prepare double polished sections and thin sections while the remaining portion was pulverized for use on XRD, XRF and stable isotope analyses.

The mineral identification work was initially performed on polished sections under reflected light petrographic microscope in order to view and analyze the ore mineral composition based on physical and optical properties such as texture, laminations, lenticles and ovoids. Apart from twenty polished thick sections, eight polished thin sections were prepared and studied under

transmitted light in order to view any transparent minerals that may be present in the manganese ore. Transmitted and reflected light petrographic microscope fitted with Motic Live 2.0 camera was used to view and capture images of interest. Out of twenty polished thick sections made, about eight polished thick sections were chosen and coated with carbon for further SEM analyses.

The XRD analyses on representative samples were performed at Mintek and Council for Geosciences to determine the mineralogy of manganese on various zones and confirm the observations and interpretations from petrographic microscopy, SEM and XRF studies. The XRD analyses were initially performed on dried and pulverized manganese samples pressed into round pellets at Council for Geoscience. Samples were scanned from 2 to 70° 2θ, $Cu_{K\alpha}$ radiation, at a speed of 0.02° 2θ, steps size of 0.5s with Lynxeye detector and generator settings of 40 kV and 40mA. Phase concentrations were determined as semi quantitative estimates, using relative peak heights/areas proportions.

Another set of XRD analyses were performed at Mintek in order to compare the results with those obtained from Council for Geoscience. The measurements were carried out on a Scan D 500 diffractometer with the following settings: Tube anode material → $Cu_{K\alpha}$ radiation; Type → 2θ; Angle range → 5^o to 80^o 2θ; Step size → 0.020^o; Step time → 1s; Time started: 0s; Generator settings → 40kV and current → 30mA.

Standard petrographic techniques on polished thin sections were initially conducted on a transmitted light microscope to view the transparent minerals that may be present in the manganese ore. Most minerals, however, in the manganese ore are opaque, so polished sections were prepared for use on reflected light microscope. Microscope studies on polished sections

were conducted on Nikon microscope fitted with a camera at Mintek and Olympus polarizing microscope fitted with a Motic live 2.0 camera at the Fort Hare Geology department. The petrographic microscope adjusted to various magnifications and fitted with a camera was used to identify various minerals based on their physical and optical properties and to capture images.

The polished thick sections were later coated with carbon and the SEM analyses were undertaken on a Jeol JSM-5600 model with energy dispersive (EDS) link at the University of Fort Hare with operating conditions at 15kV and 15mA on cobalt standard. Qualitative mineral compositions were initially obtained on the SEM using both the backscatter and secondary electron modes. X-ray line scan and spectral images of various mineral phases were also obtained on the SEM.

3.3 Results from microscopic study of lithostratigraphic zones

3.3.1 Introduction

The manganese ore at Kalagadi Manganese mine is microscopically characterized by microcrystalline, white and brown carbonate or oxide-rich ovoids with elongated laminae and lenticles of various sizes. Braunite and kutnahorite are the most dominant oxide and carbonate species intergrown in a matrix occasionally with other minor and trace minerals.

The braunite-rich manganese ore in the KMF is termed the braunite-lutite or manganolutite. Other oxides such as hematite, hausmannite and jacobsite together with carbonates such as, Mg-calcite, calcite, dolomite and rhodochrosite were determined in certain zones in minor or trace amounts. Sulphate mineral, barite, which is sometimes rich in strontium (Sr-$BaSO_4$) was determined by SEM analyses inside oxide rich ovoids and along the veins while silicate minerals, serpentine and garnet, are present mostly in trace amounts. The mineralogy of the

manganese ore in various zones varies from top to bottom of the orebody. Mg-calcite is the second most abundant carbonate mineral in the manganese ore and it was determined in all samples analyzed by XRD at Mintek and Council for Geoscience. Mn-calcite has been previously reported by many authors as the second abundant carbonate species after kutnahorite in this region but it was only determined as a trace by SEM and microscope in few zones. The minerals encountered in the study together with their possible mode of origin are summarized at the end of this chapter.

3.3.2 Zone description

The Upper and Basal low grade zones of the LMO are characterized by enrichments of carbonate content inside ovoids which is often intergrown in the matrix with braunite. The central economic zone is slightly depleted in carbonate content and rather enriched in braunite content with ovoids often partially oxidized. The replacement of carbonates by oxides such as hausmannite and braunite inside an ovoid or laminae contributes to the increased grade of the economic zones.

Diagenesis of different minerals that were determined by XRD and observed under microscope and on SEM is also discussed at the end of this chapter. Petrographic studies were initially attempted on polished thin sections under transmitted light microscope but with little success due to the manganese minerals opaqueness. There is however, few transparent minerals determined in the few zones that were studied under transmitted light and the images were captured. The microscopic field description of lithostratigraphic zones serves to supplement the macroscopic observations, and is based mainly on observable minerals, texture, occurrence and abundance of ovoids, lenticles (stretched ovoids) and laminations. The following table summarizes the microscopic description of the Lower Manganese Orebody from the bottom to the top.

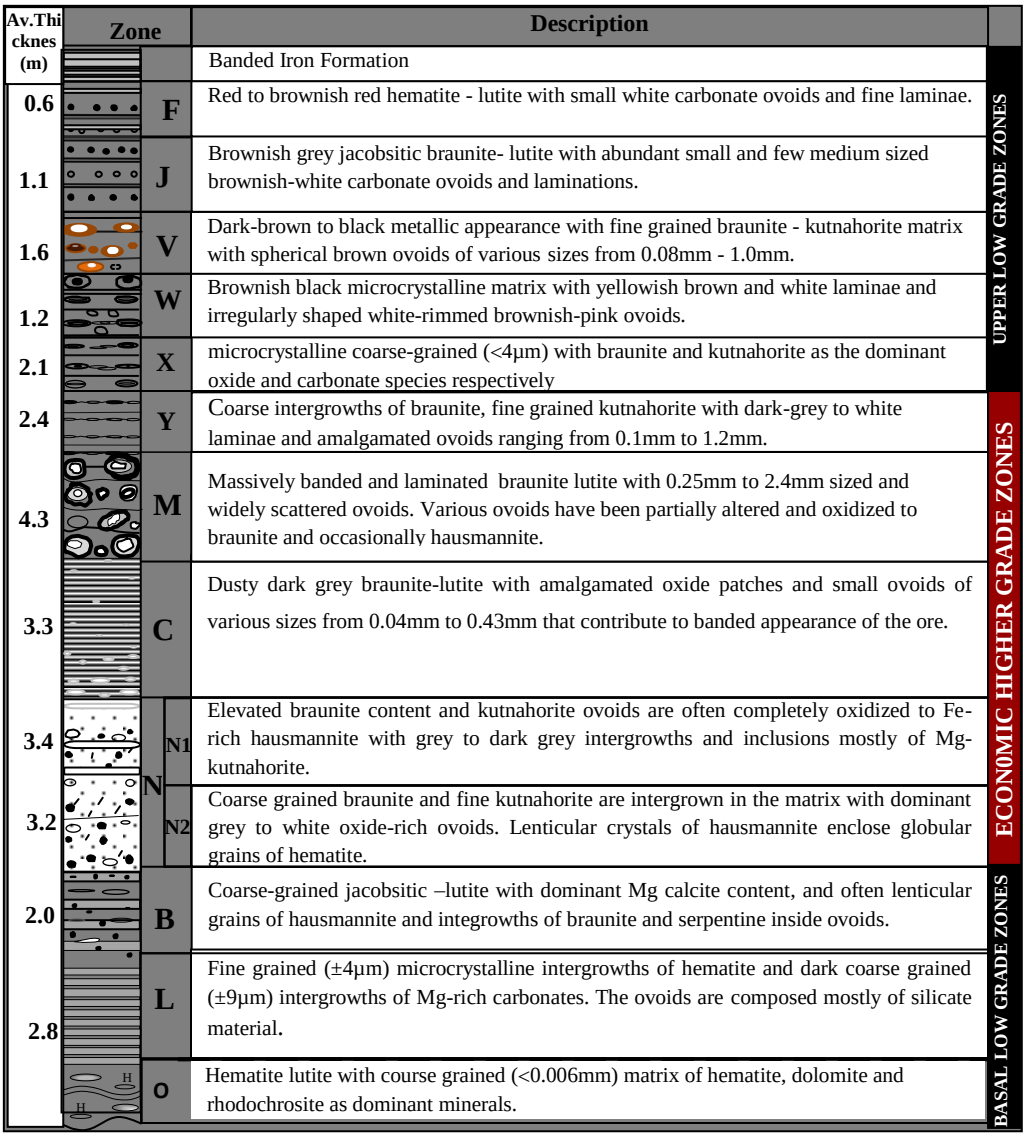

Figure 3.1. Mineralogical and Petrographic description of the Lower Manganese Orebody at Kalagadi, mine from the bottom to the top with a brief description of each zone.

3.3.3 O-zone

Under reflected light, the O - zone is characterized by fine grained (±6µm) concretioanry matrix of hematite (white), rhodochrosite and dark inclusions of serpentine material with 1.5mm sized lenticles and 0.05mm sized ovoids. The hematite and rhodochrosite are of primary origin and are macroscopically responsible for the pinkish-red appearance of the ore while serpentine is of secondary origin.

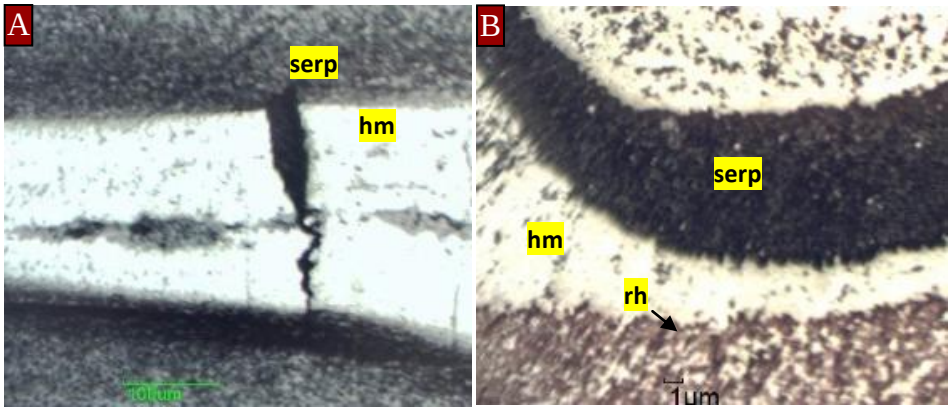

Figure 3.2. Reflected light photomicrographs (different scales) of a typical O-zone. **A**). Shows a matrix of hematite (hm) – rhodochrosite (rh) containing a white hematite-rich lamina under plane polarized light. **B**), Enlarged view of laminae of serperntine (serp) and hematite under cross polarized light.

3.3.4 L-zone

The frequently occurring ore minerals are hematite and Mg- calcite while calcite, braunite and kutnahorite occur in minor and trace amounts respectively. The ore under reflected light is characterized by white fine-grained (±4µm) microcrystalline intergrowths of hematite and dark coarse grained (±9µm) intergrowths of Mg-rich carbonate and serpentine minerals. The ovoids are composed mostly of Mg-calcite and serpentine while the hematite in the matrix is integrown kutnahorite, Mg-rich calcite, calcite and serpentine.

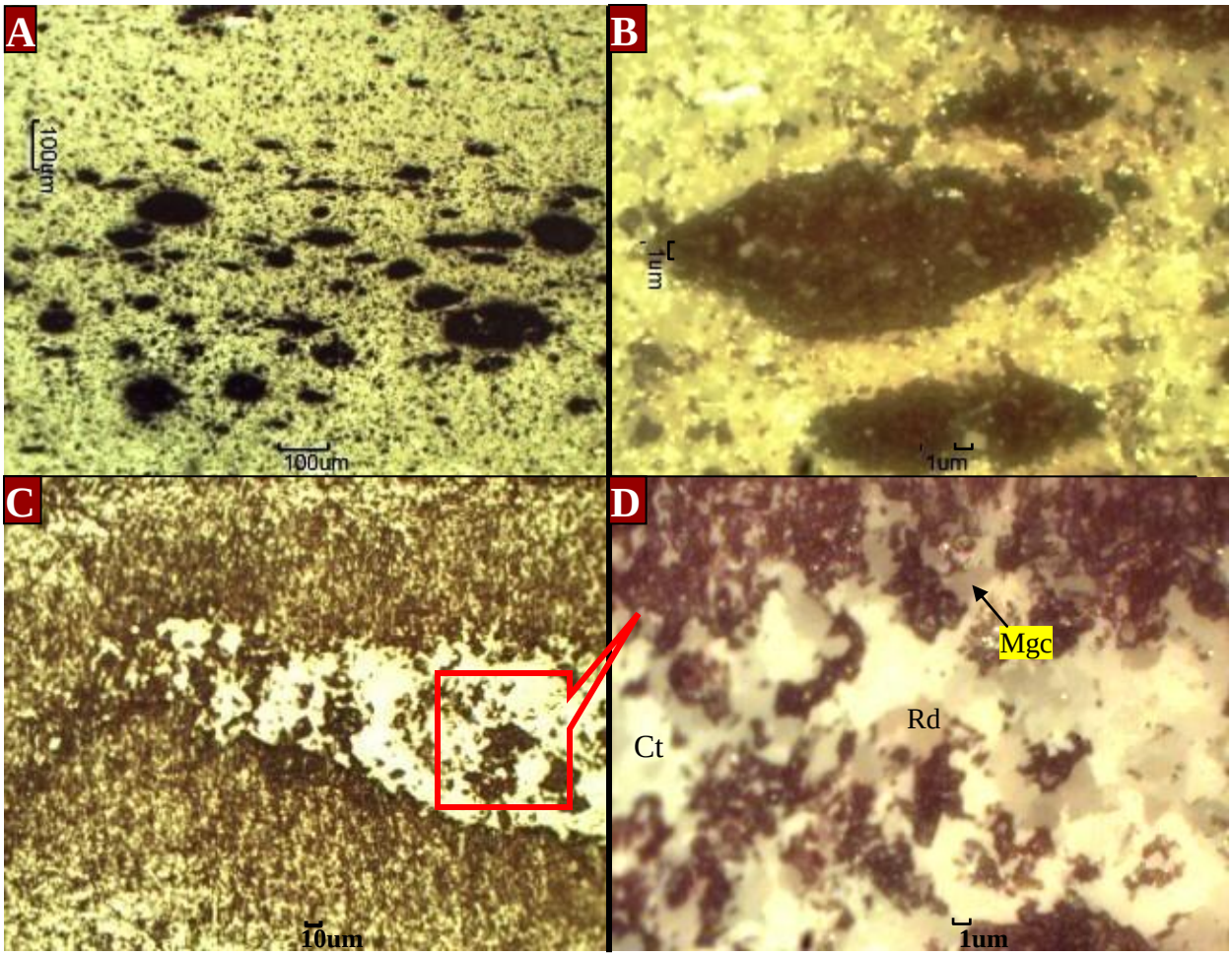

Figure 3.3. Reflected light photomicrographs of L-zone. **A**). Coarse-grained matrix of hematite (ht), kunahorite (kt) and Mg-calcite rich with ovoids containing garnet (gnt and serpentine. **B**) Enlarged view of ovoids containing dark green and gray carbonate ovoids in a hematite (pure white) — kutnahorite (dark-gray) matrix. **C**) Carbonate laminae in a matrix. **D**) Cross polarizing light showing an enlarged view of a lamina containing subhedral coarse cyrstallites of white calcite (ct), brownish-white rhodochosite (Rd), and Mg-calcite (Mgc) as shown in C.

3.3.5 B-zone

The Mg-calcite as determined by XRD is the most dominant carbonate species while kutnahorite, hematite and braunite occur in major quantities. Jacobsite, which is associated with magnetic character of the ore occurs in minor quantities while hausmannite is present in trace amounts. The zone is laminated with coarse-grained matrix of braunite and kutnahorite bearing greyish white to dark-grey carbonate ovoids ranging in size from 0.25mm - 1.8mm. Integrowths of coarse-grained lenticular hausmannite is observed inside a kutnahorite ovoid and often form as replacements (Figure 3.4). Braunite, kutnahorite and Mg–calcite are of primary origin while serpentine and hausmannite appear to be of secondary origin.

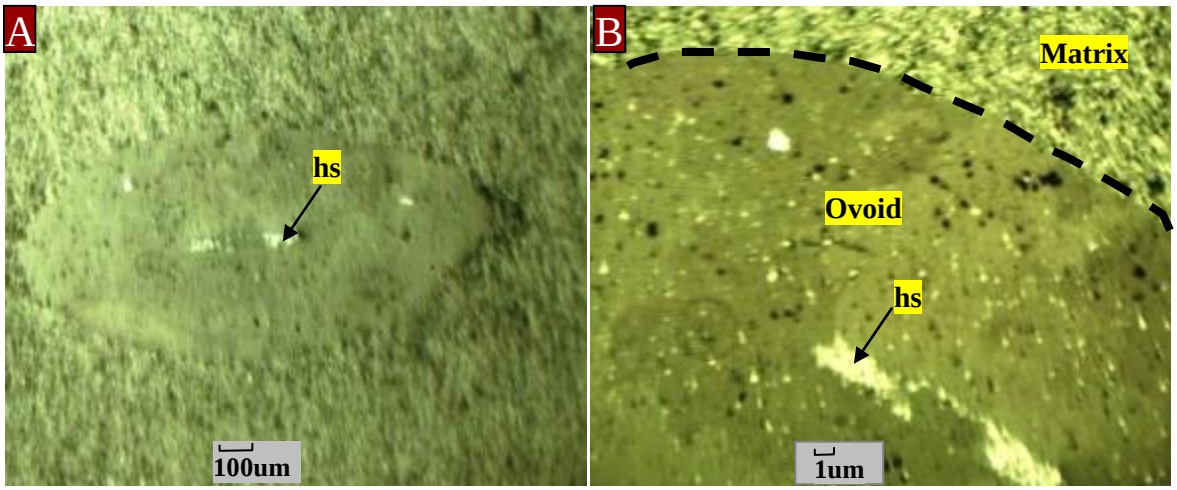

Figure 3.4. Reflected light photomicrographs (different scales) of B- zone.
A). Granular intergrowth of braunite (light grey) and kutnahorite (dark-grey) in a matrix with ovoids composed of kutnahorite and intergrowths of dark green silicate material (serpentine) and white hausmannite (hs). **B**) Enlarged view of a kutnahorite ovoid (below dotted line) together with intergrowths of alumino silicate material (dark green) and subhedral crystals of hausmannite (pure white) as replacements.

3.3.6 N2 – subzone

The N2-subzone represents the base of the Central Economic zone of the LMO. The subzone is microscopically characterized by coarse-grained matrix of braunite and kutnahorite with grey to white oxide-rich ovoids. The ovoids range in size from 0.1mm – 0.75mm and are completely or partially oxidized to hausmannite (Figure 3.6–D).

Braunite is the dominant oxide mineral while kutnahorite and Mg-calcite are major carbonate mineral species. Hematite, alumino silicate material (serpentine) and hausmannite occur in minor concentrations. Traces of rounded to sub-angular crystals of hematite and darkish/brownish green serpentine minerals are mostly concentrated inside a hausmannite-rich ovoid while barite is mostly concentrated along the veins.

Under reflected light and on SEM, pure white globular grains of hematite are enclosed in patchy lenticular grains of hausmannite in a braunite-kutnahorite matrix (Figure 3.5–A). Thick light-grey and white oxide-rich ovoids and laminae with occasionally microcrystalline fine grained (<6μm) kutnahorite and coarse grained (>6μm) Mg-kutnahorite, are observed.

Reflected light and SEM studies revealed the presence of at least two types of ovoids as shown in (Figure 3.6). The most dominant is a pure hausmannite-rich ovoid occassionally enclosing intergrowths of hematite, manganocalcite or Mg-kutnahorite (Figure 3.6 – C and D). The other type is that of manganocalcite ovoids partially replaced by braunite and/or hausmannite. Braunite and kutnahorite are of primary origin while hausmannite, hematite and serpentine are secondary and hence are often found replacing carbonate minerals (Figure 3.5–C and 3.6-B).

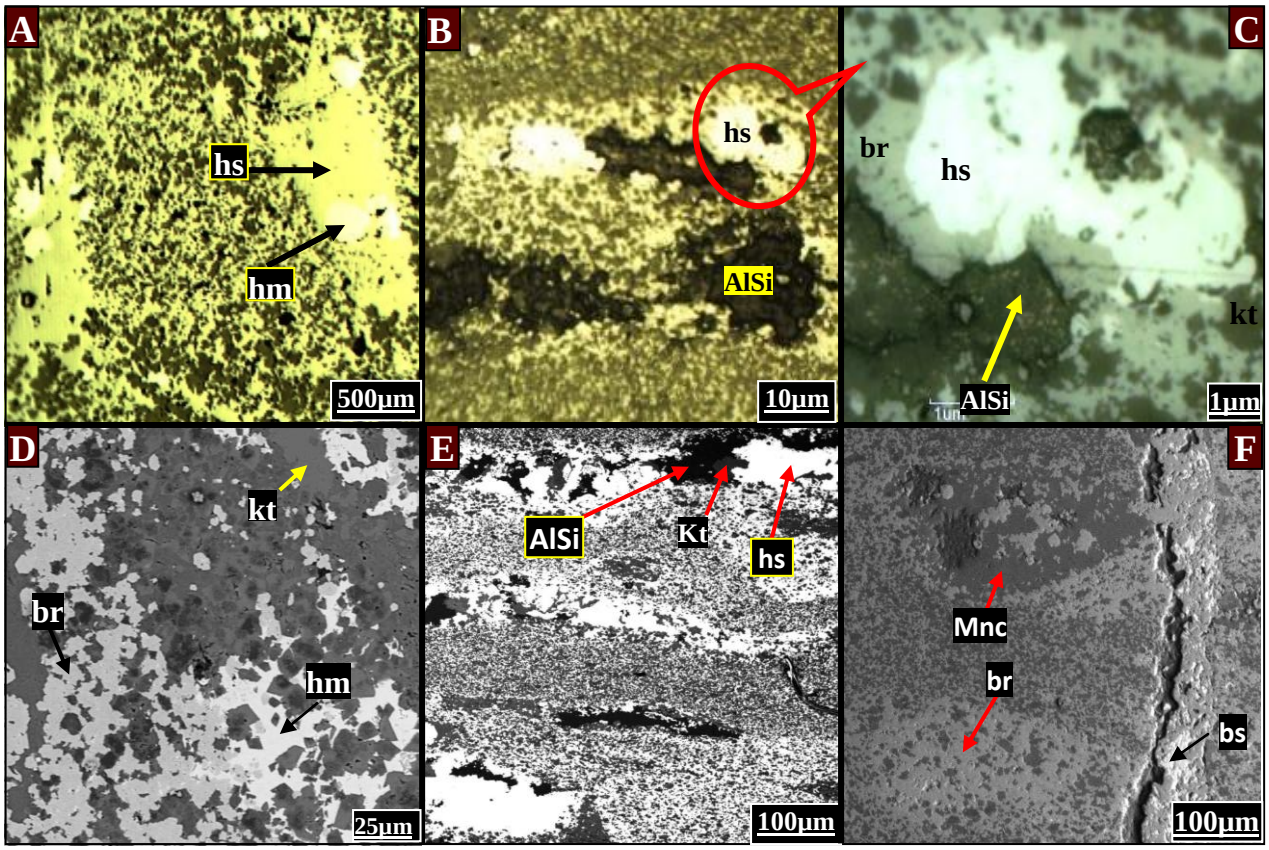

Figure 3.5 (**A)** Reflected light (plane polarized) photomicrographs of N2- subzone displaying an elongated creamish white subhedral granullite of hausmannite (hs) enclosing white globules of hematite (hm). **(B)** Braunite-kutnahorite matrix containing laminae of Mg–kutnahorite, serpentine mineral, hausmannite and braunite **(C)** Enlarged view of the top-right section of image (B). Note the replacement of braunite (br) by hausmannite (hs) and a cavity of dark green to grey serpentine and Mg kutnahorite contents. **(D)** SEM photomicrograph of the microcrystalline matrix of fine grained kutnahorite, coarse grained Mg-kutnahorite, crystallites of hematite (pure white) and braunite (grayish white). **(E)** Laminae with light grey kutnahorite, dark silicate material (serpentine and garnet) and white braunite. **(F)** Barite (bs) concentrations along the Mg-calcite fissure. Also note the occurrence of a small Mn-calcite (Mnc) ovoid with slight replacements of braunite and a braunite rich ovoid containing intergrowths of Mn calcite.

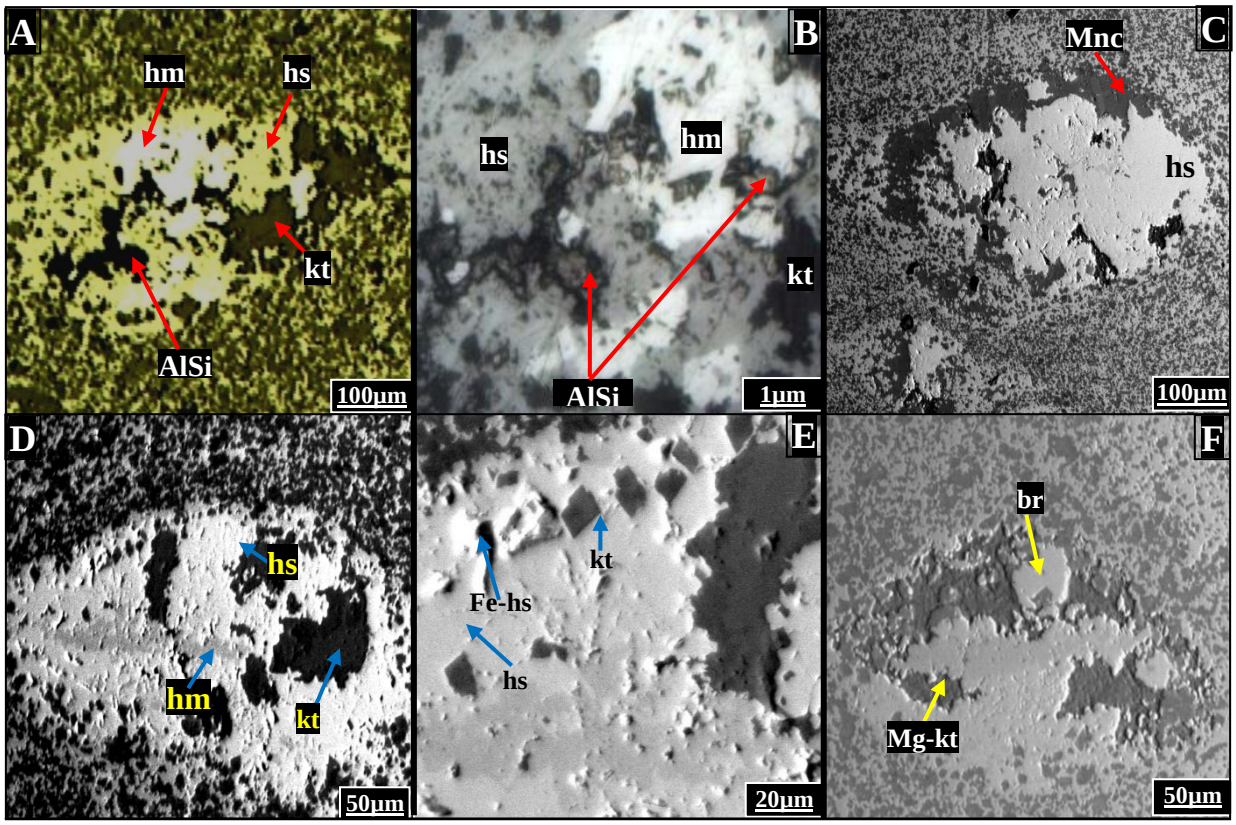

Figure 3.6 Photomicrographs(**A** to **I**) showing the various degree of oxidation inside ovoids of N2-subzone**. (A).** Reflected light (plane polarizing light) photomicrograph of an ovoid showing dark silicate material (AlSi), kutnahorite which is partially oxidised to hausmannite (hs) hosting irregular crystallites of hematite (hm). **(B).** Enlarged view of an interior of an ovoid shown in image **A** viewed under cross polarizing light microscopy. **(C).** Manganocalcite(Mnc) ovoid partially replaced by hausmannite enclosing dark gray patches of coarse grains of Mg–calcite(dark gray). **(D).** Hausmannite and dusty hematite replacing a Mg–kutnahorite ovoid(dark areas). **(E).** Enlarged interior of an ovoid (shown in **D**) with hausmannite - hematite assemblage and angular inclusions of manganocalcite. **(F).** The Mg kutnahorite ovoid partially replaced by euhedral grain braunite.

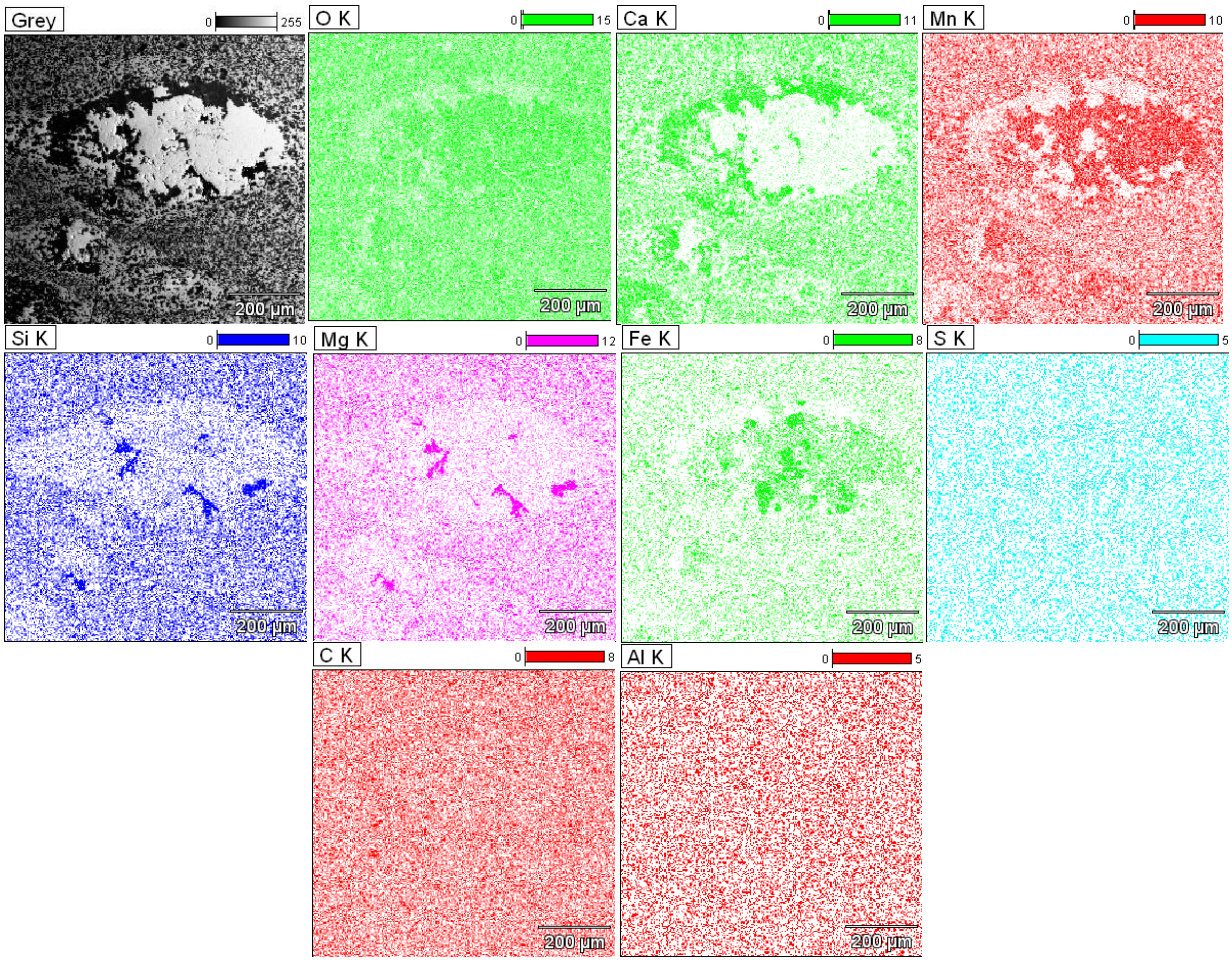

Figure 3.7. SEM spectral images of N2-subzone showing the element distribution inside ovoids and in a matrix (shown in Figure 3.6–C). The larger ovoid displays elevated carbonate (Ca) patches, mostly on the rims while other elements are lower indicating the dominance of carbonate material. The concentrations of Mn, O and Fe contents are the most dominant inside an ovoid while Si and Mg are depleted and this is compliant with the presence of hausmannite and hematite. The negative correlation on Mn with Fe inside an ovoid is attributed to the development of hematite at the expense of manganese. The dark patches/inclusions in the ore are composed of elevated contents of Mg and Si and O while and such observations suggest the dominance of alumino silicate mineral or enstatite ($MgSiO_2$). Braunite (Mn, Si and O) is mainly concentrated outside an ovoid in the matrix.

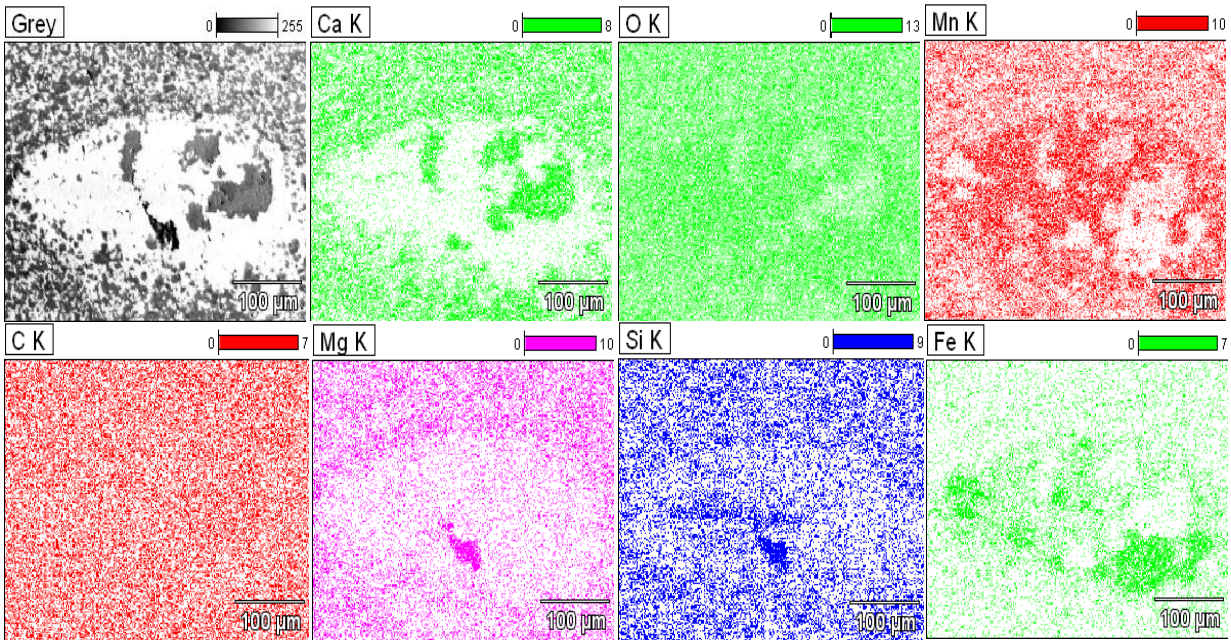

Figure 3.8 SEM spectral images of N2-subzone showing concentration of various elements inside and outside an ovoid shown in Figure 3.8–D. Note the elevated concentrations of braunite (Mn, Si and O) with patches of hematite and manganocalcite inside an ovoid.

3.3.7 N1-subzone

The N1-subzone is microscopically characterized by coarse-grained microcrystalline matrix of braunite and kutnahorite, oxidized oval shaped ovoids with dark to grey intergrowths, few thin lenticles and thick white and dark laminae. Braunite content may reach 56% with kutnahorite and Mg–calcite present in major quantities (from 11% to 25%) while hematite and hausmannite are generally present in minor concentrations (5% to 10%). The kutnahorite ovoids in most cases are completely oxidized to Fe-rich hausmannite and often contain grey to dark grey intergrowths and inclusions of Mg-kutnahorite (Figure 3.9–D and B).

The euhedral and lenticular crystals of hausmannite inside ovoids occur mostly in association with pure white grains of hematite and white traces of needle-like crystals of barite and braunite

contents. Elevated Mn, Fe and O (Figure 3.9–B) contents as observed from weight percent abundance *(analytical point 2* of Figure 3.9-A) and spectral images (Figure 3.10) by SEM suggest the dominance of Fe-rich hausmannite variety and hematite (Fe and O) and lower carbonates (Ca) and braunite (Mn, Si and O) contents.

It is therefore evident that ovoids are devoid of carbonate content and are oxidized to hausmannite rather than braunite as observed on other economic subzones. The oxide - carbonate ratio in a matrix increases towards the base with ovoids and laminae partially and completely replaced by Fe-rich hausmannite or braunite. This is a characteristic defining the N2-subzone below. Braunite and kutnahorite are of primary origin followed by hausmannite, hematite, calcite, and later alumino silicate material (serpentine and garnet).

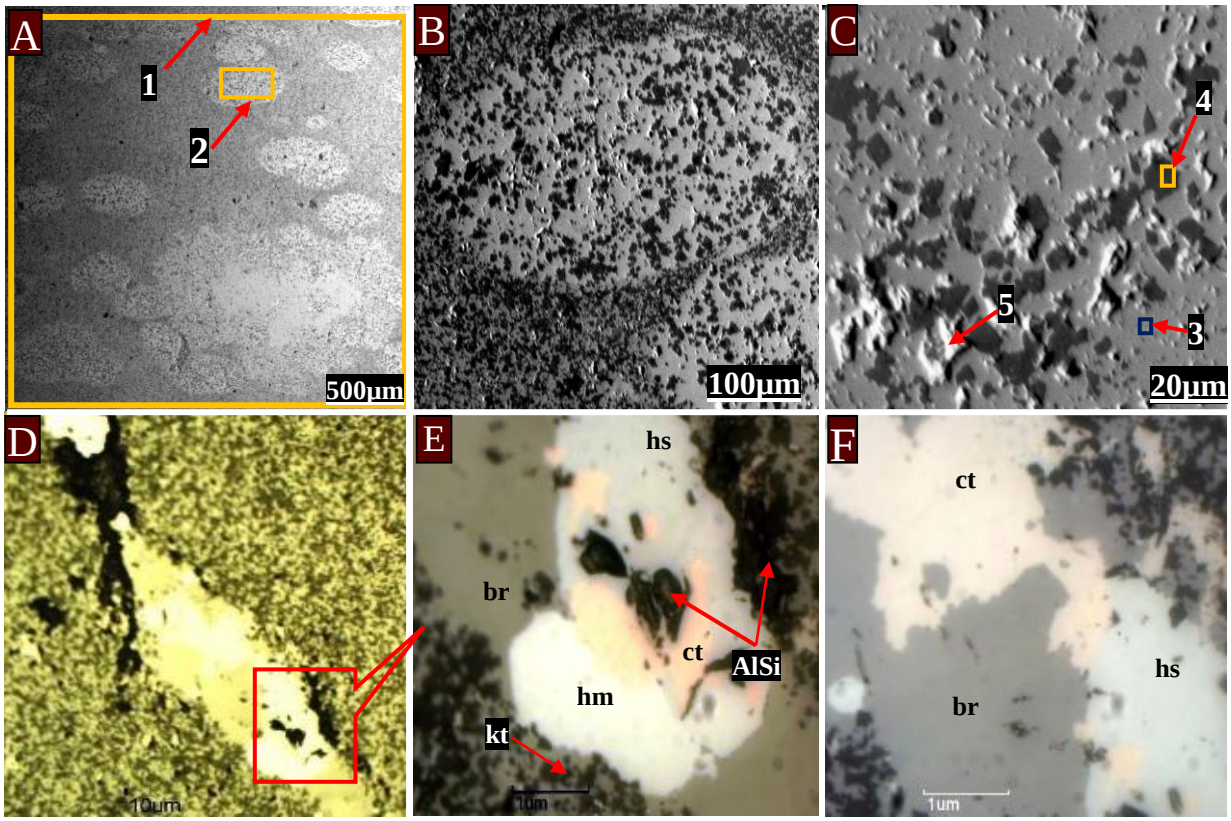

Weight % composition

Point	*C*	*O*	*Na*	*Mg*	*Si*	*S*	*Ca*	*Mn*	*Fe*	*Ba*	*Total*
1	6.08	34.78	–	2.92	2.22	0.1	9.2	39.06	5.63	–	**99.99**
2	5.6	31.58	–	1.69	0.29	0.09	5.67	32.8	22.28	–	**100**
3	4.44	25.82	–	0.41	0.37	0	–	66.12	2.84	–	**100**
4	7.47	43.65	–	4.45	–	0.22	20.33	20.4	2.25	1.23	**100**
5	7.59	24.32	1.33	0.46	–	9.24	0.94	14.42	0.54	40.65	**99.49**

Figure 3.9 SEM (A-C) and reflected light (D-F) photomicrographs (different scales) of N1-subzone. **A).** Braunite–kutnahorite matrix with oxidized carbonate ovoids. Also shown is the approximate mineralogical composition (table) of the manganese ore (*analytical point 1)* and interior of an ovoid *(analytical point 2)*. **B).** Enlarged view of oxidized ovoids with dark intergrowths and inclusions of Mg-kutnahorite**. C).** Mineralogical composition of an interior of an ovoids with enrichment of Fe-rich hausmannite (hm) and hematite (*analytical points 2 and 3*) , dark grey sub–angular intergrowths of Mg kutnahorite (*analytical point 4*) and trace amounts of manganese barite (*analytical point 5*). **D**). Coarse-grained braunite and fine grained kutnahorite matrix with hausmannite (hs) hosting subhedral grain of hematite (white). **E**). Enlarged view (*highlighted lower part*) of braunite-rich laminae hosting irregular crystals of hematite (hm) and calcite (ct). **F**). Enlarged view of an upper part of a braunite laminae shown in **D** with calcite (ct) and hausmannite coexisting.

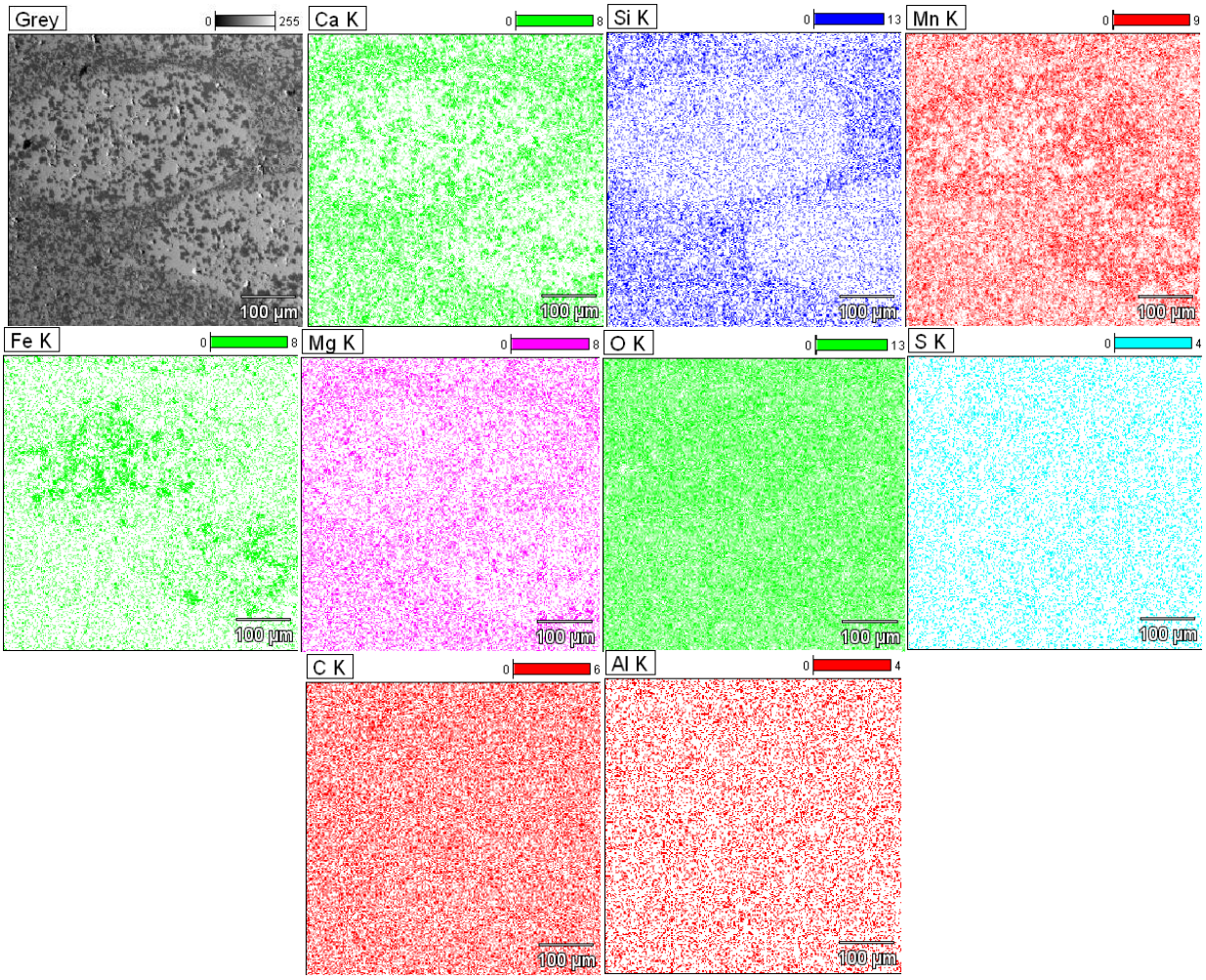

Figure 3.10 SEM spectral images of N1-subzone showing the elemental distribution and mineral phases in the manganese ore. The ovoids show elevated concentrations of Mn, O and Fe while Ca, Mg and Si are depleted and this corresponds to enrichments of Fe-rich hausmannite and depletion of carbonates and braunite inside ovoids. The Ba contents are present in negligible amounts (Figure 3.9 D – *4* & *5*). Elevated Mn, Si, O and Mg characterize the braunite-kutnahorite matrix while the Fe content is depleted.

3.3.8 C-zone

The massively banded C-zone is macroscopically characterized by dusty appearance, coarse-grained macrocrystalline matrix of braunite-kutnahorite and fine laminations with occasionally abundant small oxide rich ovoids. X-ray diffraction analyses revealed the elevated carbonate content such as Mg-calcite and kutnahorite intergrown with braunite in a matrix. Microscopic observations revealed the presence of white amalgamated oxide patches and small ovoids of various sizes from 0.04mm to 0.43mm that contribute to banded appearance of the ore (Figure 3.12–D). The ovoids are altered and oxidized to hausmannite and braunite, which is occasionally intergrown with hematite and Mg–kutnahorite (Figure 3.12-B).

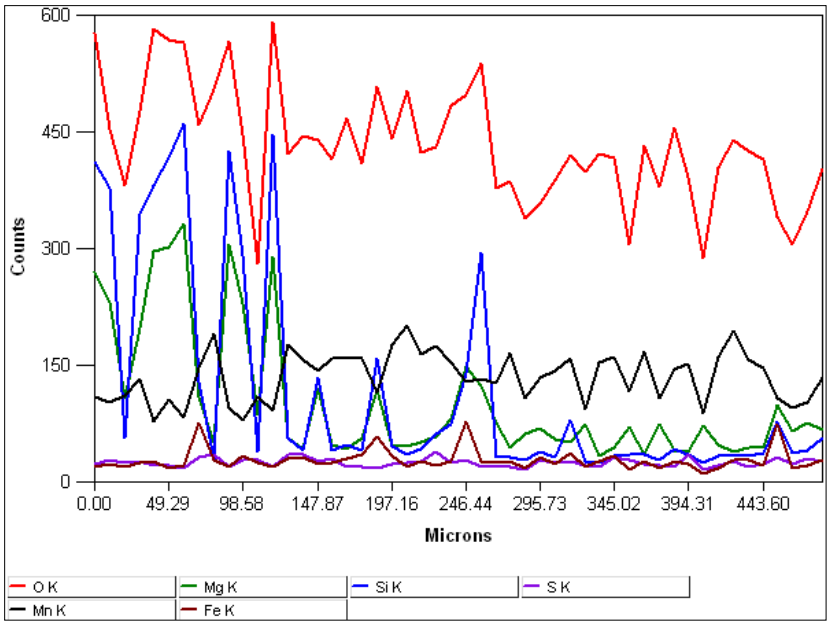

Figure 3.11 The x-ray line scan showing mineralogical variation inside an ovoid as shown in Figure 23.1(A). The line scan from 0µm to 130µm shows a steady rise in O, Si and Mg contents while Mn content fluctuates constantly throughout. Beyond 130µm, the O contents remain elevated, Mn remain constant while other elements drop slightly.

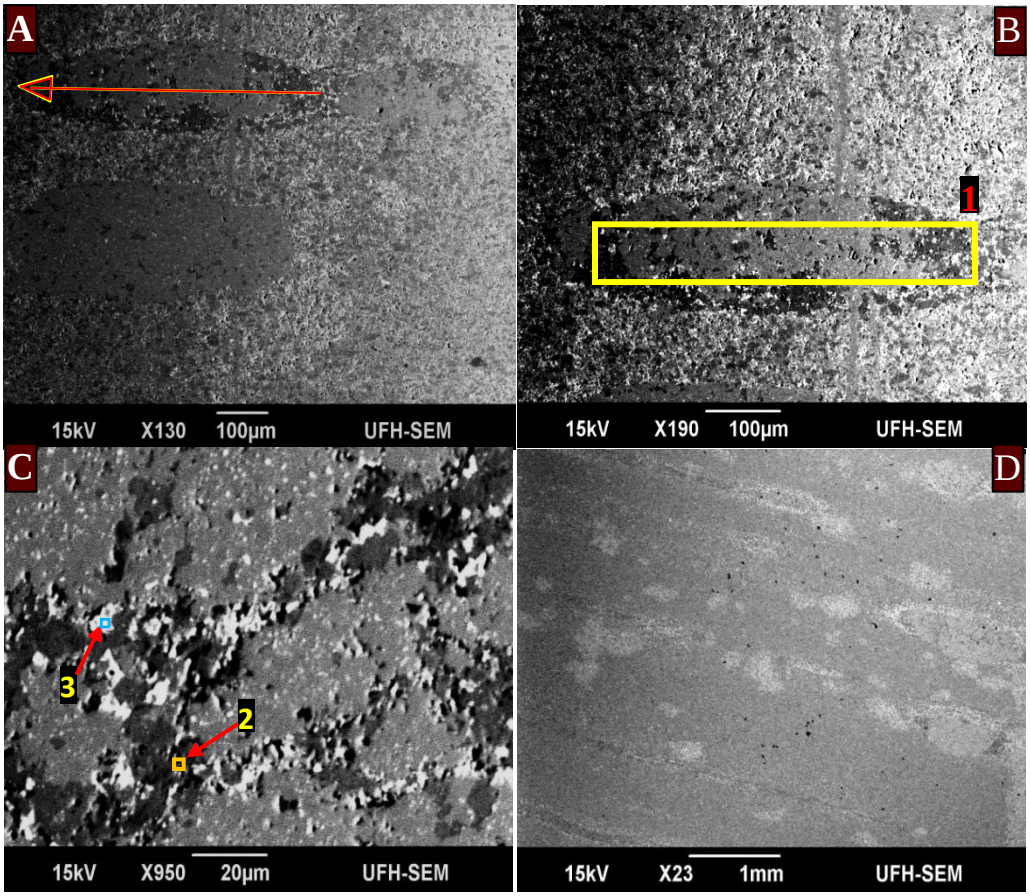

Weight % composition

Point	*C*	*O*	*Mg*	*Al*	*Si*	*S*	*Ca*	*Mn*	*Fe*	*Total*
1	7.02	40.59	1.75	–	1.26	0.00	7.67	40.87	0.82	**99.98**
2	5.86	42.30	12.16	0.22	15.84	0.01	2.81	18.59	2.20	**99.99**
3	6.65	39.61	8.78	–	10.48	0.02	2.93	26.78	4.75	**100**

Figure 3.12 SEM photomicrographs of C-zone at different scales. **(A).** Image showing oxidized carbonate ovoids in a braunite - kutnahorite matrix. The arrow inside an ovoid shows variation of elements (mineralogy) inside an ovoid and this is represented by the x-ray line scan pattern shown in Figure 3.11. **(B).** Enlarged view of an ovoid shown in the previous image **A.** Note the weight percent elemental composition of an ovoid (*analytical point 1*) **(C).** The ovoids are composed of dominantly hausmannite (see element weight % composition table – *analytical point 1*) with intergrowths of alumino silicate material, Mg–calcite, traces of hematite *(analytical point 3)* and braunite *(analytical point 2).* **(D)** The banding and laminations in the ore is attributed to dominant white small, amalgamated patchy oxide ovoids.

3.3.9 M-zone

The M-zone is a massively banded and laminated braunite lutite with 0.25mm – 2.4mm sized and widely scattered ovoids and clasts. Various ovoids have been partially altered and oxidized to braunite and occasionally hausmannite. Coarse-grained braunite is the dominant oxide mineral in the ore while Mg calcite and kutnahorite are dominant carbonate species.

Traces of hausmannite and hematite are present in small quantities and euhedral crystals (<5µm) of jacobsite inside an altered ovoid were observed. The M-zone towards the base shows an elevated ratio of braunite to kutnahorite. It is generally characterized by elevated braunite contents ranging from 48% to 53% hence it is regarded as the most economic zone.

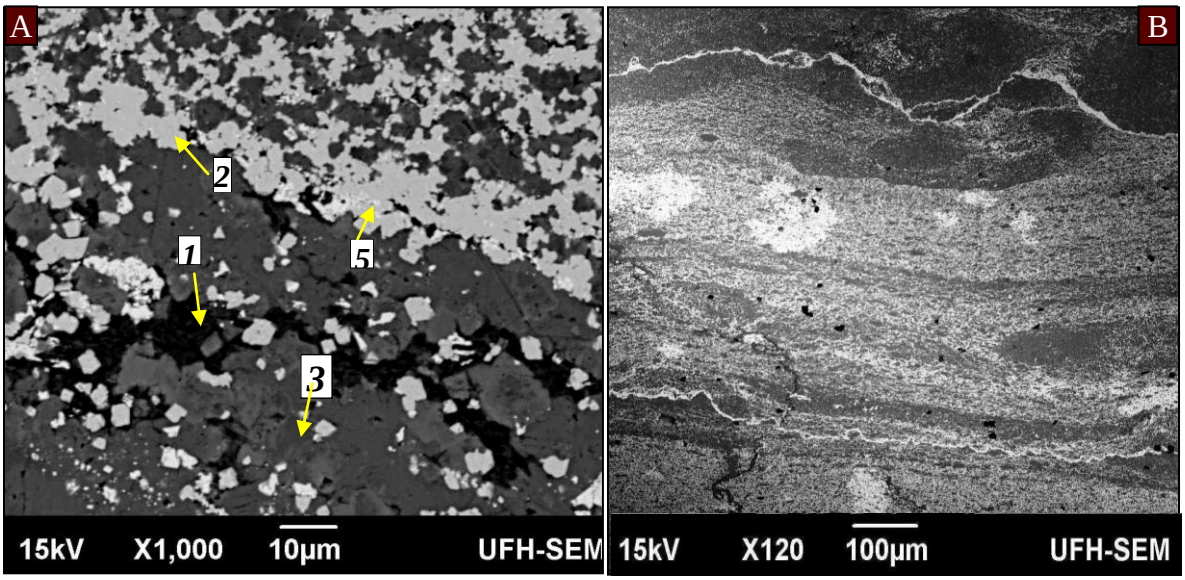

Figure 3.13 **(A).** Backscattered SEM images of M-zone showing stylolites of alumino silicate material *(1)*. Also shown are intergrowths of pure white hematite *(5)*, white braunite *(2)* and light grey manganocalcite *(3)*. **(B).** White laminae and patches of hausmannite with dark inclusions of silicate material.

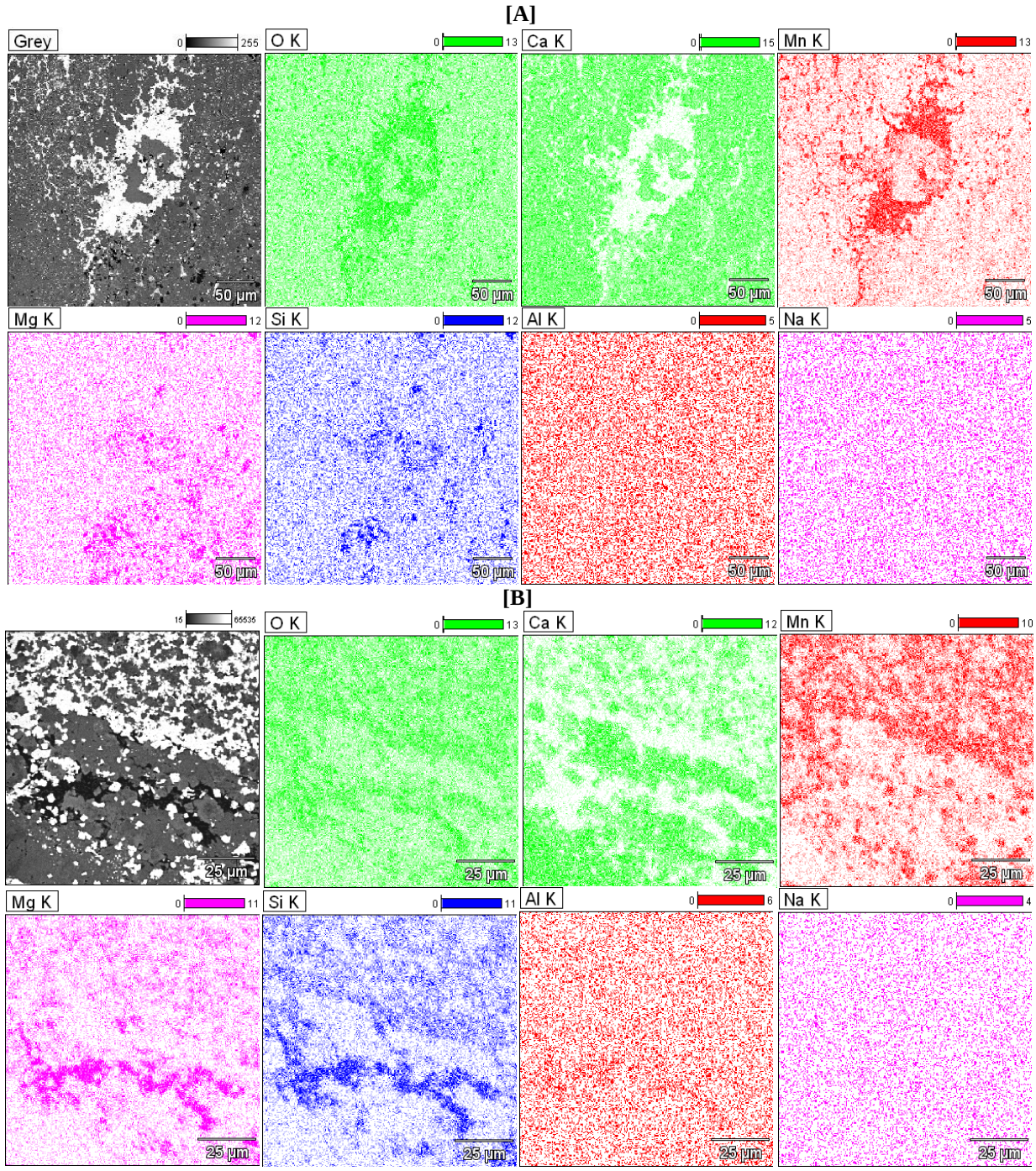

Figure 3.14 **(A)** SEM element spectral images (different scales) of M-zone showing enlarged view of carbonate laminae containing altered ovoid and dark stylolites of Mg–alumino silicate material. **(B)** Braunite-kutnahorite matrix contains fractures of Mg alumino silicate material and characterized by elevated Mg, Si, Al and O contents.

3.3.10 Y-zone

The Y-zone under the microscope is characterized by coarse-grained intergrowths of braunite, fine–grained kutnahorite, dark-gray to white laminae and amalgamated ovoids ranging from 0.1mm to 1.2mm. The ovoids display high proportions of braunite (Mn, Si and O) replacements with minor coarse inclusions of kutnahorite.

The elemental weight percent distribution analyses by SEM (Figure 3.15-A, *analytical point 1*) suggest that the ovoids are mainly enriched in braunite. Elevated Mn, Si and O contents correspond to braunite while Ca and Mg contents are associted with Mg–calcite. The euhedral subangular crystals of hausmannite occur together with braunite and are often concentrated along the fissures in the matrix. Platy slabs of strontium rich barite $(Sr,Ba)SO_4$ have been determined by SEM along the veins and brecciated zones.

Brecciated zone hosts the microcrystalline particles of Sr-barite crystals together with platy cystals of braunite (containing mainly Mg as impurity) and hausmannite in a silicate (garnet-serpentine) matrix (Figure 3.15 - C). Thick laminae dominantly composed of kutanhorite, Mg–calcite and calcite were also observed in a braunite-kutnahorite matrix. The Y-zone contains slightly high carbonate content and elevated braunite content and forms the upper portion of the Central Economic zone. The hausmannite and barite appear to be of secondary origin, braunite and kutnahorite in the matrix are of primary origin.

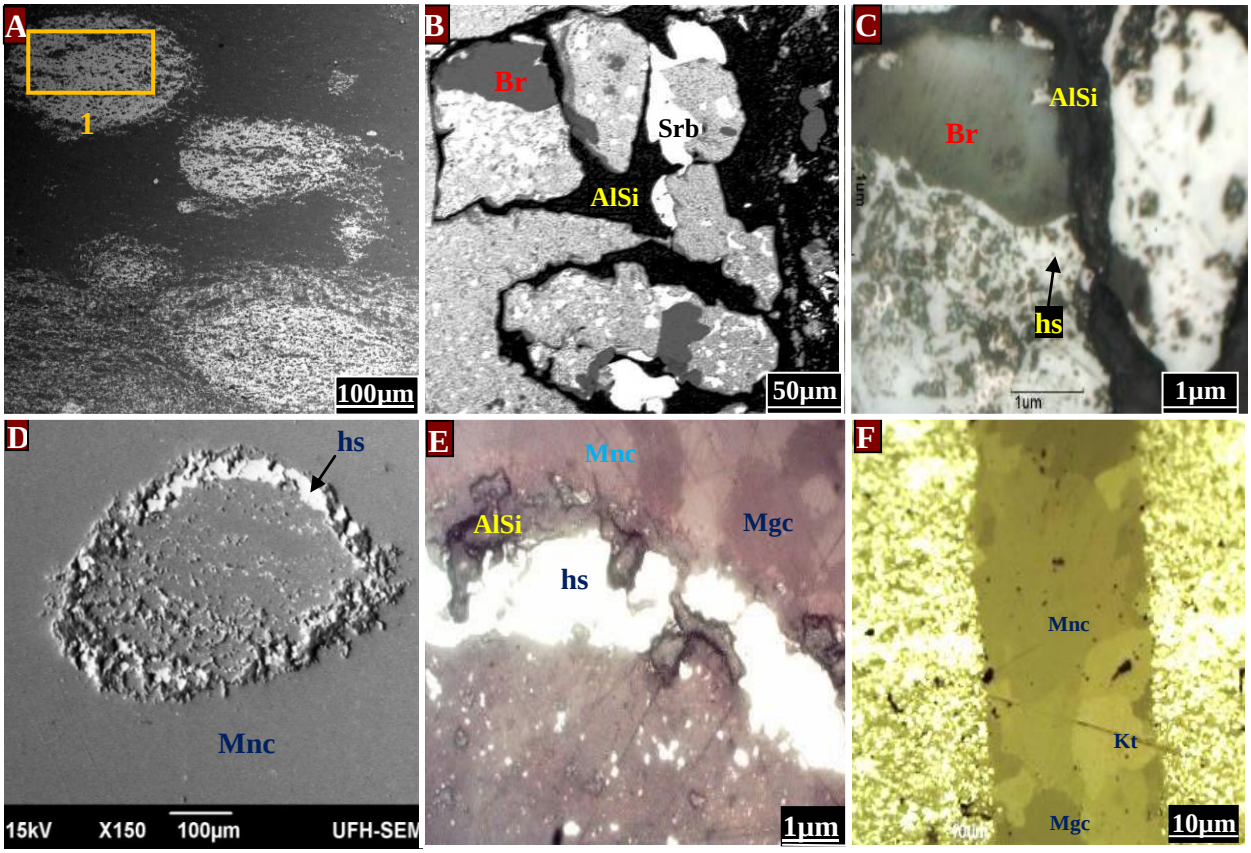

Weight% composition

Point	*C*	*O*	*Mg*	*Al*	*Si*	*S*	*Ca*	*Mn*	*Fe*	*Total*
1	5.73	33.35	4.34	0.44	6.09	0.07	8.65	38.51	2.81	99.99

Figure 3.15 **A**). Braunite–rich ovoids (by SEM) at Y-zone with minor concentrations of Mg–calcite and hematite. Note the weight % composition of elements (*analytical point 1*) inside oxide-rich ovoid where the elevated Mn, Si and O contents correspond to braunite and Ca and Mg contents with Mg–calcite and Mg–kutnahorite. **B**). Breccia texture of enlarged view (by SEM) of platy angular crystals of altered Mg-braunite (br) and mangenese Sr barite (Srb) coexisting with coarse grained hausmannite in a silicate fissure (garnet and serpentine)**. C)** Reflected light image showing the enlargement of the angular crystals as shown in image **B** (top left). Braunite coexist with hausmannite (light grey) – garnet (green to brown) – manganese strontium barite (white) assemblage in the alumino silicate (AlSi) fissure. **D**). SEM circular pattern of hausmannite (hs) and silicate (AlSi) material such as garnet and serpentine in a manganocalcite laminae. **(E).** Reflected light image of an enlarged view of hausmnnite (hs), Mn calcite (Mnc), Mg–calcite (Mgc). (**F**)**.** Reflected light image of a thick laminae composed of mixed carbonate phases such as Mg–Kutnahorite (Mg-kt), Mg–calcite and Mn calcite in a hausmannite-braunite-kutnahorite matrix.

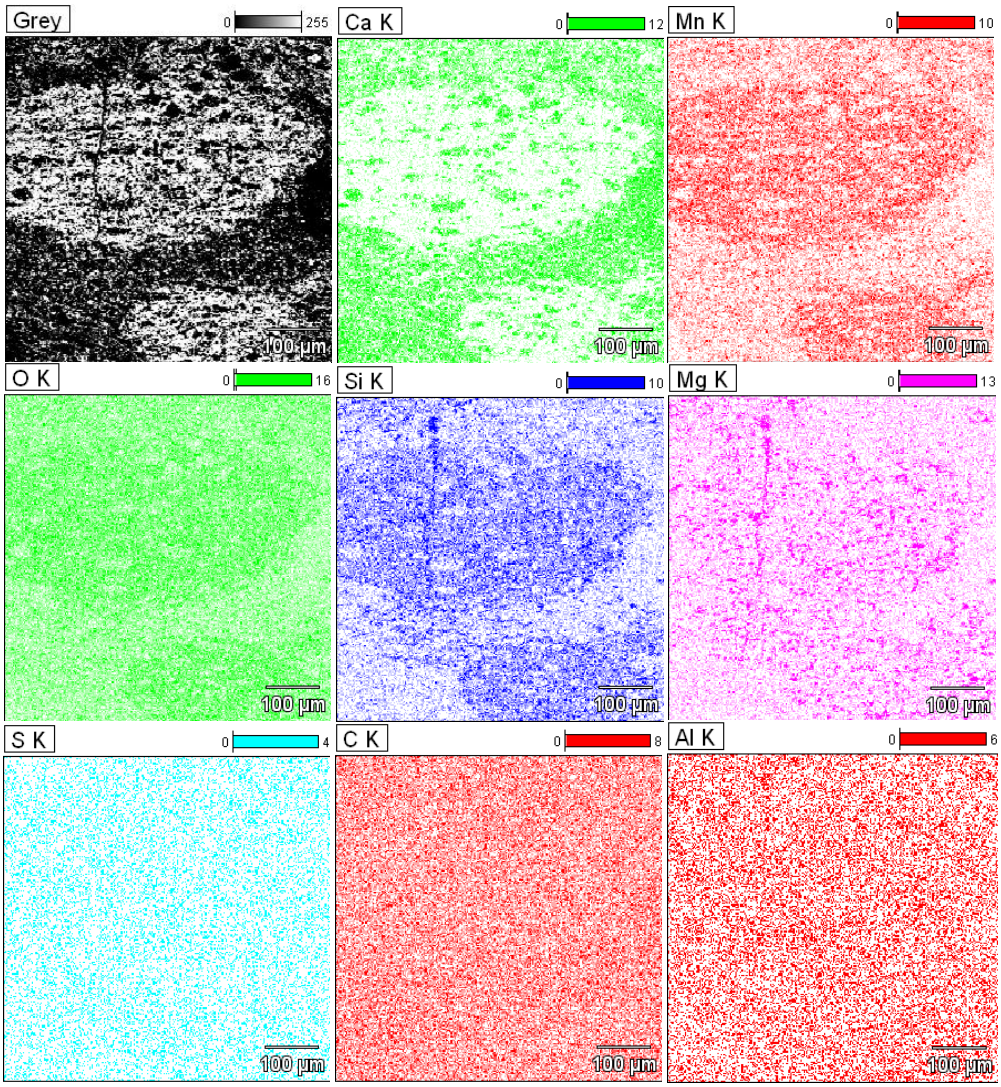

Figure 3.16 SEM spectral images showing various concentrations of elements in Y-zone. The coarse intergrowths of carbonate (Ca) content inside an ovoid are low while braunite (Mn, Si and O) contents are elevated. The Mg content is mostly concentrated inside ovoids and is mostly associated with the Mg–calcite or Mg kutnahorite. The oxidized ovoids contribute to the grade of the ore and Y-zone defines the upper portion of the central economic zone. Also note the vein crosscutting the larger ovoid.

3.3.11 X-zone

X-zone is characterized by microcrystalline coarse-grained (<4μm) braunite and kutnahorite which are dominant oxide and carbonate species respectively. The Mg-calcite determined by XRD is present as a major carbonate species while hausmannite, serpentine and hematite are present in trace amounts. Dark to light grey laminae and abundant ovoids ranging in size from 0.075mm to 0.45mm are composed of dominantly fine-grained kutnahorite and Mg-calcite. The ovoids are spherical and ellipsoidal and often contribute to the banded appearance of the ore (Figure 3.17–C). On SEM, the ovoids are characterized by elevated kutnahorite (Ca) content, low braunite (Mn, Si, O) and hematite (Fe) compared to the matrix.

Under transmitted light the X-zone is microcrystalline with laminae and scattered ovoids of manganocalcite (brown to light brown) often rimmed by calcite (white) in a matrix of braunite (dark) and kutnahotite (greenish white) (Figure 3.17–B). Dark inclusions of silicate material are observed in the matrix and outside ovoids. The zone is marked by a slight increase in carbonate content (Ca) both in the braunite-kutnahorite matrix and inside ovoid and this is attributed to the grading of the lower grade zones into more economic zones below. The X-zone therefore represents the base of the Upper low grade zones.

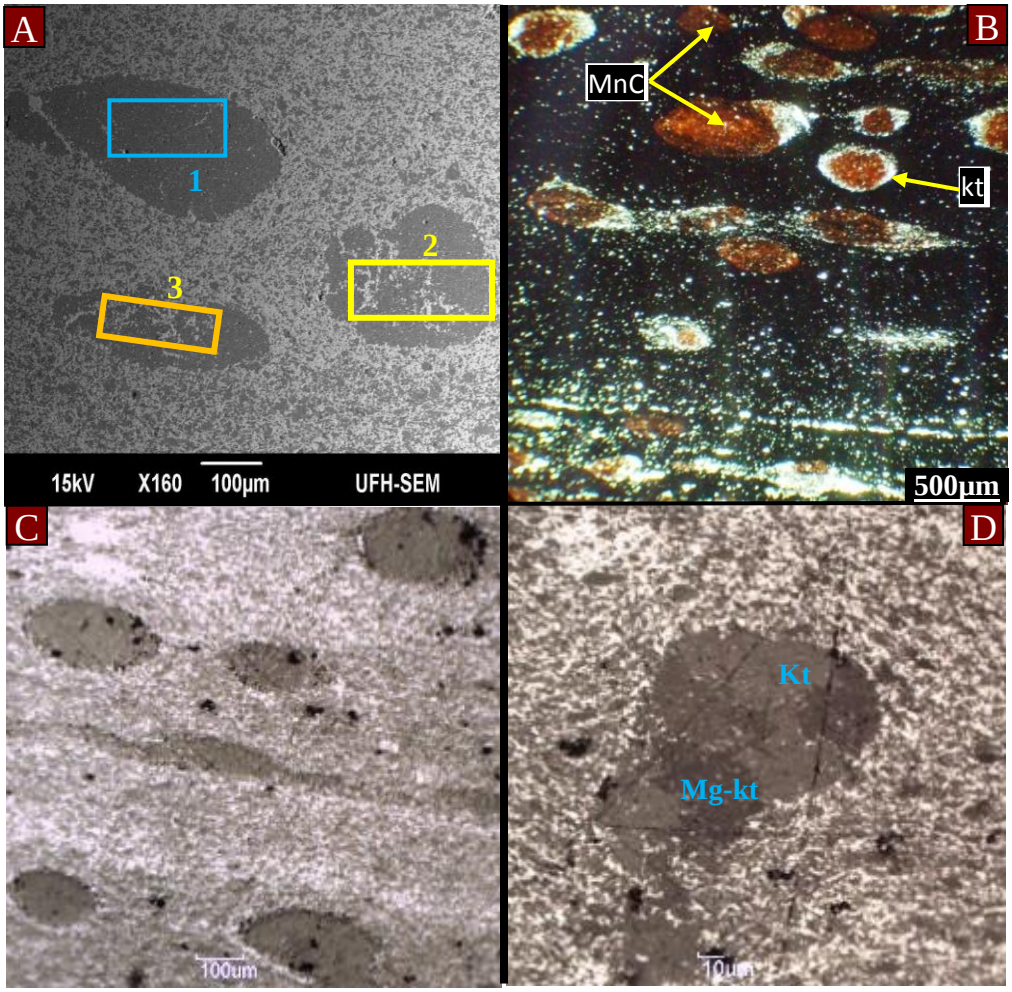

Weight % composition

Point	*C*	*O*	*Mg*	*Si*	*S*	*Ca*	*Mn*	*Fe*	*Total*
1	6.01	46.78	0.89	–	0.00	33.23	13.10	–	100.01
2	6.02	44.35	0.93	1.07	0.00	27.74	19.89	–	100.00
3	6.14	39.53	2.08	1.88	0.00	19.24	26.11	5.02	100.00

Figure 3.17**(A).** SEM images of X-zone (at different scales) showing intergrowths of braunite and kutnahorite in the matrix and ovoids. Note the table showing the weight % composition inside ovoids. The 1st ovoid shows abundance of kutnahorite and hausmannite (Mn, O), 2nd ovoid shows intergrowth of Mg-kutnahorite and braunite (Mn,Si,O) while the 3rd ovoid shows abundance of Mg–calcite, braunite (Mn,Si,O) and hematite (Fe). **(B).** Shows a transmitted light image of microcrystalline X-zone with intergrowths, laminae, scattered ovoids of manganocalcite often rimmed by kutnahorite (white) in a matrix of braunite and kutnahorite. **(C).** Reflected photomicrograph displaying dark inclusion of silicate material in the matrix and inside ovoids. **(D).** Enlarged view of an ovoid composed of dark–brown Mg–kutnahorite and light brown kutnahorite in the matrix.

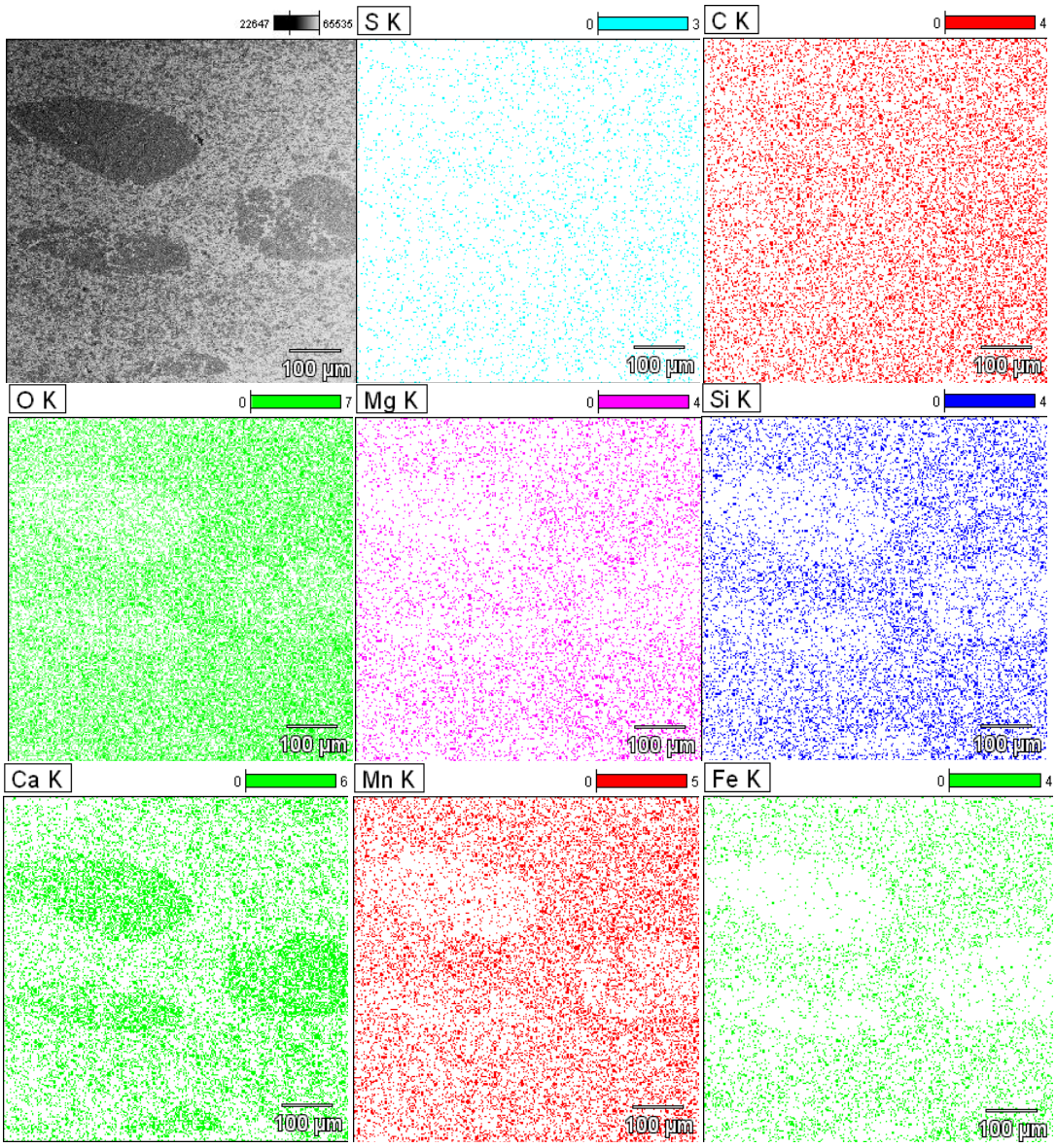

Figure 3.18 SEM spectral images showing the concentration of various elements in X-zone. The concentration of carbonate (Ca) content inside ovoids is elevated hematite (Fe, O) and braunite (Mn, Si and O) are most concentrated in the matrix. The Mg content is depleted or uniformely distributed inside ovoids.

3.3.12 W-zone

The W-zone under transmitted light microscope is characterized by brownish black microcrystalline matrix, yellowish brown to white laminae and spherical ovoids that contain a brownish-pink interior and white rims, thereby lending a somewhat "pea shaped" or "bird eye" appearance to the ore (Figure 3.19–C). The ovoids range in size from 0.08mm -1.2mm and together with some laminae are composed of dominantly white to medium brown ellipsoidal kutnahorite (pure white) ovoids.

Some ovoids are composed of light brown Mn–calcite in the core and milky white calcite in the rims. The elevated concentrations of Mn, Si, O, Ca and Mg determined by SEM represent the concentrations of braunite, Mg–calcite and kutnahorite. The low content of braunite at SKR 65 is attributed to dolomitization of the zone since dolomite is the most abundant mineral determined by XRD. Other minerals such as kutnahotite and Mg–calcite are present in major quantities while calcite, hematite and serpentine are present in variable proportions in both boreholes SKR 65 and SKR 40.

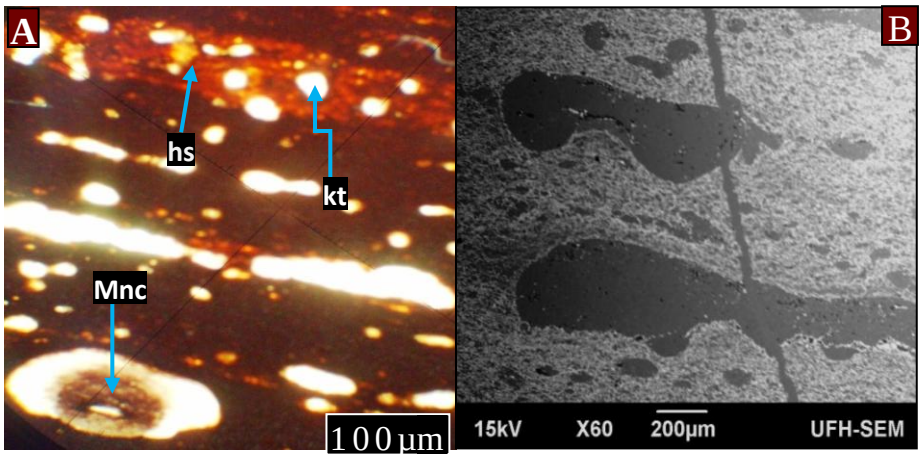

Figure 3.19 (**A).** Transmited light photomicrograph of W-zone of SKR 65 with dark–brown to reddish–brown matrix and concentrically and elongated "bird eye" Mn-calcite (Mnc) and kutnahorite (kt) ovoids and lenticles and some hausmannite (hs) laminae. **(D)** SEM photomicrograph of an elongate, amalgamated and, "bird eye" shaped ovoids that are bordered by carbonate vein.

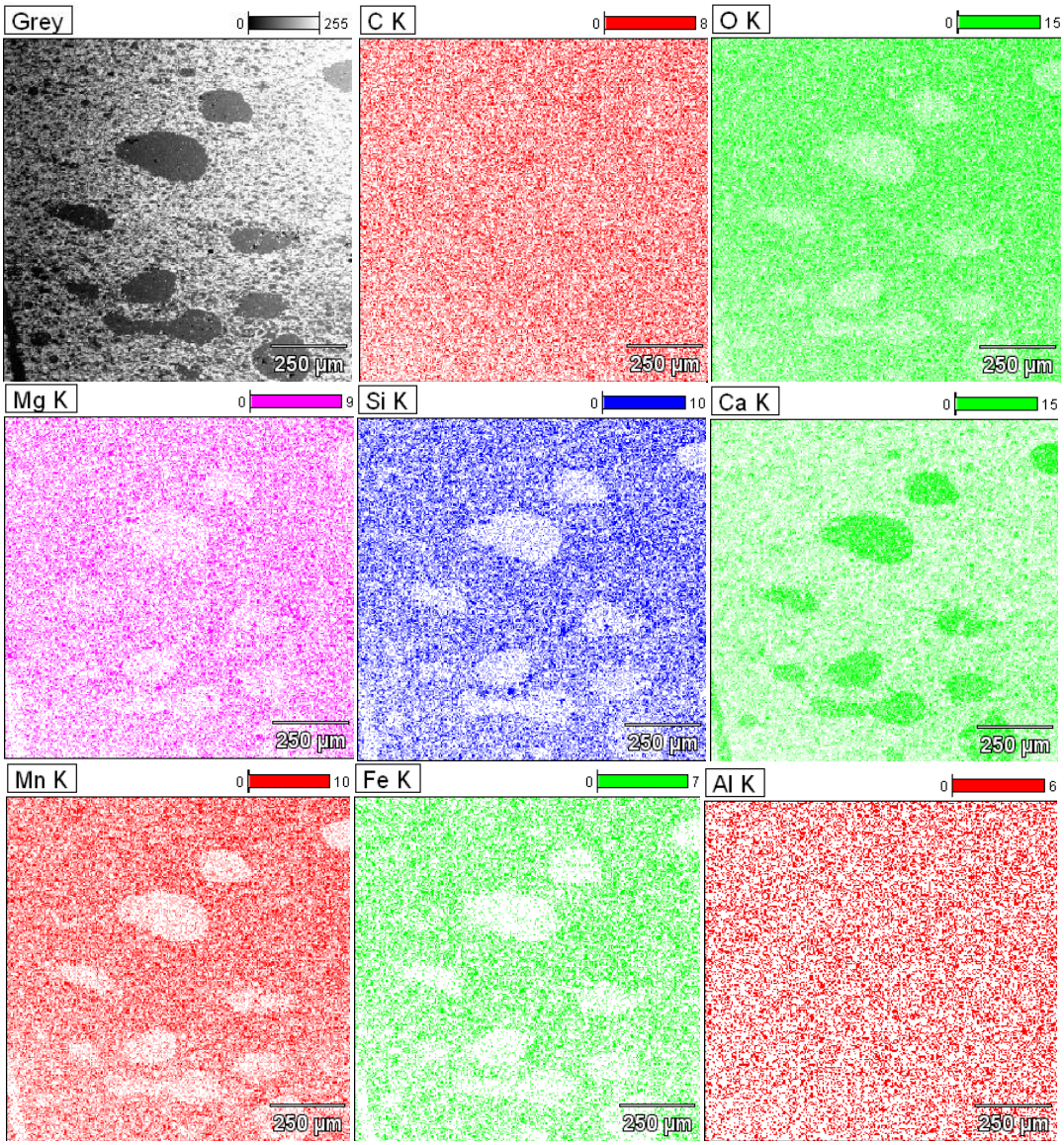

Figure 3.20 SEM spectral images of W-zone displaying elemental distribution inside ovoids and braunite – kutnahorite matrix. The ovoids are enriched in carbonates (Ca) while some elements such as Mn, Si, O, Fe and Mg are depleted and Al and C are distributed evenly. The carbonate (Ca) content is more concentrated inside ovoids while in the matrix is depleted. The elevated contents of Mn, Si and O together with Fe and Mg are compliant with braunite and hematite in the matrix.

3.3.13 V-zone

The zone is often characterized by dark-brown to black metallic appearance, fine grained braunite - kutnahorite matrix with spherical to rounded brown ovoids of various sizes from 0.08mm - 1.0mm. Coarse-grained braunite as determined by XRD is the dominant mineral and hematite, kutnahorite, calcite, Mg–calcite, hausmannite and serpentine occur in variable proportions from major to trace amounts.

The Mn-calcite ovoids are often rimmed by braunite and occasionally fine grained Ca-kutnahorite and coarse-grained Mg–kutnahorite (Figure 3.21–A). Traces of hematite are concentrated inside ovoids and in a braunite-kutnahorite matrix. Elevated contents of Ca, Mn, O and C with depleted Mg and Si contents (Figure 3.22) determined by SEM inside ovoids suggest the presence of Mn–calcite and very low concentrations of kutnahorite, braunite and/or hematite. Spectral images also show the same trend of elemental abundance (Figure 3.21). The combination of petrography microscopy and SEM analyses show that the braunite, hematite and kutnahorite are primary and are mostly intergrown in the matrix while Mg/Mn calcite and silicates are secondary.

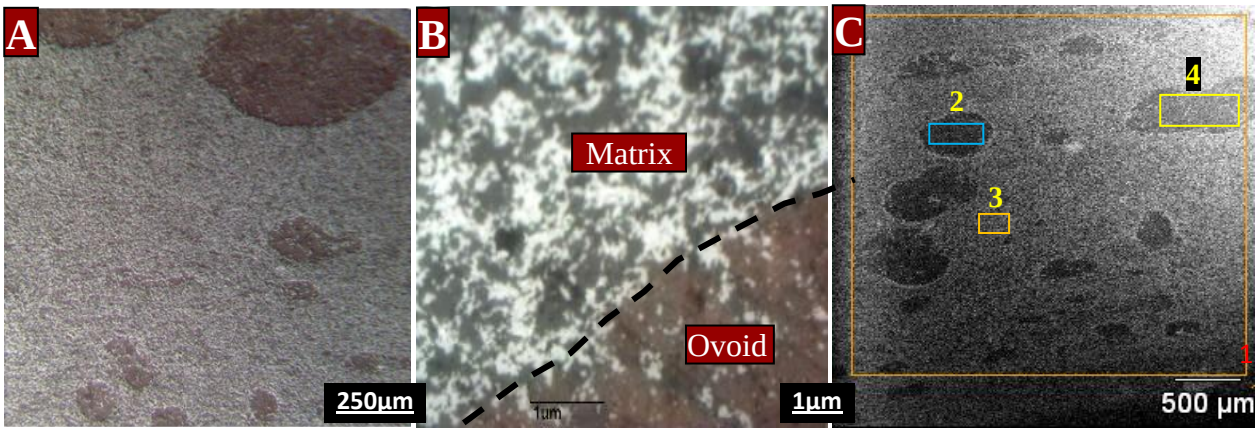

Weight % composition

Point	*C*	*O*	*Mg*	*Al*	*Si*	*S*	*Ca*	*Mn*	*Fe*	*Total*
1	6.72	38.8	2.90	0.26	3.37	0.03	15.65	25.26	6.99	99.99
2	6.70	44.1	0.81		0.58	0.04	31.06	15.65	0.79	99.75
3	6.39	37.0	3.55	0.18	4.04	0.01	12.61	27.37	8.80	99.98
4	6.42	43.8	0.70		0.63	0.02	29.52	18.22	0.62	100

Figure 3.21 . **(A).** Reflected light photomicrograph of V-zone displaying brown steel-grey ovoids of various sizes in a braunite-kutnahorite matrix. **(B).** Enlarged view (reflected light) of the braunite (white)–kutnahorite (light grey) matrix and Mn calcite (brown) ovoid. **(C).** SEM photomicrograph of V-zone showing an elemental weight % composition in a braunite-kutnahorite matrix (*analytical point 1*), inside ovoids (*analytical points 2* and *4*) and outside an ovoid (analytical point *3*).

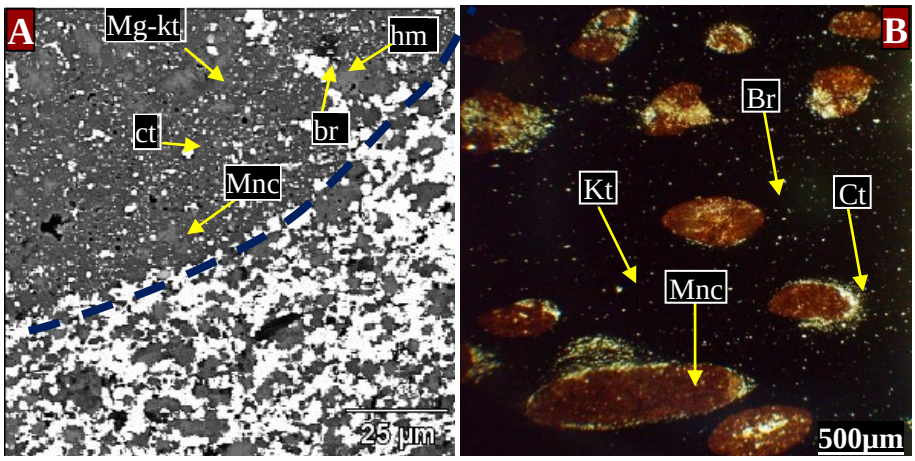

Figure 3.22 - (**A).** SEM image of V-zone showing an enlarged view of the ovoid (upper part) and the braunite-kutnahorite matrix (lower partsof the dotted line). Note concentration and intergrowths of Mg-rich kutnahorite (Mg-kt), Mn–calcite (Mc), calcite (Ct), braunite (br), and hematite (hm) in an ovoid. **(B).** Typically of **V-zone** as viewed under transmitted light with widely scattered brown to brownish white carbonate ovoids of various sizes in a braunite-kutnahorite matrix.

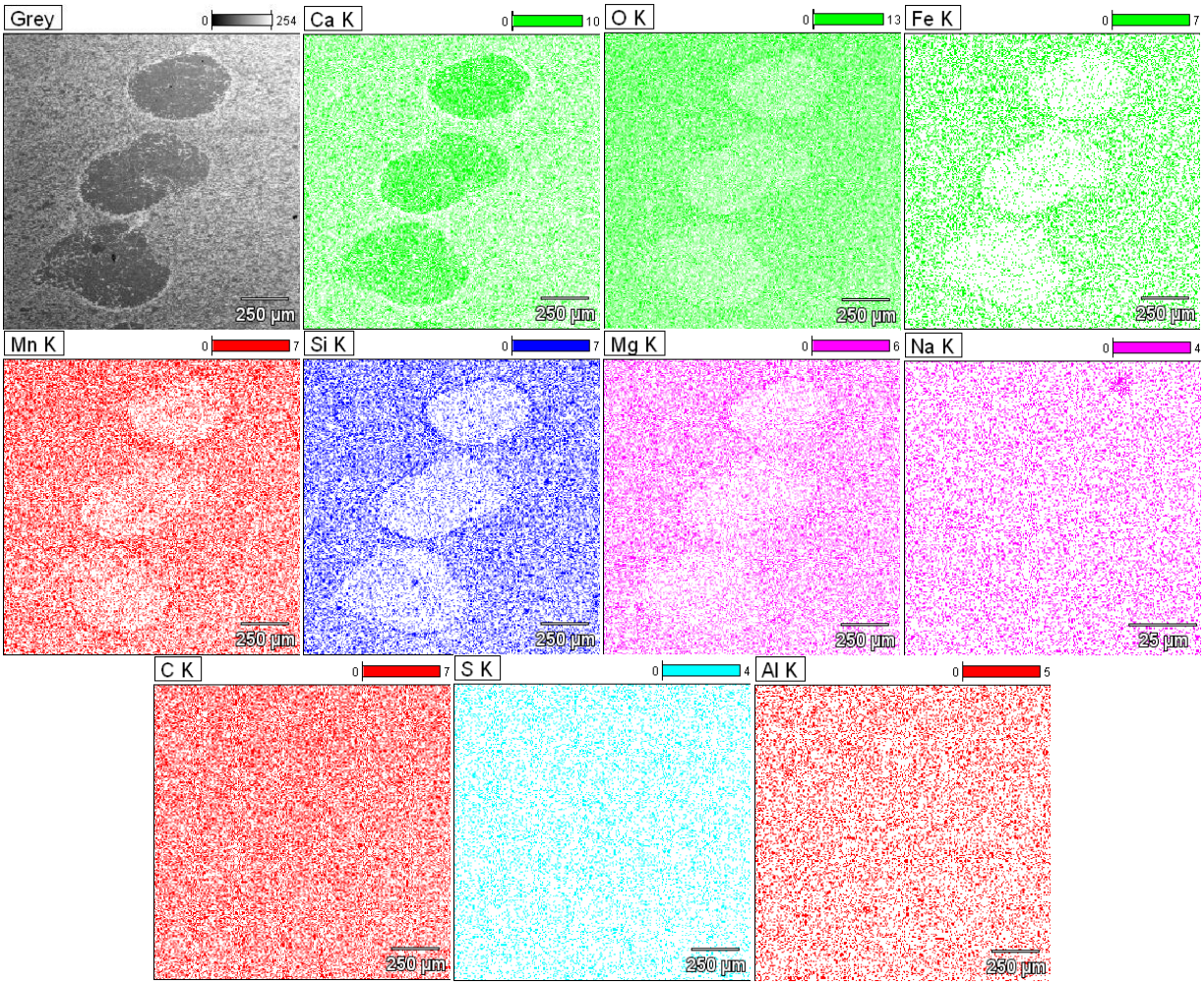

Figure 3.23. SEM spectral images of V-zone displaying elemental composition of a braunite-kutnahorite matrix bearing three carbonate ovoids. Note the elevated concentrations of Ca, lower Mn, Si and O and depleted concentrations of Fe and Mg inside an ovoid while other elements are distributed evenly. This indicates the dominance of carbonates and depletion of oxides inside an ovoid. The ovoids are rimmed by braunite and hence the concentration of Mn Si and O are elevated in the matrix while Ca contents are slightly lower. This is an indication of the dominance of braunite and lower carbonate content in the matrix.

3.3.14 J - F zones

The orebody displays both lateral and vertical variation in physical characteristics, mineralogy and chemical composition. The X-zone towards the top is characterized by eleveted hematite, kutnahorite and rhodochrosite with slightly lower braunite, calcite and jacobsite, an indication of grading into **J-zone**. Braunite content at J-zone reaches a maximum of 30% with widely scattered, small (<50μm) and medium sized (>400 μm) carbonate ovoids are characterized by dark granular grains of silicate material.The upper part (**F-zone**) of the orebody is characterized by reddish pink to brownish-red hematite-lutite. Hematite is a dominant gangue mineral, rhodochrosite which is responsible for the pink color is a major carbonate species while braunite, calcite, Mg–calcite and kutnahorite concentrations are depleted.

3.4 Discussion

Profiles for mineralogical variation in the manganese ore are created for certain zones in order to compare the results obtained from both labs (see appendix for complete XRD results). Apart from jacobsite content, data for B-zone from Mintek compared to CGS on SKR 65 show higher hematite contents, lower Mg–calcite, kutnahorite and no hausmannite, serpentine or garnet material. Mintek also reported traces of calcite on both boreholes for the zones V, W, X, Y and N2-subzones.

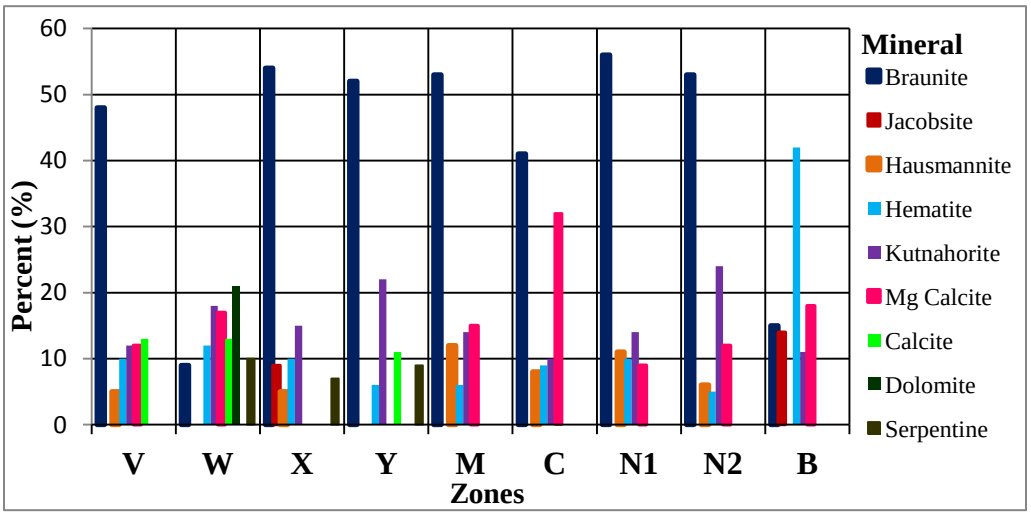

Figure 3.24 A profile of X-ray diffraction analyses of selected zones at borehole SKR 65 as reported by Mintek. The braunite content is elevated in most zones except at W and B-zones due to dolomitization and ferruginization respectively.

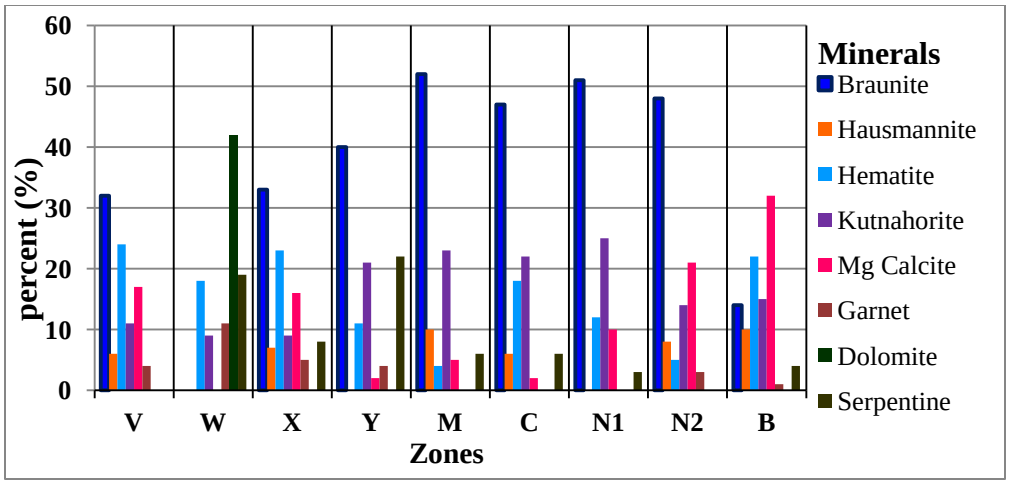

Figure 3.25 A profile of X-ray diffraction analyses of selected zones at borehole SKR 65 as reported by CGS. The braunite content is elevated in most zones while in W-zone was not detected. Garnet and serpentine were also determined in most zones.

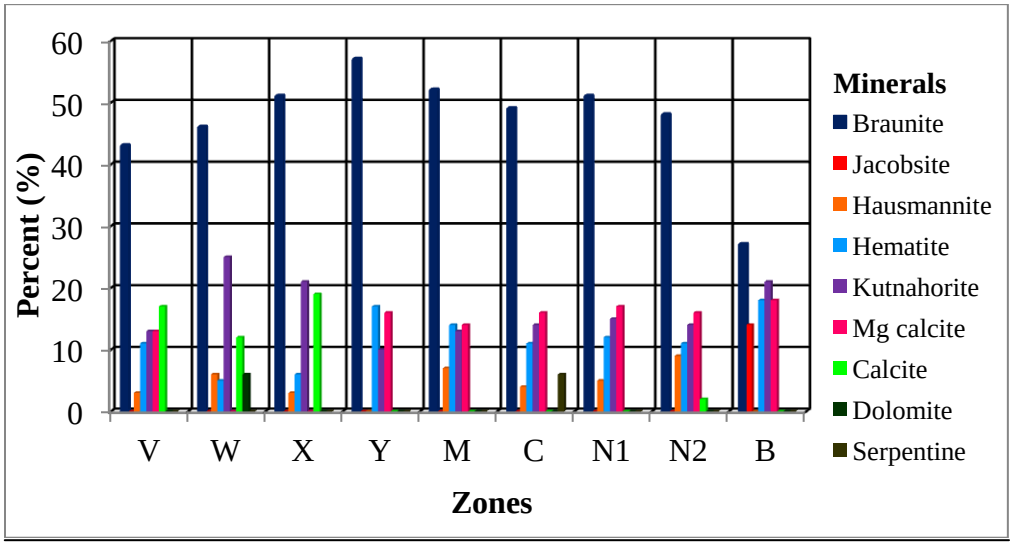

Figure 3.26 A profile of X-ray diffraction analyses of selected zones at borehole SKR 40 as reported by Mintek. Note the calcite content at V, W, X and N2 subzone. The Mg–calcite is comparably higher than kutnahorite at Y, M, C, N1 and N2 subzones.

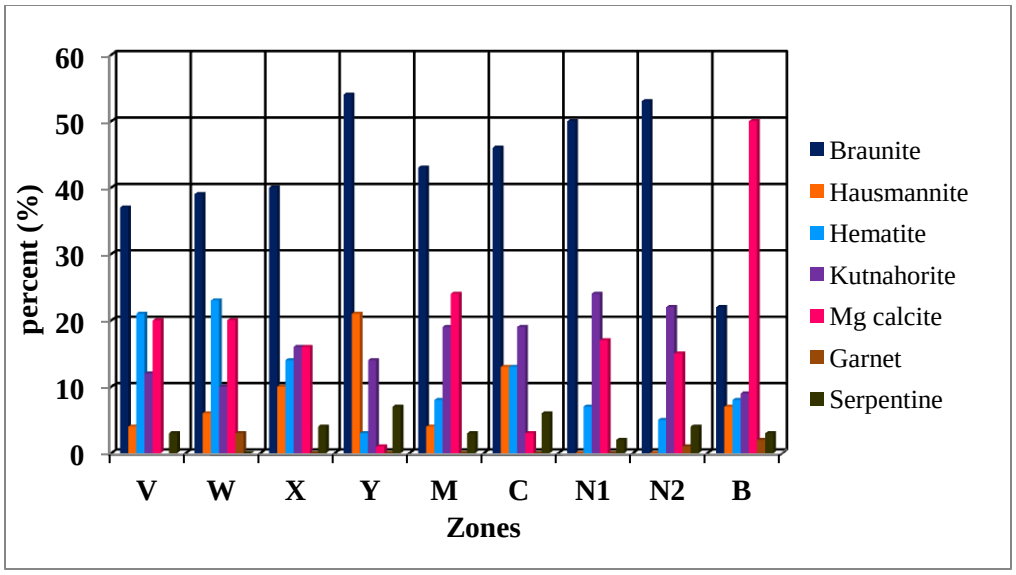

Figure 3.27 A profile of X-ray diffraction analyses of selected zones at borehole SKR 40 as reported by CGS. The Mg–calcite is elevated at B-zone and together with kutnahorite and hematite show an inverse correlation with manganese. Hausmannite is more elevated in Y-zone and hence the higher braunite content observed.

The minerals encountered in the study are further explained based on the time sequence and genetic order of deposition, refered to a paragenetic sequence. This is achieved through detailed microscopic studies by observing certain features such as textures, banding, laminations, ovoids, open-space fillings and replacements in order to understand development and post depositional history of the ore. Furthermore, it is known that certain minerals can be deposited simultaneously or one after another and this provides clues on the sequence of mineral formation. A summary of list of minerals encountered in the study and their genetic sequence of formation is discussed.

The paragenetic sequence and evolution of manganese minerals in the Kalahari deposit has been extensively studied by many authors and can be further subdvided into sedimentation, diagenesis and metamorphism in origin. A table highlighting the depositional history of the manganese ore and gauge minerals is presented below and the latter two are further grouped into four broad categories, oxides, carbonates, silicates and sulphates.

Table 3.1. List of minerals encountered in the study with their ideal chemical composition, texture and possible mode of formation.

Mineral	Chemical Formula	Texture	Mode of Formation
Braunite	$Mn^{2+}Mn_6^{3+}SiO_{12}$	Mostly microcrystalline	Primary
Kutnahorite	$Ca\ (Mn,Mg)(CO_3)_2$	Mostly microcrystalline	Primary
Mg calcite	$(Ca, Mg)CO_3$	Mostly crystalline	Primary → secondary
Mn calcite	$(Ca,Mn)CO_3$	microcrystalline	Primary
Hematite	Fe_2O_3	Crystalline to granular	Primary
Hausmannite	Mn_3O_4	Granular	Primary or Secondary
Calcite	$CaCO_3$	Crystalline (globular)	Secondary
Jacobsite	$Mn\ Fe_2O_4$	Granular	Primary or secondary
Garnet(Andradite)	$Ca_3F_2Si_3O_{12}$	concretionary	Secondary
Serpentine	$(Mg, Fe)_3Si_2O_5(OH)_4$	granular	Secondary
Barite	$BaSO_4$	granular	Secondary

.

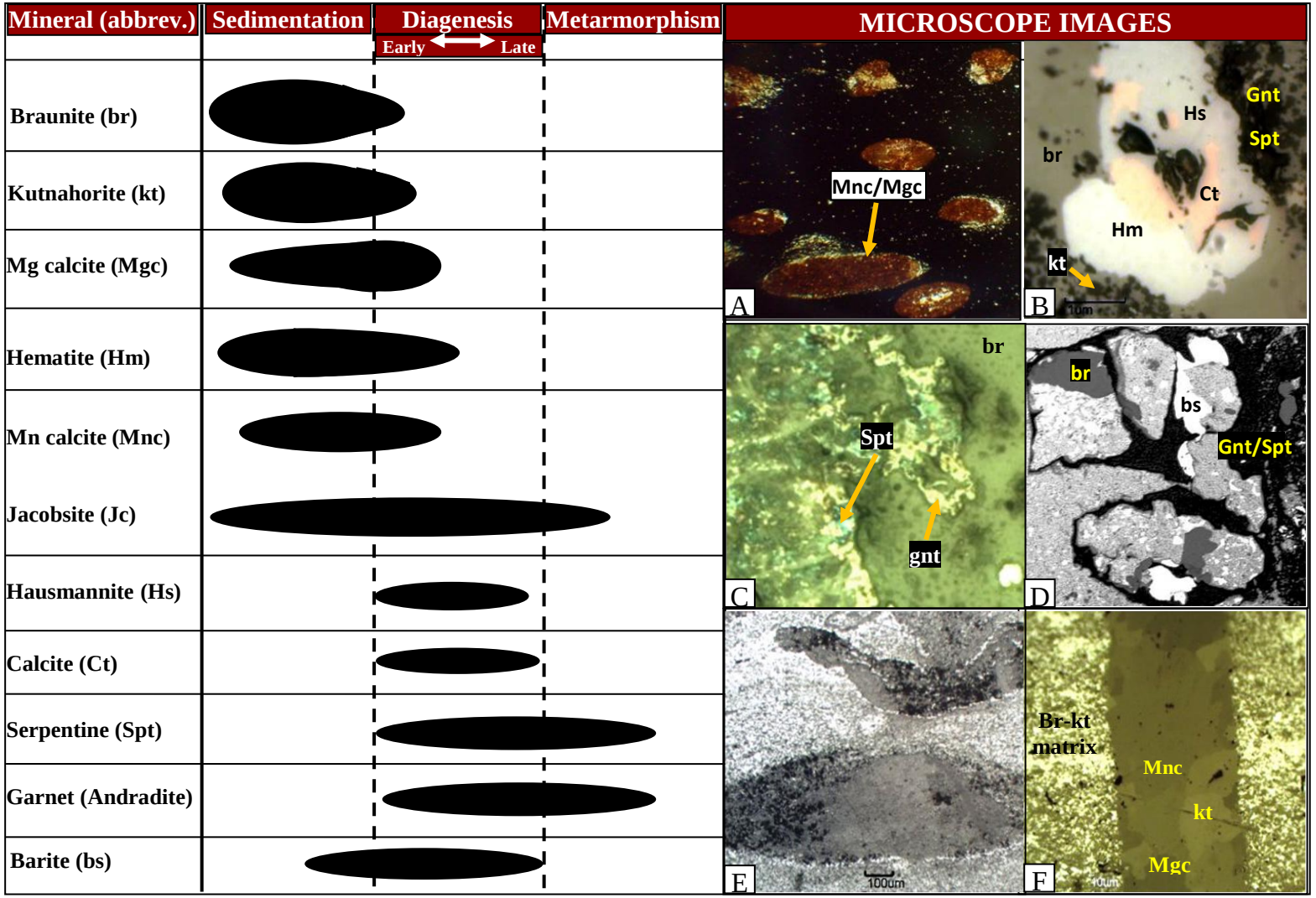

Figure 3.28 The paragenetic sequence diagram for minerals encountered in the study with some petrographic and SEM images. **A).** Mg/Mn-calcite ovoids in a braunite (dark)-kutnahorite (white) matrix under transmitted light. **B)** – **C)** Reflected light images showing mineral associations such as braunite (br), hausmannite (hs), hematite (hm), calcite (ct), kutnahorite (kt), garnet (gnt)-yellowish brown and serpentine (serp) – green. **D)** Backscattered light image (SEM) showing subheudral platy grains of barium sulphate (bs) and braunite (br) along an alumino silicate material. **E)** to **F)** Reflected light images showing carbonate ovoids and laminae.

Oxides

Hausmannite (Mn_3O_4) is the second most common manganese oxide mineral and occurs in most zones. It was determined in almost all samples investigated by an XRD and forms pure white to light grey euhedral to subhedral crystals (20µm to 120µm) under reflected light microscope and SEM. Hausmannite under reflected light is often characterized by greyish-white to creamish white colour while on transmitted light it is brownish red. Review of literature reveals that the structure of hausmannite is tetragonal almost similar to that of Fe_30_4 spinel.

The coarse-grained intergrowths and subangular crystals (±3mm) of hausmannite are easily distinguished in Y, M, C and N – subzones and occur mostly in association with calcite, recrystalized hematite and braunite inside manganocalcite/kutnahorite ovoid or laminae. The Fe-rich variety of hausmannite is prominent at N2-subzone and Nel et al. (1986) have previously reported Y-zone (Figure 3.12 - C, point 3) and the replacements of Mn calcite by hausmannite.

The SEM spectral images indicate that the hausmannite rich ovoids and laminae are enriched with Mn and O but devoid of Si while braunite rich ovoids show enrichments of Mn, O and Si. The hausmannite is of early to late diagenetic origin as it replaces mostly primary minerals in ovoids and laminae. The hausmannite defined is also similar to the oxidation hausmannite described by Kleyenstüber (1984) as an oxidation product derived from carbonates of Mamatwan-type ore (Figure 3.9-E and Figure 3.10 - D & E) and it occurs as irregular patches. Hausmannite coexists inside ovoids or laminae with braunite, hematite, calcite, Mg-calcite and/or alumino silicate materials (Figure 3.15-B) and in rare cases with barite (Figure 3.9 - C, *point 5*). The suggestion by

Kleyenstüber (1984, as cited in Gutzmer and Beukes 1996) that the hausmannite replacement in a carbonate laminae is later than hausmannite replacements in Mn-bearing carbonates ovoids could be correct. Close observations on Kalagadi mine show that the hausmannite inside ovoids can replace an early diagenetic kutnahorite (Figure 3.9- C and D) and primary braunite in some laminae (Figure 3.9 – D to F).

However Gutzmer and Beukes (1996) suggested that the hausmannite in ovoids and that on laminae are of similar composition and character. The abundance of hausmannite often gives ore a shiny metallic appearance and form through low temperature oxidation of manganese-rich carbonates in the Mamatwan type ore (van Staden, 2002). The ovoids in the M and N subzones are partially or completely oxidized to hausmannite (Nel et al, 1986) at Kalagadi Manganese mine.

Hematite (**Fe_2O_3)** is an abundant gangue mineral in the manganese ores and is concentrated mostly in the upper low grade zones and basal low grade zones as microcrystalline subhedral replacements or inclusions in a carbonate laminae or ovoids. Hematite is more abundant in the topmost and lowermost zones while in the middle zones it is intergrown mostly with braunite and kutnahorite in the matrix hence it is of primary origin. Hematite is also often enclosed by hausmannite inside ovoids and laminae in a braunite-kutnahorite matrix and such observations suggest that it may also be of secondary origin.

Jacobsite ($MnFe_2O_4$) is a member of the spinel group mineral, is a primary mineral and an alteration product of the manganese-bearing minerals, and has been determined by XRD in the upper J and V-zones and lower B-zone. It occurs as fine-grained intergrowths in the braunite-

kutnahorite matrix and often occurs in association with hausmannite and hematite in some laminae. Kleyenstüber (1984) and van Staden (2002) also indicated the development of jacobsite at the top and at the bottom of the LMO. However, Nel et al. (1986) at Mamatwan mine reported the occurrence of jacobsite only at the base of the orebody and has since attributed the absence of jacobsite at the top of the orebody to the oxidation prior the deposition of the Kalahari Group. Jacobsite, under SEM, is characterized by elevated concentrations of Fe, O and Mn in order of abundance and is mostly associated with braunite, hausmannite, and kutnahorite.

Sulphates

The **barite** (**$BaSO_4$)** is a rare gangue mineral in the manganese ore and it has been identified in trace quantities on SEM along the veins and inside the oxide-rich ovoids of N-subzones (Figure 3.9–C and F). The Sr-barite observed at Y- zone is concentrated along fissures as platy granular crystallite and is often associated with braunite and hausmannite in an Mg-rich silicate matrix (Figure 3.9).

The barium sulphate replaces diagenetic kutnahorite and the silicate material inside ovoids, veins and fissures. The occurrence of barite in the low grade Manganese-Type ore has not been previously reported (Kleyenstuber, 1984 and Gutzmer and Beukes, 1996) until recently (Preston, 2001 and van Staden, 2002). The occurrence of such scarce gaunge mineral is often associated with hydrothermal Wessel type ore as vein or the vug-fillings (Gutzmer and Beukes, 1995 and 1996).

Carbonates

Kutnahorite – Ca (Mn, Mg) (CO_3)$_2$ is a common and dominant carbonate mineral in the manganese ore and its dominance is characteristic common of the entire Kalahari deposit. The texture of kutnahorite is fine-grained (<6µm) with dark-grey intergrowths inside ovoids and in matrix. It is mostly intergrown with braunite in the matrix and occasionally found in association with hausmannite, hematite and Mg-calcite. Elemental spectral images from SEM analyses show patches of Ca and Mg both inside the ovoids and occasionally as intergrowth in a matrix.

Preston (2001) identified these patchy images as Ca-kutnahorite or Mg-kutnahorite at Mamatwan mine and similar composition was also described by Van Staden at Gloria mine. Kleyenstüber (1984) identified the Mg kutnahorite (Ca (Mn, Mg) (CO_3)$_2$) as the most common carbonate species with Ca-kutnahorite (Ca Mn (CO_3)$_2$) as representing the excess $CaCO_3$ in the ore. The suggestion by Nel et al. (1986) that Mg-rich kutnahorite (dark-gray) is later in a diagenetic sequence compared to Ca-rich/ Mg-poor kutnahorite (light-gray) is therefore correct.

Mg-calcite [(Ca, Mg)CO_3] is a calcite species rich in magnesium and a gangue carbonate in the manganese ore. The Mg-rich calcite is the second most abundant carbonate species and was determined on all samples analyzed by XRD and it occurs as dark-to-dark-grey granular crystals (<10µm) mostly inside ovoids. However, the high concentrations of Mg–calcite as determined in the study were not previously reported in the Kalahari Manganese Field. Instead, the Mn-calcite [(Ca,Mn)CO_3] in the low grade Mamatwan type ore and surrounding mines has been previously

reported, at Gloria mine by van Staden, (2001) and Chetty (2008) and at Mamatwan mine by Nel et al. (1986) and Preston (2001).

This Mn-rich calcite variety was not determined on the samples submitted for XRD analyses and the manganese is thought to have been replaced by magnesium. Pure calcite ($CaCO_3$) was also identified on certain zones by XRD and under transmitted light microscope since it is a transparent mineral and is mostly concentrated in the matrix and on the rims of ovoid especially in the upper low grade zones.

Rhodochrosite ($MnCO_3$) is a carbonate species and is only restricted to the upper F and J zones and the lower L-zones. Nel et al. (1986) identified Ca-rhodochrosite and rhodochrosite among the manganese carbonate species in the upper and lower parts of the ore bed at Mamatwan mine, and they occur in association with hematite lutite. Rhodochrosite under microscope was not easily identified but review of literature on the ore of this type suggests that it is of primary origin.

Silicates

Braunite ($Mn^{2+}Mn_6^{3+}SiO_{12}$) is the most dominant mineral and a major constituent of the manganese ore. The two polymorphs of braunite, the braunite I and II are known in the Kalahari deposit (Kleyenstuber 1984, 1993; Miyano and Beukes, 1987). The former is found in the sedimentary Mamatwan-type ore in the south while (together with the latter) it is mostly found in the hydrothermally altered Wessels type ore. The microcrystalline crystals of primary braunite (Kleyenstüber, 1993) are commonly intergrown with kutnahorite in a matrix and occasionally replace the carbonate ovoids (Figure 3.16) and this suggests sedimentary to early diagenetic origin for braunite. Close observations show that the braunite-rich ovoids as observed in Y – zone are often intergrown with coarse-grained Mg kutnahorite in the braunite-kutnahorite matrix.

Serpentine ($(Mg, Fe)_3Si_2O_5(OH)_4$ is a magnesium iron silicate hydroxide determined in trace quantities by XRD analyses. Two members of serpentine, antigorite – $Mg_6(OH)_8Si_4O_{10}$ and caryopilite - $Mn_6(OH)_8Si_4O_{10}$ were described in detail by van Staden (2001) at Gloria mine as occurring along bedding-parallel carbonate veinlets, along the margins of carbonate ovoids and in stylolites. The black fissures, intergrowths and inclusions in the manganese ores, ovoids and laminae represent the silicate material such as serpentine. Serpentine material is often bluish to greenish in colour, and is considered to be of secondary origin and is late in a digenetic sequence.

Garnet (andradite – $Ca_3F_2Si_3O_{12}$)

Garnet mineral was reported in trace quantities in some of the zones analyzed by XRD at CGS. Various species of garnet are known and observations under reflected light microscope analyses suggest that andradite which is recognizable from its brown to brownish-yellow as the only garnet species occurring along the veins.

It often occurs in association with serpentine and together form dark to brownish green bands and zoning while hausmannite, hematite and calcite are also present in this association. Andradite is the secondary mineral and hence represent late diagenetic to metamorphism in a genetic sequence. The possibility for the occurrence of grossular **(**$Ca_3Al_2(SiO_4)_3$), another variety of garnet, cannot be ruled out. Although it was not positively identified by microscope, SEM analyses often displayed higher picks of aluminum (Al) and calcium (Ca) contents. The occurrence of these varieties of garnet in the Kalahari deposit has often been associated with hydrothermal Wessels-Type ores.

3.5 Conclusion

The results from this chapter show that:

1) About twelve different mineral associations, of the LMO at the Kalagadi Mine have been identified by XRD, SEM and petrographic microscope. The identification and observation of the minerals and textures provided clues to the origin, paragenetic sequence and/or post depositional alteration history of the ore.
2) The following minerals were identified in order of abundance: braunite, kutnahorite, Mg-calcite, hausmannite, hematite, serpentine and dolomite, jacobsite, calcite, rhodochrosite and trace amounts of garnet. Mn-calcite and barite were only identified as traces by SEM and/or petrography microscope. The occurrence of garnet mineral as reported by CGS was confimed by microscopy and it often occurred in association with serpentine. A table of all minerals encountered throughout the study, their chemical composition, texture and possible mode of formation is presented above.
3) Close observation shows the existence of negative relationship between manganese versus carbonate and hematite minerals. The uppermost zones (F, J, V, W, X) and the lowermost zones (B and L) are often characterized by either or both elevated carbonate and hematite contents while depleted manganese contents.

4) It is concluded that, the ore in the upper zones is capped by ferruginized zones (F and J) and is generally characterized by elevated carbonate content both inside ovoids and in the matrix. Ovoids in these zones are enriched in carbonate content than in the matrix and the Mg/Mn-calcite is occasionally replaced by minor quantities of hausmannite, serpentine and braunite (subzones V, W and X). The replacement of carbonates by hausmannite is evidence of diagenetic or hydrothermal alteration and the variation in ore grade is attributed to change in carbonate concentrations (Kleyenstűber, 1993). The carbonate content inside an ovoid

decreases towards the middle economic zones where the ovoids are more enriched in hausmannite and/or braunite. The central economic zone is capped at the top by fine grained Y-zone bearing ovoids that are oxidized to braunite. The central economic zone includes Y, M, C and N subzones and is characterized by varying degrees of oxidation and alteration.

5) The M, C and the N1subzones are often characterized by almost pure hausmannite-rich ovoids with occasionally coarse dark intergrowths and inclusions of Mg kutnahorite and alumino silicate material respectively. Nyame (2007) suggested that the dark inclusion in carbonate minerals represent the post depositional diagenetic or metamorphic replacements of carbonates by alumino silicate mineral. The sedimentary features such as fine laminations and "dusty" hematite (Preston, 2001) and the diagenetic dark inclusion and intergrowths of alumino silicate material such as garnet and serpentine are interpreted as representing sedimentation followed by post depositional diagenetic alteration.

6) The Mg patches in the ore are associated mostly with Mg–calcite, Mg silicate material and to a lesser extent Mg-kutnahorite. The SEM spectral images show that the dark areas are enriched in Mg, which is intimately intergrown, with Si inside ovoids and laminae while other elements are depleted. Such association represents the silicate material. Nel et al. (1986) who tentatively attributed such observation to the oxidation of braunite-kutnahorite lutite during diagenesis had also observed the presence of almost pure braunite ovoids at Mamatwan mine. The occurrence of a scarce gaunge mineral, barite as observed on N and B-zones is known in the Mamatwan-Type ore.

3.6 References

Beukes, N.J. (1983). Palaeoenvironmental setting of iron formations in the depositional basin of the Transvaal Super group, South Africa. In: Trendall, A.F., and Morris, R.C. (eds). Iron formations, facts and problems, Elsevier, Amsterdam, 131-209.

Chetty, D. (2008). A geometallurgical evaluation of the ores of the northern Kalahari manganese deposit, South Africa, Unpublished PhD Thesis, Rand Afrikaans University (now University of the Johannesburg, Johannesburg, South Africa).

De Villiers, J.E. (1983). The Manganese Deposits of Griqualand West, South Africa: Some Mineralogic Aspects: Economic Geology. Vol. 78, p. 1108-1118.

Beukes, N.J., and Gutzmer, J. (1996). A volcanic-exhalative origin for the world's largest Kalahari Manganese Field, A discussion of the paper by D.H. Cornell and S.S. Schütte, Mineral Deposita, Vol. 31, p. 242-245.

Gutzmer, J., and Beukes, N.J. (1995). Fault controlled metasomatic alteration of Early Proterozoic sedimentary manganese ores in the Kalahari Manganese Field, South Africa. Economic Geology, Vol. 90, p. 823-844.

Gutzmer, J. (1996). Genesis and alteration of the Kalahari and Postmasburg manganese deposits, Griqualand west, South Africa. Unpublished PhD. Thesis, University of the Johannesburg, Johannesburg, South Africa).

Gutzmer, J., and Beukes, N.J., and Yeh, H.W., (1997). Metasomatic and supergene fault-controlled alteration of Early Proterozoic sedimentary manganese ore at Mamatwan Mine, Kalahari manganese field, South Africa. South African Journal of Geology, Vol.100, p. 53-71.

Kleyenstüber, A.S.E. (1984). The mineralogy of the manganese bearing Hotazel Formation of the Proterozoic Transvaal Sequence in Griqualand West, South Africa. Transactions of the Geological Society of South Africa, Vol. 87, p. 257-272.

Kleyenstüber, A.S.E. (1993). Significant characteristics of the manganese ores and some of the minerals occuring in the Proterozoic Kalahari Manganese Field, South Africa. Resource Geology Special Issue, No 17, p 2-11.

Miyano, T., and Beukes N .J. (1987). Physicochemical environments for the formation of quartz-free manganese oxide ores from the early Proterozoic Hotazel Formation, Kalahari Manganese Field, South Africa: Economic geology, Vol. 82, p. 706-718.

Nel, C.J., Beukes, N .J., and De Villiers, J.E. (1986). The Mamatwan manganese mine of the Kalahari manganese field, in Anhaeuser, C.R. and Maske, S., eds., Mineral deposits of Southern Africa. Johannesburg, Geological Society of South Africa, p.963-978.

Nyame, F.K. (2007). Petrography and geochemistry of intraclastic manganese-carbonates from the 2.2 Ga Nsuta deposit of Ghana: Significance for manganese sedimentation in the Palaeoproterozoic of West Africa. Journal of African Earth Sciences, Vol 50, p. 133-147.

Jennings, M. (1986). The Middleplaats manganese ore deposit, Griqualand West. In: Annhaeusser, C.R. and Maske, S. (eds.), Mineral deposits of Southern Africa. Geological Society of South Africa., Johannesburg, Vol. 1, p. 979-983.

Preston, P.C.C. (2001). Physical and chemical characterization of the manganese ore bed at the Mamatwan mine, Kalahari Manganese Field, Unpublished MSc. Dissertation, Rand Afrikaans University (now University of the Johannesburg, Johannesburg, South Africa.

Tsikos, H., Beukes, N.J., Moore, J.M. and Harris, C. (2003). Deposition, Diagenesis, and Secondary Enrichment of Metals in the Paleoproterozoic Hotazel Iron Formation, Kalahari Manganese Field, South Africa. Economic Geology Vol. 98, p. 1449–1462.

Tsikos, H., and Moore, J.M. (1998). The Kalahari manganese field: an enigmatic association of iron and manganese. South African Journal Geology Vol. 101 (4), p. 287-290.

van Staden, A. (2002). Characterization of the lowermost manganese ore bed of the Hotazel Formation, Gloria Mine, Northern Cape Province, Unpublished MSc. Dissertation University of the Johannesburg, South Africa).

CHAPTER 4

GEOCHEMISTRY

4.1 Introduction

A total of 22 pulverized manganese ore samples, representative of various zones in both drill core SKR 40 and SKR 65 were analyzed at CGS to determine major and trace element composition and to supplement the mineralogical identification. The aim was to establish the consistency and compare the whole-rock analyses with the mineral chemistry obtained by microscopy and XRD

Additional XRF data of major elements for the two boreholes were obtained from Kalahari Resources in order to compare their results with the data analyzed at Council for Geosciences. The geochemical relations comprising the entire LMO from the top to the bottom are also presented and discussed. Ternary plots are created to show the variation in composition of minerals. Many authors such as Nel et al. (1986), Tsikos & Moore (1997), Du Plooy (2002), Preston (2001), van Staden (2002) and Chetty (2008) have studied the general geochemistry of the Mamatwan type ores and/or associated Banded Iron Formation previously.

4.2 Methodologies

Whole-rock chemical compositions were completed on a glass bead made from the powdered sample fused with lithium tetraborate using XRF spectrometry at CGS following the procedure developed by Norrish and Hutton (1968). The SARM-50, an international dolerite reference material from MINTEK and IGGE, a soil reference material from China was also utilized for quality control. The collected samples were washed with distilled water to remove impurities and

left to dry, after which the samples where analysed for major trace elements using XRF. The collected rock samples were crashed and then oven dried at 75ºC after which, 500g of the powder, representative of the whole sample, were separated and kept for future use. The results obtained on each borehole are compared to better understand the mineralogical variation on both boreholes. Detailed sample preparation from rock samples into powders is given in chapter 2. The detection limits for major oxides TiO_2, Al_2O_3, Na_2O and K_2O are <0.01wt% while Cr_2O_3 is <0.001wt%. Detection limits for various trace elements ranges from: < 2ppm for Br, Mo, Ta, Pb and U; < 3ppm for Bi, Hf, Th, Ti, and Yb; < 5ppm for Cs and < 10ppm for Ce, Nd and Sm.

4.3 Results

Apart from MnO, the most abundant chemical constituents across Kalagadi mine lease are Fe_2O_3, SiO_2, CaO and MgO and they vary in each zone across the mine lease area. The oxides TiO_2, Na_2O, K_2O, Al_2O_3, and Cr_2O_3 are depleted with concentrations not exceeding 0.01wt% and 0.001wt% respectively whereas P_2O_5 concentrations are low ranging from 0.02 wt% to 0.3wt %) (Table 4.1 and 4.2).

Trace element concentrations of Ba, Zn and Sr in most zones are slightly elevated ranging from 100ppm to 3.9% (about 36000ppm) respectively while Co, Cu, Ni, Y, As, Zr, V and La rarely exceed 50ppm. In certain zones, Cu, Zn, Ni, Co and V commonly associated with volcanogenic hydrothermal input in chemical precipitates may reach up to 70ppm. Geochemical data tables, from both analyzed data and unpublished mine records reveal the consistency in vertical variation as well

as lateral variation in bulk chemical composition. Termary diagrams are presented to highlight the variation of different minerals based on chemical composition.

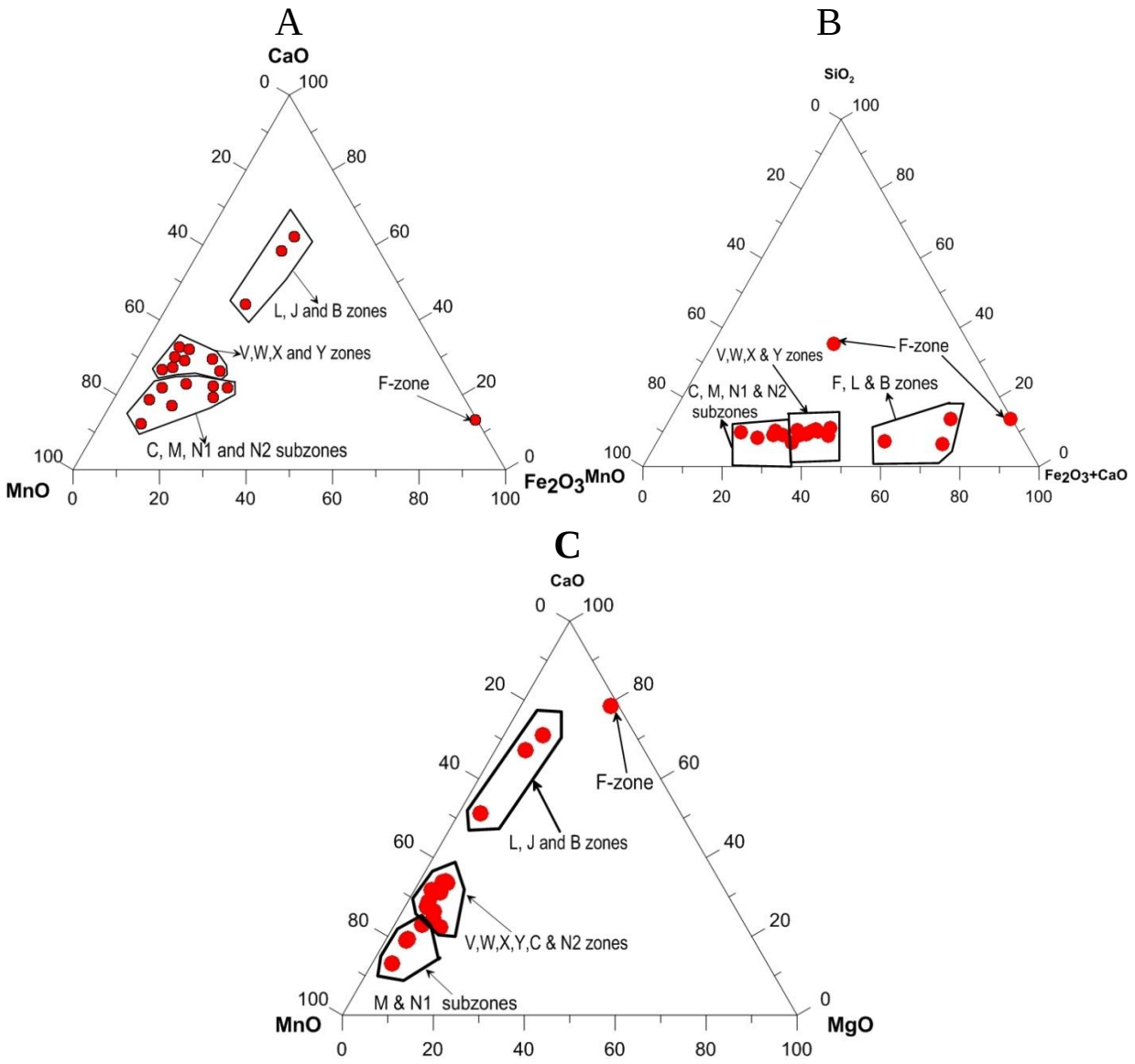

Figure 4.1 Ternary plot showing chemical variation in composition of hausmannite (A), braunite (B) and kutnahorite in the Lower Manganese Orebody of the Kalagadi mine.

Table 4.1: Results of major (wt%) and trace (ppm) elements analyzed by X-ray fluorescence spectrometry. Borehole SRK 65.

1. Major elements (wt%)									
	Subzones								
	V-zone	W-zone	X-zone	Y-zone	M-zone	C-zone	N1-zone	N2-zone	B-zone
SiO_2	8.42	9.43	8.30	7.31	7.28	8.77	7.22	7.07	5.35
TiO_2	<0.01	<0.01	<0.01	<0.01	<0.01	<0.01	<0.01	<0.01	<0.01
Al_2O_3	<0.01	<0.01	<0.01	<0.01	<0.01	<0.01	<0.01	<0.01	<0.01
$Fe_2O_3^*$	15.09	14.33	18.67	7.70	6.37	10.33	10.95	7.01	12.41
MnO^*	38.48	36.60	40.30	40.68	56.03	43.67	52.73	50.02	26.38
MgO	3.63	5.57	2.91	3.86	3.49	4.91	3.16	4.28	2.86
CaO	19.10	12.18	16.44	22.93	14.33	16.02	13.08	16.07	30.64
Na_2O	<0.01	<0.01	<0.01	<0.01	<0.01	<0.01	<0.01	<0.01	<0.01
K_2O	<0.01	<0.01	<0.01	<0.01	<0.01	<0.01	<0.01	<0.01	<0.01
P_2O_5	0.217	0.204	0.237	0.211	0.234	0.224	0.217	0.217	0.219
Cr_2O_3	<0.001	<0.001	<0.001	<0.001	<0.001	<0.001	<0.001	<0.001	<0.001
L.O.I.	18.93	25.18	16.85	20.93	16.89	19.67	16.38	18.94	25.51
Total	**99.92**	**99.95**	**99.93**	**99.91**	**99.93**	**99.91**	**99.94**	**99.94**	**99.90**
H_2O^-	0.18	0.34	0.19	0.14	0.10	0.23	0.15	0.13	0.22
2. Trace element analyses (ppm)									
As	4.4	<4	4.6	<4	10	<4	<4	<4	8.1
Ba	193	161	162	909	246	179	521	8,058	1,127
Bi	<3	<3	<3	<3	<3	<3	<3	<3	<3
Br	<2	<2	<2	<2	<2	<2	<2	<2	<2
Ce	<10	<10	<10	<10	<10	<10	<10	<10	<10
Co	50	46	48	50	36	40	49	41	44
Cr	9	6.4	37	17	14	14	26	22	41
Cs	<5	<5	<5	<5	<5	<5	<5	<5	<5
Cu	23	116	9.4	31	16	5	17	31	26
Ga	1.9	<1	1.2	<1	<1	<1	2.3	<1	<1
Ge	<1	<1	<1	<1	<1	<1	<1	<1	<1
Hf	<3	<3	<3	<3	<3	<3	<3	<3	<3
La	26	35	20	38	11	17	45	28	25
Mo	<2	<2	<2	<2	<2	<2	<2	<2	<2
Nb	<1	<1	<1	<1	<1	<1	<1	<1	<1
Nd	<10	<10	<10	<10	<10	<10	<10	<10	<10
Ni	13	12	13	15	11	14	16	13	11
Pb	4.3	11	4.6	4.2	2.9	4.9	4.6	<2	2.3
Rb	11	7.5	10	4	2.8	7.7	3.2	<2	2.9
Sc	<3	<3	<3	<3	<3	<3	<3	<3	4.5
Se	3.4	2.5	2.6	1.7	2.3	2.3	2.2	<1	1.5
Sm	<10	<10	<10	<10	<10	<10	<10	<10	<10
Sr	174	107	146	141	114	216	99	152	74

Ta	<2	<2	<2	<2	<2	<2	<2	<2	<2
Th	<3	<3	<3	<3	<3	<3	<3	<3	<3
Tl	<3	<3	<3	<3	<3	<3	<3	<3	<3
U	<2	<2	<2	<2	<2	<2	<2	<2	<2
V	7.4	9.6	17	16	9.6	11	20	17	19
W	<3	6.4	5.1	3.6	<3	<3	3.8	5.8	<3
Y	7.3	8.0	8.4	5.5	4.8	7.2	6.1	5.8	5
Yb	<3	<3	<3	<3	<3	<3	<3	<3	<3
Zn	149	30	151	62	187	12	237	138	155
Zr	3.5	5.2	4.0	2.8	<2	3.1	4.0	2.9	2.9

*** Total Fe as Fe_2O_3; Total Mn as MnO**

Table 4.2: Results of major (wt%) and trace (ppm) elements analyzed by X-ray fluorescence spectrometry. Borehole SRK 40.

1. Major elements (wt %)											
	F- zone	**J-zone**	**V –zone**	**X-zone**	**Y-zone**	**M-zone**	**C-zone**	**N1-zone**	**N2-zone**	**B-zone**	**L-zone**
SiO_2	38.36	4.33	9.08	7.41	7.24	8.50	6.85	8.26	7.61	8.29	5.45
TiO_2	<0.01	0.01	<0.01	0.01	<0.01	<0.01	<0.01	<0.01	<0.01	<0.01	<0.01
Al_2O_3	0.1	0.27	<0.01	0.21	<0.01	<0.01	<0.01	<0.01	<0.01	<0.01	<0.01
Fe_2O_3*	45.7	11.99	15.60	5.57	8.11	7.63	6.13	5.15	6.79	12.33	11.81
MnO*	0.162	10.63	41.58	39.94	42.91	62.05	44.63	47.11	45.57	37.21	13.96
MgO	1.79	4.54	4.30	3.41	3.44	3.30	2.62	3.49	3.14	3.96	3.61
CaO	7.07	37.05	16.46	22.14	20.99	9.83	21.91	19.06	19.70	20.80	36.11
Na_2O	<0.01	<0.01	<0.01	0.008	<0.01	<0.01	<0.01	<0.01	<0.01	<0.01	<0.01
K_2O	0.02	0.08	<0.01	<0.01	<0.01	<0.01	<0.01	<0.01	<0.01	<0.01	<0.01
P_2O_5	0.171	0.046	0.272	0.048	0.204	0.231	0.210	0.201	0.211	0.202	0.184
Cr_2O_3	0.001	0.002	<0.001	<0.001	<0.001	<0.001	<0.001	<0.001	<0.001	<0.001	<0.001
L.O.I.	6.01	30.58	17.20	20.6	20.85	12.75	21.43	20.42	20.84	20.76	31.58
Total	**99.384**	**99.528**	**99.75**	**99.338**	**99.93**	**99.91**	**99.87**	**99.94**	**99.88**	**99.94**	**99.96**
H_2O^-	0.08	0.13	0.22	0.11	0.22	0.08	0.11	0.13	0.15	0.24	0.22
2. Trace element analyses in ppm											
As	4.7	<4	6.9	14	5	<4	8.6	<4	6.9	Insufficient Sample	18
Ba	30	201	175	190	194	3.6%**	220	1.4%**	284		885
Bi	<3	<3	<3	<3	<3	<3	<3	<3	<3		<3
Br	<2	<2	<2	<2	<2	<2	<2	<2	<2		<2
Ce	11	10	<10	<10	<10	<10	<10	<10	<10		<10
Co	<1	26	55	28	45	51	51	65	41		58

Cr	<3	<3	9.7	<3	<3	22	7.1	20	9.2		13
Cs	<5	<5	<5	<5	<5	<5	<5	<5	<5		<5
Cu	14	4.1	6.4	7.3	2.5	13	10	7.7	4.4		16
Ga	<1	<1	1.3	<1	1.5	<1	<1	<1	1.6		<1
Ge	<1	<1	<1	<1	<1	<1	<1	<1	<1		<1
Hf	<3	<3	<3	<3	<3	<3	<3	<3	<3		<3
La	<10	25	18	26	25	42	18	<10	22		16
Mo	<2	<2	<2	<2	<2	<2	<2	<2	<2		<2
Nb	1.6	1.9	<1	2.1	<1	<1	<1	<1	<1		<1
Nd	<10	<10	<10	<10	<10	<10	<10	<10	<10		<10
Ni	2.4	8.1	14	9.5	15	14	10	18	11		14
Pb	<2	<2	4.8	<2	3.6	<2	3.6	4.8	2.6		3.1
Rb	2.2	6.2	5.2	<2	5.4	<2	<2	3.2	3.5		3.8
Sc	<3	<3	<3	<3	<3	<3	<3	3.3	<3		<3
Se	2.1	<1	2.3	1.3	2.6	<1	1.8	<1	2		2.1
Sm	<10	<10	<10	<10	<10	<10	<10	<10	<10		<10
Sr	221	274	148	114	149	134	222	131	227		78
Ta	<2	<2	<2	<2	<2	<2	2.2	<2	<2		2.2
Th	<3	<3	<3	<3	<3	<3	<3	<3	<3		<3
Tl	<3	<3	<3	<3	<3	<3	<3	<3	<3		<3
U	<2	<2	2.7	<2	<2	<2	<2	2.2	<2		<2
V	4.3	34	12	42	16	22	8.6	26	9.1		14
W	4.1	<3	3.9	<3	<3	7.5	<3	4.6	3.7		<3
Y	12	7.2	7.6	4.9	6.9	5.7	6.9	5.9	6.8		9.5
Yb	<2	<2	<3	<2	<3	<3	<3	<3	<3		<3
Zn	14	11	148	13	340	222	169	138	181		172
Zr	7.8	7.3	4.4	6.7	2.2	2.5	<2	3.8	2.6		5.7

* **Total Fe as Fe_2O_3 ; Total Mn as MnO**

****Elevated Ba concentrations in weight percent** e.g 3.6%* and 1.4%* are equivalent to 36000ppm to 14000ppm respectively.

4.3.1 Major elements

Various subzones comprising the LMO of the mines operating in the Kalahari deposit have been previously grouped into: Basal Low Grade Zone (lowermost zones), Central Economic Zone (Middle zones) and Upper Low grade zone (Upper zones).

The following are the results for the distribution of major oxides from botton to top as determined on certain zones of the LMO.

Basal Low Grade zone (L and B)

The base of the orebody is gradually diminishing in manganese (Mn) content from ≤ 30% at B-zone to L-zone finally dropping to ≈0% at a transition zone. The basal low grade zone therefore comprises braunite-jacositic B-zone and hematitic braunite lutite of L-zone. The carbonate (CaO) content on L-zone of borehole SKR 40 attains a maximum of 36% while manganese (MnO) content reaches a maximum of 11%. Hematite, calcite and kutnahorite are the most abundant minerals while rhodochrosite is found in minor quantities. The L-zone of borehole SKR 65 was however not analysed due to insuffient material and therefore comparisons are not possibble. However, the data for these two boreholes from unpublished mine records show variation of manganese (Mn) from 15% to 22%.

The B-zone at SKR 40 is characterized by elevated manganese (MnO) and silica (SiO_2) contents and low carbonate (CaO) compared to SKR 65 (Figure 4.2). The Al_2O_3 and P_2O_5 concentration vary from 0.05ppm to 0.2ppm, while K_2O, Na_2O, Cr_2O_3 and TiO_2 values are negligible (<0.001 to 0.05ppm). The loss of ignition (L.O.I) values and carbonate content towards the base of the orebody

are high while Mn/Fe ratios are negligible low. The B-zone attains a maximum thickness of ±1m at SKR 65 and the detailed data obtained from Kalahari Resources shows a variation of manganese (Mn) content from 20% at 263.17m to 22% at 264.14m (Figure 4.2–A). On the other hand, the SKR 40 attains a thickness of ±2m and varies in manganese (Mn) content from 30% at 311.5m to 17% at 313.5m (Figure 4.2– B).

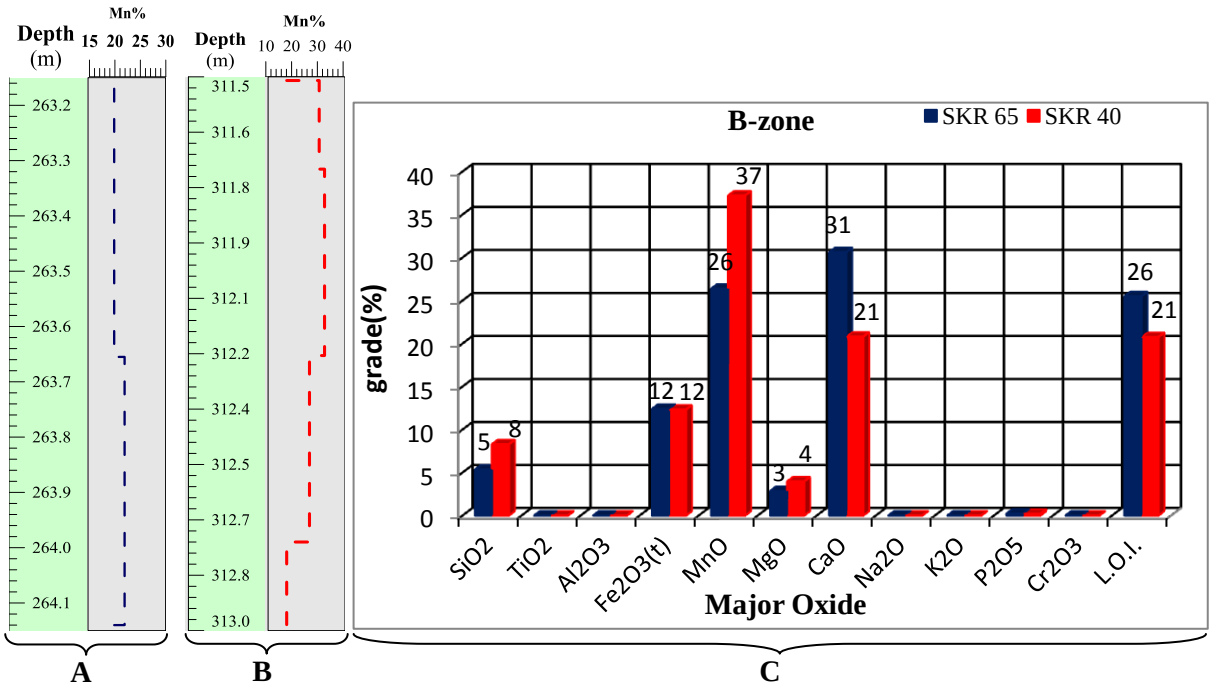

Figure 4.2 (**A**). Detailed variation of manganese (Mn) content with depth at B-zone of borehole SKR 65 while (**B**) shows variation of manganese (Mn) content at borehole SKR40. The data used in plotting A and B were obtained from Kalahari Resources in other to have a complete view of the detailed mineralogical variation in the entire zone. (**C**). Distributions of major oxides at borehole SKR 65 (blue) and SKR 40 (red) are as observed in the study. Note elevated CaO and lower MnO contents at SKR 65 as compared to slightly higher MnO and Fe content with low CaO at SKR 40.

Central Economic Zone (Y, M, C and N-subzones)

The economic mineable zone contains high concentration of manganese ranging from 30% to 40% Mn or 40% and 60 %MnO. The zone comprises Y, M, C and N subzones, among which M-subzone is the most economic followed by N–subzones. The N-zone represents the base of the economic zone of the LMO and is further subdivided into N1-subzone (top) and N2-subzone (bottom), based on physical, chemical and mineralogical differences as explained in previous chapters.

N2-subzone

The N2-subzone above B-zone is characterized by increase in manganese (MnO) content with SKR 65 and SKR 40 attaining a maximum 50% and 45% respectively. The Fe content is consistent in both boreholes while CaO and SiO_2 contents are more elevated at SKR 40. The loss of ignition values, which represent the released carbon dioxide, ranges from 21% and 19% at SKR 40 and SKR 65 respectively, slightly more than the CaO values.

This subzone attains a maximum thickness of ±5m at SKR 65 and the detailed major element analyses from Kalahari Resources show a variation of manganese (Mn) from 39% - 41% at the top (257m) to 32% towards the base at depth of 262.4m (Figure 4.3–A). The SKR 40 attains a thickness of ±2.5m and varies in manganese (Mn) content from 38% at 308.5m to 34% at 311m depth (Figure 4.3–B). The P_2O_5 contents at SKR 65 and SKR 40 attain a maximum of 0.21% while other elements such as TiO_2, Al_2O_3, Na_2O, K_2O and Cr_2O_3 are all below detection limit (Figure 4.15 and 4.16). The lower contents of CaO and MgO with elevated MnO contents correspond to the depletion in carbonates and enrichments in braunite contents, respectively.

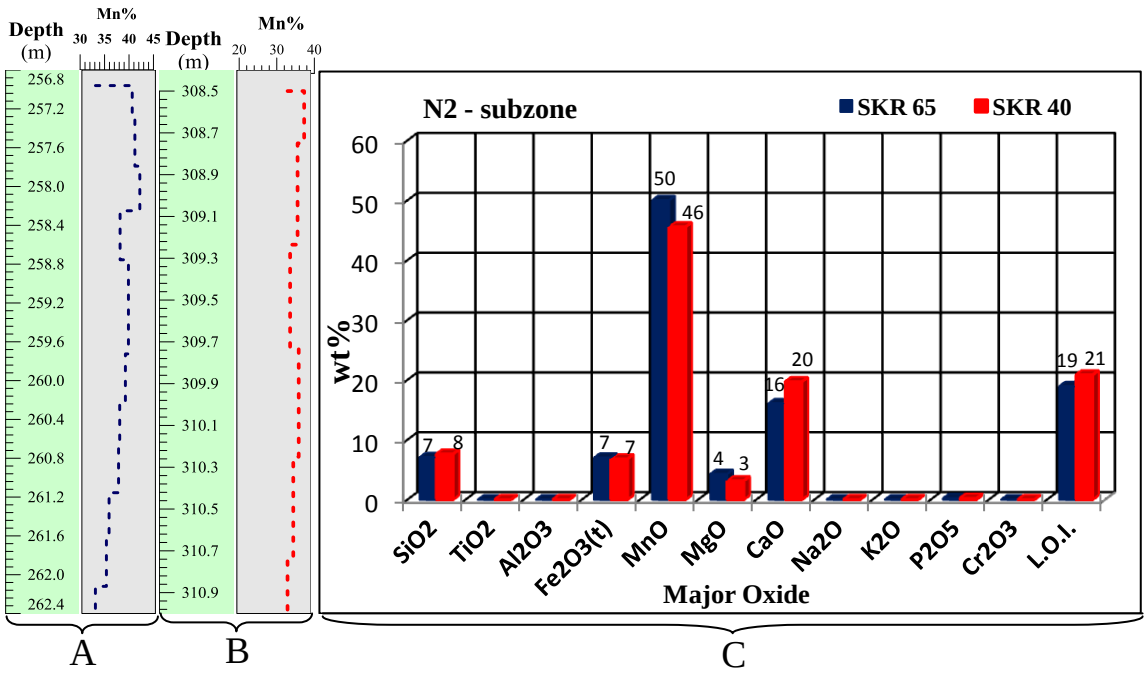

Figure 4.3 (**A**). Detailed variation of manganese (Mn) content with depth at N2-subzone of borehole SKR 65 while (**B**). Shows variation of manganese (Mn) content of borehole SKR 40. The unpublished mine records show that the manganese (Mn) content at SKR 65 varies from about 41% at the top to 32% towards the base while at SKR 40 it varies from 35 % at the top to 33% towards the base of the orebody. (**C**). Major oxide distributions as observed on N2-subzone of SKR 65 (blue) and SKR 40 (red). Note the elevated CaO and lower MnO contents at SKR 40 and higher MnO and lower CaO contents at SKR 65.

N1 – subzone

The N1-subzone is characterized by elevated concentrations of manganese content. Mineralogically, the ovoids are partially oxidized to hausmannite (Mn_3O_4) and the carbonate species are often intergrown in a matrix with braunite. The SKR 65 contains higher manganese (MnO) content of about 53% and lower carbonate (CaO) content of about 13% compared to lower manganese content of 47% and elevated carbonate (CaO) contents of 19% at SKR 40. At SKR 65,

the N1-subzone attains a maximum thickness of ±1.9m and the XRF data from Kalahari Resources shows a variation of manganese (Mn) content from 35% at the top (255m) to 41% towards the base (257m). The N1 subzone at SKR 40 attains a thickness of 1.84m and varies in manganese (Mn) content from 39% at the top (306m) of the zone to 40% at about (308m), towards the base (Figure 4.3 - A and B). The P_2O_5 contents at SKR 65 and SKR 40 attain a maximum of 0.21% and 0.20 wt% respectively while other elements such as TiO_2, Al_2O_3, Na_2O, K_2O and Cr_2O_3 are all below detection limit (Figure 4.15 and 4.16).

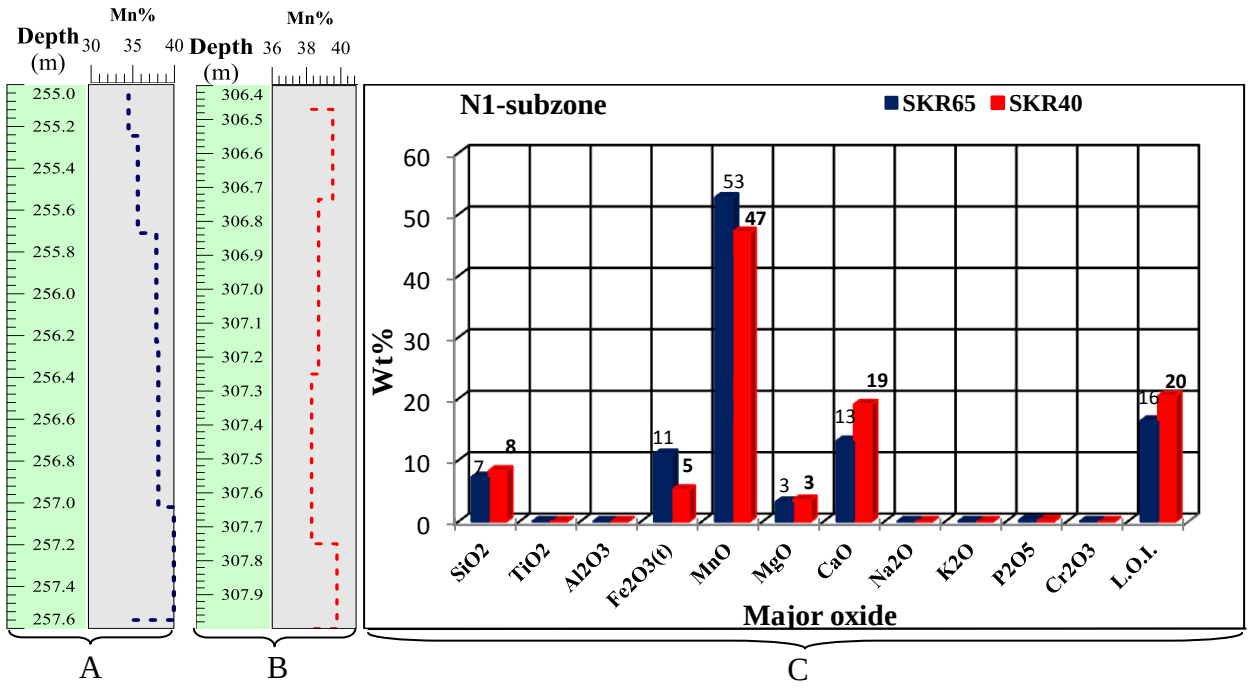

Figure 4.4. (**A**). Detailed variations of manganese (Mn) content with depth at N1-subzone of borehole SKR 65 while (**B**). Shows variation of manganese (Mn) content at borehole SKR 40. The Mn content at SKR 65 varies from about 35% at the top, 38% in the middle to 41% at the base while at SKR 40 varies from 38% at the top, 41% in the middle to 39% towards the base of the orebody. (**C**). Major oxide distributions as observed in N2-subzone of SKR 65 (blue) and SKR 40 (red). Note the elevated CaO and lower MnO contents at SKR 40 and higher MnO and lower CaO contents at SKR 65. The Fe_20_3 content is elevated in SKR 65 while SiO_2 slightly higher in SKR 40.

C-zone

The C-zone is characterized by dominant fine brownish white laminations and small, amalgamated ovoids. The concentration of manganese (MnO) in both boreholes diminishes slightly to 44% and 45% while carbonate (CaO) content increases to 16% and 22% in SKR 65 and SKR 40, respectively. The SiO_2, Fe_2O_3 and MgO contents are elevated in borehole SKR 65 while CaO content is low.

A detailed analyses of the entire C-zone from unpublished mine records indicate that SKR 65 attains a maximum thickness of ±4m and varies in Mn content from 24% in a carbonate dominated portion (251m) to 30% at 253m and finally attaining 32% at 254m - 255m (Figure. 4.5 – A). The manganese (Mn) content at SKR 40 is slightly elevated and varies from 27% to 34% at the top and finally reaches 41% Mn at the base (Figure 4.5 - B). The P_2O_5 contents at SKR 65 and SKR 40 attain a maximum of 0.22% and 0.21% respectively while other elements such as TiO_2, Al_2O_3, Na_2O, K_2O and Cr_2O_3 are all below detection limit (Figure 4.15 and 4.16).

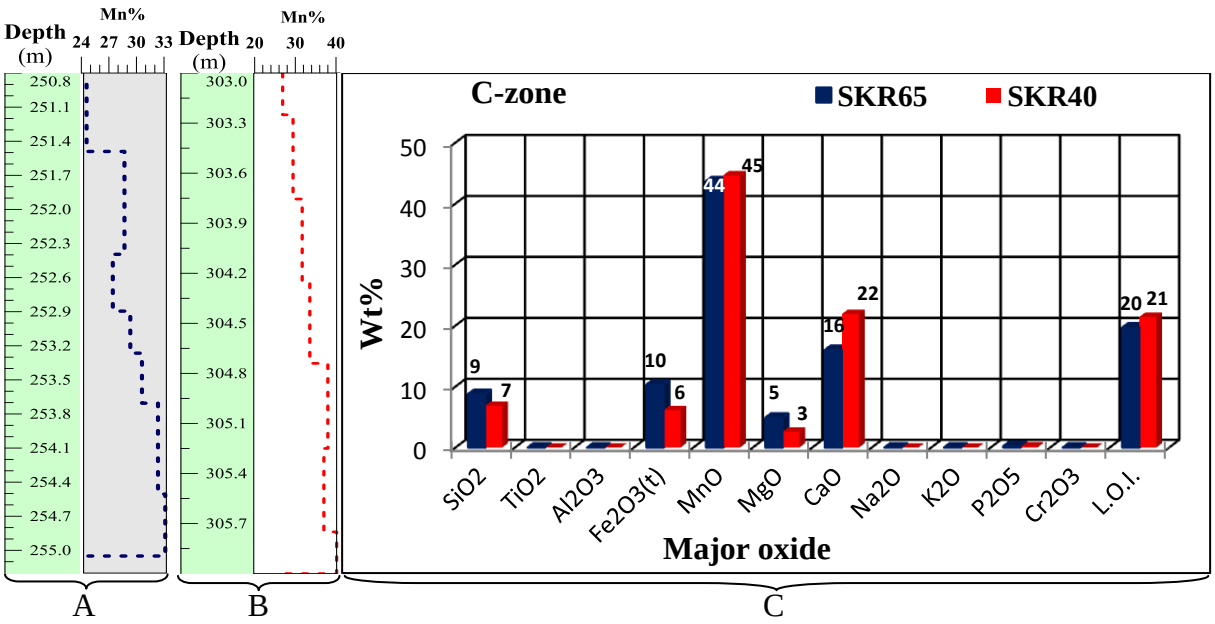

Figure 4.5 Detailed variation of manganese (Mn) content with depth at C-zone of borehole SKR 65 while (**B**) shows variation of manganese (Mn) content at borehole SKR 40. The unpublished mine records show that the manganese content at SKR 65 varies from about 24% at the top, 30% in the middle to 33% at the base while at SKR 40 varies from 27% at the top, 34% in the middle to 41% towards the base of the orebody. (**C**). Major oxide distributions as observed on C-zone of SKR 65(blue) and SKR 40 (red). Note the elevated CaO and lower MnO contents at SKR 40 and higher MnO and lower CaO contents at SKR 65. The Fe_20_3 content is elevated in SKR 65 while SiO_2 slightly higher in SKR 40.

M-zone

Mineralogically, the M–zone is characterized by high braunite and hausmannite contents and chemically attains manganese (MnO) content of 56% to 62% at SKR 65 and SRK 40, respectively. The M-zone attains a maximum thickness of ±1.06m at SKR 65, is located at a depth between 250.01m to 251.07m while SKR 40 is ±2.1m thick, and occurs at depth of 300.15m - 302.26m. The variation of manganese content in each borehole and thickness is shown by the data obtained from Kalahari Resource (Figure 4.6 - A and B). The manganese (Mn) content in borehole SKR 65 varies

from 37% at depth of about 250m to 36% at 251m and finally drops to 31% towards the base (251.1m). The decline of manganese content to 31% corresponds to the very high carbonate (CaO) contents (Figure 4.6-A). Manganese (Mn) content at borehole SKR 40 ranges from 35% to 38% at depth of 300m – 301m then drops to 33% - 29% at 302m (Figure 4.6-B). The M-zone is the most economic zone and the slight decline in manganese content towards the base indicates grading of the ore to C-zone below. The P_2O_5 contents at SKR 65 and SKR 40 attain a maximum of 0.23% while other elements such as TiO_2, Al_2O_3, Na_2O, K_2O and Cr_2O_3 are all below detection limit.

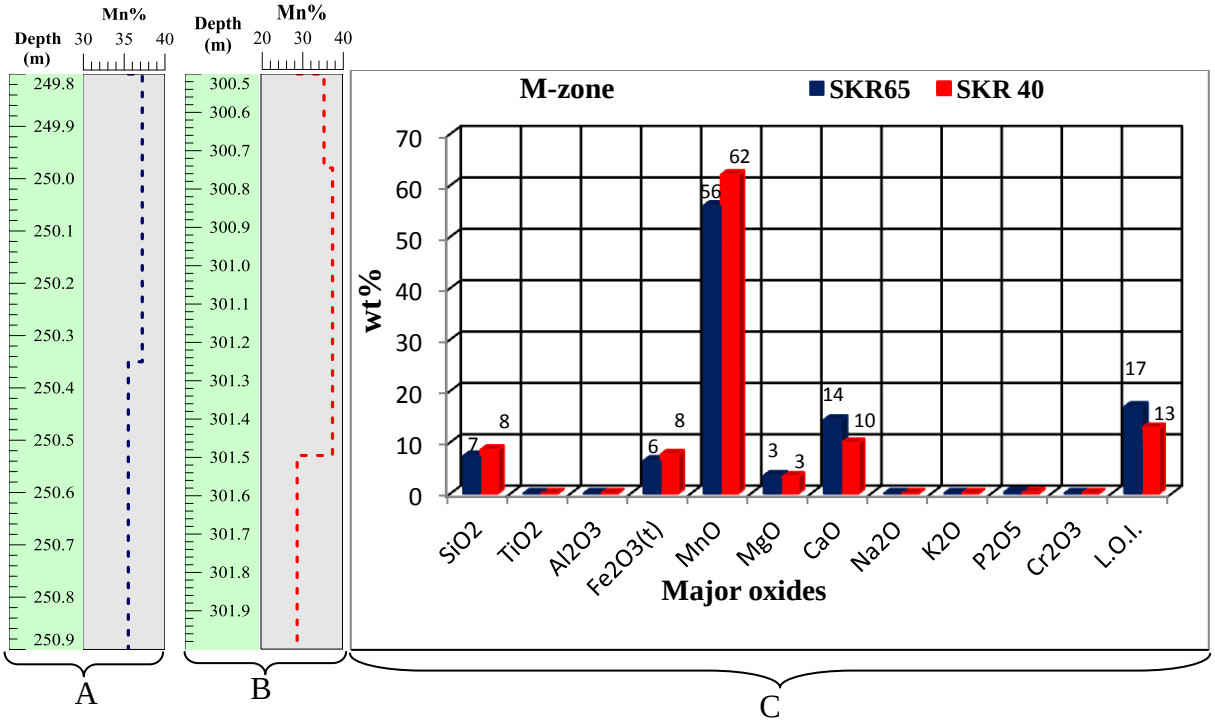

Figure 4.6 Detailed variations of manganese (Mn) contents with depth at M-zones of borehole SKR 65 (**A**) and SKR 40 (**B**). The unpublished mine records show that the manganese (Mn) content at SKR 65 varies from about 37% at the top and 36% at the bottom while at SKR 40 varies from 35% at the top, 37% in the middle and finally drops to 29% at the bottom of the orebody. **(C)** Shows the major oxide distribution on the two boreholes as observed from the study. The SKR 40 shows the elevated MnO, SiO_2 and Fe_20_3 contents and low CaO contents compared to SKR 65.

Y-zone

The manganese content at Y-zone attains a maximum of 43% MnO or 33% Mn at SKR 40 and 41% MnO or 32% Mn at SKR 65. The total carbonate content determined by XRD at both labs varies from 23% to 33% and 15% to 26% at borehole SKR 65 and SKR 40 respectively. Such elevated carbonate content is accounted for by high concentrations of CaO contents ranging from 21% to 23 % and MgO is mostly associated with the carbonates. The Y-zone at SKR 40 attains a maximum thickness of ±2m while SKR 65 is ±0.7m.

The detailed analyses for the entire Y-zone for both boreholes were obtained from Kalahari Resources in order to have a complete view of the change of mineralogy and grade with depth. The data for Y-zone at SKR 65 show variation of manganese (Mn) content from 29% – 31% at depth of 249.1m – 249.3m respectively (Figure 4.7–A) while SKR 40 shows a variation of 28% Mn to 35% Mn content from 299m–300.6m (Figure 4.7–**B**). The P_2O_5 contents at SKR 65 and SKR 40 attain a maximum of 0.21% and 0.20 respectively while other elements such as TiO_2, Al_2O_3, Na_2O, K_2O and Cr_2O_3 are all below detection limit.

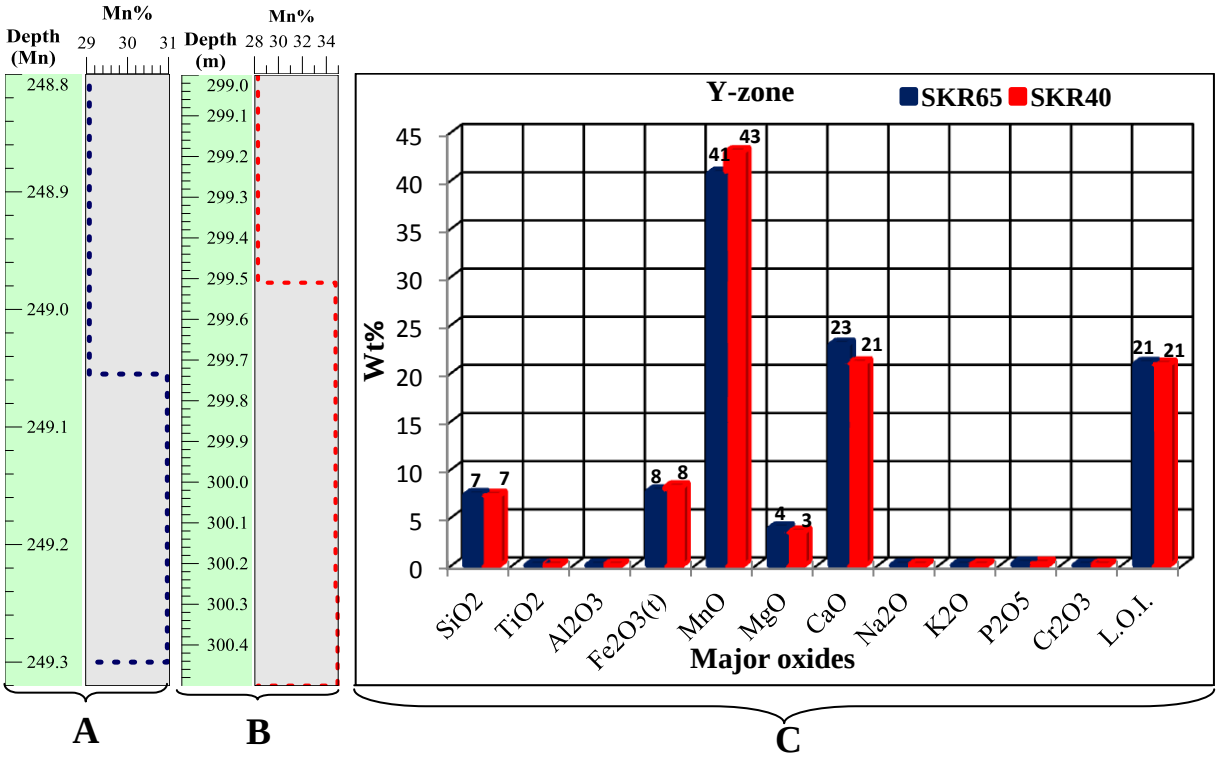

Figure 4.7 Detailed variations of manganese (Mn) contents with depth at Y-zones of borehole SKR 65 (**A**) and SKR 40 (**B**). The unpublished mine records show that the manganese (Mn) content at SKR 65 varies from about 29% at the top and 31% at the bottom while at SKR 40 varies from 28% at the top to 35% at the bottom of the orebody. **(C).** Shows the major oxide distribution on the two boreholes. Note the elevated CaO contents in both boreholes reaching and the equal contents in SiO_2, Fe_20_3 and L.O.I. The SKR 65 shows slightlylower MnO, CaO contents and elevated CaO contents compared to SKR 40.

Upper Low Grade Zone (J, F, V, W and X)

The Upper low grade zone encompasses the J, F, V, W and X subzones and is characterized by elevated hematite, rhodochrosite, calcite and kutnahorite contents while manganese content normally varies from 0% at the top to 30% towards the middle economic zone. The concentrations of Fe_2O_3, CaO, SiO_2 and MgO are compliant with the development of hematite and Mg-rich carbonates (kutnahorite, and calcite) at the expense of manganese. The MgO content reaches a maximum of 5wt%, slightly higher than previously reported for the manganese ores in this region.

X-zone

The X-zone in both drill cores is characterized by elevated manganese (MnO) contents of up to 40% with SKR 65 containing higher content of Fe_2O_3 while SKR 40 contains higher carbonate (CaO) content and almost equal proportions of MgO (Figure 4.8–C). The elevated concentration of Fe_2O_3 and SiO_2 in SKR 65 is comparable with the increase in braunite, jacobsite and hematite content in the ore. The X-zone at SKR 65 attains a maximum thickness of ±0.8m and detailed analyses for the entire zone obtained from unpublished mine records show variation of Mn content from about 29.6% at depth of 248m to about 28.9% at 248.8m (Figure 4.8 - A). The SKR 40 is ±0.5m thick and varies in Mn from 28% and 26% at 298m and 298.5m respectively.

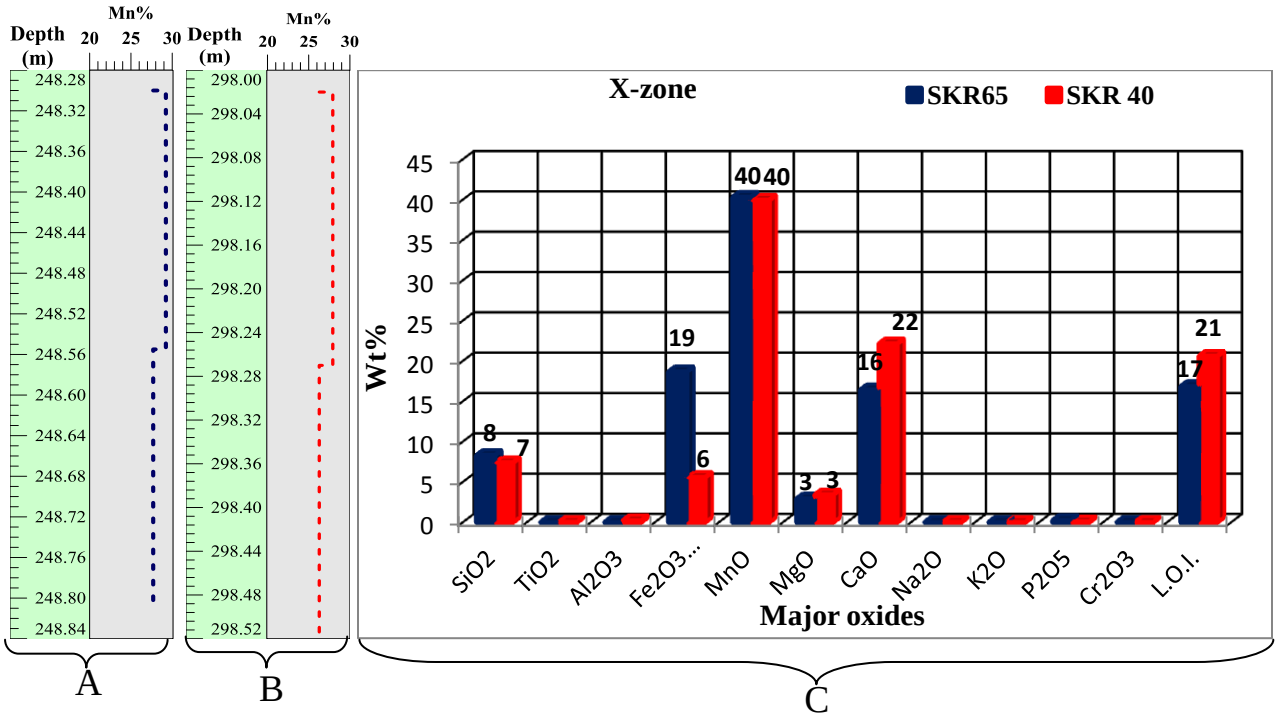

Figure 4.8 Detailed variation of manganese (Mn) contents with depth at X-zones of borehole SKR 65 (**A**) and SKR 40 (**B**). The unpublished mine records show that the manganese (Mn) content at SKR 65 varies from about 29.6% at the top and 28.9% at the bottom while at SKR 40 varies from 28% at the top to 26% at the bottom of the orebody. **(C).** Shows the major oxide distribution on the two boreholes observed from the study. The MnO content is equal in both boreholes and Fe_20_3 content is elevated at borehole SKR 65 while CaO is higher on SKR 40.

W-zone

The concentrations of MnO, CaO and Fe_2O_3 in W-zone are slightly comparable with those of V-zone although MgO and SiO_2 are elevated. The manganese (MnO) content at SKR 65 attains a maximum of 37% while CaO and Fe_2O_3 contents attain a maximum of 12% and 14% respectively. However, the selected section of W-zone analysed by XRD contains a considerably low braunite contents with elevated concentration of dolomite and serpentine and this is probably due to

dolomitization. A detailed variation of manganese content with depth in each borehole is shown by the data obtained from Kalahari Resource (Figure 4.9 - A and B). The W- zone at borehole SKR 40 is not well developed and the sample material was insufficient for major and trace elements analyses. However, XRF data obtained from Kalahari Resources shows variation of Mn content from 32% at the top (296m – 296.7m) to 28 % at the bottom (297.8m – 298m).

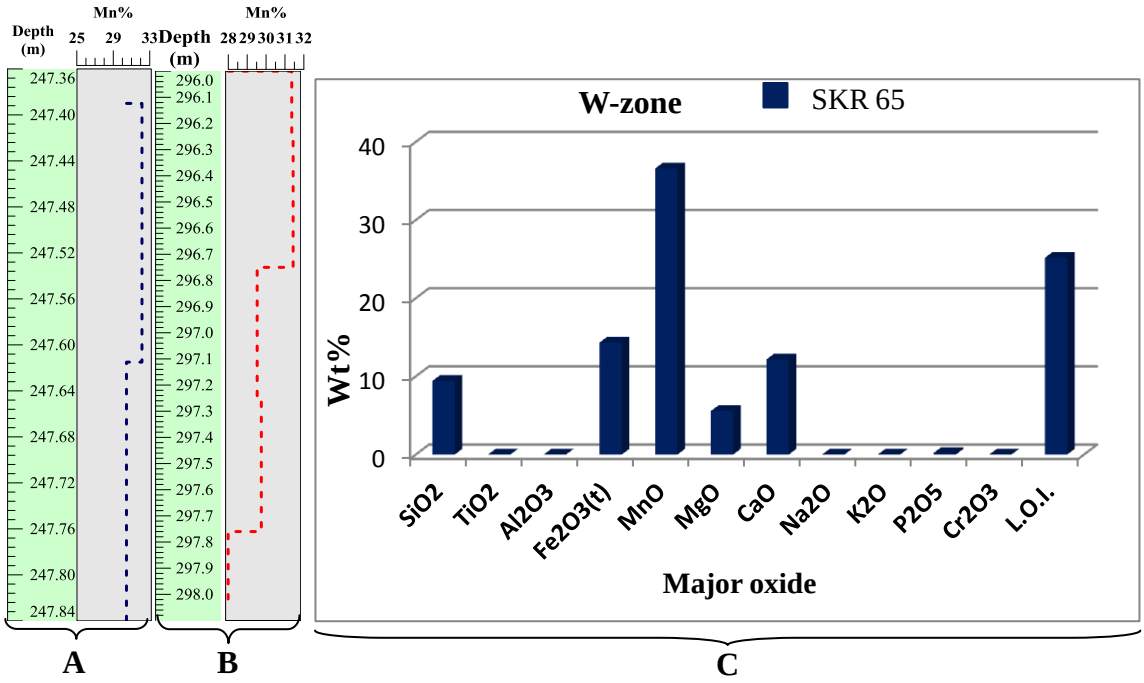

Figure 4.9 Detailed variation of manganese (Mn) contents with depth at W-zones of borehole SKR 65 (**A**) and SKR 40 (**B**). The unpublished mine records show that the variation of manganese (Mn) content varies from about 35% at the top, 29.6% in the middle to 28% at the bottom of SKR 65 while SKR 40 varies from 32% at the top and 30% at the bottom of the orebody. **(C)**. Shows the major oxide distribution on borehole SKR 65 as observed from the study.

V-zone

Below the ferruginized zones, the orebody is marked by an increase in MnO, CaO, SiO_2 and MgO while total Fe_2O_3 content decreases slightly and this is consistent with the increase in braunite, hausmannite, kutnahorite, Mg-rich calcite and/or Mn-rich calcite and a decline in hematite content. The manganese content is slightly elevated with MnO reaching 38% at SKR65 and 42% at SKR 40 while SiO_2 also increases accordingly. The CaO content is slightly elevated at SKR 65 while Fe_2O_3 content is low and the P_2O_5 is 0.21% in most zones.

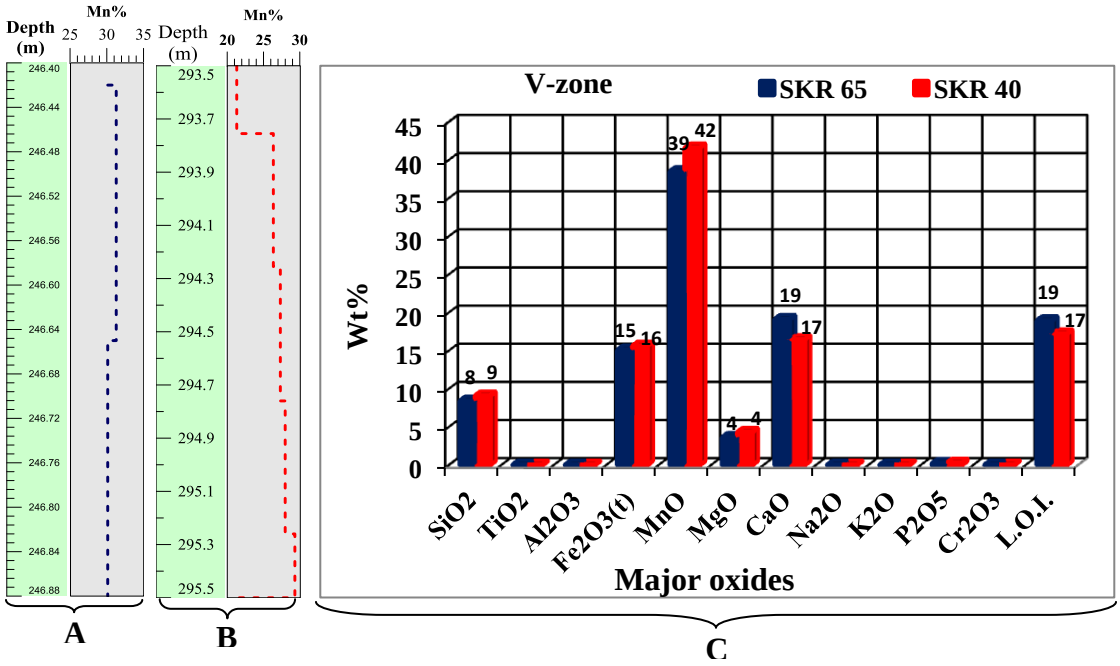

Figure 4.10 Detailed variation of manganese (Mn) content with depth at V-zones of borehole SKR 65 (**A**) and SKR 40 (**B**). The unpublished mine records show the variation of manganese (Mn) content from 31% at the top to 30% at the bottom of SKR 65 while SKR 40 varies from 21% – 27% at the top to 28% at the bottom of the orebody. (**C**) The analyzed data from the study shows that SKR 40 compared to SKR 65 is slightly elevated in MnO, total Fe_2O_3 and SiO_2 contents and lower CaO contents. The MgO contents vary equally in both zones.

F and J zones

The upper part of the orebody is capped by red to reddish pink hematite lutite with kutnahorite and rhodochrosite and occasionally calcite as carbonate species. The F and J zones constitute the uppermost part of the LMO and together constitute the ferruginized zone. The MgO and CaO contents in F-zone are slightly elevated while total Fe_2O_3 content attains a maximum of 45% due to the presence of hematite and occasionally jacobsite. The manganese content is depleted with low Mn/Fe ratios of about 1.

The concentrations of Al_2O_3, TiO_2, Na_2O, Cr_2O_3 and K_2O in almost all the zones are either very low or below detection limit <0.01 % which is negligible. The occurrences of these oxides are not immediately evident since there is no manganese or gangue minerals associated with the oxides that were encountered throughout the study. However, the Al_2O_3, could be probably associated with garnet detected by XRD as a trace and together with trace amounts Na_2O and K_2O, associated with clay minerals leached from the overlying Kalahari Group. The F and J zones at borehole SKR 40 show Al_2O_3 concentrations of about 0.1% and 0.3% respectively. The majority of the zones in both boreholes show elevated P_2O_5 content of about 0.2% compared to other minor oxides.

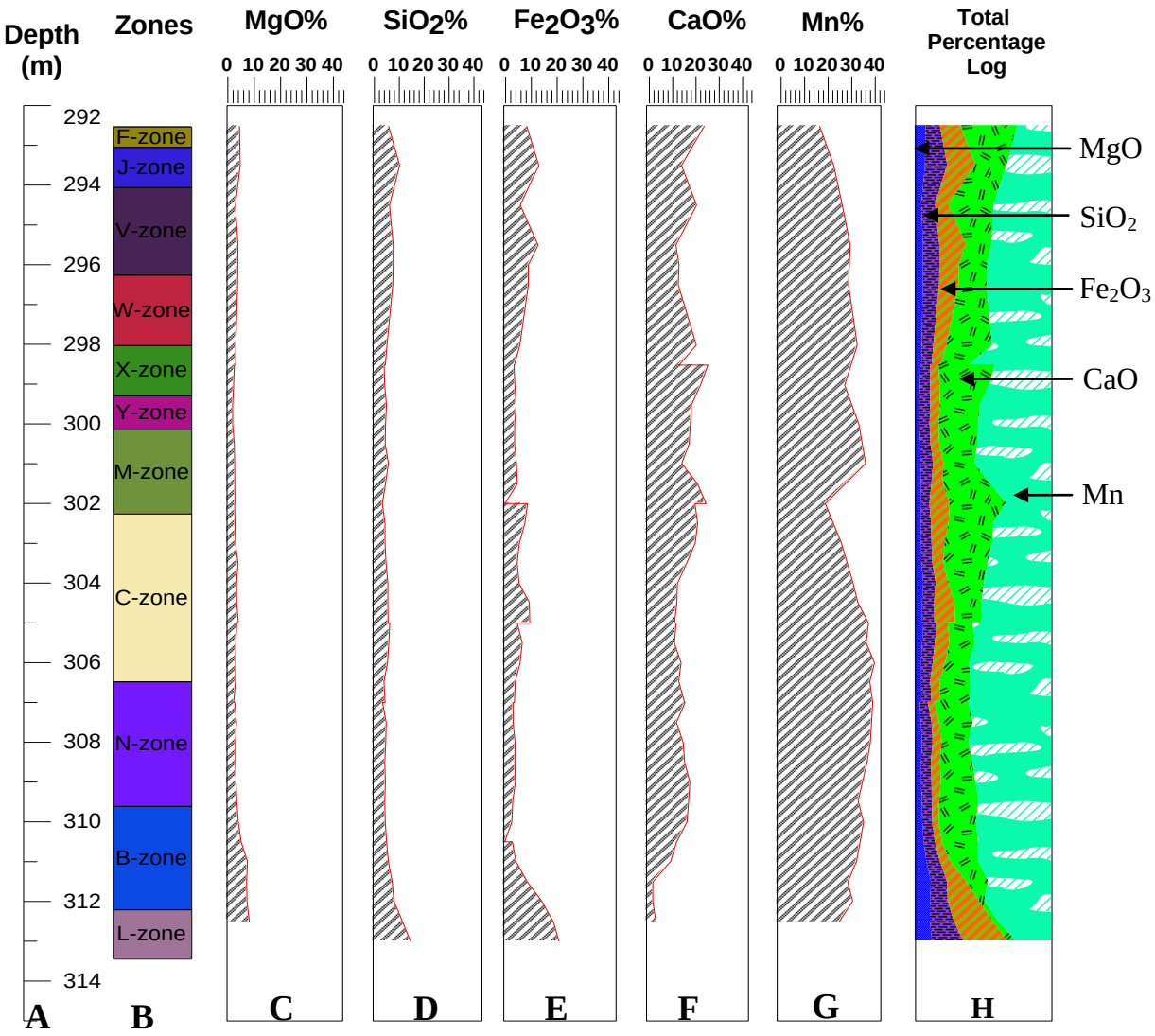

Figure 4.11 A profile plot (same scale) of the Lower Mn Orebody showing the variation of the dominant major oxides and manganese ore at borehole SKR 40 with depth. (**A** - **G**): The MgO ranges from 3% to 6% and is well developed at the top (F to X-zone) and at the base (B to L-zone). The SiO_2 content ranges from 6% to 15% and is more concentrated in the upper zones (F to X-zone) and the lowermost zones while total Fe (Fe_2O_3) varies from 8% to 22% across the orebody. The CaO is the most dominant oxide and represents the dominance of carbonates. The Mn content varies from 18% to 40% and shows a negative variation with CaO. **(H)** A variation plot showing the total percentage of the oxides normalized to 100%. Data obtained from Kalahari Resources.

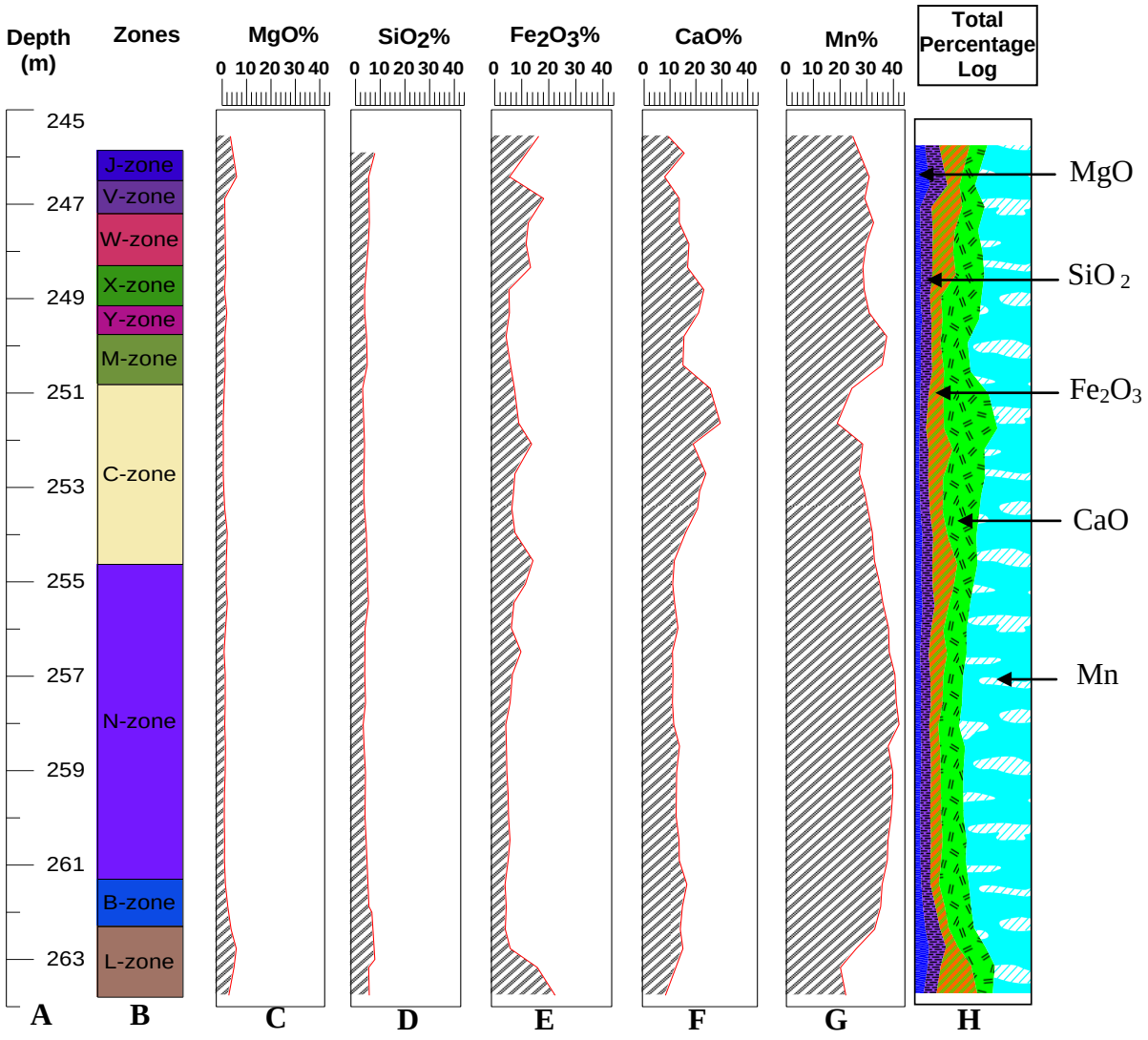

Figure 4.12 A profile plot (same scale) of the LMO showing the variation of the four dominant major oxides and manganese ore at borehole SKR 65 with depth. **A – G:** The MgO and SiO_2 contents at upper J to V zones and lower B to L zones attain a maximum of 8% to 10% and the remaining zones vary from 2% to 4% and 4% to 6% in MgO and SiO_2 respectively. The CaO is the most dominant oxide and it represents the dominance of carbonate. The Mn content varies from 20% to 42% and shows inverse negative correlation with CaO. **(H)** A variation plot showing the total percentage of the oxides normalized to 100%. Data obtained from Kalahari Resources.

Serpentine	Rhodochrosite	Dolomite	Calcite	Calcite(Mg)	Kutnahorite	Hematite	Hausmannite	Jacobsite	Braunite	Zone	Thickness (m)
	7		10		22	18		13	30	**J**	0.64
	-	-	13	12	12	10	5	-	48	**V**	0.70
10	-	21	13	17	18	12	-	-	9	**W**	1.10
7	-	-	-	-	15	10	5	9	54	**X**	0.85
9		-	11		22	6		-	52	**Y**	0.61
		-		15	14	6	12	-	53	**M**	1.06
		-	8	33	10	9	-	-	41	**C**	3.81
		-		9	14	10	-	11	56	**N1**	2.20
		-		12	25	5	6		53	**N2**	4.47
			-	18	11	42	-	14	15	**B**	1.00

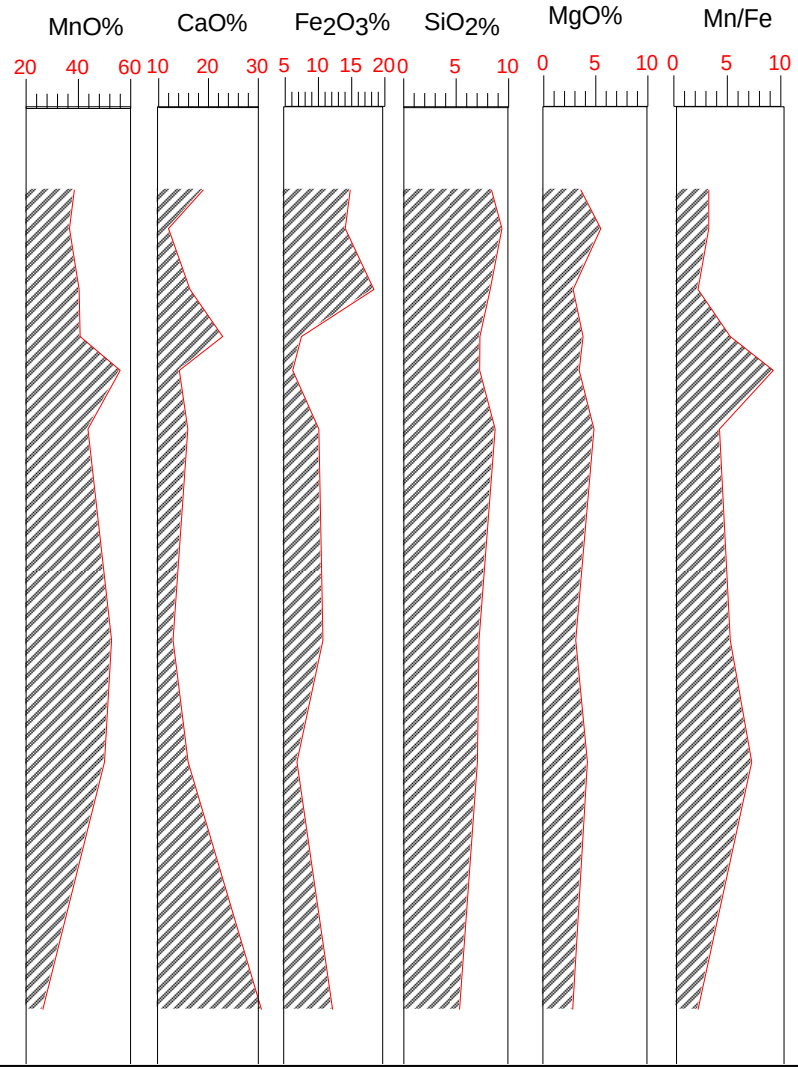

Figure 4.13 A profile showing a comparison of mineralogy (XRD) and geochemical results (dominant major oxides and manganese) at borehole SKR 65.Note the variation of manganese (MnO) content and major oxides from the top to the bottom of the orebody. The XRD analyses are expressed in percentage (%) and added up to one hundred percent (100%).

Serpentine	Rhodochrosite	Dolomite	Calcite	Calcite (Mg)	Kutnahorite	Hematite	Hausmannite	Jacobsite	Braunite	Zone	Thickness (m)
	17				32	51				**F**	
3				12	10	20	4	19	32	**J**	1.26
			17	13	13	11	3		43	**V**	2.20
		7	12		25	5	6	-	46	**W**	1.77
			19		21	6	3		51	**X**	1.26
				16	11	17	-	-	57	**Y**	0.86
				16	13	14	4		52	**M**	2.11
6				16	14	11	4		49	**C**	4.20
				17	15	12	5		50	**N1**	2.00
				16	14	11	9		48	**N2**	2.82
				18	21	18		14	27	**B**	0.78
			18	37	17	26				**L**	2.40

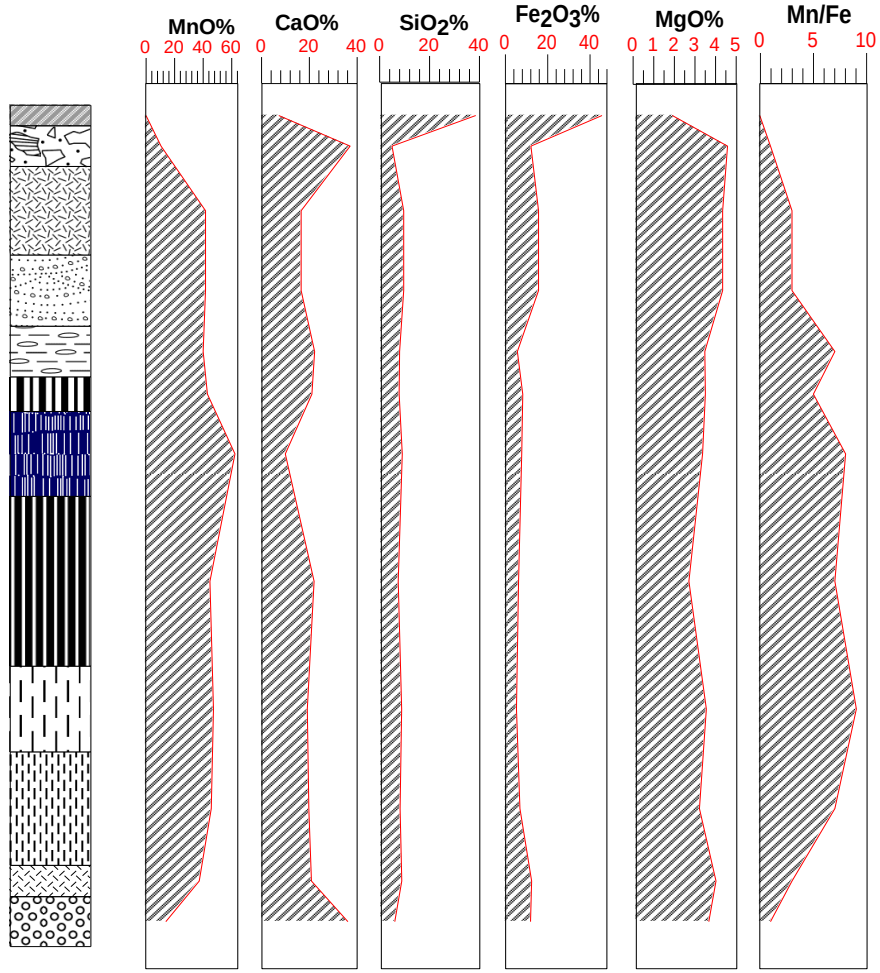

Figure 4.14. A profile showing a comparison of mineralogy and the geochemical results (dominant major oxides and manganese) at borehole SKR 40.Note the variation of manganese (MnO) content and major oxides from the top (F-zone) to the bottom of the orebody. The XRD analyses are expressed in percentage (%) and add up to one hundred percent (100%).

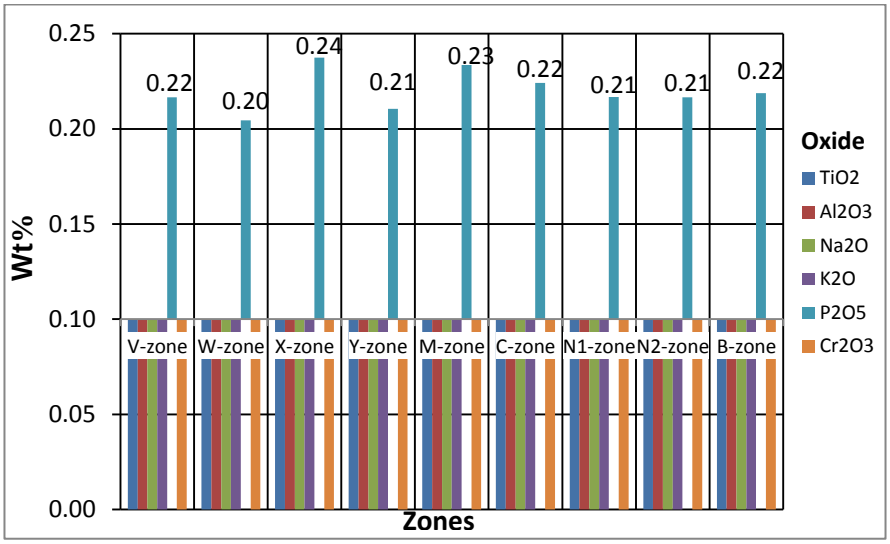

Figure 4.15 The weight percent distribution of less dominant oxide element of Al_2O_3, TiO_2, Na_2O, K_2O and P_2O_5 at SKR 65. The P_2O_5 concentration is slightly elevated above 0.2wt% in most zones while other oxides are below detection limit (<0.01wt%).

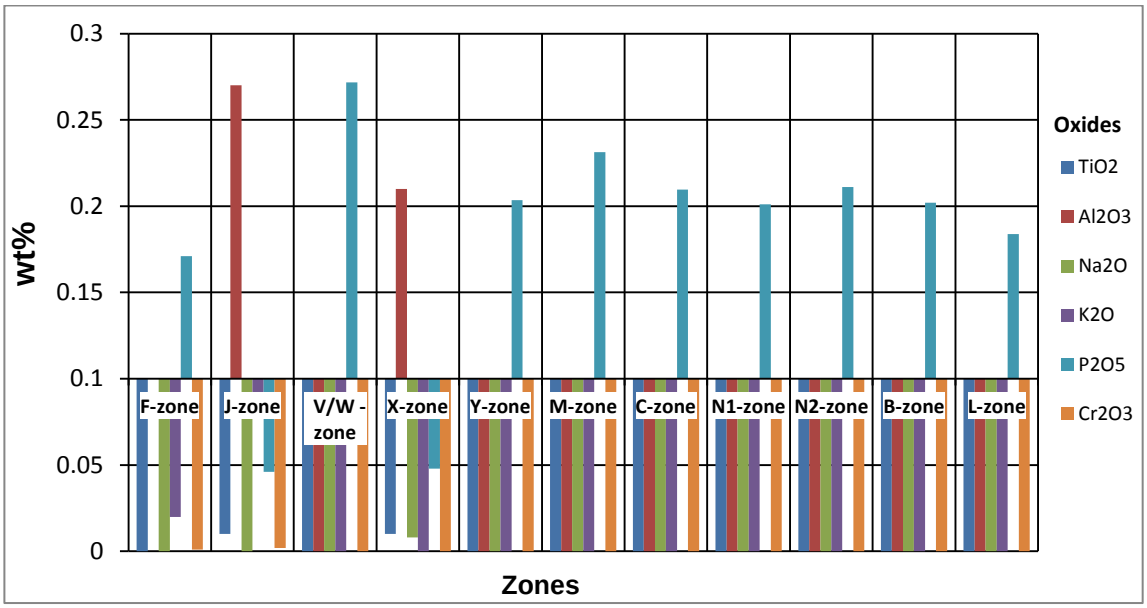

Figure 4.16 The weight percent distribution of less dominant oxide elements Al_2O_3, TiO_2, Na_2O, K_2O and P_2O_5 as on SKR 40. The P_2O_5 concentration in most zones is slightly elevated above 0.15%. The Al_2O_3 at J and V-zones ranges from 0.2 to 0.27%.

4.3.2 Trace elements

The trace elements analyses Bi, Br, Ce, Cs, Ge, Hf, Mo, Nb, Sc, Sm, Ta, Th, TI, U, Yb are below detection limit. The most abundant trace elements at J-zone of the LMO in their decreasing order of abundance are Sr, Ba, V, Co, La, Zn, Ce, Ni, Zr, Y and Rb ranging from 6ppm to 274ppm while F-zone is slightly enriched with Sr, Ba, V, Co, La, Zn, Ce, etc. The Ba content at B-zone, N1 – subzone, N2-subzone and Y-zone at SKR 65 is at 1127ppm, 521ppm, 8058ppm and 909ppm respectively.

On the other hand, M-zone and NI-subzone at SKR 40 recorded highest Ba contents of 3.6% (36000ppm) and 1.4% (1400ppm). The barite concentrations determined by SEM inside hausmannite rich ovoids and along the fissures in a braunite-kutnahorite matrix are compliant with elevated Ba contents in N- subzones of SKR 65. The elevated Ba and Sr contents at Y-zone of both boreholes are compliant with the Sr-barite concentrations inferred by SEM and the strontium content is hosted in barite.

High concentrations of trace elements barium (909ppm) and strontium (149ppm) are consistent with the traces of Sr-barite detected by SEM along the alumino silicate/silicate fissures. Towards the base (B and L zones), the Lower manganese orebody also displays an elevated content of barium (Ba). The elevated concentration of trace elements of zinc (Zn) in most zones together with slightly elevated (mostly < 60ppm) contents of Cu, Ni, Co La and V remain unexplained since there are no mineral phases hosting such elements which were detected hence they are present as impurities in the ore. However, they may have incorporated in the lattice structure of precipitating Mn and Fe content or during diagenesis.

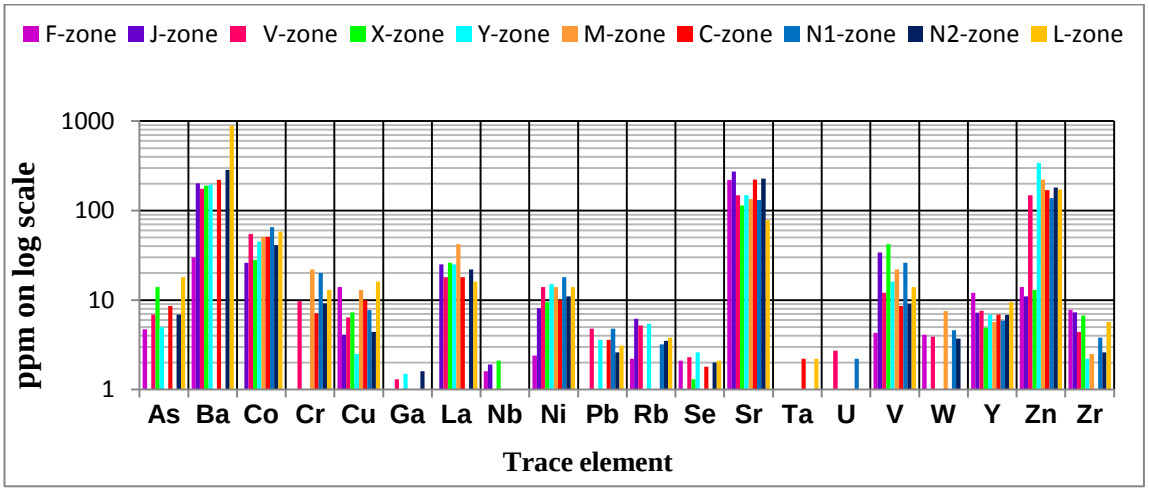

Figure 4.17. The plot of trace elements in ppm observed on various zones as determined in SKR 40. The Ba, Sr and Zn concentrations are the most dominant and are often greater than 100ppm. The Co, La and Ni contents occurs mostly above 10ppm but below 100ppm. The Ba content attains a maximum of 3.9% (about 36000ppm) at borehole SKR 40.

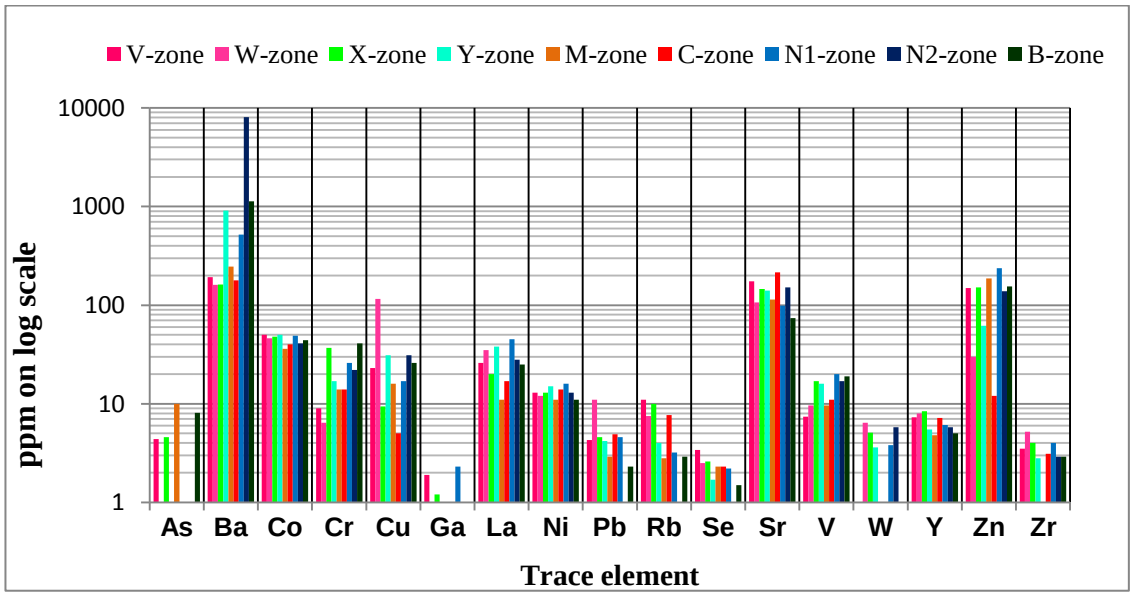

Figure 4.18. The semi-log plot of trace element (ppm) abundance at various zones as determined in SKR 65. The Ba, Sr and Zn concentrations are the most dominant and often occur in amounts greater than 100ppm. The Co, La and Ni contents are present in concentration mostly above 10ppm but below 100ppm.

4.4 Discussion

4.4.1 Correlation of major and trace elements

The manganese ore shows a strong negative correlation with carbonate content and occasionally with hematite content as discussed below.

Correlation coefficient matrices in order to determine if any relatiotionship exists between various elements of the manganese ore. Results for the individual analyses of major and trace elements are listed in table 4.1 and 4.2. Major elements such as TiO_2, Al_2O_3, Na_2O, K_2O and Cr_2O_3 together with some trace elements cannot be correlated, as they are negligibly small.

The MnO shows a negative relationship with oxides of Fe, Si, Ca, Mg and trace elements Cu and La and a positive relationship with oxide of P and trace element of Ba, Sr, Zn, Co, Ni and V. It is suggested that oxides of manganese (Mn) and iron (Fe) precipitated from seawater enrironment and in the process adsorbed trace elements due to their lattice structure and their affinity for ions.

The negative correlation of oxides of manganese (Mn) and iron (Fe) is characteristic of many manganese deposits and such non-coherence may be interpreted to suggest precipitation under different environmental and pH conditions. It is important to note that the iron phase in the manganese ore is contributed mostly by hematite and to a lesser extent by other Fe-rich manganese oxides such as jacobsite and Fe-rich hausmannite. Geochemical analyses show that the Si (together with Mg) may have been largely contributed by silicates (notable garnet and serpentine) rather than braunite as it shows no sympathethic relationship with oxide of

manganese. Nyame et al. (2002) viewed the negative relationship between Mn versus Ca, Mg and Si in the nodules of the Proterozoic Nsuta deposit as an indication that these elements (Ca, Mg and Si) originated from the surrounding depositional or diagenetic waters during the formation of nodules.

The negligibly small amount of alumina content in the manganese ore at Kalagadi mine is attributed to low amounts of aluminium silicate leached from the Kalahari calcretes and sands above. High concentrations of oxides of Ca in the ore indicate the abundancy of carbonate-bearing manganese minerals and they show a linear negative relationship with MnO.

The negative relationship between oxides of Ca, Fe versus Mn is also shown by the fact that economic zones of the LMO are characterized by lower carbonate (kutnahorite and/or Mg-calcite), hematite contents, and elevated braunite content and the opposite is observed in the low grade zones. Trace elements Cu and La show no relationship and hence their existence reflects dissolution and incorporation into the manganese lattice structure.

The good correlation (R = 0.86) between oxide of Mn and trace element of Ba is associated with the presence of barite in the manganese ore. The trace element of Ba also exhibits strong correlation with Zn and intermediate relationship with the oxide of P respectively. On the other hand, Ba is poorly correlated with the rest of major and trace elements.

Oxide of Fe is positively correlated with oxide of Si, Ca and M and trace elements Co, Cu La while showing negative relationship with oxide of Mn and P and together with trace elements Zn, Ba, Sr, Ni and V. The correlation data shows that most trace elements are

present in an adsorbed state, in precipitating oxides of Mn and Fe and some during diagenesis.

Elements like SiO_2, CaO, MgO, Co, Cu and La get adsorbed in Fe_2O_3 phase as the show positive correlation with Fe-oxide.

Table 4.3 Average compositions of six major oxides and selected trace elements (above) of certain zones (except W-zone) of the Lower Manganese Orebody at Kalagadi Manganese mine with their correlation coefficient matrices (below). The data is based on two boreholes analysed in the study. Values in italics are not averaged as the second borehole data was either insufficient or negligibley small.

Zone	**Major oxides elements in wt%**						**Trace elements in ppm**							
	MnO	**Fe_2O_3**	**SiO_2**	**CaO**	**MgO**	**P_2O_3**	**Ba**	**Sr**	**Zn**	**Co**	**Cu**	**Ni**	**La**	**V**
V	40.03	15.35	12.01	17.78	3.97	0.25	184.00	161.00	148.50	52.50	14.70	13.50	22.00	9.70
W	36.60	14.33	9.43	12.18	5.57	0.20	161.00	107.00	30.00	46.00	116.00	12.00	35.00	9.60
X	40.12	12.12	6.94	19.29	3.16	0.14	176.00	130.00	82.00	38.00	8.35	11.25	23.00	29.50
Y	41.80	7.91	7.71	21.96	3.65	0.20	551.50	145.00	201.00	47.50	16.75	15.00	31.50	16.00
M	59.00	7.00	7.46	12.10	3.40	0.23	18123.00	124.00	204.50	43.50	14.50	12.50	26.50	15.80
C	44.20	8.23	7.45	19.00	3.77	0.22	200.00	219.00	90.50	45.50	7.50	12.00	17.50	9.80
N1	49.90	8.05	6.19	16.10	3.33	0.21	7260.50	115.00	187.50	57.00	12.35	17.00	*45.00*	23.00
N2	47.80	6.90	6.93	17.90	3.71	0.21	4171.00	189.50	159.50	41.00	17.70	12.00	25.00	13.05
B	32.00	12.37	8.84	25.72	3.41	0.21	*1127.00*	*74.00*	*155.00*	*44.00*	*26.00*	*11.00*	*25.00*	*19.00*
	MnO	**Fe_2O_3**	**SiO_2**	**CaO**	**MgO**	**P_2O_5**	**Ba**	**Sr**	**Zn**	**Co**	**Cu**	**Ni**	**La**	**V**
MnO	1.00	-0.73	-0.48	-0.59	-0.34	**0.25**	**0.86**	**0.28**	**0.52**	**0.09**	-0.38	**0.35**	-0.13	**0.02**
Fe_2O_3		1.00	**0.80**	**0.06**	**0.48**	-0.02	-0.55	-0.36	-0.57	**0.08**	**0.48**	**-0.30**	**0.12**	-0.11
SiO_2			1.00	**0.02**	**0.47**	**0.51**	-0.35	-0.08	-0.21	**0.24**	**0.32**	**-0.19**	**0.06**	-0.55
CaO				1.00	**-0.46**	-0.20	-0.53	-0.07	**0.19**	-0.14	-0.43	-0.14	-0.30	**0.26**
MgO					1.00	**0.20**	-0.31	-0.05	-0.64	0.09	-0.05	-0.64	**0.59**	-0.64
P_2O_5						1.00	**0.29**	**0.21**	**0.37**	**0.55**	-0.01	0.23	-0.11	-0.76
Ba							1.00	-0.16	**0.56**	**0.03**	-0.20	**0.18**	**0.06**	**0.10**
Sr								1.00	-0.07	-0.08	-0.37	-0.02	-0.55	-0.44
Zn									1.00	**0.31**	-0.62	**0.53**	-0.05	**0.15**
Co										1.00	-0.01	**0.83**	**0.08**	-0.19
Cu											1.00	-0.20	**0.74**	-0.38
Ni												1.00	**0.30**	**0.10**
La													1.00	-0.09
V														1.00

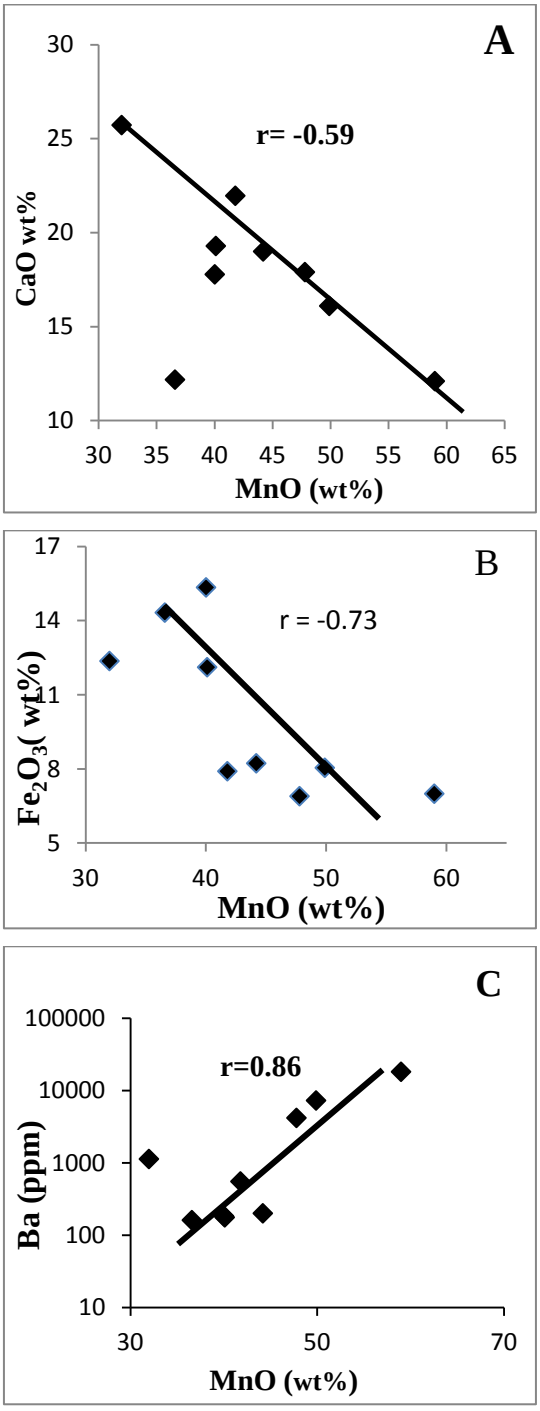

Figure 4.19 Shows correlation between oxide of (**A**) Mn and Ca; (**B**) Mn and Fe and (**C**)Mn and Ba.

4.4.2 Depositional environment

The sodium (Na) and magnesium (Mg) contents calculated from the data obtained from both this study and Kalahari Resources ranges from 0.005% to 0.05% and 1% to 3.4% respectively. The sodium and magnesium are mobilized by weathering with the former being more soluble in water. The elevated concentrations of magnesium, often above 1wt% content is thought to correspond with High Mg–calcite in the manganese ore. The High Mg-calcite is commonly precipitated from marine water because Mg is more abundant than Ca in the marine environment.

Nicholson (1992) presented a summary of an average composition of manganese oxides for fresh water and marine depositional environments and further established a diagnostic plot of Na vs Mg (Figure 4.20). It is important to note that SKR 65 and SKR 40 sodium (Na) values obtained from the study are lower compared to the data obtained from Kalahari Resources while magnesium (Mg) is uniformly consistent. The analyzed geochemical data from the study area plot mostly on marine to shallow marine field and hence the possibility of a freshwater chemical environment for deposition of manganese ore is excluded.

The Ca, Mg, Na and K have been diagnostically used to distinguish between the lacustrine and marine environments. Trace element analyses on the other hand have been previously used either in unity or with major oxides to differentiate sedimentary marine and hydrothermal Mn deposits. Nicholson (1992) postulated that the sedimentary marine oxide display enrichments in Na-K-Ca-Mg-Sr while those formed in the deep oceanic environments

show additional enrichments of Co-Cu-Ni. At Kalagadi mine, the barium (Ba) and strontium (Sr) contents attain a maximum of 3.6%wt (36000ppm) and 274ppm respectively while Co, Cu and Ni are slightly enriched with values ranging from 26ppm - 65ppm, 3ppm - 116ppm and 3ppm - 15ppm respectively and such values deviate from deep oceanic deposits.

The elevated Ba levels of up to 4.9% in fresh water deposits (Nicholson, 1988) and often hydrothermal deposits are known and hence it cannot be used in isolation as a guide to genesis (Nicholson, 1992).

The geochemical data from the study shows lower aluminum (Al) compared to the data supplied by Kalahari Resources while the Silica (Si) content varies constantly. The Si-Al diagram of Choi and Hariya (1992) distinguishes between hydrothermal and hydrogenous deposits. Most of the samples (except one) from both labs contain low silica contents and the data from the Kalagadi mine plot on the hydrogenous plot (Figure 4.21). The MnO_2 (Mn^{4+} , O^{2-}) is insoluble in a marine environment and is normally reduced to MnO (Mn^{2+}, O^{2-}) to enhance solubility and mobility during weathering, transport, deposition and diagenesis.

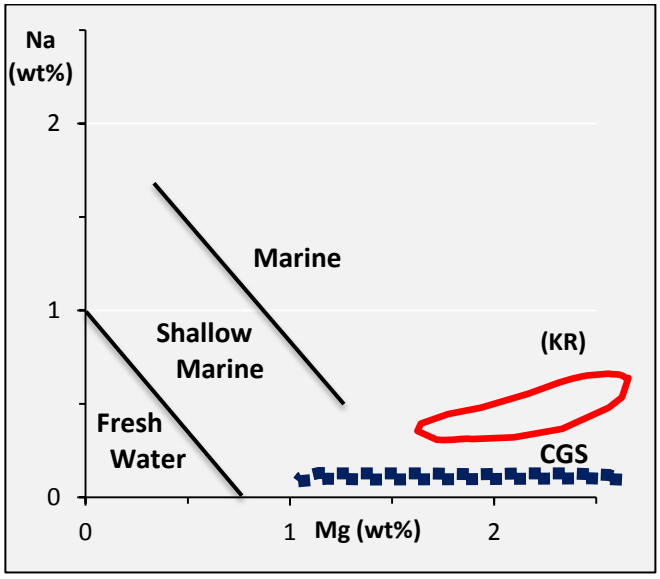

Figure 4.20 The Na vs Mg diagnostic plot to differentiate between marine and fresh water deposits (after Nicholson 1992). The solid red line shows data obtained from Kalahari Resources (KR) while blue little squares show the data analysed from Council for Geoscience (CGS).

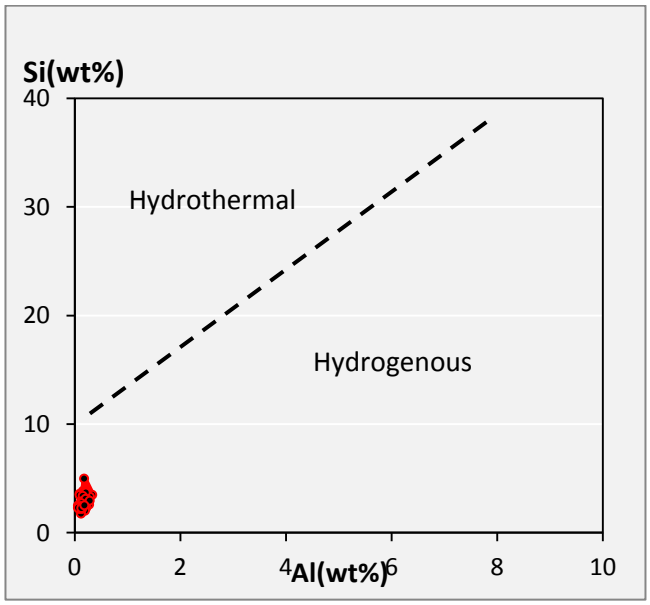

Figure 4.21 Si vs. Al discrimination diagram for the Kalagadi samples (Choi and Hariya, 1992). Note that all samples show low Al content and plot on hydrogenous.

4.5 Conclusions

The results from the study show that:

1) Chemically the LMO at Kalagadi mine is characterized by a manganese content of up to 62 % (MnO) or 42% (Mn) and Mn/Fe ratios of 4 to 9. The XRF analyses are compliant with the mineralogical results observed and determined by microscopic, (SEM) and XRD. The manganese is a minor constituent in the upper and lower zones of the stratigraphic column while carbonates (CaO) and iron (total Fe_2O_3) contents are elevated.
2) The MgO and SiO_2 contents are consistent with Mg-rich carbonates and silicate material respectively and are more elevated at the top and bottom of the orebody. The dominant major oxide elements of MnO, CaO, SiO_2, MgO and total Fe (Fe_2O_3) are comparable with the results obtained from Kalahari Resources. However, the data obtained from Kalahari Resources shows elevated Al_2O_3, Na_2O, and K_2O and lower P_2O_5 content compared to the results obtained from the study.
3) The top (F to J-zone) of the orebody is capped by elevated hematite (Fe_2O_3) and carbonate contents such as rhodochrosite, kutnahorite, Mg calcite and calcite with depleted manganese content. The decrease in Fe_2O_3 content with increasing CaO, SiO_2 and MnO towards the base of F-zone is an indication of grading of the ore from hematitic to jacobsitic braunite-lutite of J-zone. The MgO content is slightly elevated mainly in the upper and lower zones and increase with increasing CaO content.

4) The most abundant trace elements are barium (Ba), strontium (Sr) and zinc (Zn) occur in concentrations above 100ppm in almost all the zones. The trace elements cobalt (Co), lanthanide (La), nickel (Ni), vanadium (V) and copper (Cu) are present in variable proportions, mostly from >5ppm but <100ppm. The enrichments of Cu, Zn, Ni, Co and V trace elements in the host rock or orebody are commonly associated with volcanogenic hydrothermal input in chemical precipitates (Tsikos and Moore, 1997) and slightly elevated Co and Ni concentrations are often associated with organic matter.
5) Therefore, it can be concluded that the depositional environment for the manganese ore on the mine lease is that of marine to shallow marine with probable some influence of volcanic activity.

4.6 References

Chetty, D. (2008). A geometallurgical evaluation of the ores of the northern Kalahari manganese deposit, South Africa, Unpublished PhD Thesis, University of the Johannesburg, South Africa).

Choi, J.H., and Hariya, Y. (1992). Geochemistry and depositional environment of Mn oxide deposits in the Tokoro Belt, Northeastern Hokkaido, Japan. Economic Geology, Vol. 87; no. 5; p. 1265-1274

Du Plooy, A.P. (2002). Geochemistry and mineralogy of supergene altered manganese ore below the Kalahari unconformity in the Kalahari manganese field, Northern Cape Province, South Africa, Unpublished MSc. Dissertation, Rand Afrikaans University (now University of the Johannesburg, Johannesburg, South Africa).

Nel, C.J., Beukes, N.J. and De Villiers,J.E. (1986). The Mamatwan manganese mine of the Kalahari manganese field, in Anhaeuser, C.R. and Maske, S., eds., Mineral deposits of Southern Africa: Johannesburg, Geological Society of South Africa, p.963-978.

Nicholson, K. (1988). An ancient manganese-iron deposit of freshwater origin, Islay, Argyllshire: Scottish Journal of Geology, Vol. 24, p.175-187.

Nicholson, K. (1992). Contrasting mineralogical-geochemical signature of manganese oxides: Guides to Metallogenesis: Economic Geology Vol, 87, 1992, p. 1253-1264.

Nyame, F.K., Beukes, N.J., Kase, K., and Yamamoto, M., (2002). Compositional variations in manganese carbonate micronodules from the Lower Proterozoic Nsuta deposit, Ghana: product of authigenic precipitation or post-formational diagenesis. Sedimentary Geology, Vol. 154, p. 159–175.

Preston, P.C.C. (2001). Physical and chemical characterization of the manganese ore bed at the Mamatwan mine, Kalahari Manganese Field, Unpublished MSc. Dissertation, Rand Afrikaans University (now University of the Johannesburg, Johannesburg, South Africa.

Tsikos, H., and Moore, J.M. (1997). Petrography and geochemistry of the Palaeoproterozoic Hotazel Iron Formation, Kalahari Manganese Field, South Africa. Implications for Precambrian manganese metallogenesis. Economic Geology Vol.92, p. 87-97.

van Staden, A. (2002). Characterization of the lowermost manganese ore bed of the Hotazel Formation, Gloria Mine, Northern Cape Province, Unpublished MSc. Dissertation, University of the Johannesburg, Johannesburg, South Africa).

CHAPTER 5

CARBON AND OXYGEN ISOTOPES

5.1 Introduction

The stable isotope studies on manganese carbonates of the KMF have been conducted, more recently by Tsikos et al. (2003) for the manganese carbonate ore and associated BIF in the hydrothermally altered Wessels-Type ore and sedimentary Mamatwan-Type ore. Preston (2001) and van Staden (2002) in their studies also reported the bulk carbonate stable isotope in the manganese at Mamatwan and Gloria mine operating in the Mamatwan-Type ore.

The stable isotope data at Kalagadi Manganese mine is also compared to the other data of the world's manganese deposits of various ages such as Palaeoproterozoic Nsuta, Ghana (Nyame and Beukes, 2006), Late Jurassic Molango, Mexico (Okita et al. 1992), Early Jurassic Ürküt, Hungary (Polgari et al. 1991), Ordovician Taojiang, China (Delian et al. 1992), Cambrian Usa deposit (Kuznetskii Alatau area) (Kuleshov and Bych, 2002) and Kyzyltash deposits of the southern Urals, Russia (Kuleshov and Brusnitsyn, 2005).

The source of the water filling pore space and fractures in rocks varies mostly from fresh/meteoric and seawater. The carbon isotope composition for fresh water carbonates ranges from -4‰ to -9‰ PDB (Anderson and Arthur, 1983) while those derived from seawater carbonates are around 0‰. Living organisms generally show depleted $\delta^{13}C$ values of up to -34‰.Öztürk and Frakes (1995) reported and interpreted the carbon isotopes from -5‰ to -7‰ PDB at Binkilic manganese deposit in Turkey as suggestive of modern fresh waters.

Andrews (2006) suggested that the $\delta^{13}C$ isotopes are controlled by the amount of interaction a system has with atmospheric CO_2 derived from soil organic matter and inorganic carbon derived from limestone at depth. The $\delta^{18}O$ composition of marine carbonates, though variable, are close to 0‰ and hence elevated compared to non-marine carbonate which normally shows negative values on PDB scale. The oxygen isotope composition has also been utilized to uncover paleotemperature conditions under which certain rock deposits and sediments formed.

According to Andrews (2006), the $\delta^{18}O$ isotopes vary because of three main factors: 1) water temperature; 2) the amount of $\delta^{18}O$ in the water; and 3) other factors such as evaporation and biological components. Rosales et al. (2004) also suggested and attested to the fact that ,the $\delta^{18}O$ composition of marine carbonates may be influenced by isotopic composition and variation in salinity of the water mass from which they precipitate, the temperature of the water, the biogenic fractionation (vital effect), and the diagenetic processes.

According to Kasting et al. (2006) minerals precipitated from seawater at low temperatures are enriched in $\delta^{18}O$ compared to the parent solution, while minerals formed at higher temperatures show less enrichment of oxygen isotope. Kuleshov and Brusnitsyn (2005) reported isotopic compositions in the range of –51.4‰ to –10.8‰ $\delta^{13}C$ and 14.4‰ to 21.4‰ $\delta^{18}O$ for rhodochrosite and calcite on manganese ores in the South Faizuly and Kyzyltash deposits of the southern Urals. Nyame and Beukes (2006) reported the $\delta^{13}C$ and $\delta^{18}O$ values for the manganese carbonates at Nsuta manganese mine in a range of -20.8‰ to -1.5‰ and 12.2 ‰ to 19.6 ‰, respectively. The $\delta^{13}C$ and $\delta^{18}O$ values for the manganese carbonate

ores of the Usa manganese deposit varies from –18.4‰ to –0.7‰, and 18.4‰ to 23.0‰ respectively (Kuleshov and Bych, 2002).

Delian et al. (1992) reported $\delta^{13}C$ values for black shale-hosted Mn carbonates of Taojiang deposit in China in a range of -22 to -9‰, showing negative variation with manganese. The $\delta^{13}C$ values reported by Nyame and Beukes (2006) for the Nsuta manganese deposit range from -20.9 to -1.5‰ while the Urkut manganese deposit varies from -30.78 to -1.24 (Polgari et al. 1991) and Molango manganese deposits range from -16 to -5‰ (Okita 1987 in Polgari et al. 1991). The carbon isotope values for the Taojiang, Nsuta, Urkut and Molango deposits therefore show an influence of organic carbon during diagenetic stage while fewer samples from Usa, Nsuta and Urkut deposits show evidence of precipitation of Mn carbonates from seawater (≈0‰).

Stable isotope compositions of different manganese carbonate ores (rhodochrosite, calcareous rhodochrosite) from the Usa deposit (Kuznetsk Alatau) as suggested by Kuleshov and Bych (2002) are of diagenetic to sedimentary origin ($\delta^{13}C$ = -18.4 to -0.7‰ for the ores and -1.9 to 1.0‰ for host rock) and are thought to have formed with the participation of oxidized organic carbon. Apart from that, manganese ores in the Usa deposit shows a direct correlation with carbon isotopic composition.

Kuleshov and Brusnitsyn (2005) reported carbon ($\delta^{13}C$) isotope values for the manganese carbonates (rhodochrosite and calcite) in the Kyzyltash deposits of the southern Urals in a range from -28.1 to -10.8‰. The carbon in these carbonate ores is associated with carbon dioxide derived from mainly microbial decomposition of organic matter and possibly small amounts of methane (from positive correlation of Ca and $\delta^{13}C$) generated during diagenesis.

5.2 Methologies

A total of ten pulverized samples of bulk carbonates in the manganese ore representing certain zones were submitted to the University of Cape Town to determine the oxygen and carbon isotopes of bulk carbonate content on the manganese ores. The analyses were carried out on a Finnigan Mat 252 mass spectrometer and all samples were reacted at 100^{o}C to ensure that any carbonate mineral present was reacted.

The abundant carbonate minerals in the analyzed samples are the kutnahorite and Mg−calcite and occassionally calcite. Semi-quantitative results from XRD were used to calculate the approximate total carbonates present in each sample and the content varied from 20% to 60%. The acid-CO_2 fractionation factor was assumed to be that of the dominant carbonate, the reproducibility of $\delta^{13}C$ was better than 0.1 per mil, and for $\delta^{18}O$ about 0.1 per mil. The measurements of carbonates samples were undertaken on CO_2 liberated during reaction with 100% H_3PO_4 at various temperatures. The oxygen and carbonate isotope data are reported as $\delta^{18}O$ values in per mil relative to Standard Mean Ocean Water (SMOW) and $\delta^{13}C$ are reported in per mil relative to Pee Dee Belemnite (PDB).

5.3 Results

The M-zone of borehole SKR 40 is most depleted in $\delta^{13}C$ attaining about -12‰ but enriched in $\delta^{18}O$ reaching 19.80‰ when compared to the most of the data. This zone as determined by XRD is characterized by elevated manganese and low carbonates (CaO) content. The M-zone at borehole SKR 65 also shows the lower $\delta^{13}C$ values of -11.25‰ while $\delta^{18}O$ values attain a maximum of 19.78‰.

The X-zone below compared to the most data shows enrichments of up to -8.50‰ $\delta^{13}C$ but slight depletion of about 18.22‰ in $\delta^{18}O$ contents. The $\delta^{13}C$ values of W-zone shows a slight decline of about -9.04‰ while $\delta^{18}O$ are slightly enriched at 18.57‰ compared to X zone above. The Y and C-zones compared to the most analyzed zones hold almost similar values and are most enriched in $\delta^{13}C$ attaining -7.96‰ and -7.49‰ respectively but most depleted in $\delta^{18}O$ with 17.79‰ to 17.55‰.

The V-zone share almost similar $\delta^{13}C$ and $\delta^{18}O$ values with W-zone, reaching -9.29‰ and 18.68‰. The $\delta^{13}C$ values at N1 and N2 subzones gradually decline to -11.35‰ and -10.67‰ and this persists to B-zone before increasing to -9.33‰. Similarly, the $\delta^{18}O$ values increases from about 19‰ to 20‰ at N1 and N2 subzones and finally reaching 22‰.

Table 5.1 Oxygen and Carbon of the samples data mostly SKR 65 (except M-zone) in the Kalagadi mine with associated manganese and carbonate species as determined by XRD. The $\delta^{18}C$ PDB values are obtained using relationship: $\delta^{18}O$ (SMOW) = 1.030 $\delta^{18}C$ (PDB) + 30.86 (**$\delta^{18}O$ in PDB** is calculated using the above formula developed by Friedman & O'Neil, 1977).

Zone	$\delta^{13}C$ PDB	$\delta^{18}O$ PDB	$\delta^{18}O$ SMOW	%cc	Mn	CaO
M (SKR 40)	-12.26	-13.37	19.80	22	48.4	9.83
X	-8.50	-13.79	18.22	100	31.4	16.43
W	-9.04	-14.01	18.57	11	28.7	12.18
Y	-7.96	-12.04	17.79	43	27.2	24.71
C	-7.49	-12.77	17.55	78	34	16.02
V	-9.29	-11.86	18.69	70	29	19.10
N1	-11.35	-12.91	18.83	43	41.1	13.08
N2	-10.67	-13.02	19.58	52	39	16.07
M (SKR 65)	-11.25	-10.01	19.78	33	43.4	14.33
B	-9.33	-11.83	21.68	73	20.1	30.64

5.4 Discussion

The stable isotope data can be classed into Group I and II, based on $\delta^{18}O$ and $\delta^{13}C$, Mn and $\delta^{13}C$, CaO and $\delta^{13}C$, and Mn and $\delta^{18}C$ correlation as shown below.

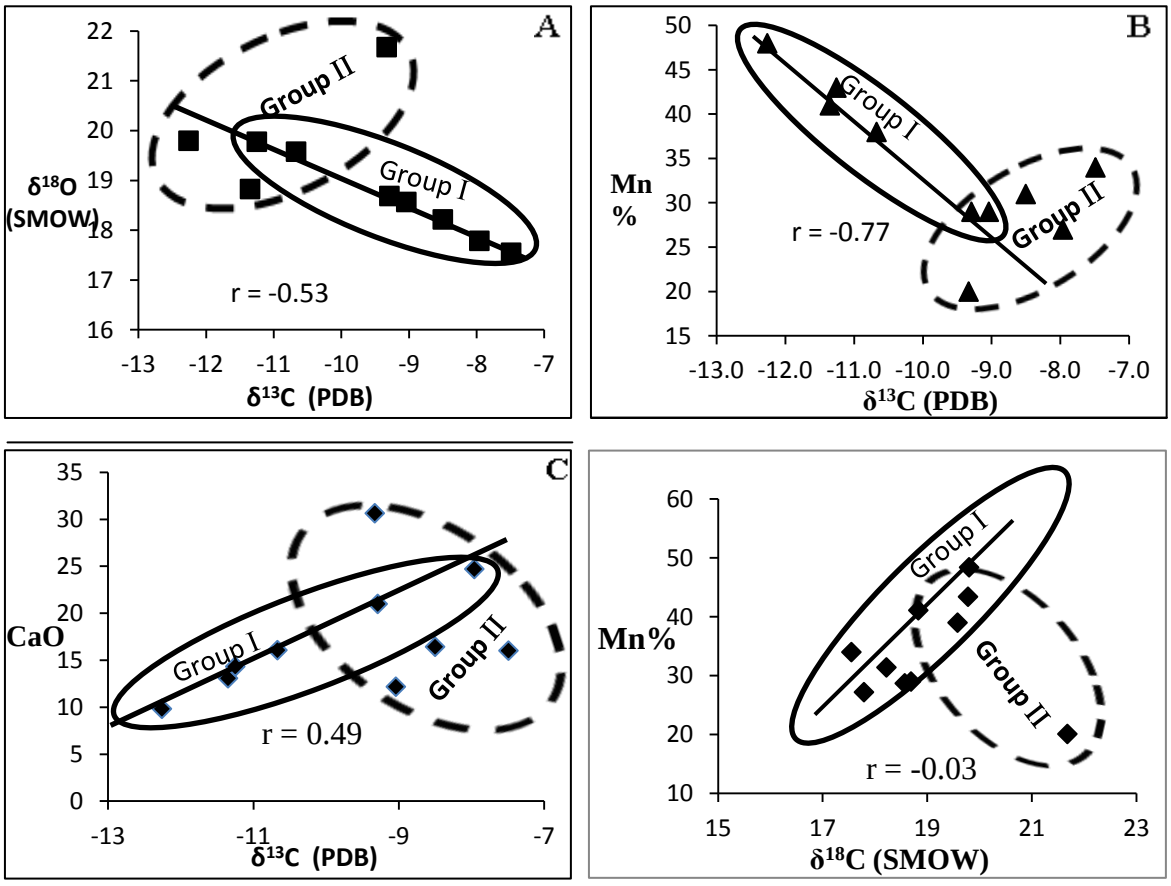

Figure 5.1 (**A**). The $\delta^{18}O$ and $\delta^{13}C$ isotope plot for the manganese carbonate samples at Kalagadi mine showing an overal negative correlation. (**B**). Scatter plot of Mn content versus $\delta^{13}C$ showing negative correlation. (**C**) Carbonate (CaO) and $\delta^{13}C$ are positively correlated. Mn and $\delta^{18}C$ show a negative correlation.

Group I is characterized by linear correlation between on $\delta^{18}O$ and $\delta^{13}C$, Mn and $\delta^{13}C$, CaO and $\delta^{13}C$, and Mn% and $\delta^{18}C$ values. Group I shows a negative linear correlation between $\delta^{18}O$ (SMOW) and $\delta^{13}C$ (PDB), and Mn% and $\delta^{13}C$ (PDB) and a positive linear relationship between CaO and $\delta^{13}C$ (PDB), and Mn% and $\delta^{18}C$ (SMOW).

Group II is fairly scattered, but there is a slight positive correlation between $\delta^{18}O$ (SMOW) and $\delta^{13}C$ (PDB), Mn% and $\delta^{13}C$ (PDB), CaO and $\delta^{13}C$ (PDB), and Mn% and $\delta^{18}C$ (SMOW). Group II shows an evidence of metamorphism or alteration compared to group I.

It is evident from Figure 5.1 that stable isotopes ($\delta^{13}C$ and $\delta^{18}O$) of the Kalahari Manganese Field (Mn ore and BIF) including that of the Kalagadi Manganese mine overlap with those of the Usa, Taojiang, Kyzyltash and Nsuta deposits while Ürküt and Molango deposits show comparable $\delta^{13}C$ signatures but heavy $\delta^{18}O$ signatures. The $\delta^{13}C$ signatures for the above deposits range from that of seawater (± 0.7‰) to fresh water (-6‰) and finally to that of water mixed with organic carbon released during bacterial oxidation (-32‰).

The $\delta^{18}O$ signatures for these deposits on the other hand range from 12‰ to 32‰ and such values are interpreted to indicate the diagenetic alteration of the manganese ore. The oxygen $\delta^{18}O$ isotope signatures for the Mn carbonates in the other deposits of various ages in the world directly overlap with that of Kalahari Manganese Field (BIF and ores) and Kalagadi Manganese mine (from 12‰ to 24‰ SMOW) except for the Urkut and Molango deposits which show heavy (from 25‰ to 32.5‰ SMOW) values and hence barely overlap.

Minimal metamorphism or metasomatism of Mn carbonates is also reported from Mamatwan mine and Nsuta deposit (Nel et al. 1986 and Nyame and Beukes 2006); Usa deposit (Kuleshov and Bych, 2002); Kyzyltash deposits (Kuleshov and Brusnitsyn, 2004) and Taojiang deposit (Delian et al. 1992) while the Urkut and Molango deposits are unmetamorphosed (Polgari et al. 1991).

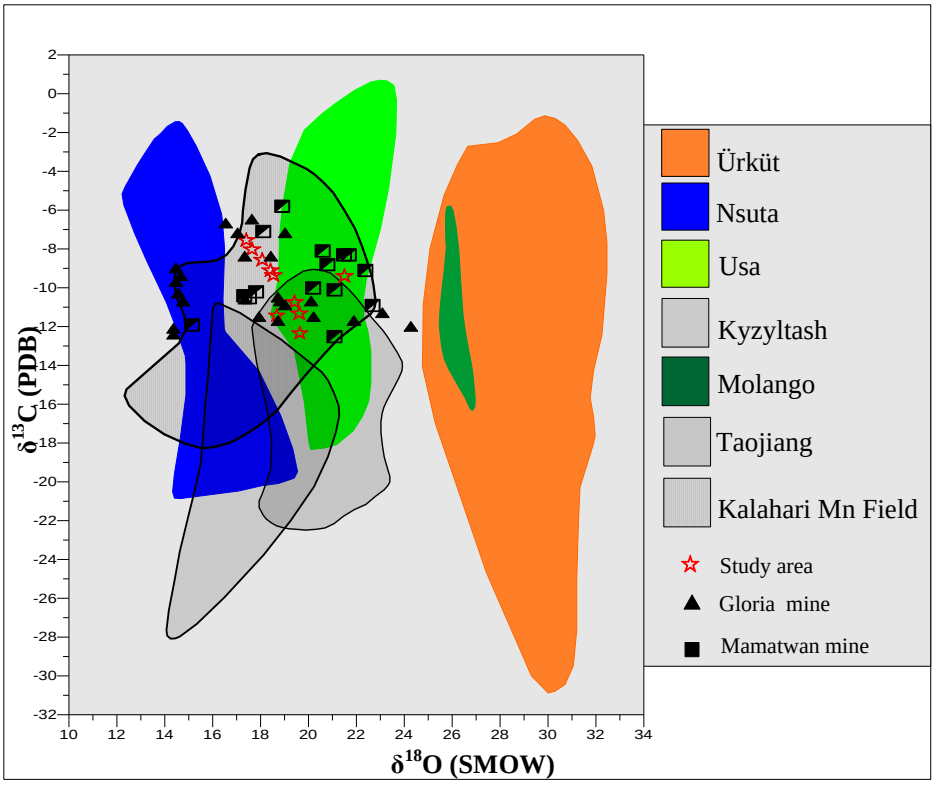

Figure 5.2 Comparison plot of carbon and oxygen isotope from Kalagadi mine with literature data from mines in the Kalahari Manganese Field, South Africa and some major Mn deposits of the world. Data are from the Paleoprotezoic Kalahari Manganese Field (Tsikos et al. 2003), and surrounding mines (Preston, 2001 at Mamatwan mine and Van Staden, 2002 at Gloria mine); Jurassic Ürküt, Hungary (Polgari et al. 1991); Jurassic Molango, Mexico (Okita et al. 1988); Ordovician Taojiang,

China (Delian et al. 1992); Cambrian Usa deposit, Russia (Kuleshov and Bych, 2002) and Kyzyltash (southern Urals), Russia (Kuleshov and Brusnitsyn, 2005).

The difference in $\delta^{13}C$ signatures (lowest to highest) at Kalagadi mine compared to Mamatwan mine range from 1‰ to 2‰ while at Gloria mine is from 0.2‰ to 0.9‰. This difference in isotopic compositions of the Kalagadi mine ores compared to Mamatwan and Gloria mine is partly because few samples were submitted for analyses compared to other two mines. The stable isotope composition of carbonates in manganese ores is also compared with other manganese deposits of various ages throughout the world. The observed difference between the Kalagadi Manganese mine and other deposits of the world is attributed mainly to the occurence of different and more than one carbonate species in the ore.

The isotopic composition of the bulk carbonate contents at Kalagadi Manganese mine fall within the boundary of the KMF as reported by Tsikos et al. (2003) especially for manganese ore. Tsikos et al. (2003) conducted a detailed stable isotope study on the manganese ore and associated BIF of the hydrothermally altered Wessel type ore in the north and with the sedimentary Mamatwan-type ore in the south of the KMF.

The carbonate isotope compositions reported for the entire KMF range from -18 to -4‰ $\delta^{13}C$ and 12 to 20‰ $\delta^{18}O$ for the BIF while the alternating manganese units range from -12 to -8‰ $\delta^{13}C$ and 14‰ to 22‰ $\delta^{18}O$. The oxygen $\delta^{18}O$ isotope values for the Kalahari Manganese Field are interpreted to suggest involvement of either meteoric water or a low-temperature hydrothermal fluid in the oxidation, leaching, and enrichment of the iron formation (Tsikos et al. 2003).

5.5 Conclusions

1) The results for isotopic composition of bulk carbonates in the manganese ores at Kalagadi Manganese mine are therefore comparable with the other mines operating in the Kalahari deposit and some other deposits manganese deposits worldwide.
2) The overall, $\delta^{13}C$ and $\delta^{18}O$ values for the manganese carbonate ores at Kalagadi Manganese mine are negatively correlated (Figure 5.1−A) while the combined data for manganese (Mn) is negatively correlated with $\delta^{13}C$. Such observations may indicate minimal action of organic carbon during manganese precipitations where the organic matter is oxidized and manganese content reduced. On the other hand, the manganese carbonates (CaO) are positively correlated with carbon isotope and this indicate diagenetic alteration and the involvement of biogenic carbonate during sedimentation.

3) The mean $\delta^{13}C$ at Kalagadi mine is -9.7‰ and at least four samples of the analyzed data show $\delta^{13}C$ isotopic signatures within a range expected for fresh water while the rest shows slightly lower values, possibly due to mixing of seawater with organic carbon. This is a characteristic common in other huge manganese deposits throughout the world. The lighter $\delta^{13}C$ values such as those observed at Kalagadi mine and other deposits are associated with the carbon in the manganese ore that originated from organic matter during diagenesis.

4) The stable isotope values at Mamatwan and Gloria mine also fall within the boundary of the Kalahari Manganese Field with very few samples lying beyond. The carbon ($\delta^{13}C$ = -12.3 to -7.5‰) isotope therefore is strongly comparable to the carbon ($\delta^{13}C$ = -12.5 to -8.1‰) isotope data for Mn-carbonates at Kalahari Manganese Field by Tsikos et al. (2003) while the $\delta^{18}O$ contents attains a maximum of 23‰ which is slightly heavier than at Kalagadi mine (20‰).

5) The oxygen isotope data suggest that low-temperature hydrothermal fluids mixed with heated meteoric water (possible from volcanic source) responsible for the precipitation of Mn carbonate ores.

6) The manganese carbonate stable isotope analyses at Kalagadi mine is also comparable with the data obtained from other mines in the entire Kalahari deposit. The oxygen $\delta^{18}O$ isotopes (18‰ to 22‰) at Kalagadi Manganese mine are therefore also interpreted to indicate slight metamorphism of the ore, as unmetamorphosed ores normally show $\delta^{18}O$ signatures in a range of 25‰ to 30‰ SMOW (Maynard, 2010). The abundance of sedimentary features (banding, lenticles etc) and minerals in the ore together with few minerals of late diagenetic to early metamorphism (garnets and serpentines) also indicate that the low to medium pressure and temperature of metamorphism.

5.6 References

Anderson, T.F., and Arthur M.A. (1983). Stable isotopes of oxygen and carbon and their application to sedimentologic and paleoenvironmental problems. In: M.A. Arthur et al. (editors), Stable Isotopes in Sedimentary Geology. Soc. Econ. Paleont. Mineral., ShortCourse IO: 1.1-1.151.

Andrews, J.E. (2006). Palaeoclimatic records from stable isotopes in riverine tufas: Synthesis and review: Earth-Science Reviews, Vol. 75, p. 85-104.

Delian, F. Tiebing, L. and Jie, Y. (1992). The process of formation of manganese carbonate deposits hosted in black shale series. Economic Geology, V. 87, p. 1419-1429

Friedman, I., and O'Neil, J. R. (1977). Compilation of stable isotope fractionation factors of geochemical interest in U.S. geological Survey Professional Papers, p. 440-KK.

Kasting, J.F., Tazewell, H.M., Klaus, W., Veizer J., Shields G., Jaffrés J. (2006). Paleoclimates, ocean depth, and the oxygen isotopic composition of seawater: Earth and Planetary Science Letters 252, p. 82–93.

Kuleshov, V. N., and Bych, A. F. (2002). Isotopic Composition ($\delta^{13}C$, $\delta 1^{8}O$) and Origin of Manganese Carbonate Ores of the Usa Deposit (Kuznetskii Alatau). Lithology and Mineral Resources, Vol. 37, No. 4, p. 330–343. Translated from Litologiya iPoleznye Iskopaemye, No. 4, p. 381–396.

Kuleshov, V. N., and Brusnitsyn, A. I. (2005). Isotopic Composition ($\delta^{13}C$,$\delta 1^{8}O$) and the Origin of Carbonates from Manganese Deposits of the Southern Urals: Lithology and Mineral Resources, Vol. 40, No. 4, 2005, p. 364–375. Translated from Litologiya i Poleznye Iskopaemye, No. 4, 2005, p. 416–429.

Maynard, B.J. (2010). The Chemistry of Manganese Ores through Time: A Signal of Increasing Diversity of Earth-Surface Environments. Economic Geology, Vol. 105, p. 535–552.

Nyame, F.K., and Beukes, N.J. (2006). The genetic significance of carbon and oxygen isotopic variations in Mn bearing carbonates from the Palaeo-proterozoic (~2.2GA) Nsuta deposit in the Birimian of Ghana: Carbonates and Evaporites, Vol. 21, no. 1, p. 21-32.

Okita, P.M., Maynard, J.B., Spiker, E.C., and Force, E.R., (1988). Isotopic evidence for organic matter oxidation by manganese reduction in the formation of stratiform manganese carbonate ore. Geochim Cosmochim. Acta, Vol. 52, p. 2685– 2697.

Okita, P.M. 1987 cited in Polgari, M. Okita, P.M., Hein, J.R. (1991). Stable isotope evidence for the origin of the Urkut manganese ore deposit, Hungary. Journal of Sedimentary Petrology. Vol. 61, p 384–393.

Öztürk, H., and Frakes, L.A. (1995). Sedimentation and diagenesis of an Oligocene manganese deposit in a shallow subbasin of the Paratethys: Thrace Basin, Turkey: Ore Geology Reviews, Vol. 10, Issue 2, p 117-132.

Ozturk, H., and Hein. J.R. (1997). Mineralogy and stable isotopes of black shale-hosted Manganese ores, southwestern Taurides, Turkey: Economic Geology, Vol. 92, p. 733-744

Polgari, M., Okita, P.M., Hein, J.R. (1991). Stable isotope evidence for the origin of the Urkut manganese ore deposit, Hungary. Journal of Sedimentary Petrology. Vol. 61, p 384–393.

Preston, P.C.C. (2001). Physical and chemical characterization of the manganese ore bed at the Mamatwan mine, Kalahari Manganese Field, Unpublished MSc. Dissertation, Rand Afrikaans University (now University of the Johannesburg, Johannesburg, South Africa.

Rosales, I., Quesada, S. and Robles, S. (2004). Paleotemperature variations of Early Jurassic seawater recorded in geochemical trends of belemnites from the Basque Cantabrian basin, northern Spain. Palaeogeography, Palaeoclimatology, Palaeoecology Vol. 203, p. 253-275

Tsikos, H. Beukes, N.J. Moore, J.M., and Harris, C. (2003). Deposition, Diagenesis, and Secondary Enrichment of Metals in the Paleoproterozoic Hotazel Iron Formation, Kalahari Manganese Field, South Africa: Economic Geology Vol. 98, p. 1449–1462.

Tsikos, H., and Moore, J.M. (1997). Petrography and geochemistry of the Palaeoproterozoic Hotazel iron-formation, Kalahari Manganese Field, South Africa: Implications for Precambrian manganese metallogenesis. Economic Geology, Vol. 92, p. 87-97.

CHAPTER 6

SUMMARY AND CONCLUSIONS

The Lower Manganese Orebody at Kalagadi mine is subdivided into eleven textural distinct zones. The Y, M, C and N – subzones represent the economic portion of the orebody and reach average of 10m. It should however be noted that the, Y-zone macroscopically by dusty brown appearance and hence may be erroneously mined as a waste.

Mineralogically, the economic zones at Kalagadi Manganese mine are characterized by enrichments of braunite and hausmannite not only in the matrix but also as replacements insides ovoids. Therefore, replacements of ovoids by these oxides contribute to the elevated manganese content in these zones. The M and N subzones are the most economic zones mainly due to dominance oxidized carbonate ovoids and laminae.

The X-zone at both SKR 65 and SKR 40 contains elevated manganese content, however close observations from additional boreholes from unpublished mine records show lack of consistency in grade. However, the experience at Mamatwan shows that X-zone is of high grade. Apart from that, although this zone at Gloria mine could not be distinguished from Y-zone, the XY-zone suggest by van Staden (2002) appear to be of economic value. Based on the above observations, it is therefore recommended that X-zone may be included to other economic zones during mining but the economic gain from this zone is not guaranteed due to the observed inconsisteny. It is therefore suggested that, about 11m of the orebody (including X-zone) can be mined rather than 8m initially anticipated during preliminary inverstgations on

the mine lease area. Therefore, about 3m of the ore that could have been mined as waste can now bemined.

Other zones such as W, V, J and (X) zones are considered low grade and hence cannot be mined due to their low manganese content and elevated carbonate and hematite contents in the matrix, ovoid and laminae.

Observations from the fieldworks and borehole information show no major effects of structural feature such as faults that may cause complexities during mining and affect the quality of the ore. Therefore, there is no particular trend or anomaly from the mineralogical and geochemical analyses to suggest the influence of any structural feature.

The mineralogy, mineral paragenesis and geochemistry of the manganese ore at Kalagadi mine is comparable to the other mines in the region. All the minerals encountered in this study are known in the entire Kalahari deposit except for Mg-calcite instead of traditional Mn-calcite previously reported by other authors for the manganese. Further study in this area is recommended to ascertain the presence of this mineral.

The manganese content at Kalagadi mine on average range from 30% Mn - 40% Mn and the ore show slight effect of metamorphism. The abundance of sedimentary features (banding, lenticles etc) and minerals in the ore together with few minerals of late diagenetic to early metamorphism (garnets and serpentines) indicate the influence of low to medium pressure and temperature of metamorphism on the manganese ore.

The oxygen $\delta^{18}O$ isotopes (18‰ to 22‰) at Kalagadi mine are also interpreted to indicate slight metamorphism of the ore.

The oxygen $\delta^{18}O$ isotope values for the Kalahari Manganese Field are interpreted to suggest involvement of either meteoric water or a low-temperature hydrothermal fluid in the oxidation, leaching, and enrichment of the iron formation. The oxygen isotope data suggest that low-temperature hydrothermal fluids mixed with heated (possible from volcanic source) marine water responsible for the precipitation of Mn carbonate ores. The manganese carbonate stable isotope analyses at Kalagadi mine is also comparable with the data obtained from other mines in the entire Kalahari deposit.

Lastly, the Lower manganese orebody at Kalagadi Manganese mine shows a strong correlation with that of Gloria mine in the northeast and it can be correlated with that of Mamatwan mine in the south. It is however not surprising that physical and mineralogical characteristics of various zones at Kalagadi mine are compatible with that of Gloria mine, which is also an underground operation and also at close proximity.

The individual physical characteristic of various zones are hoped to aid in the easy identification of the mineralized sections of the orebody.

REFERENCES

Anderson, T.F., and Arthur M.A. (1983). Stable isotopes of oxygen and carbon and their application to sedimentologic and paleoenvironmental problems. In: M.A. Arthur et al. (editors), Stable Isotopes in Sedimentary Geology Soc. Econ. Paleont. Mineral. ShortCourse IO: 1.1-1.151.

Andrews, J.E. (2006). Palaeoclimatic records from stable isotopes in riverine tufas: Synthesis and review: Earth-Science Reviews, Vol. 75, p. 85-104.

Astrup, J., and Tsikos, H. (1998). Manganese. *in* Wilson, M.J., and Anhaeusser, C.R., (eds), Mineral Resources of Southern Africa: Pretoria, South Africa, Council for Geosciences, Handbook 16, p. 450–460.

Bau, M., Romer, R.L., Lüders, V., and Beukes, N.J. (1999). Pb, O, and C isotopes in silicified Mooidraai dolomite (Transvaal Supergroup, South Africa): Implications for the composition of Paleoproterozoic seawater and 'dating' the increase of oxygen in the Precambrian atmosphere. Earth and Planetary Science Letters, Vol. 174, p. 43–57.

Beukes, N.J., and Gutzmer, J. (1996). A volcanic-exhalative origin for the world's largest Kalahari Manganese Field, A discussion of the paper by D.H. Cornell and S.S. Schütte, Mineral Deposita, Vol. 31, p. 242-245.

Beukes, N.J. (1983). Palaeoenvironmental setting of iron formations in the depositional basin of the Transvaal Super group, South Africa. In: Trendall, A.F., and Morris, R.C. (eds). Iron formations, facts and problems, Elsevier, Amsterdam, p. 131-209.

Beukes, N.J., Kleyestüber, A.S.E., and Nel, C.J. (1982). Volcanogenic-sedimentary cycles in the Kalahari manganese field. Sedimentology, Vol. 82, Geological Society of South Africa, Extended Abstracts, p. 93-97.

Boardman, L.G. (1941). The Black Rock manganese deposit in the south-eastern Kalahari: Geological Society of South Africa Transaction, Vol. 44, p. 51-60.

Burger, A.M. (1994). Fault controlled hydrothermal alteration of Palaeoproterozoic manganese ore in Wessels mine, Kalahari manganese field. Unpublished MSc.

Dissertation, Rand Afrikaans University (now University of the Johannesburg, Johannesburg, South Africa).

Chetty, D. (2008). A geometallurgical evaluation of the ores of the northern Kalahari manganese deposit, South Africa, Unpublished PhD Thesis, University of the Johannesburg, South Africa).

Choi J, H., and Hariya, Y. (1992). Geochemistry and depositional environment of Mn oxide deposits in the Tokoro Belt, Northeastern Hokkaido, Japan: Economic Geology, Vol. 87; no. 5; p. 1265-1274

Cornell, D.H., and Schütte, P. S.S. (1995). A volcanic-exhalative origin for the world's largest (Kalahari) Manganese field: Mineral Deposita, Vol. 30, p. 146-151.

Delian, F., Tiebing, L., and Jie, Y. (1992). The processes of formation of manganese carbonate deposits hosted in black shale series. Economic Geology, V. 87, p. 1419-1429

De Villiers, J.E. (1983). The Manganese Deposits of Griqualand West, South Africa: Some Mineralogic Aspects.Economic Geology Vol. 78, p. 1108-1118.

Dorland, H. (2004). Provenance ages and timing of sedimentation of selected Neoarchean and Paleoproterozoic successions on the Kaapvaal Craton. Unpublished PhD thesis, University of Johannesburg, South Africa.

Du Plooy, A.P. (2002). Geochemistry and mineralogy of supergene altered manganese ore below the Kalahari unconformity in the Kalahari manganese field, Northern Cape Province, South Africa, Unpublished MSc. Dissertation, Rand Afrikaans University (now University of the Johannesburg, Johannesburg, South Africa).

Eglington, B.M., Steven M. Reddy, S.M., and Evans, D. A. D. (2009). The IGCP 509 database system: design and application of a tool to for Palaeoproterozoic tectonic domains, large igneous provinces capture and illustrate litho- and chrono-stratigraphic information and ore deposits; with examples from Southern Africa. Geological Society, London, Special Publications 2009; Vol. 323, p. 27-47.

Frakes, L., and Bolton, B. (1992). Effects of ocean chemistry, sea level, and climate on the formation of primary sedimentary manganese ore deposits. Economic Geology, Vol. 87, p. 1207-1217.

Friedman, I., and O'Neil, J. R. (1977). Compilation of stable isotope fractionation factors of geochemical interest in U.S. geological Survey Professional Papers, p. 440-KK.

Gutzmer, J., and Beukes, N.J. (1995). Fault controlled metasomatic alteration of Early Proterozoic sedimentary manganese ores in the Kalahari Manganese Field, South Africa. Economic Geology, Vol. 90, p. 823-844.

Gutzmer, J. (1996). Genesis and alteration of the Kalahari and Postmasburg manganese deposits, Griqualand west, South Africa. Unpublished PhD. Thesis, Rand Afrikaans University (now University of the Johannesburg, Johannesburg, South Africa).

Gutzmer, J., and Beukes, N.J. (1996). Mineral paragenesis of the Kalahari Manganese Field. Ore Geology Reviews, Vol. 11, p. 405-428.

Gutzmer, J., Beukes, N.J. (1997). Effects of mass transfer, compaction and secondary porosity on hydrothermal upgrading of Paleoproterozoic sedimentary manganese ore in the Kalahari Manganese Field, South Africa. Mineralium Deposita, Vol. 32, p. 250-256.

Gutzmer, J., and Beukes, N.J., and Yeh, H. W. (1997). Metasomatic and supergene fault-controlled alteration of Early Proterozoic sedimentary manganese ore at Mamatwan Mine, Kalahari manganese field, South Africa. South African Journal of Geology, Vol.100, p. 53-71.

International Manganese Institute, (2008). Manganese Ore Production. Available online at http://www.manganese.org/about_mn/production.

Internet, 2009. *Tittle of web page.* www.kalahariresources.co.za, visited in 2009 and 2011.

Jennings, M. (1986). The Middleplaats manganese ore deposit, Griqualand West. In: Annhaeusser, C.R., and Maske, S., (eds.), Mineral deposits of Southern Africa. Geological Society of South Africa., Johannesburg, Vol. 1, p. 979-983.

Kasting, J.F., Tazewell H.M., Klaus W., Veizer J., Shields G., Jaffrés J. (2006). Paleoclimates, ocean depth, and the oxygen isotopic composition of seawater: Earth and Planetary Science Letters 252, p. 82–93.

Kleyenstüber, A.S.E. (1984). The mineralogy of the manganese bearing Hotazel Formation of the Proterozoic Transvaal Sequence in Griqualand West, South Africa. Transactions of the Geological Society of South Africa, Vol. 87, p. 257-272.

Kleyenstüber, A.S.E. (1993). Significant characteristics of the manganese ores and some of the minerals occuring in the Proterozoic Kalahari Manganese Field, South Africa. Resource Geology Special Issue, No 17, p 2-11.

Kuleshov, V. N., and Bych A. F. (2002). Isotopic Composition ($\delta^{13}C$, $\delta 1^{8}O$) and Origin of Manganese Carbonate Ores of the Usa Deposit (Kuznetskii Alatau). Lithology and Mineral Resources, Vol. 37, No. 4, p. 330–343. Translated from Litologiya iPoleznye Iskopaemye, No. 4, p. 381–396.

Kuleshov, V.N., and Brusnitsyn A. I. (2005). Isotopic Composition ($\delta^{13}C$,$\delta 1^{8}O$) and the Origin of Carbonates from Manganese Deposits of the Southern Urals: Lithology and Mineral Resources, Vol. 40, No. 4, 2005, p. 364–375. Translated from Litologiya i Poleznye Iskopaemye, No. 4, 2005, p. 416–429.

Maynard, B.J. (2010). The Chemistry of Manganese Ores through Time: A Signal of Increasing Diversity of Earth-Surface Environments: Economic Geology, Vol. 105, pp. 535–552.

Miyano, T., and Beukes, N .J. (1987). Physicochemical environments for the formation of quartz-free manganese oxide ores from the early Proterozoic Hotazel Formation, Kalahari Manganese Field, South Africa: Economic geology, Vol. 82, p. 706-718.

Nel, C.J., Beukes, N .J., and De Villiers., J. E. (1986). The Mamatwan manganese mine of the Kalahari manganese field, in Anhaeuser, C.R. and Maske, S., eds., Mineral deposits of Southern Africa: Johannesburg, Geological Society of South Africa, p.963-978.

Nicholson, K. (1988). An ancient manganese-iron deposit of freshwater origin, Islay, Argyllshire. Scottish Journal of Geology, Vol. 24, p.175-187.

Nicholson, K. (1992). Contrasting mineralogical-geochemical signature of manganese oxides: Guides to Metallogenesis: Economic Geology Vol, 87, 1992, p. 1253-1264.

Norrish, K., and Hutton, J.T. (1968) An accurate X-Ray Spectrographic method for the analyses of a wide range of geological samples, Geochim.et Cosmochim.Acta, p. 431, 33.

Nyame, F.K., Beukes N.J., Kase K., and Yamamoto M., (2002). Compositional variations in manganese carbonate micronodules from the Lower Proterozoic Nsuta deposit, Ghana: product of authigenic precipitation or post-formational diagenesis: Sedimentary Geology, Vol. 154, p. 159–175.

Nyame, F.K., and Beukes N.J. (2006). The genetic significance of carbon and oxygen isotopic variations in Mn bearing carbonates from the Palaeo-proterozoic(~2.2GA) Nsuta deposit in the Birimian of Ghana: Carbonates and Evaporites, Vol. 21, no. 1, p. 21-32.

Nyame, F.K. (2007). Petrography and geochemistry of intraclastic manganese-carbonates from the 2.2 Ga Nsuta deposit of Ghana: Significance for manganese sedimentation in the Palaeoproterozoic of West Africa. Journal of African Earth Sciences, Vol 50, p. 133-147.

Okita, P.M., Maynard, J.B., Spiker, E.C., and Force, E.R. (1988). Isotopic evidence for organic matter oxidation by manganese reduction in the formation of stratiform manganese carbonate ore: Geochim Cosmochim. Acta, Vol. 52, p. 2685– 2697.

Okita, P.M. 1987 cited in Polgari, M., Okita, P.M., Hein, J.R. (1991). Stable isotope evidence for the origin of the Urkut manganese ore deposit, Hungary. Journal of Sedimentary Petrology. Vol. 61, p. 384– 393.

Öztürk, H., and Frakes, L.A. (1995). Sedimentation and diagenesis of an Oligocene manganese deposit in a shallow subbasin of the Paratethys: Thrace Basin, Turkey: Ore Geology Reviews, Vol. 10, Issue 2, p 117-132.

Ozturk, H., Hein, J.R. (1997). Mineralogy and stable isotopes of black shale-hosted Manganese ores, southwestern Taurides, Turkey: Economic Geology, Vol 92 p. 733-744

Polgari, M., Okita, P.M., and Hein, J.R. (1991). Stable isotope evidence for the origin of the Urkut manganese ore deposit, Hungary. Journal of Sedimentary Petrology, Vol. 61, p 384– 393.

Polteau, S., and Moore, J.M., and Tsikos, H. (2006). *The geology and geochemistry of the Palaeoproterozoic Makganyene diamictite.* Precambrian Research, 148 (3&4). p. 257-274.

Preston, P.C.C. (2001). Physical and chemical characterization of the manganese ore bed at the Mamatwan mine, Kalahari Manganese Field, Unpublished MSc. University of the Johannesburg, South Africa.

Rosales, I., Quesada, S., and Robles, S. (2004). Paleotemperature variations of Early Jurassic seawater recorded in geochemical trends of belemnites from the Basque Cantabrian basin, northern Spain: Palaeogeography, Palaeoclimatology, Palaeoecology, Vol. 203, p. 253-275.

Schneiderhan, E. A., Gutzmer, J., Strauss H. , Mezger K., and Beukes N. J. (2006) The chemostratigraphy of a Paleoproterozoic MnF- BIF succession – the Voëlwater Subgroup of the Transvaal Supergroup in Griqualand West, South Africa, South African Journal of Geology, Vol.109, p.63-80.

Tsikos, H., Beukes, N.J., Moore, J.M., and Harris, C. (2003). Deposition, Diagenesis, and Secondary Enrichment of Metals in the Paleoproterozoic Hotazel Iron Formation, Kalahari Manganese Field, South Africa: Economic Geology, Vol. 98, p. 1449–1462.

Tsikos, H., and Moore, J.M. (1997). Petrography and geochemistry of the Palaeoproterozoic Hotazel iron-formation, Kalahari Manganese Field, South Africa: Implications for Precambrian manganese metallogenesis. Economic Geology, Vol. 92, p.87-97.

Tsikos, H., and Moore, J.M. (1998). The Kalahari Manganese Field: an enigmatic association of iron and manganese. South African Journal Geology, Vol. 101 (4), p. 287-290.

Van Niekerk, H.S. (2006). The origin of the Kheis Terrane and its relationship with the Archean Kaapvaal Craton and the Grenvillian Namaqua Province in Southern Africa, unpublished MSc. Dissertation, University of Johannesburg, South Africa.

van Staden, A. (2002). Characterization of the lowermost manganese ore bed of the Hotazel Formation, Gloria Mine, Northern Cape Province, Unpublished MSc. Dissertation, University of the Johannesburg, Johannesburg, South Africa).

APPENDIX

(a) Relative abundance (in %) of ore and gangue minerals present in Kalagadi Mine. SKR 65

- Analysis done at Mintek

Zone	Braunite	Jacobsite	Hausmannite	Hematite	Kutnahorite	Calcite(Mg)	Calcite	Dolomite	Rhodochrosite	Serpentine
J	30	13	-	18	22	-	10	-	7	-
V	48	-	5	10	12	12	13	-	-	
W	9		-	12	18	17	13	21		10
X	54	9	5	10	15	-	-	-	-	7
Y	52	-	-	6	22	-	11	-	-	9
M	53	-	12	6	14	15	-	-	-	-
C	41	-	8	9	10	32	-	-	-	-
N1	56	-	11	10	14	9	-	-	-	-
N2	53	-	6	5	24	12	-	-	-	-
B	15	14	-	42	11	18	-	-	-	-
L	-	-	-	51	32	-	-	-	17	-

– → not detected

(b).Relative abundance (in %) of ore and gangue minerals present in Kalagadi Mine. SKR 65

- Analysis done at Council for Geosciences

Zone	Braunite		Hausmannite	Hematite	Kutnahorite	Calcite(Mg)	Garnet	Dolomite	Quartz	Mica	Serpentine
J	*		*	*	*	*	*	*	*	*	*
V	32		6	24	11	17	4	-	-	-	5
W	-		-	18	9	-	11	42	-	-	19
X	33		7	23	9	16	5	-	1	-	8
Y	40		-	11	21	2	4	-	-	-	22
M	52		10	4	23	5	-	-	-	-	6
C	47		6	18	22	2	-	-	-	-	6
N1	51		-	12	25	10	-	-	-	-	3
N2	48		8	5	14	21	3	-	-	-	-
B	14		10	22	15	32	1	-	-	4	4
L	*		*	*	*	*	*	*			*

(c).Relative abundance (in %) of ore and gangue minerals present in Kalagadi Mine. SKR 40

- Analysis done at Mintek

Zone	Braunite	Jacobsite	Hausmannite	Hematite	Kutnahorite	Calcite(Mg)	Calcite	Dolomite	Rhodochrosite	Serpentine
F	-	-	-	51	32	-	-	17		-
J	32	19	4	20	10	12	-	-	-	3
V	43	-	3	11	13	13	17	-	-	-
W	46	-	6	5	25	-	12	6	-	-
X	51	-	3	6	21	-	19	-	-	-
Y	57	-	-	17	10	16	-	-	-	-
M	52	-	7	14	13	15	-	-	-	-
C	49	-	4	11	14	16	-	-	-	6
N1	51	-	5	12	15	17	-	-	-	-
N2	48	-	9	11	14	16	2	-	-	-
B	27	14	-	18	21	18	-	-	-	-
L		-	-	28	17	37	18	-	-	-
				-	-	-	-	-	-	-

(d).Relative abundance (in %) of ore and gangue minerals present in Kalagadi Mine. SKR 40

- Analysis done at Council for Geosciences

Zone	Braunite		Hausmannite	Hematite	Kutnahorite	Calcite(Mg)	Garnet	Dolomite	Quartz	Mica	Serpentine
F	*		*	*	*	*	*	*			*
J	*		*	*	*	*	*	*			*
V	37		4	21	12	20		-			3
W	39		6	23	10	20	3	-			-
X	40		10	14	16	16	-	-			4
Y	54		21	3	14	1	-	-			7
M	43		4	8	19	24	-	-			3
C	46		13	13	19	3	-	-			6
N1	50		-	7	24	17	-	-			2
N2	53		-	5	22	15	1	-			4
B	22		7	8	9	50	2	-			3
L			-	27	19	46		-			8

– → not detected

* → not submitted/insufficient sample material